The Nek2 protein kinase: its phosphorylation, activation and inhibition

Thesis submitted for the degree of
Doctor of Philosophy
at the University of Leicester

By

Donna-Marie Cheary BSc (Hons) (Leicester)
Department of Biochemistry
University of Leicester

April 2009

DECLARATION

Unless otherwise acknowledged, the experimental work in this thesis has been carried out by the author in the department of Biochemistry at the University of Leicester between October 2005 and October 2008. The work has not been submitted, and is not presently being submitted for any other degree at this or any other University.

Signed: Date:

Department of Biochemistry
University of Leicester
University Road
Leicester
LE17RH

DONNA-MARIE CHEARY BSc (Hons)

THE NEK2 PROTEIN KINASE: ITS PHOSPHORYLATION, ACTIVATION AND INHIBITION

ABSTRACT

Nek2 is a cell cycle-regulated protein kinase localised to the centrosome. Nek2 is involved in regulating mitotic events and centrosomal activity through phosphorylation of various substrates including C-Nap1, Rootletin and PP1. Nek2 is overexpressed in cancer cell lines and primary tumours. Overexpression of active Nek2 is characterised by the premature splitting of centrosomes and altered microtubule nucleation. Activation of Nek2 is dependent upon dimerisation and autophosphorylation. Using mass spectrometry, 13 sites of autophosphorylation have been identified in the Nek2 kinase. Individual phosphorylation sites were mutated and the effect that this had on Nek2 activity *in vitro* and *in vivo* was characterised. Phosphomimiking mutation of T170 or S171 created hyperactive Nek2A kinases. However, mutation of the C-terminal autophosphorylation sites had no effect upon Nek2A activity. The proposal that the C-terminal domain of Nek2 acts as an autoinhibitory domain was investigated although the removal of C-terminal residues did not create a hyperactive Nek2 kinase. An investigation into the role of a novel αT-helix found at the N-terminal end of the T-loop of an inactive Nek2 crystal structure, found that mutation of αT-helix residues resulted in loss of Nek2A kinase activity. Phospho specific antiserum directed against the Nek2 T175 autophosphorylation site was purified and characterised. This reagent should prove to be a valuable tool for detection of active Nek2 kinase in tumours as well as cells in culture. Furthermore, the intramolecular interactions of C-Nap1 and Nek2 were investigated to determine how centrosome cohesion is regulated. Protein binding assays revealed that C-Nap1 can form hetero- and homo-dimers and that the ability of C-Nap1 to heterodimerise is compromised as a consequence of phosphorylation by Nek2. Finally, the consequences of Cdk1 inhibition upon Nek2A activity and centrosome cohesion were investigated. Inhibition of Cdk1 in cells induced a substantial G_2/M arrest accompanied by premature centriole disengagement resulting in multipolar spindle formation observed in cells released from Cdk1 inhibition.

ACKNOWLEDGEMENTS

I am very grateful to the Biochemistry Department at the University of Leicester for giving me the chance to study for a PhD with them. I would like to thank Prof. Andrew Fry for his support and encouragement over the past 3 years and for his careful reading of this manuscript. I would also like to thank the members of lab 242, past and present, who have offered support and guidance during the past 3 years. In particular, I would like to thank Joanne Baxter for the detailed handover she gave me to enable the continued analysis of the Nek2 autophosphorylation sites. I also want to offer my thanks to my committee members, Dr. Christine Wells and Prof. Maggie Manson for their help and advice during the course of the project.

Lastly I would like to thank my husband Martin for his encouragement and support and for putting up with an untidy house during my writing up period!

I would like to dedicate this manuscript to my Grandpa John who bravely battled cancer in silence until diagnosed terminal. I hope he would be proud of me x

CONTENTS

Declaration II
Abstract III
Acknowledgements IV
Contents V
Abbreviations XII
Figures XVI

Chapter One Introduction

1.1 The eukaryotic cell cycle.. 2
1.2 Regulation of the cell cycle.. 5
1.3 The mitotic spindle... 6
  1.3.1 Microtubules... 6
  1.3.2 Spindle assembly.. 8
  1.3.3 Microtubule nucleation.. 9
  1.3.4 Microtubule anchoring and release.. 11
1.4 The centrosome.. 12
  1.4.1 Centrosome structure... 12
  1.4.2 Centrosome duplication... 14
    1.4.2.1 Centriole disengagement.. 14
    1.4.2.2 Centriole duplication... 14
    1.4.2.3 Centrosome maturation, disjunction and separation......... 18
  1.4.3 Centrosome functions.. 19
  1.4.4 Centrosomes and cancer.. 21
1.5 Cell cycle regulation of the centrosome.. 22
  1.5.1 Cyclin-dependent kinases.. 22
  1.5.2 Polo-like kinases.. 24
  1.5.3 Aurora kinases... 27

1.6 **NIMA-related kinases** 29
1.6.1 Mitotic Neks: Nek6, Nek7 and Nek9……………………………... 32
1.6.2 Ciliary Neks: Nek1 and Nek8.. 33
1.6.3 Miscellaneous Neks: Nek3, Nek4, Nek5, Nek10 and Nek11 34
1.7 **The Nek2 protein kinase**... 35
1.7.1 Nek2 structure.. 36
1.7.2 Nek2 functions... 40
1.7.3 Nek2 regulation.. 42
1.7.4 Nek2 substrates.. 44
1.7.5 Nek2 in cancer cells... 49
1.8 **Project Aims**... 50
1.8.1 Background to project.. 50
1.8.2 Experimental objectives... 50

Chapter Two Materials and Methods

2.1 **Materials**.. 56
2.1.1 Chemical suppliers... 56
2.1.2 Radioisotopes... 58
2.1.3 Vectors and constructs.. 58
2.1.4 Antibodies.. 58
2.1.5 Bacterial strains.. 60
2.1.5 Buffers and solutions.. 60
2.2 **Molecular Biology Techniques**... 61
2.4.1 Growth and maintenance of bacterial strains................................. 61
2.4.2 Transformation of competent bacteria... 61
2.4.3 Plasmid preparation (small scale)... 61
2.4.4 Plasmid preparation (large scale).. 61
2.4.5 Quantification of DNA concentration.. 62
2.4.6 Restriction digestion... 62
2.4.7 DNA gel electrophoresis.. 62

2.4.8 DNA sequencing………………………………………………………. 62
2.4.9 Oligonucleotide design for mutagenesis…………………………. 62
2.4.10 Site-directed mutagensis…………………………………………. 63
2.3 Protein Techniques.. 64
2.5.1 SDS-Polyacrylamide Gel Electrophoresis (SDS-PAGE).............. 64
2.5.2 Coomassie blue staining... 64
2.5.3 Silver staining... 65
2.5.4 Western blotting... 65
2.5.5 In *Vitro* Translation (IVT)... 66
2.5.6 In *vitro* pull-down assays.. 66
2.5.7 Immunoprecipitation (IP)... 66
2.5.8 Kinase assay.. 67
2.4 Protein Expression and Purification.. 67
2.6.1 Expression of protein in bacteria.. 67
2.6.2 Purification of His and GST tagged fusion proteins....................... 68
2.5 Cell Biology Techniques.. 68
2.2.1 Maintenance and storage of cells... 68
2.2.2 Transfection of cells.. 69
2.2.3 Cell extractions... 69
2.2.4 Cell cycle analysis... 69
2.6 Immunofluorescence Microscopy... 70
2.7 Antibody Generation and Purification...................................... 70
2.7.1 Phosphospecific antibody generation.. 70
2.7.2 Preparation of affinity purification columns................................ 71
2.7.3 Affinity purification of Nek2 phosphospecific antibodies.............. 71
2.8 Quantification Techniques... 71
2.8.1 Quantification of protein concentration.. 71
2.8.2 Scintillation counting.. 71
2.8.3 Quantification of kinase activity.. 72
2.8.4 Quantification of centrosome splitting... 72
2.8.5 Quantification of protein band intensity………………………….. 72

2.8.6 Statistics 73

Chapter Three Autophosphorylation of the Nek2 Protein Kinase

3.1 Introduction.. 75

3.2 Results

3.2.1 Validating the activity assays with wild type Nek2A and kinase-inactive Nek2A.. 78

3.2.2 Phosphomimetic mutations of T170 and S171 increase Nek2A kinase activity... 80

3.2.3 Mutation of S356 and S368 does not alter Nek2A kinase activity or localisation... 82

3.2.4 Mutation of S296 or S428 creates hyperactive Nek2A proteins...... 82

3.2.5 Individual mutation of S387 does not affect Nek2A kinase activity……….. 87

3.2.6 Deletion of the last 61 residues from the C-terminus creates a hyperactive Nek2A protein... 87

3.2.7 Mutation of A163G in the αT-helix leads to loss of Nek2A kinase activity... 91

3.2.8 Mutation of other residues within the αT-helix results in loss of Nek2A kinase activity... 94

3.2.9 Mutation of the gatekeeper residue M86, leads to loss of Nek2A kinase activity.. 94

3.3 Discussion... 98

Chapter Four Generation and Characterisation of a Nek2 Phosphospecific Antibody

4.1 Introduction.. 104

4.2 Results

4.2.1 Prescreening of rabbit sera.. 106

4.2.2 The immune serum stains centrosomes more strongly than the pre-immune serum.. 106

4.2.3 The immune sera from rabbits 10654 and 10659 detect the peptides more strongly than the pre-immune sera......................... 109

4.2.4 The purified pT175 antibody detects the phosphorylated peptide more strongly than the non-phosphorylated peptide...................... 109

4.2.5 Generation and characterisation of an inactive Nek2-KD-K37R/D141A kinase.. 112

4.2.6 pT175 Ab C detected the Nek2 KD-K37R but not Nek2-KD-K37R/D141A protein.. 114

4.2.7 pT175 antibody C detects endogenous Nek2 in U2OS lysates and stains the centrosome and midbody in U2OS cells........................ 117

4.2.8 The six potential Nek2 pT175 phosphospecific antibodies generated by HuCAL technology.. 117

4.2.9 AbD1 detects centrosomes in prophase U2OS cells...................... 120

4.2.10 AbD1, 2, 3 and 6 detect Nek2-KD-K37R and Nek2 KD-K37R-D141A bacterially expressed proteins.. 120

4.2.11 Recombinant antibodies AbD1, 2 and 3 detect the full-length recombinant His-Nek2A protein preferentially after ATP incubation.. 123

4.2.12 AbD1 detects specifically the mitotic kinase Nek2A *in vitro*........ 123

4.2.13 Recombinant AbD1 detects centrosomes specifically from prophase to metaphase…………….…………………………….. 127

4.2.14 Nek2A does not colocalise with kinetochores…………………… 127

4.3 Discussion.. 130

Chapter Five Investigation into the effect of Cdk1 Inhibition on Nek2 activation

5.1 Introduction.. 134

5.2 Results

5.2.1 RO-3306 induces a reversible G2/M arrest in U2OS cells........... 136

5.2.2 RO-3306 inhibits Cdk1 but not Nek2A kinase *in vitro* 136

5.2.3 RO-3306 does not prevent premature centrosome splitting in response to Nek2A overexpression……………………………… 136

5.2.4 Cdk1 inhibition induces centrosome defects…………………….. 139

5.2.5 Release of Cdk1 inhibition leads to multipolar spindle formation 139

5.3 Discussion... 144

Chapter Six Characterisation of Nek2 and C-Nap1 in Centrosome Cohesion and Assembly

6.1 Introduction.. 151

6.2 Results

6.2.1 Purification of GST-C-Nap1-CTD and –NTD proteins................. 153

6.2.2 Intramolecular interactions of C-Nap1.. 153

6.2.3 *In vitro* phosphorylation of C-Nap1 by Nek2 kinase..................... 155

6.2.4 The ability of the C-Nap1-CTD and NTD to form heterodimers is reduced as a consequence of phosphorylation by Nek2A.......... 158

6.2.5 Identification of sites in C-Nap1 phosphorylated by Nek2……… 158

6.3 Discussion... 163

Chapter Seven Final Discussion

7.1 Nek2 regulation by autophosphorylation.. 169

7.1.1 Is there a common mechanism for activation of Nek kinases?.......... 170

7.1.2 Does the C-terminal domain of Nek2 act as an autoinhibitory domain?... 170

7.1.3 Does mutation of residues comprising the αT-helix result in hyperactivity?... 171
7.1.4 Does mutation of the M86 gatekeeper residue alter Nek2A activity?... 171
7.2 Generation of Nek2 phosphospecific antibodies....................................... 172
7.3 Does Nek2 activation occur upstream or downstream of Cdk1?............ 173
7.4 Nek2 interactions with C-Nap1... 175
7.4.1 Nek2, C-Nap1 and the intercentriolar linkage.................................... 175
7.4.2 Does a Nek2 target consensus sequence exist?.................................. 177
7.5 Concluding remarks... 178

Chapter Eight **References** 180

ABBREVIATIONS

A260	Absorbance at 260 nanometres
APC/C	Anaphase promoting complex/cyclosome
Asp	Abnormal spindle protein
ATP	Adenosine triphosphate
ATRX	alpha-thalassemia mental retardation syndrome X-linked
BCA	Bicinchoninic acid
BCIP	5-bromo-4-chloro-3-indolyl phosphate
bp	base pairs
53-BP1	p53 binding protein 1
BSA	Bovine serum albumin
C-	Carboxyl
Cdc20	Cell division cycle 20
Cdh1	Cadherin 1
Cdk	Cyclin dependent kinase
cDNA	Complementary deoxyribonucleic acid
CENPJ	Centromere protein J
cm	Centimetre
C-Nap	Centrosomal Nek2 associated protein 1
CPAP	centrosomal P4.1-associated protein
CTD	C-terminal domain
DMEM	Dulbeccos modified eagle’s medium
DMSO	Dimethylsulfoxide
DNA	Deoxyribonucleic acid
DTT	Dithiothreitol
EDTA	Ethylene diamine tetra acetic acid
EGTA	Ethylene glycol-bis (aminoethylether) N,N,N’N’-tetraacetic acid
FCS	Foetal calf serum
G	Growth phase
g/l	Grams per litre

GFP	Green fluorescent protein
γ-TuRC	γ-tubulin ring complex
HEPES	N-2-hydroxyethylpiperazine-N’-2-ethanesulphonic acid
HMGA2	High mobility group AT-hook 2
IF	Immunofluorescence
IgG	Immunoglobulin G
IMS	Industrial methylated spirit
IPTG	β-D-isopropyl-thiogalactopyranoside
IVT	In vitro translation
kDa	Kilo Dalton
KIF3A	kinesin family protein 3A
l	Litre
LATS2	large tumour suppressor 2
LB	Luria-bertani
M	Molar
mA	Milliamp
MAPK	Mitogen activated protein kinase
MCAK	Mitotic centromere-associated kinesin
Mg	Milligram
Min	Minutes
ml	Millilitre
mM	Millimolar
MPM-2	Mitotic pro monoclonal 2
mRNA	Messenger ribonucleic acid
MTOC	Microtubule organising centre
N-	Amino-
NBT	Nitroblue tetrazolium
NDEL1	Nuclear distribution gene E (*A-nidulans*)-like 1
Nek2	NIMA-related kinase
ng	Nanogram
NIMA	Never in Mitosis

Nlp	Ninein-like protein
NTD	N-terminal domain
OD	Optical density
OFD2	Outer dense fibre 2
O/N	Overnight
PAGE	Polyacrylamide gel electrophoresis
PBD	Polo box domain
PBS	Phosphate buffered saline
PCM	Pericentriolar matrix
PCR	Polymerase chain reaction
PKA	Protein kinase A
Plk	polo-like kinase
PMSF	phenylmethylsulphonyl fluoride
PP1	Protein phosphatase 1
Rac1	Ras-related C3 botulinum toxin substrate1
RCC1	Regulator of chromosome condensation 1
RhoA	Ras homolog gene family member A
RhoGEF	Ras homolog nucleotide exchange factor
RNA	Ribonucleic acid
rpm	Revolutions per minute
SCF	Skp-cullin-F-box
SDS	Sodium dodecyl sulphate
SPB	Spindle pole body
SPD	Spindle defective 2
TACC3	Transforming acidic coiled-coil protein 3
TEMED	N,N,N’N’-tetramethylethylenediamine
TPX2	Targeting protein for Xklp2
TRIS	Tris (hydroxymethyl) aminomethane
mg	Microgram
µl	Microlitre
µM	Micromolar

V	Volts
(v/v)	Volume per volume ratio
(w/v)	Weight per volume ratio
ZYG	Zygote defective 1

FIGURES

1.1 The Eukaryotic Cell Cycle………………………………………………. 3
1.2 Mitosis…………………………………………………………………… 4
1.3 The Mitotic Spindle…………………………………………………... 7
1.4 Centrosome Structure.. 13
1.5 The Centrosome duplication cycle…………………………………… 15
1.6 Protein kinase regulation of the centrosome duplication cycle……… 23
1.7 NIMA-related kinases………………………………………………… 30
1.8 Crystal structure of the N-terminal catalytic domain of Nek2……….. 37
1.9 The structure of Nek2A, Nek2B and Nek2C ………………………… 39
1.10 Nek2 substrates.. 45
1.11 Mass Spectrometry reveals thirteen autophosphorylation sites within Nek2A…………………………………………………………………… 51
1.12 A summary of data available before starting this project on Nek2A autophosphorylation sites…………………………………………….. 52

3.1 Assays to determine Nek2A kinase activity *in vitro* and *in vivo*.......... 79
3.2 Mutation of T170 or S171 to glutamate or aspartate, respectively, results in hyperactive Nek2A proteins……………………………... 81
3.3 Mutation of S356 or S368 does not alter Nek2A kinase activity…….. 83
3.4 Mutation of S356 or S368 does not alter Nek2A activity or localisation in cells……………………………………………………. 84
3.5 Mutation of S296 or S428 has no effect upon Nek2A kinase activity... 85
3.6 Mutation of S296 or S428 does not alter Nek2A activity in cells……. 86
3.7 Mutation of S387 does not affect Nek2A activity……………………. 88
3.8 Mutation of S387 has no effect on Nek2A activity in cells…………... 89
3.9 Deletion of C-terminal residues does not alter Nek2 localisation to the centrosome…………………………………………………………... 90
3.10 Deletion of the last 61 residues from the C-terminus creates a hyperactive Nek2A protein……………………………...………. 92
3.11 Mutation of A163 in the αT-helix inactivates Nek2………………….. 93
3.12 Additional mutations in the αT-helix cause loss of Nek2A activity…. 95

3.13 Mutation of the gatekeeper residue M86 leads to loss of Nek2A activity………………………………………………………………… 97
3.14 A summary of the consequences of mutations in Nek2A autophosphorylation sites…………………………………………….. 102

4.1 Prescreening of rabbit sera……………………………………………. 107
4.2 Immune sera 10654 and 10659 stain centrosomes more strongly than the pre-immune sera………………………………………………... 108
4.3 The immune sera for rabbits 10654 and 10659 detect phosphorylated peptide more strongly than the pre-immune sera……………………... 110
4.4 Two of the purified pT175 antibodies detect the phosphorylated peptide more strongly than the non-phosphorylated peptide…………. 111
4.5 Expression and purification of Nek2-KD-K37R and Nek2-KD-K37R/D141A proteins……………………………………………... 113
4.6 Nek2-KD-K37R/D141A kinase is an inactive kinase incapable of autophosphorylation…………………………………………………. 115
4.7 pT175 Ab C detected Nek2-KD-K37R kinase but not unphosphorylated Nek2-KD-K37R/D141A kinase…………………... 116
4.8 pT175 Ab C detects Nek2 in U2OS lysates………………………... 118
4.9 ELISA data for the six recombinant pT175 Nek2 antibodies identified by AbD Serotec…………………………………………………….. 119
4.10 The six HuCAL pT175 phosphospecific antibodies detect the phosphorylated but not the unphosphorylated peptide……………… 121
4.11 AbD1 detects centrosomes in U2OS cells……………………………. 122
4.12 AbD1, 2 and 3 preferentially detect Nek2-KD-K37R rather than Nek2-KD-K37R/D141A bacterially expressed protein………………. 124
4.13 Recombinant antibodies AbD1, 2 and 3 detect phosphorylated His-Nek2A after ATP incubation but not untreated His-Nek2……………. 125
4.14 AbD1 detects specifically the mitotic kinase, Nek2 *in vitro*………….. 126
4.15 AbD1 detects centrosomes specifically in prophase cells……………. 128
4.16 Nek2 does not colocalise with kinetochores.. 129

5.1 RO-3306 induces a G2/M arrest in U2OS cells………………………. 137
5.2 RO-3306 inhibits Cdk1 but not Nek2 kinase activity *in vitro*………... 138
5.3 RO-3306 does not prevent centrosome splitting in U2OS cells transfected with myc-Nek2A-WT…………………………………….. 140
5.4 RO-3306 induces centrosome defects in U2OS cells………………… 141
5.5 RO-3306 induces spindle defects in U2OS cells……………………... 143
5.6 Cdk1 inhibition results in premature centriole disengagement and premature recruitment of intercentriolar proteins................................. 146
5.7 A model for the role of Cdk1 in the activation of Nek2 and prevention of premature centriole disengagement................................ 148
5.8 A model for the consequences of Cdk1 inhibition by RO-3306 upon Nek2 activation and centriole disengagement...................................... 149

6.1 Purification of GST-C-Nap1-CTD and –NTD...................................... 154
6.2 *In vitro* GST pull down assays with C-Nap1 and Nek2 proteins……. 156
6.3 C-Nap1-CTD and -NTD can be phosphorylated by Nek2 kinase……. 157
6.4 The ability of C-Nap1-CTD and -NTD to form heterodimers is significantly reduced as a consequence of phosphorylation by Nek2... 159
6.5 Identification of sites within the N- and C-terminal domains of C-Nap1 phosphorylated by Nek2……………………………………... 161
6.6 Comparison of the phosphorylation consensus sequence for NIMA and those sites phosphorylated by Nek2 in C-Nap1............................. 162
6.7 Proposed model of how C-Nap1 interactions may be regulated in response to phosphorylation by Nek2.. 165

7.1 A model of the intercentriolar linkage connecting paired centrioles.. 176

Chapter One

Introduction

1.1 The Eukaryotic cell cycle

Somatic cells progress through 4 phases to divide into two new daughter cells. Following the previous cell division, cells first enter Gap1 (G_1) phase which is a period of growth before the cells then undergo a period of DNA synthesis (S) during which the chromosomes are duplicated (Figure 1.1). The cells then enter a second period of growth (G_2) phase and prepare for the final phase, mitosis (M). During mitosis, the duplicated chromosomes are segregated and the cell divides into two new daughter cells. G_1, S and G_2 are collectively called interphase. Cells spend most of their time in interphase and cycle through mitosis very rapidly. In HeLa cells a complete cell cycle takes about 22 hours. There is a fifth phase known as G_0 or quiescence when cells exit the cell cycle. Cells enter this phase in response to anti-proliferative extracellular signals (Alberts et al., 2008).

Mitosis can be divided into a series of phases known as prophase, prometaphase, metaphase, anaphase and telophase (Figure 1.2). During prophase, chromosomes condense which involves the compaction of chromatin into sister chromatids that can be distinguished by light microscopy. The two centrosomes each nucleate an array of microtubules known as an aster. The microtubules from each aster interact with each other and elongate as the centrosomes move to opposite ends of the cell. Here they organise the poles of the emerging mitotic spindle. At prometaphase, the nuclear envelope breaks down allowing the chromosomes access to the mitotic spindle microtubules. At metaphase, the chromosomes align at the equator of the spindle equidistant between the spindle poles as a result of the microtubules radiating from the centrosomes capturing the chromosomes via their kinetochores. The paired sister chromatids separate during anaphase and are pulled to the spindle poles at opposite ends of the cell by a motion called poleward flux. This equally segregates the DNA and leads to the formation of two daughter nuclei (Mitchison and Salmon, 2001; Wittmann et al., 2001). In telophase, the nuclear envelopes reform around each chromosome mass and the chromosomes decondense. The final step in mitosis is cytokinesis, during which the cytoplasm is divided equally between two daughter cells by the action of a contractile ring of actin and myosin. The contractile ring pinches the dividing cell in the middle forming the cleavage furrow. The cleavage furrow thins into a structure called the midbody, before finally separating into two individual cells, each with a single nucleus (Alberts et al., 2008).

1.2 Regulation of the cell cycle

The various events that occur within the cell cycle are regulated by a control system that checks whether environmental conditions are favourable and that each event is successfully completed before the next event begins. It also ensures that events occur only once and in the correct sequence. This control system is mediated in large part by the activity of cyclin-dependent kinases (Cdks) and the ubiquitin ligases, SCF (skp1, cullin and F-box) and anaphase-promoting complex/cyclosome (APC/C). Cyclin-Cdk complexes act at several transition points throughout the cell cycle (Alberts *et al.*, 2008). Some of these transition points can be considered as checkpoints, where progress through the cell cycle can be delayed until conditions are favourable. For example, there is a mitotic entry checkpoint in late G_2 which checks that all the DNA has been replicated before the mitotic machinery is activated. Once cells pass this point, they are committed to mitosis (Pihan and Doxsey, 1999; Pines and Rieder, 2001). At metaphase there is a spindle assembly checkpoint (SAC) which checks that all chromosomes are properly attached by their kinetochores to spindle microtubules. In the absence of such attachment, BubR1 and Mad2 proteins bind to unattached kinetochores and exert inhibitory signals (Mitchison and Salmon, 2001; Musacchio and Hardwick, 2002; Pines, 1999). This inhibits the APC/C cofactor Cdc20, preventing the activation of APC/C, which in turn prevents premature chromosome segregation and progression into anaphase until all spindle microtubules are correctly attached (Alberts *et al.*, 2008; Hansen *et al.*, 2002; Pines and Reider, 2001). There is a third checkpoint in late G_1 called the restriction point, which checks that the environment is favourable before committing the cell to DNA replication. Finally, there are DNA damage checkpoints present in G_1, S and G_2 which delay cell cycle progression if any DNA is damaged, allowing time for the DNA to be repaired (Houtgraaf et al., 2006).

Cdks are activated by the phosphatase, Cdc25, and inhibited by the kinase, Wee1 (Alberts *et al*, 2008; Pines, 1999). Cdk activity is also regulated by the binding of particular inhibitory proteins (CKIs) and changes in the expression of their regulatory partner subunits, cyclins. The ubiquitin ligase, SCF, is responsible for the ubiquitylation and destruction of G_1/S-cyclins, whereas the APC/C is responsible for the ubiquitylation and proteolysis of M-cyclins. Hence, the SCF and APC/C inactivate cyclin-Cdk complexes, thereby ensuring unidirectional progress through the cell cycle (Hansen *et al.*, 2002).

1.2 The Mitotic Spindle

1.3.1 Microtubules

In all eukaryotic cells, the accurate segregation of duplicated chromosomes is dependent on the assembly of a microtubule-based structure, referred to as the mitotic spindle. A typical mammalian mitotic spindle is thought to contain over 3000 microtubules (Compton 2000). Microtubules are present in both interphase and in mitotic cells and form a supportive network which allows the movement of proteins and organelles within a cell. Microtubules are hollow cylindrical structures, 25 nm in diameter, composed of alternating α- and β-tubulin molecules with 13 tubulin molecules per turn of the filament. Hence, each microtubule has a regular 13 filament structure (Urbani and Stearns, 1999). Microtubules are intrinsically polar structures with a rapidly growing plus end, targeted to the chromosomes or cell cortex and a slow growing minus end anchored at the centrosome (Figure 1.3). The growth and shrinkage of microtubules occurs constantly throughout the cell cycle as a result of their dynamic instability (Doxsey, 2001; Mitchison and Salmon, 2001).

There are at least 3 classes of microtubules involved in the formation of a mitotic spindle: astral, kinetochore and interpolar microtubules (Figure 1.3). Astral microtubules radiate from the centrosomes and anchor the spindle to the plasma membrane to ensure the correct positioning of the spindle. Kinetochore microtubules connect the kinetochores of chromosomes to the spindle. The interpolar microtubules radiate from centrosomes into the central spindle and interact with microtubules from the opposite centrosome. These interactions are thought to stabilise the bipolar shape of the spindle by producing outward forces through sliding of anti-parallel microtubules to balance the intense inward forces exerted by the kinetochores. In addition, these interactions may also aid the movement of spindle poles to opposite ends of the cell in anaphase B (Compton 2000). During mitosis, these microtubule-mediated interactions are continuously altered by the addition of α/β-tubulin subunits at the plus end and the removal of α/β-tubulin subunits from the minus end at the spindle pole to allow a continuous poleward microtubule flux (Mitchison and Salmon, 1992; Doxsey, 2001).

1.3.2 Spindle assembly

Spindle assembly relies on two main families of mechanochemical motor proteins which move along microtubules in an ATP-dependent manner, known as kinesins and dyneins. Kinesins and dyneins cross-link microtubules thus mediating motor-driven sliding of anti-parallel microtubules across one another (Diwan, 2006). These proteins consist of 2 or 3 heavy chains which include a globular head domain and numerous intermediate and light chains. The heavy chains contain a microtubule binding domain at the C-terminus and a globular motor domain at the N-terminus which possesses ATPase activity. The forward motor domain binds ATP allowing it to attach to microtubules more strongly. Simultaneously, the second motor domain hydrolyses its bound ATP allowing the motor domain to undergo a conformational change which results in its detachment from the microtubules, thus mediating its movement along the microtubules (Diwan, 2006; Sharpe et al., 2000).

Kinesins are generally plus end-directed motor proteins which move away from the spindle pole towards the plus ends of microtubules. There are over 40 members of the kinesin family which differ greatly in structure and function. The light chains of kinesins often possess several tetratricopeptide repeats (TPRs) at the C-terminal tail that mediate protein-protein interactions. TPRs allow kinesins to bind cargo proteins such as kinectin and Rab GTPases. BimC proteins are a family of kinesin-related motor proteins that include the mammalian Eg5 kinesin. They are homotetrameric molecules which assemble into antiparallel dimers via their tail domain. As BimC motor domains move towards the microtubule plus ends, an outward force is generated that pushes the poles apart. Abolishing bimC motor activity prevents centrosome separation and results in monopolar spindle formation (Compton, 2000).

Minus end-directed motor proteins focus the minus ends of microtubules at the spindle poles. One such motor protein is cytoplasmic dynein. The translocation of microtubules by dynein is required for spindle pole organisation in somatic cells irrespective of the presence of centrosomes (Compton, 2000; Heald et al., 2005). Dynein promotes the targeting of microtubule ends to the spindle poles by cross-linking and sliding antiparallel microtubules across one another. This cross-linking activity possessed by cytoplasmic dynein, as well as its interaction with the plasma membrane and cargo proteins, is facilitated by a large multi-protein activator called dynactin (Merdes et al., 2000). Dynactin activates dynein and acts as a tether between dynein and microtubules. Dynactin also facilitates the interaction between dynein and its subcellular cargo proteins (Quintyne and Schroer, 2002). The dynein-dynactin complex moves along astral microtubules towards the centrosome generating a force that mediates spindle orientation and centrosome separation in mitosis. In addition, this allows dynein-dependent minus end-directed microtubule transport of a number of centrosomal and spindle proteins to the spindle pole. The large structural protein, NuMA, is recruited to the spindle pole by dynein-dynactin where it fixes bundles of microtubule minus ends tightly together creating a focused structural support for the spindle pole, independent of the centrosome (Merdes et al., 2000; Compton, 2000). NuMA is likely to form a trimeric complex with dynein and dynactin as disruption of any of these proteins results in spindle defects (Compton, 2000).

1.3.3 Microtubule nucleation

Microtubules undergo many changes upon mitotic entry that alter their organisation and dynamics to permit spindle assembly. This is in part dictated by the centrosome and its associated proteins which nucleate and subsequently organise microtubules. Microtubule nucleation occurs from within the pericentriolar material (PCM) (see section 1.4.1) at ring-shaped multi-protein complexes containing γ-tubulin. γ–Tubulin is the key protein involved in the nucleation of microtubules *in vivo*. These γ-tubulin ring complexes, or γ-TuRCs, are present at the centrosomes throughout the cell cycle, but additional γ-TuRCs are recruited to the PCM during centrosome maturation at the G_2/M transition (Job et al., 2003). Although also present in the cytoplasm, they predominantly nucleate microtubules at the centrosome, presumably due to the presence of additional activators (Wiese and Zheng, 2000). The γ-TuRC is composed of 12 γ-tubulin molecules, at least 6 other proteins, referred to as γ-tubulin binding proteins (GTBPs) and a cap-shaped structure (Stearns and Winey, 1997). A number of possible GTBPs have been identified including γ-tubulin complex proteins 2 and 3 (GCP2 and GCP3) which anchor additional proteins such as pericentrin/Kendrin, ninein-like protein (Nlp) and abnormal spindle protein (Asp) to the γ-TuRC (Bornens, 2002; Delgehyr et al., 2005; Takahashi et al., 2002). Each microtubule is thought to assemble initially as a sheet which closes to form a tube. There are two proposed models to explain how γ-TuRCs nucleate microtubules. The first model for microtubule nucleation suggests that the γ-TuRC acts as a helical template for the assembly of α/β-tubulin dimers with its cap encompassing the microtubule minus ends of microtubules (Zheng et al., 1995; Keating and Borisy, 2000; Moritz et al., 2000). Microtubule capping is required to prevent depolymerisation of minus ends of microtubules after being released (Urbani and Stearns, 1999). The γ-tubulin molecules interact with each other laterally and with α-tubulins longitudinally at the minus end of one protofilament, thus promoting polymerisation and elongation of the microtubule.

In contrast, the second ‘protofilament’ model proposes that γ-tubulin molecules interact with each other longitudinally and with α/β-tubulin dimers laterally causing the γ-TuRC to unwind and form the first protofilament. This promotes the assembly of additional α/β-tubulin subunits laterally creating a sheet which grows and curls to form a microtubule (Job et al., 2003; Keating and Borisy, 2000; Moritz et al., 2000).

γ-Tubulin is essential for microtubule nucleation to occur. γ-Tubulin is present at the centrosome throughout the cell cycle, although its concentration increases during mitosis when it is required for mitotic spindle formation (Khodjakov and Rieder, 1999). The recruitment of γ-tubulin to the centrosome may be dependent upon dynactin. Dynactin interacts with dynein via its sidearm subunit, $p150^{GLUED}$. Overexpression of fragments of the $p150^{GLUED}$ results in unfocused and disorganised microtubule arrays and a failure to recruit γ-tubulin (Quintyne et al., 1999). Microinjection of dynein antibodies also results in failed γ-tubulin recruitment to the centrosome in *Xenopus* cells (Young et al., 2000). Together, these data suggest that the dyenin/dynactin complex may transport γ-tubulin from the cytoplasm along microtubules to the centrosome and that this is necessary for microtubule nucleation to occur.

Pericentrin localises to the PCM surrounding the centrioles and has been implicated in microtubule nucleation and organisation. Pericentrin forms a complex with γ-tubulin generating a reticular lattice that contacts the minus ends of nucleated microtubules at the centrosome (Doxsey et al., 1998). Pericentrin may therefore act as a structural scaffold for microtubule nucleating complexes. The pericentrin-γ-tubulin lattice assembles in G_1, enlarging until mitosis and disassembling after mitosis. In the absence of microtubules or in response to microinjection of anti-dynein or anti-dynactin antibodies, the recruitment of pericentrin and γ-tubulin is inhibited, thus preventing the assembly of this lattice (Young et al., 2000). This suggests that dynein is required to mediate the transport of pericentrin and γ-tubulin along microtubules and facilitate their anchorage at the centrosome. Cells depleted of pericentrin and γ-tubulin exhibit a reduced microtubule nucleating ability. Together, these data suggest that the assembly of the pericentrin-γ-tubulin lattice represents a second mechanism for the anchorage and organisation of microtubule nucleation sites at the centrosome in mammalian cells (Dictenberg et al., 1998).

1.3.4 Microtubule anchoring and release

Microtubule nucleation and anchoring mechanisms are both thought to control the microtubule array and centrosome movements during division. Once microtubules are nucleated from the PCM, they are released or severed from their nucleating sites and are either released into the cytoplasm or become anchored at centrosomal or non-centrosomal sites such as apical domains in epithelial cells (Abal, 2002; Mogensen, 1999). It is likely that the microtubules are transported by dynein-dynactin motor protein complexes, to centrosomal sites where they become anchored. However, overexpression of dynactin causes the abnormal release of microtubules from the centrosome leading to unfocused microtubule arrays and defective spindle pole separation. This supports an additional role for dynactin in microtubule anchorage (Bornens, 2002; Vaisberg et al., 1993). The centrosomal site of microtubule anchorage is thought to be based at the distal appendages of the mother centriole.

One protein which has been implicated in microtubule nucleation is ninein. Ninein exists as two splice variants of 245 kDa and 249 kDa that largely consist of coiled-coil regions (Bouckson-Castaing et al., 1996; Hong et al., 2000). Ninein localises at the distal appendages of the mother centriole via its C-terminus and anchors γ-TuRCs via its N-terminus (Delgehyr et al., 2005). Ninein also localises to apical non-centrosomal sites in epithelial cells where microtubule minus ends are anchored following its release from the centrosome (Mogensen et al., 2000; Moss et al., 2007). This is thought to be necessary for the stabilisation of apico-based arrays in epithelial cells (Moss et al., 2007). Overexpression of mutants only encoding the C-terminal domain of ninein result in displacement of ninein and γ-TuRCs from the centrosome causing defective microtubule nucleation and anchoring, whereas, overexpression of mutants lacking the central coil-coil motif only disturbed ninein localisation at the centrosome and microtubule anchoring activities (Delgehyr et al., 2005). In addition microinjection of ninein antibodies results in disrupted centrosome integrity (Dammermann and Merdes, 2000). Therefore, ninein is thought to play a dual role as a microtubule minus-end capping protein facilitating the docking of the γ-TuRC at the centrosome during microtubule nucleation and as a microtubule anchoring protein (Mogensen et al., 2000). A protein similar to ninein has been discovered, named ninein-like protein (Nlp). Nlp may also play a role in microtubule anchoring. However, this protein shall be discussed in detail in a later section.

1.4 The centrosome

1.4.1 Centrosome structure

The centrosome is a non-membranous organelle of 1-2 μm^3 in volume. It consists of a pair of barrel-shaped centrioles, 0.5 μm in length and 0.2 μm in diameter, each formed from 9 sets of triplet microtubules. The two centrioles are arranged perpendicular to each other, surrounded by PCM (Figure 1.4). The PCM contains an array of structuralcoiled-coil proteins as well as many regulatory proteins held within a meshwork of fibres (Anderson et al., 2003; Doxsey, 2001). This matrix is thought to provide a framework for anchoring proteins involved in microtubule nucleation and cell cycle progression. The duplicated centrosomes form the two poles of the mitotic spindle in metaphase. They are thought to direct microtubule nucleation and organisation, hence determining spindle orientation and controlling cell polarity (Alberts *et al.*, 2008; Doxsey, 2001). The older centriole, known as the mother, and the younger centriole, called the daughter, are linked at their proximal ends by interconnecting fibres referred to as the intercentriolar linkage. Evidence for the linkage has arisen from isolated centrosome preparations in which the centrioles remain paired. Also electron dense material has been observed between the two centrioles (Paintrand *et al.*, 1992). In G_1 the mother centriole is located near the cell centre, whilst the daughter is found to oscillate around the mother centriole. These correlated movements suggest that the intercentriolar linkage is flexible (Piel *et al*., 2000). The centrioles are polar structures with a proximal and distal end. During centriole duplication new procentrioles emerge from the side wall at the proximal ends of centrioles. The mother centriole can be distinguished from the daughter centriole as it contains distal and subdistal appendages. The composition of these appendages is unknown, but they are considered to facilitate microtubule anchoring and attachment of centrioles to the plasma membrane during ciliogenesis (Marshall, 2001). Indeed, the mother centriole has the ability to act as a basal body and nucleate the microtubules found within primary cilia. This activity may be dependent on the presence of distal and subdistal appendages, as centrioles which lack appendages due to the deletion of ODF2 (an appendage marker), lose the ability to nucleate cilia (Ishikawa et al., 2005; Piel et al 2000). Each centrosome undergoes duplication and separation once during each mitotic cycle.

1.4.2 Centrosome duplication

1.4.2.1 *Centriole disengagement*

Centrosome duplication occurs once per cell cycle and involves a series of events shown in Figure 1.5. At anaphase the two centrioles at each pole disengage and lose their perpendicular arrangement in preparation for templated synthesis of procentrioles. Centriole disengagement (also called centriole disorientation) is mediated by the cysteine protease, separase, that also destroys centromeric cohesin, thus triggering sister chromatid segregation (Waizenegger et al., 2000). Experiments using *X. laevis* cell free extracts suggest that the ubiquitin ligase, APC/C, may degrade proteins such as securin which subsequently frees separase to trigger centriole disorientation (Freed et al., 1999; Tsou and Stearns, 2006).

Shugoshin 1 (Sgo1) is a protein implicated in protection of sister chromatid cohesion. Recently, a shorter splice variant of Sgo1, called sSgo1, has been identified which localises to the centrosomes of the mitotic spindle and protects cohesion at paired centrioles until early anaphase (Wang et al., 2006). The centrosomal localisation and function of sSgo1 is regulated by its phosphorylation by Plk1 (Wang et al., 2008). sSgo1 displacement from the centrosome possibly by dephosphorylation or cleavage by separase is thought to trigger centriole disengagement. This is supported by studies in which Sgo1 depletion by RNAi induces the formation of multiple centrosome structures in mitotic cells that result from separation of paired centrioles. Introduction of sSgo1 in Sgo1-depleted cells rescues premature centriole separation but not sister chromatid separation. So whereas Sgo1 is responsible for sister chromatid cohesion, sSgo1 appears to be required for centriole cohesion (Wang et al., 2008). Following centriole disengagement at the end of mitosis the two centrioles separate and acquire their own distinct cloud of PCM, although they appear to regain their close proximity prior to centriole duplication. Disengagement is thought to constitute a licensing step, required for a further round of centriole duplication (Tsou and Stearns 2006).

1.4.2.2 *Centriole duplication*

During S phase, each centriole duplicates by nucleating the growth of a new daughter pro-centriole from its side at a right-angle (Figure 1.5). Similar to DNA replication, centrosome duplication is semi-conservative. This has given rise to the templated model of pro-centriole formation which suggests that the new centriole is formed from an existing structure on the maternal centriole (Kochanski and Borisy, 1990). A second mechanism for centrosome

duplication is known as the '*de novo*' pathway. The *de novo* pathway occurs in the absence of a parental centriole. Instead, many centriolar structures are formed which, upon mitotic entry, each acquire the ability to nucleate and organise microtubules. This can lead to the assembly of multipolar spindles (La Terra et al., 2005; Tsou and Stearns, 2006). A control pathway must therefore exist to prevent *de novo* formation occurring in the presence of a functional centrosome.

Mutagenesis and genome-wide RNAi screens in *C. elegans* have identified a number of proteins that are essential for centriole duplication (Dammermann et al., 2004; Kirkham et al., 2003; Gonczy et al., 2000). These include the protein kinase, ZYG-1 (zygote defective 1), and the coiled-coil spindle assembly proteins, SAS-4, SAS-5, SAS-6 and SPD-2 (spindle defective 2). The *C. elegans* oocyte does not contain centrioles. However, during fertilisation, the sperm donates two centrioles which duplicate and the oocyte donates the proteins which form the PCM. RNAi depletion of maternal genes encoding ZYG-1, SAS-4, SAS-5 and SAS-6 prevents centriole duplication following fertilisation, leading to the formation of monopolar spindles following the second round of mitosis (Dammermann et al., 2004; Kirkham et al., 2003; Liedel and Gonczy, 2005). This indicates that these proteins are required for centriole formation to occur. In contrast, SPD-2 is essential for centrosome maturation. SPD-2 depleted embryos fail to acquire sufficient PCM during centrosome maturation. Therefore microtubule nucleation fails and mitotic spindles cannot form (Dammermann et al, 2004). However, in *C. elegans* centriole duplication was also prevented in SPD-2 depleted embryos (Leidel and Gonczy, 2003). A stepwise pathway has been proposed based on RNAi and electron tomography studies which state that SPD-2 and ZYG-1 are the first proteins to be recruited to centrioles. Their role is then to promote the recruitment of SAS-5 and SAS-6 which physically interact and appear co-dependent for their centriole localisation (Leidel et al., 2005). This initiates the development of daughter centrioles in S-phase by the formation of a central tube suggesting that SAS-5 and SAS-6 may act to maintain its structural integrity. SAS-5 and SAS-6 also facilitate the recruitment of SAS-4 to the centrioles which is required for the assembly and maintenance of microtubules onto the central tube (Kirkam et al., 2003; Leidel and Gonczy et al., 2003; Pelletier et al., 2006). SAS-4 has also been suggested to play a role in regulating centriole size as SAS-4 depletion results in stunted centrioles (Kirkham et al., 2003).

Following the identification of several proteins implicated in centriole duplication in *C. elegans*, a search was initiated to find homologues of these proteins in other eukaryotes. Indeed, the centriole duplication pathway identified in *C. elegans* may be conserved amongst eukaryotes. A human homologue of SAS-6 has been identified and named HsSAS-6. HsSAS-6 is essential for centriole duplication in somatic cells (Leidel et al., 2005). A homologue of SAS-4 has been found in *Drosophila*, *DSAS-4* and in humans, known as CPAP or CENPJ. Recent research suggests CPAP (centrosomal P4.1-associated protein)/CENPJ (centromere protein J) plays a direct role in centriole duplication (Kleylein-Sohn et al., 2007). ZYG-1 is functionally similar to Sak in *Drosophila* and Plk4 in humans (Dutcher, 2007; Kleylein-Sohn et al., 2007). Similar to ZYG-1, loss of Plk4 in human cells results in a step-wise reduction of centriole numbers (Habedanck et al., 2005). Furthermore overexpression of Plk4 induces centriole overduplication (Bettencourt-Dias et al., 2005; Kleylein-Sohn et al., 2007). As yet no orthologues of SAS-5 have been identified. Finally, a mammalian homologue of SPD-2 has been proposed as Cep192 which regulates the recruitment of the PCM and centrosome maturation (Zhu et al., 2008). Hence, a number of proteins involved in centriole duplication in *C. elegans* appear to be conserved in other organisms, although additional proteins have also been identified which are required for centriole duplication, as the process is likely to be more complex in higher organisms. Nevertheless, understanding the mechanisms underlying centrosome duplication that exist in *C. elegans* will help elucidate the mechanisms that exist in humans.

The mechanisms that regulate centrosome duplication ensuring that it only occurs once per cycle are poorly understood. Using cell fusion experiments, it was shown that a block to reduplication normally exists in cells, which is thought to be intrinsic to the centrosomes (Wong and Stearns, 2003). In somatic mammalian cells, Cdk2/cyclinA activity is necessary for centriole duplication to occur (Meraldi et al., 1999). In comparison, in *Xenopus* egg extracts, Cdk2/cyclin E is an essential factor for centrosome duplication. Centrosome duplication is blocked in the presence of Cdk2 inhibitors or by immunodepletion of Cdk2 or cyclin E which was restored by the addition of Cdk2/cyclin E (Hindcliffe et al., 1999; Matsumoto et al., 1999). Centrosome duplication also depends on the phosphorylation status of the tumour suppressor protein, retinoblastoma (Rb). Expression of an Rb mutant which lacked the Cdk phosphorylation sites inhibited centriole duplication (Meraldi et al., 1999). Rb inhibits the activity of the transcription factor, E2F, which otherwise promotes S-phase progression (Meraldi et al., 1999). Together, this evidence suggests that phosphorylation and inactivation of Rb and the subsequent activation of E2F is required for centrosome duplication in addition to Cdk2-cyclin A activity. A second tumour suppressor protein, p53, is also involved in centrosome duplication. p53 transcriptionally regulates p21, which inhibits Cdk2 activity. This is supported by the observation that reduced p21 activity results in increased Cdk2/Cyclin E activity, leading to reduplication and amplification of centrosomes (Mantel et al., 1999). In addition, gene knockout of p53 in somatic cells resulted in a significant number of cells with increased centrosome numbers (Fukasawa, 2008). The process of centriole duplication is complex and it is likely that many other proteins contribute to its regulation. Clearly, research will be required to fully understand the mechanisms which regulate centriole duplication through the cell cycle.

1.4.2.3 *Centrosome maturation, disjunction and separation*

During G_2/M phase, the new daughter centrioles elongate until full length is achieved in mitosis. The PCM also undergoes structural reorganisation in a process known as centrosome maturation. This involves the recruitment of additional proteins such as γ-tubulin to enhance microtubule nucleating ability and initiate the separation of the duplicated centrosomes (Blagden and Glover, 2003; Khodjakov and Rieder, 1999). In early prophase, the close association between the two parental centrioles breaks down, allowing the two centriole pairs to separate in a process known as centrosome disjunction (Figure 1.5) (Nigg, 2002).

One model for centrosome cohesion has been proposed which suggests that the close proximity between parental centrioles is a direct result of cytoskeletal forces, and that alterations to the cytoskeleton may have a direct effect upon centrosome cohesion (Thompson et al., 2004). However, the second model for centrosome cohesion postulates the existence of linker proteins which connect parental centrioles. Evidence supporting the existence of this linkage includes electron microscopy images of fibers between centrioles that are still present in the absence of microtubules (Paintrand et al., 1992). In addition, centrosomes are seen as paired dots even after isolation from cultured cells, while in live cells the mother and daughter centrioles make correlated movements that suggest they are held together by a physical tether (Bornens, 2002; Piel et al., 2000). The linker structure is thought to be composed of the coiled-coil proteins, C-Nap1 and rootletin (discussed in more detail in later sections). C-Nap1 and rootletin dissociate from the centrosome when activity of the Nek2 kinase exceeds that of its inhibitor, PP1, thus mediating centrosome disjunction at the G_2/M transition (O'Regan et al., 2007). Recent research suggests that the protein Cep68 also contributes to the linker structure (Bahe et al., 2002). Depletion of C-Nap1, rootletin or Cep68 by siRNA induces substantial centrosome splitting. Electron microscopy showed that Cep68 colocalises with rootletin fibers emanating from the proximal ends of centrioles and, like C-Nap1 and rootletin, dissociates from the centrosome at the onset of mitosis. Furthermore Cep68 and rootletin depend on C-Nap1 for their localisation at the centriole. This supports previous findings that C-Nap1 does not form the central region of the linker structure, but is present at the proximal ends of centrioles and acts as a docking site for the adjoining rootletin fibers. Together this evidence strongly suggests that centrosome cohesion is mediated by a direct mechanism involving these proteins. These two models are not mutually exclusive and it is likely that centrosome cohesion is regulated by both cytoskeletal interactions and the presence of an intercentriolar linker between the parental centrioles. Indeed, it is possible that the cytoskeleton may contribute to transport of structural or regulatory components important for the linker to the centrosome (Meraldi and Nigg, 2001).

At the onset of mitosis, the centrosomes separate and move to either end of the cell forming the two spindle poles. This movement is dependent upon the activity of motor proteins such as the kinesin, Eg5. Microinjection of anti-Eg5 antibodies blocks centrosome separation resulting in mitotic arrest and monopolar spindle formation (Blangy et al., 1995). In turn the localisation of Eg5 to the centrosome is dependent upon its phosphorylation status, which is regulated by Cdk1 (Sawin and Mitchison, 1995).

1.4.3 Centrosome Functions

The main function of the centrosome is to act as a microtubule organising centre (MTOC), mediating events such as microtubule nucleation, release and anchoring (Anderson, 1999). Perhaps most critically, the centrosome organises the spindle poles in order to regulate mitotic spindle assembly and positioning, thus defining the plane of cytokinesis and ensuring equal segregation of chromosomes into two daughter cells (Nigg, 2004). The role of the centrosomes in spindle assembly is crucial and mistakes may contribute to the formation of human cancers and conditions such as microcephaly, which is associated with small brain size at birth (Woods et al., 2005). One such centrosome abnormality is the presence of more than two centrosomes per cell which can result in multipolar spindles and inaccurate chromosome segregation, which may cause aneuploidy (Nigg, 2002).

Interestingly, there is accumulating evidence from various organisms that centrosomes are not essential for mitotic spindle assembly. Firstly, cells which have had their centrosomes removed by laser ablation can still form bipolar spindles (Hinchcliffe et al., 2001). Secondly, in *Xenopus* egg extracts mitotic spindle assembly can occur in the presence or absence of centrosomes. In the absence of centrosomes microtubules form an antiparallel array focused around chromatin which is driven by microtubule-associated motor proteins (Heald et al., 1997). Thirdly, in *Drosophila*, DSas-4, a relative of Sas-4 in *C. elegans,* is an essential regulator of centrosome duplication. DSas-4 mutant flies fail to develop centrosomes by the third larval stage but intriguingly a mitotic spindle still assembles. However, these flies lack cilia and flagella and die soon after birth (Basto et al., 2006). Finally, mouse oocytes also lack functional centrosomes. Hence, microtubule polymerisation occurs at multiple MTOCs which are recruited to the chromosomes which appear to be the main organiser of spindle assembly (Brunet and Maro, 2005). Together, these studies suggest that centrosomes are not essential for spindle assembly. However, centrosomes are considered essential for the correct positioning of the mitotic spindle, which is vital in cells that undergo asymmetric divisions. Astral microtubules associated with the centrosome control spindle positioning by directly contacting the cell cortex and anchoring themselves at appropriate positions to orientate the mitotic spindle in mammalian cells (Basto et al., 2006). Misorientation of the spindle may put chromosomes in the path of a cleaving cell leading to chromosome loss and aneuploidy or to the missegregation of critical developmental determinants (Cowan and Hyman, 2004; Higginbotham and Gleeson, 2007).

The centrosome has also been suggested to play a role in cytokinesis or mediate a checkpoint that monitors cytokinesis, as cells lacking centrosomes display cytokinesis defects (Khodjakov and Reider, 2001). At telophase, a hypothetical cytokinesis checkpoint is turned on. The maternal centriole has been shown to move to the midbody between dividing cells. As the actomyosin bridge constricts, microtubules depolymerise and the centriole appears to move back to the centrosome prior to checkpoint inactivation and finally, cell cleavage (Piel et al., 2000). However, the significance of these observations remains to be confirmed. Further evidence which supports a role of centrosomes in cytokinesis is the characterisation of a novel protein at the maternal centriole known as centriolin, which is required for the later stages of cytokinesis (Gromley et al., 2003). A role of the centrosome in regulating the G_1/S transition, thus activating DNA replication, has also been implicated. Cells which lack centrosomes generally fail to complete cytokinesis, but those cells that do divide show a G_1 arrest preventing DNA replication (Hinchcliffe et al., 2001; Khodjakov and Reider, 2001). It is unclear how centrosomal defects induce a G_1 arrest. It is possible that centrosomes may be required to activate DNA replication (Hinchcliffe et al., 2001). Alternatively, centrosomes may mediate the G_1-S transition indirectly by controlling a checkpoint that monitors centrosome number and DNA content (Mikule et al., 2007).

In addition to their role as MTOCs, centrosomes also form the basal bodies that nucleate the growth of cilia and flagella (Eley et al., 2005). Cilia and flagella are cellular projections that mediate movement of the cell and substances surrounding the cell or act as sensory organelles (Bettencourt-Dias and Glover, 2007). In recent years many human diseases characterised by defective cilia, so-called ciliopathies, have been found to be caused by mutations in the genes that encode centrosomal or basal body components (Adams et al., 2008; Badano et al., 2006; Fleigauf et al., 2007). The basal body organises the assembly of the axoneme, a microtubule based structure that determines the rigidity and motility of cilia.

1.4.4 Centrosomes and cancer

A cancerous growth or tumour consists of cells which have evaded the normal cell cycle controls and limits. Cancer usually arises from an accumulation of defective processes including the activation of oncogenes, loss of tumour suppressor function and deregulation of the cell cycle and in some cases deregulation of the centrosome cycle (Brinkley and Goepfert, 1998). The changes in centriole arrangement and the movement of centrosomes in mitosis are thought to determine the organisation of mitotic spindle microtubules which in turn determines the accuracy of chromosome segregation (Doxsey, 2001). Misalignment of chromosomes on the metaphase plate can lead to chromosome missegregation, characteristic of many tumours (Nigg, 2002). Cancer cells from a wide array of tumours exhibit multipolar spindles, which are often associated with supernumerary centrosomes, and these can lead to aneuploidy (Saunders et al., 2005). In comparison, monopolar spindles lead to a complete failure of chromosome segregation and subsequent tetraploidisation (Brinkley, 2001). Centrosome aberrations may arise as a result of loss of coordination between the centrosome duplication cycle and cell division cycle or a failure in cell division. This may result in centrosome duplication failure or centrosome overduplication within a single cell cycle, aborted cell division or cell fusion (Brinkley, 2001; Nigg, 2002; Pihan and Doxsey, 1999). Aborted cell division is thought to be the primary cause of excessive centrosome numbers (Nigg, 2002).

There is a strong correlation between aberrant centrosome numbers and aneuploidy. Abnormal centrosome numbers have been observed in many cancer types, including bladder, breast, colon and prostate tumours, and are therefore considered to be a key event in tumour progression (Saavedra et al., 2003; Schneeweiss et al., 2003; Yamamoto et al., 2004). Mouse tumour models suggest centrosomal abnormalities occur at the pre-invasive stage of tumourigenesis (Brinkley and Goepfert, 1998). However, other researchers found that aberrant centrosomes were only seen when accompanied by chromosomal abnormalities suggesting centrosomal abnormalities occur during late tumour progression (Saunders et al., 2005).

In addition to aberrant centrosome numbers, there are other centrosome abnormalities such as increased size, excess PCM and inappropriate phosphorylation of centrosomal proteins (Salisbury et al., 2002). However, abnormal centrosomes are most certainly associated with tumour progression, hence there has been a huge interest in the identification of mutations and abnormal expression patterns of centrosomal proteins in cancer cells (Nigg, 2001). Some of these centrosomal proteins which have been investigated include the mitotic protein kinases Cdk1, Plk1, Aurora-A and Nek2 (Nigg, 2001). However, which proteins are likely to be involved in the deregulation of the centrosome cycle in cancer cells are yet to be determined.

1.5 Cell cycle regulation of the centrosome

During the cell cycle, the centrosome undergoes a number of structural and functional changes as described above, which are controlled in large part by cell cycle-dependent protein phosphorylation. This is regulated by the activity of protein kinases and phosphatases (Fry and Faragher, 2001) (Figure 1.6). The important kinases involved in centrosome regulation include members of the Cdk, Polo-like kinase (Plk), Aurora kinase and NIMA-related kinase families (Figure 1.6) and some of the roles of these kinases in centrosome regulation are discussed below (Nigg, 2001; Mayor *et al.*, 1999).

1.5.1 Cyclin-dependent kinases (Cdks)

Cyclin-dependent kinases (Cdks) contain a catalytic subunit which is activated in the presence of a cyclin regulatory subunit. Mammalian cells have several Cdks which regulate different stages of the cell cycle. Cdk1 is required for cells to enter mitosis, Cdk2 regulates S-phase progression and Cdk4/6 regulates passage through the G_1 restriction point (Alberts et al., 2008). In terms of the centrosome cycle, Cdks regulate centrosome duplication and maturation, microtubule nucleation and dynamics and they are responsible for the recruitment of proteins to the centrosome (Mayor *et al.*, 1999; Fry and Faragher, 2001). As discussed above, a study in S-phase arrested *Xenopus* egg extracts found that Cdk2 drives several rounds of centrosome duplication (Hinchcliffe et al., 1999). Meanwhile, injection of the Cdk inhibitors (CKIs), p21 or p27, blocks centrosome duplication in *Xenopus* embryos (Lacey et al., 1999). Cdk2 activity is also required for the separation of paired centrioles in *Xenopus*

extracts as depletion of Cdk2 or its activating partners cyclin A and E prevents centriole separation (Lacey et al., 1999). Similar results have been obtained in somatic cells (Matsumoto et al., 1999; Meraldi et al., 1999). As a positive regulator of centrosome duplication, Cdk2-cyclin E has been shown to phosphorylate a number of key proteins at unduplicated centrosomes such as breast cancer suppressor 1 (BRCA1), p53 and Nucleophosmin (NPM)/B23. All of these may be important negative regulators of centrosome duplication. Phosphorylation of BRCA1, p53 and NPM/B23 by Cdk2-cyclin E stimulates their dissociation from the centrosome, which in turn promotes centrosome duplication (Deng, 2002; Fukasawa, 2007; Okuda et al., 2000).

It has been shown that Cdk1 is required for centrosome maturation. There is evidence from different organisms that NIMA-related kinases or Plks may be involved in targeting Cdk1 to centrosomes (Wu et al., 1998; Jackman et al., 2003). Activated Cdk1-cyclin complexes promote the centrosomal recruitment of the plus-end-directed kinesin motor protein Eg5 amongst many other centrosomal proteins. Following phosphorylation by Cdk1, Eg5 then stimulates centrosome separation allowing spindle assembly (Blangy et al., 1995; Sawin and Mitchison, 1995). This suggests that Cdk1 may be involved in centrosome separation. Cdk1 has been implicated in the regulation of microtubule dynamics during mitosis through phosphorylating a number of microtubule associated proteins including β-tubulin and XMAP215, a protein which stabilises microtubule plus ends (Fourest-Lieuvin et al., 2006; Vasquez et al., 1999). Furthermore, the addition of Cdk1/cyclin B stimulates increased microtubule nucleation from centrosomes in interphase *Xenopus* egg extracts (Ohta et al., 1993).

1.5.2 Polo-like kinases (Plks)

Plks are a family of serine/threonine, cell-cycle regulated kinases that are highly conserved from yeast to humans. Polo kinase was first identified in *Drosophila* where it was shown to have multiple roles throughout mitosis (Glover, 1995; Tavares et al., 1996). In *Drosophila* Polo is responsible for recruiting CP190 and the microtubule-associated protein, Asp, which in turn recruits γ-TuRC and organises microtubule asters (Donaldson et al., 2000). Polo and Asp have been shown to immunoprecipitate together and exist as a complex, independent of microtubules. Asp is phosphorylated by Polo *in vitro* which transforms it into an MPM2 epitope (Avides et al., 2001). Overexpression of mutant *asp* or microinjection of anti-Asp antibodies or immunodepletion of Asp in *Drosophila* results in bipolar spindles with broad unfocused spindle poles and an abnormal distribution of γ-tubulin causing mitotic and meiotic defects, which could be reversed by the addition of phosphorylated Asp (Avides et al., 2001; Avides and Glover, 1999). Furthermore, embryonic extracts depleted of Polo are unable to rescue the nucleating ability of centrosomes stripped with salt, but the addition of phosphorylated Asp or active Polo restores this activity (Avides et al., 2001). Therefore, it is proposed that phosphorylation of Asp by Polo stimulates microtubule nucleation from centrosomes and stimulates the ability of Asp to organise these microtubules into asters thus mediating mitotic spindle formation (Avides et al., 2001). Recently, a novel centrosome component Kizuna (Kiz) has been identified as another Plk1 substrate which maintains spindle pole integrity. Ablation of Kiz in cultured HeLa cells induces spindle pole fragmentation resulting in multiple γ-tubulin containing foci. This has led to the proposal that in the absence of Kiz, the PCM breaks down in response to increased tension exerted by microtubule-kinetochore interactions (Fry and Baxter, 2006; Oshimori et al., 2006).

Following the identification of Polo in *Drosophila*, *Xenopus laevis* was found to express 3 Plks known as Plx1, Plx2 and Plx3 (Cheng et al., 2003). Meanwhile, the mammalian Plk family consists of Plk1, Plk2 (Snk), Plk3 (Prk/Fnk) and Plk4 (Sak). Plks consist of an N-terminal catalytic domain and a regulatory C-terminal domain (CTD) which contains a conserved sequence motif, the polo-box domain (PBD). The PBD contains two polo boxes linked by a polo-box cap (Barr et al., 2004). Overexpression of the PBD alone induces mitotic defects such as spindle abnormalities and micronucleated cells (Seong et al., 2002). A crystallisation study identified the PBD as a phospho Ser/Thr binding motif. Phosphopeptides, e.g. from the Cdc25 protein, were shown to bind a positively charged cleft between the two polo boxes. Plk kinase activity is activated in response to phosphopeptide binding. This is thought to target Plk1 towards specific substrates. Plk can therefore be primed for phosphorylation at specifc points of the cell cycle. Mutation of residues within the PBD results in loss of centrosome localisation (Elia et al., 2003). Hence, the PBD is thought to regulate both the subcellular localisation and interaction of the kinase with its substrates. Moreover, the Plk CTD may exert an autoinhibitory effect via the interaction of the PBD with the catalytic domain. This autoinhibition can be relieved by the binding of a phosphopeptide to the PBD and the phosphorylation of Thr-210 which activates Plk1 (Barr et al., 2004; Cheng et al., 2003; Jang et al., 2002).

Plk2 and Plk4 are proposed to play roles in centrosome duplication. Plk2 exhibits maximal activity at the G_1/S-transition. Overexpression of inactive Plk2 in S-phase arrested cells or reduction of Plk2 by RNAi results in failure of centrosome duplication (Warnke et al. 2004). At present, Plk2 is classed as a centrosomal protein and its activity is required for centrosome duplication at the G_1-S transition. However, further research is required to determine how Plk2 regulates centrosome duplication. In comparison, more is known about Plk4 which exhibits highest kinase activity in late S-G_2 transition. Experiments involving loss-of-function and gain-of-function mutations provide evidence that Plk4 is also a key regulator of centrosome duplication. Overexpression of Plk4 promotes the formation of multiple procentrioles per maternal template which disengage from the pre-existing centriole following mitosis, resulting in centrosome amplification (Kleylein-Sohn et al., 2007). In contrast depletion of Plk4 by RNAi leads to monopolar spindle formation and incorrect centriole numbers (Habedanck et al., 2005). Plk4 is therefore considered essential for centrosome duplication in mammalian cells.

The most studied Polo-like kinase in humans, Plk1, is thought to be required for centrosome maturation and establishment of the mitotic spindle (Figure 1.6). Plk1 activity peaks at the G_2/M transition and Plk1 protein associates with the mitotic spindle poles until metaphase, after which it is redistributed to the midzone of the spindle (Golsteyn et al., 1995). Microinjection of anti-Plk1 antibodies results in immature centrosomes that fail to recruit γ-tubulin and MPM-2 phosphoepitopes leading to improper spindle formation (Lane and Nigg, 1996). Further support for a role for Plk1 in centrosome maturation has arisen from the identification of Cdc25c as a substrate of Plk1 (van de Weerdt et al., 2008). It has been demonstrated that Plk1 activates the Cdk1-cyclin B complex required for mitotic entry by phosphorylating the phosphatase Cdc25c. This data implies that Plk1 plays a role in centrosome maturation and mitotic entry at the G_2/M transition (Lane and Nigg, 1996; Mayor et al., 1999). However, cells depleted of Plk1 are still able to enter mitosis suggesting that Plk1 is not essential for M-phase entry. Nevertheless, these cells arrested in prometaphase due to unstable microtubule-kinetochore interactions, suggesting that Plk1 is essential for proper spindle formation (Sumara et al., 2004).

Increased Plk1 expression has been found in a variety of cancers, including those derived from breast, prostate and bladder. Furthermore, Plk1 overexpression is linked to many higher grade tumours and associated with poor prognosis (de Carcer et al., 2007). These observations highlight Plk1 as an attractive target in the design of anti-cancer agents. Therefore, a number of small molecule inhibitors against Plk1 are currently being developed which significantly reduce the viability of cancer derived cell lines (Gumireddy et al., 2005).

These include BI2536 and TAL which have proved successful as potent inhibitors of Plk1 function *in vitro* (Taylor and Peters, 2008). However, all Plk1 drugs developed to date also inhibit Plk2 and Plk3 to varying extents (Taylor and Peters, 2008). Future research will hopefully lead to the development of a Plk1 specific inhibitor which could be a potential anti-cancer drug.

1.5.3 Aurora kinases

Aurora kinase was first identified in *S. cerevisiae* as Ipl1p, while two Aurora kinases were found in *Drosophila* named aurora and IAL. Three mammalian Aurora kinases have now been identified and named Aurora-A, -B and -C (Nigg, 2001). Aurora kinases consist of an N-terminal catalytic domain and a C-terminal regulatory domain which varies greatly in length and sequence. Aurora-A activity is low in G_1/S, increases in G_2 and peaks at mitotic onset, whereas Aurora-B activity peaks later in mitosis (Andrews et al., 2003). Aurora-A localises to the centrosomes and mitotic spindle from S-phase until telophase, whereas Aurora-B localises to the midzone in anaphase and translocates to the bridge between two dividing cells during cytokinesis. Aurora-C is predominantly expressed in the testis but little is known about its function (Fry et al., 2000; Nigg, 2001).

Aurora-A is activated by phosphorylation and by the binding of multifunctional protein, TPX2 which resides in the hinge region between the C- and N-terminal lobes of the catalytic domain of Aurora-A. This alters the conformation of the catalytic domain so that the activation loop and the residues forming the ATP binding site are positioned in such a way that substrate binding is facilitated (Bayliss et al., 2003). In the absence of TPX2, the phosphorylated activation loop adopts a more flexible and looser conformation that blocks the substrate binding site and exposes the crucial threonine 288, which is then susceptible to dephosphorylation (Bayliss et al., 2003). In early mitosis Aurora-A is necessary for centrosome maturation and separation, which in turn are necessary for mitotic spindle assembly (Figure 1.6). Aurora-A depletion in *C. elegans* and *Drosophila* results in failure of γ-tubulin accumulation at the centrosome leading to loss of centrosomal microtubules (Hannak et al., 2001; Berdnik and Knoblich, 2002). Overexpression of active Aurora-A or kinase-dead Aurora-A in any cell line results in polyploidy and centrosome amplification (Dutertre et al., 2002; Meraldi et al., 2002). In the presence of protein Bora, Aurora-A activates Plk1 leading to Cdk1 activation, thus Aurora-A and Bora cooperatively regulate mitotic entry. Bora interacts with Plk1 to promote the accessibility of the Plk activation loop for phosphorylation by Aurora-A (Seki et al., 2008). Plk1 is thought to be responsible for recruiting Aurora-A to the centrosome where it activates a number of downstream targets which promote centrosome maturation (Chan et al., 2008; Seki et al, 2008). These downstream targets include the serine/threonine kinase LATS2 and NDEL1 which are phosphorylated by Aurora-A and targeted to the centrosome in G_2/M (Barr and Gergely, 2007; Mori et al., 2007). Centrosome maturation fails in response to LATS2 siRNA knock down supporting a role for LATS2 in centrosome maturation (Toji et al., 2004). Another group found that overexpression of a constitutively phosphorylated mutant of NDEL1 restored centrosome maturation and separation in Aurora-A depleted cells (Mori et al., 2007). This suggests that NDEL1 is involved in centrosome maturation and is likely to be involved in other Aurora-A activated processes. Indeed NDEL1 strongly interacts with TACC3, another Aurora-A target. Recent evidence suggests that NDEL1 is required for TACC3 recruitment to the centrosome in addition to phosphorylation on Ser 558 by Aurora-A. TACC3 then promotes the stabilisation and polymerisation of microtubules in mitosis (Kinoshita et al., 2005; Mori et al., 2007). Despite this evidence for a role for Aurora-A in centrosome maturation, Aurora-A does not localise to centrosomes until duplication is complete. It is possible that Aurora-A activates an inhibitor of duplication to prevent reduplication and that deregulation of Aurora-A activity leads to centrosome amplification, but further evidence is required to support this hypothesis (Dutertre et al., 2002; Meraldi et al., 2002).

Mutation of the *aurora* gene in *Drosophila* or expression of a dominant negative mutant of Aurora-related kinase, Eg2, in *Xenopus* or siRNA mediated depletion of Aurora-A in human cells all prevented centrosome separation leading to monopolar spindle formation (Glover et al., 1995; Roghi et al., 1998; Marumoto et al., 2003). It is possible that the role of Aurora-A in centrosome separation could be linked to its role in centrosome maturation. It is not understood how Aurora-A regulates centrosome separation. One possibility is in part by phosphorylating the BimC-like kinesin protein, Eg5 (Giet et al., 1999). Eg5 induces movement of microtubules and tethers microtubule plus ends. Therefore Eg5 may generate a force capable of pushing overlapping microtubules apart, thus mediating centrosome separation. However, there is no evidence that Eg5 activity depends on phosphorylation by Aurora-A (Barr and Gergely, 2007; Dutertre et al., 2002). Depletion of Aurora-A generates relatively few and short astral microtubules implying that interactions between spindle poles and the cell cortex may also contribute to centrosome separation (Barr and Gergely, 2007).

Aurora-A has been found to be overexpressed in many cancer cell lines and primary tumours and possesses transforming potential (Dutertre et al., 2002). Therefore, Aurora-A is an attractive target for the development of anti-cancer therapies. A number of small molecule inhibitors of Aurora kinases have been developed which proved successful in clinical trials (Matthews et al., 2006). ZM447439 (AstraZeneca) and Hesperadin (Boehringer Ingelheim) are two drugs which have proved useful as specific inhibitors of Aurora function, inducing growth arrest or apoptosis of cancer derived cell lines (Ditchfield et al., 2005). Millenium pharmaceuticals have recently developed a potential Aurora-A inhibitor, MLN-8054 (Taylor and Peters, 2008). Although effective *in vitro*, a significantly higher concentration of the drug is required to inhibit Aurora-A function *in vivo*, which may result in low level inhibition of Aurora-B. More characterisation of the drug is required and further research should help confirm whether this is an effective Aurora-A inhibitor (Taylor and Peters, 2008). The development of Aurora kinase inhibitors will help to elucidate the functions of Aurora kinases *in vivo* and may potentially generate an anti-cancer drug.

1.6 NIMA-related kinases

NIMA-related kinases, or Neks, are serine/threonine protein kinases which share homology with the NIMA (Never In Mitosis A) kinase of the filamentous fungus, *Aspergillus nidulans* (Lu et al., 1993) (Figure 1.7). NIMA is a 79 kDa protein which shows cell cycle regulated activity peaking at the G_2/M transition (Krien et al., 1998; Osmani et al., 1991b). In general, NIMA-related kinases consist of a highly basic non-catalytic C-terminal domain and an N-terminal catalytic domain containing all the motifs characteristic of serine/threonine protein kinases (Hanks and Hunter, 1995). The length and sequence of the C-terminal domains varies greatly between the NIMA-related kinases, which suggests that they may have different functions and may be regulated in a different manner (Fry and Nigg, 1997). NIMA localises to spindle pole bodies during mitosis where it plays a role in microtubule organisation and mitotic spindle formation, although the mechanism remains obscure (O’Regan et al., 2007). The use of synthetic peptides led to the identification of a putative consensus site for phosphorylation by NIMA. This site was FRxS/T with the phenyalanine at position -3 being particularly important (Lu et al., 1994). NIMA itself is phosphorylated at multiple serine/threonine residues and can undergo autophosphorylation, while the activity and stability of NIMA is tightly regulated by changes in its phosphorylation state (Lu et al. 1993). NIMA contains several putative Cdk1 phosphorylation sites raising the possibility that it is

activated by Cdk1. The presence of active NIMA is essential for cells to progress from G_2 into mitosis, while overexpression of NIMA drives cells into mitosis irrespective of their cell cycle stage. This is characterised by premature chromatin condensation and spindle assembly (O’Connell et al., 1994; Osmani et al., 1987). Interestingly, temperature-sensitive mutations in the *nimA* gene induce a G_2 arrest even in the presence of active Cdk1, highlighting the essential nature of NIMA for mitotic entry in *Aspergillus* (O’Connell et al., 2003; Osmani et al, 1988).

Other eukaryotes also express NIMA-related kinases (Figure 1.7). Yeasts express a single NIMA-related kinase, this being Kin3 in the budding yeast, *Saccharomyces cerevisiae,* and Fin1 in the fission yeast, *Schizosaccharomyces pombe*. Kin3 is present during mitosis but overexpression and mutation studies have revealed no obvious defects and hence it does not appear to be essential for cell cycle progression (Barton et al., 1992; Jones and Rosamond, 1990). More is known about the function of Fin1. Fin1 localises to spindle pole bodies (SPBs; the functional equivalent of centrosomes) during the metaphase-anaphase transition suggesting that Fin1 may play a role in spindle function (Krien et al., 2002). Moreover, the introduction of two temperature-sensitive, loss-of-function mutations in the *Fin1* gene resulted in failure of microtubule nucleation from spindle poles and failure of mitotic spindle formation (Grallert and Hagan, 2002). Overexpression of Fin1 induces spindle abnormalities and premature chromatin condensation. However, a role in chromosome condensation is unlikely as the kinase activity of Fin1 peaks at the metaphase-anaphase transition after chromosome condensation has occurred. Recent research has shown that Fin1 only binds to mature SPBs which are at least two cycles old (Grallert et al., 2008). Fin1 binds the older SPB in association with septum initiation network (SIN) inhibitors once the SIN which controls mitotic exit is active. Loss of Fin1 activity results in SIN activation on both SPBs in anaphase B and promotes premature septation which divides the cell into two daughter cells. This research suggests that Fin1 contributes to the inhibition of SIN activity on the old SPB until the cell is ready to divide (Grallert et al., 2004).

The most closely-related NIMA homologue is the NIM1 protein of *Neurospora crassa.* NIM1 is 75% identical in sequence to NIMA in the catalytic domain and is the only NIMA-related kinase to be capable of complementing an *Aspergillus nimA* mutant (Pu et al., 1995). These studies in lower eukaryotes suggest that NIMA-related kinases play roles within mitosis and possibly at centrosomes/SPBs. Furthermore, overexpression of NIMA in a number of higher eukaryotes results in premature mitotic entry, and overexpression of an inactive NIMA mutant in human cells induces a G_2 arrest (Lu and Hunter, 1995). The observation that proteins involved in cell cycle control are highly conserved from yeast to humans prompted the search for a mammalian homologue of NIMA. This resulted in the identification of Nek1 in mice, closely followed by Nek2 in humans (Letwin et al., 1992; Schultz et al., 1994). In fact, higher eukaryotes were found to express multiple Nek kinases compared to the single NIMA-related kinase found in fungi. The human genome encodes eleven NIMA-related kinases which have been named Nek1 to Nek11. These are illustrated in Figure 1.7 and described in more detail below.

1.6.1 Mitotic Neks: Nek6, Nek7 and Nek9

Nek6, Nek7 and Nek9 appear to act in concert to regulate mitotic events in vertebrate cells. Nek9, also called Nercc1, shares 40-50% identity with other Nek proteins in the N-terminal kinase domain. It has a long C-terminal domain that contains an RCC1-like domain and a coiled-coil motif (O'Connell et al., 2003). Deletion of the RCC1 domain creates a hyperactive kinase implying that this region may mediate an autoinhibitory mechanism (Roig et al., 2002). Nek9 is also capable of autophosphorylation and activation of Nek9 seems to depend on phosphorylation of T-210 within the activation loop. Meanwhile, the C-terminal domain of Nek9 contains numerous sites for phosphorylation by Cdk1/cyclin B, but it has not yet been shown whether this has any physiological relevance. A phosphospecific antibody generated against the T-210 site showed that active Nek9 localises to spindle poles during mitosis (Roig et al., 2005; Belham et al., 2003). *Xenopus* Nek9 was also observed at spindle poles (Roig et al., 2005). Interference with Nek9 function by antibody microinjection caused spindle abnormalities and prometaphase arrest or chromosome missegregation, whilst depletion of Nek9 from *Xenopus* egg extracts strongly impaired spindle assembly *in vitro* (Belham et al., 2003). Taken together, these studies support a direct role for Nek9 in the regulation of mitotic spindle organisation and chromosome segregation (O'Regan et al, 2007; Roig et al., 2002).

Nek9 is proposed to act upstream of Nek6 and Nek7. The C-terminal domain of Nek9 interacts with Nek6 and Nek7 at a site between the RCC1-like domain and the coiled-coil motif (Roig et al., 2002). Nek9 subsequently phosphorylates Nek6 at Ser-206 and Nek7 at S-195 within their activation loops, thus increasing their activity at mitotic onset (Belham et al., 2003). The protein sequences of Nek6 (314 residues) and Nek7 (303 residues) are 87% identical and only differ in a small region at their extreme N-termini. Nek6 and Nek7 are the smallest of the mammalian NIMA-related kinases consisting of only a catalytic domain

(O'Connell et al., 2003). The abundance and activity of Nek6 is upregulated in mitosis, whereas Nek7 protein levels are relatively constant throughout the cell cycle (Belham et al., 2003; Kim et al., 2007). Nek7 localises to the centrosome at mitotic onset, unlike Nek6 which is found diffusely distributed in the cytoplasm (Kim et al., 2007). Nek6 and Nek7 exhibit similar expression patterns in various tissues but, upon serum starvation, Nek7 activity is enhanced, whereas Nek6 activity is inhibited (Minoguchi et al., 2003). However, overexpression of kinase-inactive Nek6 or Nek7, or knock-down of either kinase by siRNA-mediated depletion produces similar phenotypes including metaphase arrest. Furthermore, spindle defects and nuclear abnormalities are observed in these cells accompanied by increased apoptosis (Yissachar et al., 2006; Yin et al., 2003). These studies suggest that Nek6 and Nek7 kinases are involved in mitotic spindle organisation at the metaphase-anaphase transition, but their exact function and whether they have distinct roles remains a mystery. In summary, a mitotic Nek cascade model has been proposed in which Nek9 is activated at mitosis onset which leads to Nek6 and Nek7 activation downstream of Nek9. Nek6 and Nek7 then mediate formation of the mitotic spindle by a mechanism that remains to be elucidated.

1.6.2 Ciliary Neks: Nek1 and Nek8

Surprisingly, Nek1 was identified by screening a mouse cDNA expression library with anti-phosphotyrosine antibodies. However, the N-terminal catalytic domain of Nek1 is 42% identical to NIMA and contains all the sequence motifs typical of serine/threonine kinases (Letwin et al., 1992). Nevertheless, though Nek1 mainly phosphorylates serine and threonine residues, Nek1 is capable of phosphorylating tyrosine residues at least *in vitro* (Hanks and Hunter, 1995). Nek1 may play a specific role in meiosis since Nek1 is highly expressed in the male and female germ lines (Letwin et al., 1992). However, two spontaneous mutations found in the mouse Nek1 gene, known as Kat and Kat2J, lead to a complicated array of defects including male sterility, polycystic kidney disease (PKD) and facial dysmorphism. These phenotypes are typical of ciliopathies, diseases that arise due to defective cilia or flagella (Adams et al., 2008; Badano et al., 2006). Indeed, recent evidence has emerged supporting a role for Nek1 in cilium organisation. Microtubules within the ciliary axomere are nucleated from basal bodies and Nek1 was found to localise to the basal body region. Furthermore, Nek1 overexpression inhibited ciliogenesis without affecting centrosome integrity in kidney epithelial cells. In addition, Kat2J expressing mouse embryonic fibroblasts exhibit a reduced number of primary cilia (Shalom et al., 2008; White and Quarmby, 2008), while a ciliary targeting motif has been identified within the C-terminal coiled-coil region of Nek1 (White and Quarmby, 2008). Therefore, it is postulated that Nek1 may link cell cycle progression with primary cilium formation (Shalom et al., 2008). However, Nek1 has also been implicated in the activation of DNA damage pathways as Nek1 kinase is upregulated in response to ionising radiation and cells expressing kinase-inactive Nek1 fail to repair damaged DNA (Polci et al., 2004). A yeast two-hybrid screen using the C-terminal regulatory domain of human Nek1 as bait identified a number of proteins which interacted with the central coiled-coil region of Nek1. These proteins included KIF3A and tuberin, which are implicated in cilia formation, as well as ATRX (RAD54 homologue), 53BP1 and the PP2A subunit, B56, which are proteins involved in double strand DNA break repair at the G_2/M transition (Surpili et al., 2003). Hence, it is possible that Nek1 plays a role in DNA damage/repair pathways in addition to ciliogenesis.

Murine Nek8 was identified by the discovery of mutation in the Nek8 gene which leads to polycystic kidney disease (PKD) in mice (Liu et al., 2002). Like Nek1, Nek8 has been implicated in cilia-related diseases raising the possibility that several mammalian Neks may play a role in microtubule organisation in cilia. Depletion of Nek8 in zebrafish prevents the formation of longer cilia. However, Nek8 shares the highest homology with Nek9 as both Nek8 and Nek9 contain an RCC1-like domain. Overexpression of kinase-inactive Nek8 leads to multinucleated cells and abnormal actin cytoskeleton organisation (Liu et al., 2002; Bowers and Boylan, 2004). Together, the results from mouse and human studies provide evidence that Nek8 may be involved in regulating the actin cytoskeleton structure during G_2/M progression as well as being involved in ciliogenesis.

1.6.3 Miscellaneous Neks: Nek3, Nek4, Nek5, Nek10 and Nek11

Apart from Nek2, the remaining Neks are poorly characterised and have no clear functions. Nek3 shares 42% homology with NIMA within its catalytic domain. Northen blots and in situ hybridisation experiments show that Nek3 is preferentially expressed in mitotically active tissues such as testis, ovaries and brain. However, unlike certain other mammalian Neks its expression is not cell cycle-regulated and there is no evidence of post-translational modifications (Kimura and Okano, 2001; Tanaka and Nigg, 1999). Nek3 is localised predominantly to the cytoplasm and no association with the centrosome has been observed. Similarly, overexpression of Nek3 or antibody microinjection had no effect upon cell cycle progression (Tanaka and Nigg, 1999; Chen et al., 1999). Hence it is possible that the function of Nek3 is not related to cell cycle regulation. Indeed, a recent study has found that Nek3 phosphorylates the scaffolding protein, paxillin, and the RhoGEF, Vav2, in response to prolactin signalling (Miller et al., 2007). Paxillin is localised to focal adhesion complexes which facilitate motility, while Vav2 activates Rac1, RhoA and Cdc42 and is also involved in cytoskeletal reorganisation. In addition, Nek3 is upregulated in malignant breast tissue compared to normal breast tissue. Together, these data provide some evidence that Nek3 is involved in the regulation of the prolactin-mediated cytoskeletal reorganisation and motility of breast cancer cells (Miller et al., 2007).

Very little is known about Nek4, Nek5 or Nek10. Nek4 (also called STK2) exists as two splice variants which both localise to the cytoplasm. Similar to Nek3, the expression and localisation of Nek4 is not cell cycle-dependent and hence its function is not understood (Hayashi et al, 1999). Nek5 possesses a dead box helicase-like domain and belongs to the dead box protein family. Nek5 is predominantly nucleolar, but nothing is yet known about its function.

Nek11 exists as two splice variants, Nek11S (short isoform) and Nek11L (long isoform). The catalytic domain is most structurally similar to Nek3 and Nek4. Nek11L expression levels increase from S to G_2/M phase and its subcellular localisation also changes through the cell cycle, localising to the nucleus in interphase and microtubules during mitosis (Noguchi et al., 2002). This suggests that Nek11 may play different roles during the cell cycle. Noguchi et al. found that Nek11 was activated in cells arrested in G_1/S in response to DNA-damaging agents and replication inhibitors. This suggests that Nek11 may be involved in regulating DNA replication as part of the S-phase checkpoint in response to DNA damage. There is also evidence that Nek11 is a target of Nek2A at the nucleolus in cells arrested in G_1/S. Both Nek11 and Nek2 were detected at the nucleolus and Nek11L interacted with the autophosphorylated form of Nek2A, but not with the inactive Nek2A (K37R) mutant. Nek2A has also been shown to directly phosphorylate the C-terminal domain of Nek11 increasing Nek11 kinase activity. This study highlights a novel role for a NIMA-related kinase in nucleolar function and suggests that Nek11 and Nek2 may represent another Nek kinase cascade (Noguchi et al., 2004).

1.7 The Nek2 protein kinase

Nek2 is the most closely-related mammalian homologue of NIMA and has therefore been the most well-studied of the mammalian Neks. It also resembles fungal NIMA in terms of its cell cycle-dependent expression and substrate specificity. Most importantly, Nek2 is clearly implicated in mitotic control as will be described in detail below.

1.7.1 Nek2 structure

Nek2 consists of an N-terminal catalytic domain that shares 47% protein sequence homology with NIMA and 44% with KIN3 and a C-terminal regulatory domain (Fry *et al.*, 1999). Nek2 is a typical serine/threonine protein kinase in that it contains all 12 motifs which are highly conserved amongst kinase sequences. These sequences contain the conserved residues which mediate the catalytic activity of the kinase and mediate the transfer of the γ-phosphate of ATP to the hydroxyl group of serine or threonine residues (Hanks and Hunter, 1995). Like other kinases Nek2 is activated by phosphorylation of the central activation loop also called the T-loop (Johnson et al., 1996). Phosphorylation of the activation loop stabilises it into an open and extended conformation to allow efficient substrate binding (Huse and Kuriyan, 2002). The activation loop is anchored at its N-terminal and C-terminal ends. The N-terminal anchor contains a DFG sequence (residues 159-161 in Nek2) in which the aspartate acts as a metal bivalent ligand and chelates a Mg^{2+} ion that correctly orientates the phosphate group for phospho-transfer (Hanks and Hunter, 1995; Nolen et al., 2004). The C-terminal anchor contains the motif APE and forms hydrogen bonds with a lysine residue in order to mediate interactions at the binding interface (Nolen et al., 2004). Nek2 also contains a conserved motif of an arginine and aspartate (RD) at residues 140/141 and a conserved residue (R/K) at residue 164 (Johnson et al., 1996).

The first crystal structure of the Nek2 kinase domain has recently been published (Rellos et al. 2007). This structure was determined for the Nek2-T175A mutant complexed with a pyrrol-indoline inhibitor (SU11652). T175 is an essential autophosphorylation site (discussed in 3.1) and so this therefore represents the structure of inactive Nek2 (Figure 1.8). Previous attempts to express the wild-type Nek2 kinase for crystallisation purposes had failed as Nek2 activity is toxic to bacteria (Fry and Nigg, 1997). The Nek2 catalytic domain possesses a bilobal protein kinase fold typical of many protein kinases (Hanks and Hunter, 1995). It is separated into 2 domains known as the N-lobe and C-lobe. The N-lobe is smaller and contains β-sheets, whereas the C-lobe is larger and consists of α-helices (Ubersax and Ferrell, 2007). ATP binds in the deep hydrophobic pocket between the two lobes, beneath a conserved phosphate-binding loop. This loop is glycine-rich contributing to its flexibility (Huse and Kuriyan, 2002). The depth, charge and hydrophobicity of the active site contribute to the substrate specificity of the Nek2 kinase (Ubersax and Ferrell, 2007). Nek2 is most

structurally similar to Aurora-A (31% identity) and a structural comparison of the two kinases is shown in Figure 1.8. The activation loop appears as an unstructured region. The two kinase structures differ in length and location of secondary structural features particularly within the C-lobe. The most distinct difference is the presence of a short αT-helix in Nek2, composed of 5 amino acids directly after the DFG motif at the N-terminal end of the activation loop that is missing in Aurora-A (Figure 1.8). This means that the short β-sheet structure after the DFG motif is therefore missing in Nek2. In this inactive conformation the αT-helix is located between Glu-55 and the ATP-binding site. Thus the αT-helix acts as a barrier preventing this catalytic glutamate from accessing the active site. In the activated form of Nek2 this helix must be disrupted or moved (Figure 1.8). A helical structure after the DFG motif has been observed in inactive forms of other kinases such as ATP-bound Cdk2, EGFR kinase and Src/Hck family kinases. This supports the proposal that the αT-helix is a feature of the inactive conformation of Nek2 rather than a structure created by the inhibitor binding (Rellos et al, 2007).

Despite sharing a common catalytic mechanism, the non-catalytic domains vary greatly between different kinases. These domains contain unique features which are thought to confer substrate specificity and mediate the targeting and localisation of protein kinases, allowing them to perform a diverse array of functions. For example, the C-terminal non-catalytic domain of Nek2 contains two coiled-coil motifs, degradation motifs, a site for interaction with protein phosphatase 1 (PP1) and a targeting motif responsible for localising Nek2 to the centrosome (Fry, 2002).

The human *nek2* gene is located on chromosome 1 and Nek2 mRNA is encoded on 8 exons. Exon 1 contains the initiation codon and exon 8 contains the stop codon UAG. Three splice variants of Nek2 have been described: Nek2A (445 residues; 48 kDa), Nek2B (383 residues; 44.9 kDa) and Nek2C (437 residues; 48 kDa) (Figure 1.9) (Fry, 2002; O'Connell *et al*., 2003; Wu et al., 2007). Nek2B arises as a result of an alternative polyadenylation site within intron 7 of Nek2A (Hames, 2002). This means that Nek2B differs from Nek2A, as it lacks the second coiled-coil domain (Figure 1.8). Nek2C lacks amino acids 371-378 within the C-terminal domain of Nek2A and results from an alternative splice acceptor site in exon 8. Ectopic Nek2C predominantly localises to the nucleus compared to the predominant cytoplasmic localisations of Nek2A and Nek2B. Mutagenesis studies revealed a strong nuclear localisation sequence (NLS) within Nek2C that is generated as a direct result of the 8 amino acid deletion. Nek2A does display a weak NLS activity, but this is completely absent

in Nek2B. Hence, it is predicted that Nek2C is required to phosphorylate nuclear substrates to promote mitotic or meiotic entry (Wu *et al.*, 2007). All three isoforms of Nek2 have also been shown to localise to the centrosome during interphase (Fry *et al.*, 1998; Hames *et al.*, 2001; Wu *et al.*, 2007). However, Nek2A and Nek2C are destroyed upon entry into mitosis due to the presence of destruction motifs in the extreme C-terminal region not present in Nek2B (Fry *et al.*, 1999; Hames *et al.*, 2001; Hayes *et al.*, 2007; Wu et al., 2007). Antibodies specific for each splice variant have not yet been developed, so only total Nek2 activity can be measured. This indicates that Nek2 is a cell-cycle regulated protein, with almost undetectable activity in G_1 and high activity in S/G_2, with low activity detected in mitosis (Fry, 2002). This supports a role for Nek2 in cell cycle regulation.

1.7.2 Nek2 functions

The best studied function for Nek2 is in the separation of centrosomes at the onset of mitosis. Yeast two-hybrid screens have shown that Nek2 interacts with the protein phosphatase 1 (PP1), and two centrosomal coiled-coil proteins, C-Nap1 and rootletin, forming a regulatory complex at the proximal ends of centrioles (Fry *et al.*, 1998 a and b; Helps *et al.*, 2000; Yang *et al*., 2002). Nek2 can phosphorylate itself, PP1, C-Nap1 and rootletin at serine and threonine residues. PP1 can dephosphorylate Nek2 and C-Nap1 (Fry *et al.*, 1998b; 1999; Helps *et al.*, 2000). It has not yet been shown whether PP1 also dephosphorylates rootletin. Overexpression of Nek2 or disruption of C-Nap1 by microinjection of antibodies results in premature separation of centrosomes. This suggests that Nek2 and C-Nap1 regulate anchoring sites for the intercentriolar linkage (Fry *et al*, 1998a; 1998b; Mayor *et al*, 2000). Increased levels of PP1 inhibitors have been shown to stimulate centrosome separation (Meraldi and Nigg, 2001; Eto *et al*, 2002). In addition, damage caused by exposure to radiation inhibited the premature centrosome splitting induced by overexpression of Nek2A. This suggests that Nek2A is involved in the response to the G_2 DNA damage checkpoint (Fletcher *et al.*, 2004). At present there is sufficient evidence to support a role for Nek2 in centrosome separation, but the precise events that underlie centrosome separation have not yet been discovered.

There is also evidence that Nek2 plays a role in centrosome assembly and maintenance. *Dictyostelium* Nek2 (DdNek2) shares 54% identity to the catalytic domain of human Nek2 and contains similar structural features. Overexpression of active or inactive DdNek2 leads to supernumerary centrosomes, dispersal of centrosomes and nuclear size and shape abnormalities (Graf, 2002). This study highlights a possible structural role of Nek2 in maintaining centrosome integrity and assembly. Similarly, overexpression of active or inactive Nek2 in human cells induces centrosome dispersal (Fry et al., 1998). In addition, immunodepletion of X-Nek2B from *Xenopus* egg extracts prevented γ-tubulin recruitment to the sperm basal body and delayed the conversion of the sperm basal body into a centrosome (Fry et al., 2000). However the addition of active or inactive Nek2B rescued these defects (Twomey et al., 2004), whilst a second study found that inhibition of X-Nek2B induced centrosome fragmentation leading to abnormal spindle formation (Uto and Sagata, 2000). X-Nek2B therefore plays a role in centrosome assembly and maintenance at least in *Xenopus* embryos and this appears to be independent of its activity.

Recently, new roles have been proposed for Nek2 in chromosome segregation (Sonn et al., 2004), chromatin condensation (Di Agostino, et al., 2002), spindle checkpoint signalling (Chen et al., 2002; Lou et al., 2004), DNA damage pathways (Fletcher et al., 2004) and cytokinesis (Prigent et al., 2005; Fletcher et al., 2004). Some of these possible roles are discussed in more detail below.

Evidence has emerged suggesting that Nek2 may be involved in chromosome segregation. Nek2A and Nek2B are expressed throughout early embryogenesis in mice and, interestingly, murine Nek2A is not degraded upon mitotic entry as seen in human cells. Depletion of Nek2A by RNAi in mouse early embryos resulted in nuclear abnormalities, including dumbbell shaped nuclei, nuclear bridges and micronuclei (Sonn et al., 2004). This study highlights a requirement for Nek2 in proper chromosome segregation and could reflect its role in centrosome regulation. However, another study found that Nek2 is exclusively localised at chromosomes during porcine oocyte maturation suggesting a more direct role in regulating chromosome organisation (Fujioka et al., 2000).

Indeed, there is additional evidence that Nek2 plays a direct role in chromatin condensation. The C-terminal domain of Nek2 interacts with the DNA architectural protein, high mobility group protein A2 (HMGA2). Following phosphorylation by Nek2, HMGA2 is released from chromatin, thus promoting chromatin condensation (Di Agostino et al., 2002). This is discussed in more detail in the next section (1.7.3).

There is also some evidence that Nek2 contributes to the spindle assembly checkpoint. Nek2 was found to phosphorylate Hec1 at kinetochores, and some data support the notion that this phosphorylation is essential for accurate chromosome segregation in budding yeast (Chen et al., 2002). Nek2 has also been shown to interact with and colocalise with Mad1 at kinetochores and possibly function in spindle checkpoint signalling. However, depletion of Nek2 by RNAi had no effect upon Mad1, but interestingly it did displace Mad2 from kinetochores (Lou et al., 2004). This suggests that Nek2 may mediate the interaction between Mad1 and Mad2 at kinetochores, although Nek2 may interact with Mad2 directly (Lou et al., 2004). *In vitro* experiments have also identified the kinetochore protein, Sgo1 as a target of Nek2. Nek2 was found to colocalise with Sgo1 at the kinetochores of mitotic cells and expression of a mutant Sgo1, which was unable to undergo Nek2 phosphorylation, led to an increase in microtubule attachment errors. This suggests a role for Nek2 in regulating kinetochore-microtubule interactions in mitosis (Fu et al., 2007). However, the presence of Nek2 at kinetochores needs to be confirmed.

Overexpression of Nek2 in *Drosophila* results in cleavage furrow formation and cytokinesis failure (Prigent et al., 2005). Nek2 was also seen to associate with the actin contractile ring at the midbody during cytokinesis in *Drosophila*. Anillin and actin mediate the formation of the actin ring and the rearrangement of membrane during cytokinesis. In *Drosophila* cells overexpressing Nek2, anillin and actin were mislocalised from the cleavage furrow, resulting in the formation of membrane protrusions between each daughter cell, thus contributing to cytokinesis failure (Prigent et al., 2005). This implies that Nek2 may negatively regulate anillin localisation during cytokinesis and thus contribute to mitotic exit. This is somewhat reminiscent of the role described earlier for Fin1 in negatively regulating premature mitotic exit in fission yeast.

1.7.3 Nek2 regulation

Nek2 expression and kinase activity are regulated by transcriptional and post-translational mechanisms (Hayward and Fry, 2005). Nek2 mRNA levels are low in M and G_1 and high in S and G_2 (Twomey et al., 2004). Nek2 transcription is cell-cycle regulated by the transcription factors, E2F4 and FoxM1, which bind the Nek2 promoter (Ren *et al.*, 2002; Wonsey and Follettie, 2005). Once bound to the promoter, E2F4 recruits the Rb family proteins, p107 and p130, which act to repress Nek2 mRNA transcription in G_0 and G_1 phase. In S/G_2 phase, E2F4 is released from the promoter allowing transient expression of Nek2. In cells which lack p107 and p130, Nek2 mRNA expression is significantly increased (Ren *et al.*, 2002).

Nek2 protein levels are also regulated by degradation (Hames et al.., 2001). Nek2A and Nek2C contain a carboxyl-terminal methionine-arginine (MR) dipeptide (residues 444-445 in Nek2A) and a KEN box (residues 391-399 in Nek2A) which are not present in Nek2B (Hames et al., 2001). Nek2A is destroyed in prometaphase in the presence of an active SAC by the 26S proteasome following polyubiquitylation by the APC/C (Hayes et al, 2006). The APC/C is an E3 ubiquitin ligase that catalyses the covalent attachment of ubiquitin molecules to a particular substrate (Peters, 2006). It is a 1.5 MDa protein complex composed of least 12 different subunits. Its ubiquitylating activity depends on its interaction with three cofactors: a ubiquitin-activating enzyme (E1), a ubiquitin-conjugating enzyme (E2) and an additional co-activator protein. Co-activator proteins, such as Cdc20 (Fizzy in *Xenopus*) and Cdh1 (Fizzy-related in *Xenopus*) interact with the APC/C via their C-terminal isoleucine-arginine (IR) tails. They also contain a C-terminal WD40 domain that recognises specific sequence elements such as destruction boxes (D-boxes; RxxLxxxxN) and KEN-boxes in APC/C substrates (Peters, 2006).

In mitotic cells, the APC/C is activated, firstly, by binding to Cdc20 from prophase to anaphase and then, secondly, by binding to Cdh1 in telophase and G_1. These sequential interactions with the APC/C may account for the destruction of different proteins at specific times during mitosis (Fry and Yamano, 2006). Cdc20-activated APC/C recognises substrates containing a D-box, such as securins and mitotic cyclins. Cdh1-activated APC/C recognises both D-box and KEN box containing substrates, including Cdc20 accounting for its loss in late mitosis (Fang et al, 1998; Pfleger and Kirschner, 2008).

The destruction motifs present in Nek2A are thought to be responsible for the targeting of Nek2A/Nek2C to the anaphase-promoting complex/cyclosome (APC/C) at the onset of mitosis. Nek2A has been shown to interact with APC/C-Cdh1 via its KEN box and with Cdc20-APC/C via its extreme C-terminus (Pfleger and Kirschner, 2000). Hames et al. (2001) found that removal of the C-terminal 25 residues stabilised Nek2A significantly more than removal of the KEN box for both Cdc20-APC/C and Cdh1-APC/C. It was also demonstrated that removal of both destruction motifs was required to fully stabilise Nek2A in *Xenopus* mitotic egg extracts (Hayes et al, 2006). Nek2A has since been shown to interact directly with the APC/C via its MR-dipeptide tail independently of the adapter proteins, Cdc20 and Cdh1. However, the co-activator proteins are still required for Nek2A ubiquitylation and destruction as Cdc20 and Cdh1 are required to activate the ubiquitin ligase activity of the APC/C.

Nek2A is also tightly regulated by autophosphorylation, but this will be described in detail later.

1.7.4 Nek2 substrates

Nek2 exists in cells as a stable homodimer as a result of interaction via its leucine zipper coiled-coil motif (Fry *et al.*, 1999) (Figure 1.10). This dimerisation promotes trans-autophosphorylation, particularly on serine and threonine residues within both the N- and C-terminal domains (Fry et al., 1995). Loss of the leucine zipper motif and an inability to dimerise results in reduced Nek2 kinase activity (Fry et al., 1999). It is unknown whether the kinase activity is reduced due to loss of trans-autophosphorylation or loss of dimerisation. Nek2A and Nek2B can also form heterodimers (Hames and Fry, 2002). This may allow Nek2B to be regulated by protein phosphatase 1 (PP1) despite the fact that Nek2B lacks the PP1 binding site present in Nek2A (Helps et al., 2000) (Figure 1.10).

PP1 is a major protein phosphatase that regulates cellular processes by dephosphorylation of serine and threonine residues. PP1 interacts with Nek2A via a conserved ‘KVHF’ motif at positions 383-386 in the Nek2A C-terminus (Figure 1.9). This kinase-phosphatase complex maintains Nek2A in a dephosphorylated state. The addition of PP1 to GST-Nek2A reduces the kinase activity of Nek2A by 65% (Helps et al., 2000). Nek2 can phosphorylate PP1 on threonines 307 and 318 and this leads to inhibition of PP1, providing a positive feedback mechanism for Nek2A (Helps et al., 2000) (Figure 1.10). Nek2 can then phosphorylate other target substrates. PP1 exists as 3 isoforms, PP1α, β and γ, but only PP1α coimmunoprecipitates with Nek2 and is capable of regulating Nek2 activity (Mi et al., 2007).

The kinase-phosphatase complex of PP1 and Nek2 may be further regulated by a PP1 inhibitor, known as inhibitor-2 (Inh2). At the G_2/M transition, Inh2 binds PP1 at a site of conserved residues, IKGI, which lies next to the Nek2 binding site at the C-terminal (Eto et al., 2002). When either Inh2 or Nek2 binds PP1 it may induce conformational changes which prevents the other from binding (Egloff et al., 1997; Eto et al., 2002). Therefore, Inh2 may enhance the kinase activity of Nek2 by displacing Nek2 from PP1 (Eto et al., 2002). Overexpression of Inh2 leads to increased centrosome splitting in fibroblasts, which indicates enhanced Nek2 kinase activity (Eto et al., 2002). Inh2 has been shown to be phosphorylated by MAPK at Thr72 and the addition of MAPK inhibitors blocks Nek2 kinase activity in cells, suggesting that the binding of Inh2 to PP1 may be activated by MAPK (Di Agostino et al., 2002).

HEF1 is a component of the focal adhesion complex which plays a role in integrin-dependent attachment signalling. However in mitosis HEF1 localises to the spindle asters (Pugacheva and Golemis, 2005). HEF1 overexpression leads to aberrant centrosomes and multipolar spindles similar to Aurora-A overexpression, whereas HEF1 depletion induces centrosome splitting and monopolar spindle formation reminiscent of Nek2 overexpression. This led to the proposal that HEF1 is capable of negatively regulating Nek2A as well as positively regulating Aurora-A activity (Pugacheva and Golemis, 2005). However this model is not in agreement with the fact that Aurora-A and Nek2 are active simultaneously in the cell cycle. This study suggests a role for the centrosome in regulating cell migration but this remains to be confirmed.

C-Nap1 was first identified in a yeast two-hybrid screen using kinase-inactive Nek2A as bait (Fry et al., 1998). C-Nap1 is a 281 kDa protein consisting of globular N-terminal domain (NTD) and C-terminal domains (CTD) joined by coiled-coil domains and a central proline-rich region that might act as a hinge. Nek2 has been shown to phosphorylate C-Nap at its N- and C-terminal domains *in vitro* and it is proposed that, as a result of phosphorylation by Nek2, C-Nap1 dissociates from the centrosome at the onset of mitosis allowing centrosomes to separate (Hames, 2002; Fry et al, 1998; Helps et al., 2000; Mayor, 2002) (Figure 1.10). In support of this model, C-Nap1 and Nek2 colocalise at the proximal ends of centrioles in interphase and disruption of C-Nap1 by microinjection of antibodies results in centrosome splitting, regardless of the cell cycle stage (Mayor et al, 2000). This suggests that C-Nap1 forms part of the linker structure which keeps centrioles together during interphase. However, Immuno-EM analysis of C-Nap1 revealed tight association of C-Nap1 with centriole ends but no localisation between the centrioles and C-Nap1 is still partially present at centrosomes when premature centrosome splitting is induced by the overexpression of Nek2 (Mayor et al., 2000; Faragher and Fry, 2003). This suggests that additional proteins are likely to be involved in the intercentriolar linkage.

Indeed, another component of the intercentriolar linker is rootletin, a 220 kDa protein that also localises to the cilary rootlet and basal body (Yang et al., 2002). Rootletin is related in sequence to C-Nap1 and has a globular head domain and a tail domain of extensive coiled-coil structures. A yeast two-hybrid analysis showed that rootletin can interact directly with C-Nap1 (Bahe et al. 2005; Liu et al., 2007). Like C-Nap1, rootletin colocalises at the proximal ends of centrioles in non-ciliated cells and is displaced at the onset of mitosis. siRNA gene depletion of rootletin causes centrosome splitting, thus demonstrating that rootletin is required for centrosome cohesion (Bahe et al., 2005). Importantly, ultrastructural examinations reveal the presence of rootletin fibres at the ends and between centrioles suggesting that rootletin may constitute the bulk of the linker structure (Bahe et al., 2005). Nek2 has been shown to phosphorylate rootletin *in vitro* (Figure 1.9). Together, current data suggests a model in which rootletin serves as a physical linker between a pair of centrioles by interacting with C-Nap1, which anchors rootletin to the proximal ends of centrioles. Centrosome cohesion is thought to be regulated by the phosphorylation of C-Nap1 and rootletin by Nek2.

β-catenin regulates cell proliferation and plays a role in cell adhesion. Recent research demonstrated that β-catenin localises to the centrosome in mitosis and plays an essential role in bipolar spindle formation (Bahmanyar et al., 2008). Depletion of β-catenin results in monopolar spindle formation and failure of centrosome separation, whereas stabilisation of β-catenin results in premature centrosome splitting. β-catenin has also been shown to interact with Nek2, rootletin and C-Nap1. The localisation of β-catenin in between centrosomes was found to be dependent on the presence of rootletin and C-Nap1. Interestingly, Nek2 overexpression stimulates the relocalisation of β-catenin from in between centrosomes to binding sites directly on the centrosome following displacement of C-Nap1 and rootletin (Bahmanyar et al., 2008). This study suggests β-catenin is a component of the intercentriolar linkage and may play a role in centrosome cohesion.

Another potential centrosome substrate of Nek2 is ninein-like protein (Nlp). Nlp was first identified in a yeast two-hybrid screen using the *Xenopus* Polo-like kinase, Plx1, as the bait. It shares 37% sequence homology with the microtubule anchoring protein, ninein (Casenghi et al., 2003). Nlp localises preferentially to the mother centriole but is displaced from centrosomes at the G_2/M transition (Casenghi et al., 2003; Rapley et al., 2005) (Figure 1.10). Meanwhile, overexpression of Nlp results in aberrant spindle formation (Casenghi et al., 2003). Therefore, Nlp is proposed to play a role in microtubule anchoring during interphase possibly via interaction with components of the γ-tubulin ring complex. Mutational analysis suggests that Nek2 and Plk1 phosphorylate Nlp at distinct sites to coordinately regulate the displacement of Nlp from the mother centriole upon mitotic entry (Figure 1.10). Indeed, kinase-inactive Nek2 can inhibit phosphorylation of Nlp by Plk1 thus preventing dissociation of Nlp from the centrosome. This raises the possibility that Nek2 phosphorylation may prime Nlp for phosphorylation by Plk1 (Rapley *et al*., 2005).

Centrobin, also known as Nek2 interacting protein 2 (NIP2), was originally identified as a Nek2 substrate. In contrast to Nlp, NIP2 associates with the daughter centriole and with the cytoplasmic microtubule network (Jeong et al., 2007). Depletion of NIP2 results in microtubule misorganisation, spindle defects and abnormal nuclear morphology. This suggests that NIP2 plays a role in stabilising microtubule structure. It has been proposed that phosphorylation of NIP2 by Nek2 stimulates the movement of NIP2 to unstable microtubules, enabling NIP2 to carry out its function (Jeong et al., 2007).

High mobility group protein A2 belongs to the HMG superfamily of DNA architectural proteins. HMGA proteins bind DNA in AT-rich regions through basic domains called AT-hooks. They alter chromatin conformation by creating bends in the DNA to increase its exposure to transcription factors. HMGA1 and HMGA2 expression is confined to the testis in the adult and mainly to meiotic spermatocytes (Di Agostino et al., 2000). HMGA2 may have an essential function in the regulation of spermatogenesis as HMGA2$^{-/-}$ mice are sterile and spermatogenesis is drastically impaired. The C-terminus of Nek2 has been shown to directly interact with HMGA2 *in vivo* and *in vitro* independently of the Nek2 activation state (Figure 1.10). Phosphorylation of HMGA2 by Nek2 reduces its affinity for DNA and may promote its dissociation from chromatin allowing entry of other factors involved in the condensation of meiotic chromosomes (Di Agostino et al., 2000). Therefore, the interaction between HMGA2 and Nek2 may play an important role in the regulation of chromosome condensation in meiosis.

Hec1 (highly expressed in cancer) is localised at kinetochores and was shown to interact with Nek2 via its two C-terminal coiled-coil domains (Figure 1.10). During G_2 and M phases Hec1 is thought to be phosphorylated by Nek2 at serine 165, thus allowing Hec1 to coordinate accurate chromosome segregation (Chen *et al.*, 2002). This site lies within an FxxS motif shown to be the preferred target for NIMA and mutation of this site abolishes phosphorylation by Nek2 *in vitro*.

Shugoshin 1 (Sgo1) protects centromeric cohesion of sister chromatids until the kinetochores of chromosomes are attached to the mitotic spindle by microtubules emanating from both spindle poles. It has been shown that Sgo1 is phosphorylated by Nek2A at S14 and S507. Expression of a non-phosphorylatable Sgo1 mutant resulted in increased microtubule attachment errors (Fu et al., 2007). This suggests that Nek2A mediated phosphorylation of Sgo1 may be required for spindle microtubule attachment.

1.7.5 Nek2 in cancer cells

Centrosomal abnormalities caused by a loss of co-ordination between centrosome and chromosome segregation cycles are frequently observed in many cancers (Fry, 2002; Nigg, 2002). One common centrosomal abnormality is the presence of supernumerary centrosomes that may lead to multipolar spindles causing inaccurate chromosome segregation, characteristic of many high-grade tumours (Doxsey, 2001 and Nigg, 2002). Evidence suggests that centrosomal abnormalities may contribute to the formation of aneuploidy and could promote progression of benign cancers to more malignant types (Nigg, 2002; Pihan and Doxsey, 1999).

Other mitotic kinases that localise to centrosome, including Plk1 and Aurora-A, are often deregulated in cancer cells and may contribute to the chromosome instability typical of tumours. Nek2 mRNA was first found to be overexpressed in cell lines derived from Ewings tumours, a paediatric osteosarcoma, cholangiocarcinoma and human non-Hodgkin lymphoma (Kokuryo et al., 2007; Wai et al., 2002; de Vos et al., 2003). Furthermore, analysis of a wide range of patient samples revealed that Nek2 mRNA levels increased as follicular lymphoma (FL) advances to the more aggressive diffuse large B-lymphoma (DLBCL) (de Vos et al., 2003). This rise in Nek2 mRNA levels may be due to loss of control at the transcriptional level (de Vos *et al*., 2002; Wai *et al*., 2002). It is also possible that the Nek2 gene is amplified in certain tumours (Weiss *et al*., 2004, Loo *et al*, 2004). The Nek2 gene is regulated by the forkhead transcription factor, FoxM1, and FoxM1 expression is elevated in primary breast cancers. Cells depleted of FoxM1 fail to complete cell division promoting reduplication of centrosomes (Wonsey and Follettie, 2005). Nek2 protein levels have also now been found to be increased by 2-5 fold in some cancer cell lines derived from breast, prostate and cervical carcinomas and in high-grade invasive primary breast tumours (Hayward *et al*., 2004; Hayward and Fry, 2005). It has not yet been shown whether this increase in Nek2 expression is associated with centrosomal and spindle abnormalities, but overexpression of Nek2 has been shown to induce chromosomal instability and aneuploidy in HBL-100 non-transformed breast cells (Hayward et al., 2004). In addition, Nek2 has been shown to induce tumorigenic growth of cholangiocarcinoma. Suppression of Nek2 expression in a cholangiocarcinoma derived cell line by siRNA inhibited cell proliferation and induced cell death. Furthermore, xenograft bearing mice treated with Nek2 siRNA demonstrated longer survival periods and reduced tumour size compared to control mice

(Kokuryo et al., 2007). This provides strong evidence that Nek2 could be an effective anti-cancer drug target.

1.8 Project aims

1.8.1 Background to project

As explained in detail above, Nek2 is a cell cycle regulated protein kinase that localises to the centrosome. Nek2 is thought to play a major role in uncoupling centrosome cohesion at the G_2/M transition and may contribute to other mitotic processes. However, it is not understood how Nek2 is activated in such a precise and timely manner to carry out these processes. Moreover, the elevated Nek2 mRNA and protein levels found in various tumours highlights the importance of increasing our understanding of how Nek2 is regulated and how Nek2 may regulate its centrosomal partners.

Prior to initiating the project 13 autophosphorylation sites had been identified within Nek2A by mass spectrometry (Figure 1.11). These were generated upon expression of Nek2A in bacteria. Five sites lay within the N-terminal catalytic domain and eight sites in the C-terminal non-catalytic domain. Four of the sites within the kinase domain clustered around the activation loop suggesting that phosphorylation of multiple sites may be required for Nek2 to reach maximal activity. A number of these sites have already been studied by a previous PhD student, Dr. Baxter, in the laboratory using site-directed mutagenesis (Baxter, 2006). A summary of the data obtained by Dr. Baxter is shown in Figure 1.12.

Furthermore, a recent study performed in the laboratory in collaboration with Prof. S. Smerdon (NIMR, London) and Dr. S. Knapp (SGC, Oxford) enabled a crystal structure of the catalytic domain of human Nek2A to be obtained (Figure 1.8). Structural comparison of Nek2A and Aurora-A revealed a novel αT-helix at the N- terminal end of the Nek2 activation loop (Rellos et al., 2007) (Figure 1.8). However, this structure was of inactive Nek2 and it is not clear whether this helix is present or not in the active kinase. It is possible that it needs to melt to allow activation of Nek2 (Rellos et al., 2007).

1.8.2 Experimental objectives

A. *Mutational analysis of Nek2A autophosphorylation sites*

Nek2A mutant kinases would be generated by incorporating point mutations into a pRcCMV:myc-Nek2A vector using a site-directed mutagenesis approach. The consequence

of these mutations on Nek2A activity would be analysed by expressing the protein by *in vitro* translation (IVT), immunoprecipitating it with an anti-myc antibody and using the immunoprecipitate in a kinase assay with β-casein as the substrate. In addition, the Nek2A mutant constructs would be transiently transfected into U2OS cells. Immunofluorescence microscopy would determine whether the mutant kinases localise at the centrosome and costaining with γ-tubulin would allow quantification of the extent of centrosome splitting in transfected cells as an indicator of Nek2 activity *in vivo.*

B. ***Does the C-terminus of Nek2A acts as an autoinhibitory domain?***

The activity of three Nek2A mutants possessing C-terminal truncations of various size would be analysed by the IVT-IP kinase assay described above alongside a Nek2B construct. If the C-terminal domain acts as an autoinhibitory domain then deletion of these residues may result in a hyperactive kinase.

C. ***Does mutation of the αT-helix alter Nek2A activity?***

Based on the recent crystal structure, the Nek2 kinase domain contains an unusual T-helix at residues 162-166 (Figure 1.8). Its position suggests that it would inactivate Nek2. The activity of an A163G mutant Nek2 construct would be analysed by an IVT-IP kinase assay. This mutation should cause the αT-helix to collapse and its mutation may therefore create a constitutively active kinase. It would also be investigated whether an A163G mutation is sufficient to rescue the inactivity caused by mutation of another autophosphorylation site, S241.

D. ***Is it possible to mutate the M86 gatekeeper residue without altering Nek2A activity?***

M86 lies at the predicted position for the gatekeeper residue in the Nek2 protein kinase. Two mutants would be created changing M86 to G or A. The activity of the mutant kinases would be assessed by performing an IVT-IP kinase assay as described above. This would dictate whether M86 can be mutated to generate an analogue-sensitive Nek2 kinase.

E. ***Generate a Nek2 T175 phosphospecific antibody***

T175 is a critical autophosphorylation site within the Nek2 activation loop. Its phosphorylation directly regulates the activity of Nek2. Peptides encompassing the phosphorylated T175 site would therefore be injected into rabbits and the immune sera collected and purified. The reactivity and specificity of the resulting antibody would be analysed by dot blots, Western blotting and immunofluorescence microscopy. Furthermore, a second approach using a recombinant antibody technology would be used to generate a phosphospecific antibody which would be characterised in a similar manner.

F. ***Use of the Nek2 T175 phosphospecific antibody in cell based assays***

Immunofluorescence microscopy would be performed to compare localisation patterns using the T175 phosphospecific and total Nek2 antibodies. The development of cell based methods for testing Nek2 activity would be highly valuable in the assessment of small molecule inhibitors of Nek2.

G. ***Is Nek2 activated upstream or downstream of Cdk1?***

To determine whether Nek2 activation is dependent upon Cdk1, the effect of the specific Cdk1 inhibitor, RO-3306, upon Nek2A activity and cellular morphology, will be determined by performing kinase assays and immunofluorescence microscopy.

H. ***How does Nek2 phosphorylation regulate C-Nap1?***

It has previously been shown that Nek2 can phosphorylate the globular N- and C-terminal domains of the centrosomal linker protein, C-Nap1. However, the sites of phosphorylation have not yet been identified. Mass spectrometry would be used to identify sites on these domains phosphorylated by Nek2 *in vitro*. Moreover, yeast two-hybrid assays have shown that the N- and C-terminal domains of C-Nap1 can form homo- and hetero-dimers. Therefore it was tested whether Nek2 phosphorylation might regulate the intramolecular interactions of C-Nap1 as a mechanism to disassemble the intercentriolar linkage. For this purpose, GST-fused C-Nap1-CTD and -NTD proteins would be expressed and coupled to glutathione-sepharose beads. These would be incubated with [^{35}S]-labelled, myc-tagged Rab4, Nek2-WT, C-Nap1-CTD and C-Nap1-NTD proteins to confirm interactions *in vitro*. The GST proteins would then be incubated with purified Nek2 kinase prior to the pull down assays to determine the effect of phosphorylation upon these interactions with Nek2.

Chapter Two

Materials and Methods

Chapter 2 MATERIALS AND METHODS

2.1 Materials

2.1.1 Chemical suppliers

All reagents and chemicals were purchased from Sigma (Poole, UK) or Roche (Lewes, UK) apart from those indicated in the table below.

Reagent	**Supplier**
DNA nucleotides (dATP, dGTP, dCTP, dTTP) Glutathione Sepharose 4B^{TM} ECL Western Blotting ECL Plus Western Blotting Reagent	Amersham Pharmacia Biotech (Buckinghamshire, UK)
Poly-prep Columns Protein A Beads Precision Plus Protein All Blue Standards Ammonium Persulfate Silver Stain Concentrate and Developer	Bio-Rad (Hemel Hempstead, UK)
Hoechst 33258 (0.1 μg/ml)	Calbiochem
Super RX X-Ray film	Fuji photo film (Dusseldorf, Germany)
Glacial Acetic Acid NaCl EDTA EGTA KCl NaH_2PO_4 Oligonucleotide Primers	Fischer Scientific (Loughborough, UK)
Protogel liquid acrylamide (30% w/v)	Flowgen (Ashby-de-la-Zouch, UK)
Bovine Serum Albumin (Fraction V) Glycine Phenylmethanesulfonylfluoride (PMSF)	Fluka Biochemika (Gillingham, UK)
Dulbecco's-MEM with Glutamax	Invitrogen (Paisley, UK)

Foetal Calf Serum (FCS) Ethidium Bromide solution Geneticin Lipofectamine 2000 Gene Tailer Site-Directed Mutagenesis Kit GST-Plk1	Invitrogen (Paisley, UK)
Marvel (skimmed milk powder)	Premiere Beverages (Stafford, UK)
DNA 100 bp Generuler plus molecular weight ladder	MBI Fermentas (York, UK)
Tris	Melford Laboratories
DNA ladder 100 bp DNA ladder 1 kb Restriction endonucleases	New England Biolabs (Herts, UK)
Bacto-agar Yeast Extract Bacto-trytone	Oxoid (Basingstoke, UK)
BCA Protein Assay	Pierce (Rockford, USA)
TnT T7 Quick Coupled mix Transcription/Translation Kit T4 DNA ligase	Promega (Southampton, UK)
QIA Filter Plasmid Maxi Kit QIA Filter Plasmid Miniprep Kit QIAquick PCR purification Kit QIAquick gel extraction Kit	Qiagen (Sussex, UK)
ProTran Nitrocellulose membrane	Schleicher and Schuell (Dassel, Germany)
Cdk1-his$_6$/GST-Cyclin B his$_6$Nek2A his$_6$Nek6 his$_6$Nek7 his$_6$Aurora-A	Upstate (Dundee, UK)
3MM Chromatography Paper	Whatmann (Maidstone, UK)

2.1.2 Radioisotopes

Isotope	**Specific Activity**	**Supplier**
^{32}P-γ-[ATP]	167 Tbq/mmol	MP Biomedicals UK
[^{35}S] methionine	43.5 Tbq/mmol	NEN Life Science Products

2.1.3 Vectors and Constructs

Vector	**Application**	**Supplier**
pRcCMV-Myc-Nek2A	Eukaryotic protein expression	Fry *et al.*, 1998a
pGEX-4T-1	Bacterial protein expression	Pharmacia
pGEX-4T-2	Bacterial protein expression	Pharmacia
pGEX-C-Nap1-NTD	Bacterial protein expression	Created by R. Hames
pGEX-C-Nap1-CTD	Bacterial protein expression	Created by R. Hames
pBS-KS-C-Nap1-CTD	*In vitro* translation (T3)	Created by A. Fry
pBS-KS-C-Nap1-NTD	*In vitro* translation (T3)	Created by A. Fry
pEGFP-C1-Nek2A	Immunofluorescence	Gift from K. Tanaka

2.1.4 Antibodies

Primary Antibodies	**Working Dilution or Concentration**	**Application**	**Supplier**
Anti-GFP (Rabbit)	100 ng/ml	Immunofluorescence	Abcam
Anti-Myc (mouse)	1/1000	Immunoprecipitation Western Blotting Immunofluorescence	Cell Signalling
Anti-Nek2 (mouse)	1/1000 (1 µg/ml)	Immunofluorescence Western Blotting	Abcam
Anti-Nek2	1/1200	Immunofluorescence	Zymed

(rabbit)		Western Blotting	
Anti-Nek2 (mouse)	1/100 (1 µg/ml)	Immunofluorescence Western Blotting	BD Biosciences
Anti-γ-tubulin (Rabbit)	1/500 (6.5 µg/ml)	Immunofluorescence	Sigma
Anti-α-tubulin (mouse)	1/2000	Immunofluorescence	Sigma
Anti-centromere (human)	1/200	Immunofluorescence	Europa Bioproducts Ltd.

Secondary Antibodies	**Working Dilution or Concentration**	**Application**	**Supplier**
Goat anti-human FITC	1/200	Immunofluorescence	Sigma
Goat anti-human IgG HRP	1/5000	Western Blotting	Serotec
Goat anti-mouse IgG HRP	1/5000	Western Blotting	Sigma
Goat anti-rabbit IgG HRP	1/5000	Western Blotting	Sigma
Goat anti-mouse AP conjugate	1/7500 (0.1 µg/ml)	Western Blotting	Promega
Goat anti-rabbit AP conjugate	1/7500 (0.1 µg/ml)	Western Blotting	Promega
Goat anti-rabbit Alexa 488 nm	1/200 (10 µg/ml)	Immunofluorescence	Invitrogen
Goat anti-rabbit Alexa 594 nm	1/200 (10 µg/ml)	Immunofluorescence	Invitrogen
Goat anti-mouse Alexa 488 nm	1/200 (10 µg/ml)	Immunofluorescence	Invitrogen
Goat anti-mouse Alexa 594 nm	1/200 (10 µg/ml)	Immunofluorescence	Invitrogen

Final antibody concentrations, where known, are stated in brackets after the working dilution.

2.1.5 Bacterial strains

Strain	**Supplier**
DH5α-library efficient competent cells	Invitrogen
DH5α-T1 competent cells max efficiency	Invitrogen
One shot BL21 star (DE3) chemically competent *E. coli*	Invitrogen
Rosetta (DE3) *E. coli*	Invitrogen

2.1.6 Buffers and solutions

Buffer	**Composition**
3 x Laemmli Protein Sample Buffer	62.5 mM Tris-HCl, pH 6.8, 2% (w/v) SDS, 5% (v/v) β-mercaptoethanol, 10% (v/v) glycerol, 0.01% (v/v) bromophenol blue
10 x PBS	137 mM NaCl, 26.8 mM KCl, 2.7 mM Na_2HPO_4, 1.4 mM KH_2PO_4
TBE	89 mM Tris, 89 mM boric acid, 1 mM EDTA pH 8.0
TE	10 mM Tris pH 8.0, 1 mM EDTA
Western Blotting Transfer Buffer	25 mM Tris, 192 mM Glycine, 10% methanol (optional)
Alkaline Phosphatase Buffer	100 mM NaCl, 5 mM $MgCl_2$, 100 mM Tris-HCl pH 9.5
BCIP	50 mg/ml in DMF
NBT	50 mg/ml in 70% DMF
Kinase Assay Buffer	50 mM Hepes KOH pH 7.4, 5 mM $MnCl_2$, 5 mM β–glycerophosphate, 5 mM NaF, 4 µM ATP, 1mM DTT, 10 µCi-γ-^{32}P [ATP], dH_2O
Protein Gel Running Buffer	0.1% SDS, 0.3% Tris, 1.44% glycine

2.2 Molecular biology techniques

2.2.1 Growth and maintenance of bacterial strains

One bacterial colony was selected and streaked onto a Luria Bertani (LB) agar plate (NaCl 10 g/l, tryptone 10 g/l, yeast extract 5 g/l and agar at 2% (w/v) adjusted to pH 7.0 and autoclaved) and grown at 37^0C overnight (O/N). Bacterial stocks were prepared by firstly growing a bacterial colony in 5 ml LB medium at 37^0C in a shaking incubator O/N. Glycerol (800 µl) was added to 200 µl of this bacterial stock and stored at -80^0C. Selective medium was prepared by the addition of antibiotic (100 µg/ml ampicillin, 34 µg/ml chloramphenical or 50 µg/ml kanamycin).

2.2.2 Transformation of competent bacteria

Competent *E. coli* cells and DNA samples were thawed on ice. Approximately 100 ng of DNA was added to 50 µl of competent cells and gently tapped to mix. The sample was incubated on ice for 10 minutes before heat shock at 42^0C for 45 seconds and then returned to ice for 1 minute. Under sterile conditions 200 µl of LB was added to each vial and tapped to mix. Next the vial was incubated at 37^0C for 1 hour shaking at 225 rpm. The cell mixture (200 µl) was streaked onto a pre-warmed LB agar plate containing appropriate antibiotic using a sterilised glass pasteur pipette. The plates were inverted and incubated at 37^0C O/N.

2.2.3 Plasmid preparation (small scale)

Each bacterial colony selected from an agar plate was grown in 5 ml LB containing appropriate antibiotic whilst shaking at 37^0C O/N. The colonies were centrifuged at 805g for 15 minutes and the supernatant aspirated. The colonies were then processed using the Qiagen mini prep spin kit according to Qiagen's instruction manual. Plasmid DNA was eluted into 50 µl sterilised distilled water, yielding 5-10 ng of DNA.

2.2.4 Plasmid preparation (large scale)

Each bacterial colony selected was grown in 5 mls LB containing appropriate antibiotic whilst shaking at 37^0C for 8 hours. The starter culture (1000 µl) was added to a sterile flask containing 100 ml of LB and appropriate antibiotic. The bacterial culture was grown whilst shaking at 37^0C O/N. The culture was spun down at 6000 g at 4^0C for 20 minutes and the supernatant aspirated. The plasmid was isolated from the remaining pellet using the Qiagen

Maxi prep kit and following the instructions provided. The plasmid was diluted in appropriate volume of distilled water to obtain a 1 mg/ml concentration.

2.2.5 Quantification of DNA concentration

Concentrations of DNA were measured by UV light at OD_{260} and calculated according to the formula below:

$$A_{260} \text{ x dilution factor x } 40 = \text{DNA Concentration } (\mu g/ml)$$

2.2.6 Restriction digestion

Restriction digestion of plasmid DNA was performed using 10 units (U) restriction endonuclease to approximately 5 μg DNA. The appropriate 10 x buffer and the appropriate volume of water were added according to the manufacturer's instructions. The reaction was incubated for 2 hours at 37^0C. Double digestions were performed by the addition of a second enzyme to the reaction.

2.2.7 DNA gel electrophoresis

DNA was analysed on 1% agarose gels. Agarose (0.5 g) was mixed with 50 ml of 1 X TBE in a conical flask. The mixture was heated on full power in a microwave for approximately 2 minutes and swirled. Ethidium bromide (0.5 μl) was added and the mixture poured into a ready made gel kit and allowed to set. The comb was then removed to create the loading wells. DNA samples were mixed with 10% DNA loading dye (50% glycerol, 0.1 M EDTA, 0.3% bromophenol blue) at a ratio of 10 (sample) :1 (loading dye) and loaded onto the gel. Gene Ruler 1 Kb DNA marker (2.5 μl) was added to one well and electrophoresis performed at 80 V for 45 minutes.

2.2.8 DNA sequencing

DNA samples were sent to LARK Technologies (Takely, Essex UK) accompanied by appropriate oligonucleotides for sequencing. Upon return, the sequencing data were analysed using Gene Jockey or CLC Free Work Bench 3 computer software.

2.2.9 Oligonucleotide design for mutagenesis

Oligonucleotides were designed for site-directed mutagenesis according to recommended specifications. Oligonucleotides were approximately 30 bp in length for a forward primer (upper sequence on diagram) and 35 bp for a reverse primer (lower sequence on diagram). They possessed various essential features as illustrated:

Mutation
site
← Overlapping region → ↓ ← Extended →
5' AGCTTGGAGACTTTGGGCTAGGTAGAATATTAA 3'
3' CGTTCGTTTTGCAGTTCGAACCTCTGAAACCCGAT 5'
← Extended region →← Overlapping region →

Designs for oligonucleotides were sent to Invitrogen for synthesis. The synthesised oligonucleotides were diluted to 100 μM concentration and stored at -80^{0}C.

2.2.10 Site-directed mutagenesis

The Gene Tailor Site-Directed Mutagenesis System (Invitrogen) was used according to manufacturer's instructions. Firstly, 100 ng of plasmid DNA was combined with 1.6 μl methylation buffer, 1.6 μl 10X SAM, 4 U/μl DNA methylase and 16 μl sterile distilled water. The methylation mixture was incubated at 37^{0}C for 1 hour and then stored at -20^{0}C. Next the methylated plasmid was PCR amplified. Methylated DNA (12 ng) was combined with 1.5 μl of 10 μM forward and reverse primers, 10 mM dNTPs, 10X Expand buffer and 2.5 U of Expand enzyme to a total volume of 50 μl with sterile water. The PCR mix was thermocycled according to the cycle format:

Time (secs)	Temperature (^{0}C)	Cycles
120	94	1
30	94	25
30	48	
60 (per Kb DNA)	72	
600	72	1
∝	4	1

The PCR mix (10 μl) was analysed by DNA gel electrophoresis to check for the presence of DNA at the correct size. The reaction was stored at 4^{0}C prior to transformation into DH5α-T$_1$ *E. coli* cells.

2.3 Protein techniques

2.3.1 SDS-Polyacrylamide Gel Electrophoresis (SDS-PAGE)

Gel casting apparatus was assembled according to manufacturer's instructions (Biorad miniprotean gel system). A lower resolving gel solution was prepared to produce a final acrylamide concentration of 10, 12 or 15% as follows:

Resolving gel	**10%**	**12%**	**15%**
Protogel (30% acrylamide)	2.0 ml	2.4 ml	3.0 ml
Water	2.5 ml	2.1 ml	1.5 ml
Lower Tris (1.5 M Tris pH 8.8, 0.4% SDS)	1.5 ml	1.5 ml	1.5 ml
10% Ammonium Persulphate	75 µl	75 µl	75 µl
TEMED	5 µl	5 µl	5 µl
Protein size for analysis (kDa)	40-100	20-70	15-40

TEMED was the final component to be added. The mixture was swirled immediately and poured into the gap between the glass plates. The acrylamide mixture was covered in a layer of water-saturated isobutanol and left to set in a vertical position at room temperature. The isobutanol was then washed from the top of the gel with distilled water. Any remaining fluid was thoroughly drained. The upper stacking gel (0.65 ml 'Protogel' (30% acrylamide), 3 ml distilled water, 1.25 ml upper Tris (0.5 M Tris-HCl, pH 6.8, 0.4% SDS), 75 µl 10% APS, 5 µl Temed) was prepared to produce a final acrylamide concentration of 4% with TEMED being the final component to be added. The mixture was swirled immediately and poured onto the surface of the resolving gel. A clean Teflon comb to create the loading wells was immediately inserted into the stacking gel and removed once the stacking gel was set. The gel was then assembled with the electrophoresis apparatus. Samples were boiled with 3x Laemmli protein sample buffer for 5 minutes and the appropriate volume loaded into each well. Precision Plus marker proteins were added to one well to indicate protein size. The gel was submerged with 1x gel running buffer (0.3% Tris, 1.44% Glycine, 0.1% SDS, pH 8.3) and proteins separated at 180 volts at room temperature for 1 hour.

2.3.2 Coomassie Blue Staining

The SDS-Polyacrylamide gel was removed from the electrophoresis apparatus and the upper resolving gel discarded. The separating gel was stained with Coomassie Brilliant Blue (0.25% Coomassie Brilliant Blue, 40 % IMS, 10% acetic acid) for 30 minutes on a rocking platform. The gel was washed in destain (25% IMS, 7.5% acetic acid) for approximately 30 minutes until protein bands were clearly visible. Gels were dried under vacuum at 80^0C for 1-2 hours. Once dried, radioactive gels were placed into a cassette and exposed to X-ray film for appropriate periods of time.

2.3.3 Silver staining

Following electrophoresis the upper gel was discarded and the lower gel rinsed in distilled water for 1 minute before being submersed in 40% methanol (v/v), 10% acetic acid (v/v) for 15 minutes. The gel was then washed in distilled water 3 times at 5 minutes intervals. The gel was transferred to a solution of 25% methanol, 10% acetic acid (v/v) for 15 minutes. The gel was washed in distilled water 3 times every 5 minutes before being oxidised in 0.25 g/l sodium dithionite for 1 minute. The gel was washed briefly in distilled water then incubated in silver reagent solution supplied by Biorad for 20 minutes. After a brief wash in distilled water the gel was submersed in 33 ml of silver stain developer solution (Biorad kit) until appropriate intensity was achieved. The reaction was stopped by the addition of 5 ml of 30% acetic acid (v/v) for 5 minutes. Finally, the gel was washed in distilled water for 1 minute. This method was used to assess the specificity of potential phosphospecific antibodies generated by Serotec.

2.3.4 Western blotting

SDS-PAGE was performed as above. Following protein separation, the gel was placed on nitrocellulose membrane soaked in Western blotting transfer buffer. This membrane was then placed on 3 sheets of Whatmann 3MM filter paper soaked in transfer buffer on the bottom of a semi-dry Western blot electrophoresis apparatus (Hoeffer). A further 3 pieces of 3MM filter paper soaked in transfer buffer were then placed above the gel. Any air bubbles were carefully removed before the top electrode was fitted above the stack. The gel was left to transfer for 60 minutes at 70 mAmps. The membrane was removed and the proteins stained with Ponceau Red solution. Excess stain was washed off in H_2O and the lanes indicated in pencil. The membrane was then blocked in PBST (1 x PBS, 0.1% Tween-20) or TBST (1 x TBS, 0.1% Tween-20) containing 5% milk (non-phosphospecific antibodies) or 5% BSA (phosphospecific antibodies) and left for 1 hour at room temperature gently shaking. It is generally recommended that immunoblots using phosphospecific antibodies should be performed using BSA instead of milk. Milk contains casein which is a phosphoprotein and causes high background because the phospho-specific antibody detects the casein present in the milk. The membrane was incubated with primary antibody diluted in appropriate volume of PBST or TBST with 5% milk or 5% BSA and incubated on rollers for 1 hour at room temperature. The primary antibody solution was removed and the membrane was washed 3 times with PBST or TBST solution at 5 minute intervals. In between washes the membrane was replaced on the rollers. Next the membrane was incubated for 60 minutes with secondary antibody (AP- or HRP-conjugated) in fresh PBST or TBST containing 5% milk or 5% BSA solution. The membranes were then washed 3 times with 1 x PBS/ 0.1% Tween-20 solution at 5 minute intervals. The membranes previously incubated with AP-conjugated antibodies were then developed by adding an AP buffer containing AP reagents (0.66 mg/ml BCIP, 0.66 mg/ml NBT) and placing on a rocking platform. Once a colour change had developed, the membrane was washed gently in PBST. The membrane was scanned and air-dried on filter paper. The membranes previously incubated with HRP-conjugated antibodies were developed using an ECL protein detection kit. This involved covering the membrane in a developing solution for up to 2 minutes and then drying the membrane and wrapping it in cling film smoothing out any air bubbles. The membrane was then exposed to X-ray film for the appropriate time.

2.3.5 *In vitro* translation (IVT)

Plasmid DNA (1 μg) was gently mixed with 1 μl of ^{35}S-methionine or unlabelled methionine and added to 8 μl T7 Quick Mix on ice. The reaction mixture was incubated at 30^{0}C for 1.5 hours. This mixture (1 μl) was then added to 20 μl 3x sample buffer for SDS-PAGE analysis.

2.3.6 *In vitro* pull-down assays

In vitro protein-protein interactions were investigated using purified tagged proteins and proteins generated by IVT. Glutathione beads (100 μl) were washed three times with 1 x PBS. The beads were incubated either with 5 ml of protein for 1 hour rotating at 4^{0}C. The beads were then washed three times in NETN buffer and finally resuspended in 1 ml of NETN buffer (1 mM EDTA pH 8, 20 mM Tris HCl pH 8, 100 mM NaCl, 0.5% Nonident P40). The beads (250 μl) were centrifuged at 300 g for 2 minutes and the supernatant removed. The beads were then resuspended in 1 ml of NETN buffer and incubated with 7 μl of protein translated *in vitro* for 2 hours rotating at 4^{0}C. Following three washes in NETN buffer, a fraction of the beads was resuspended in 20 μl of 3 x Laemmli protein sample buffer, whilst the remainder was stored at 4^{0}C. Binding efficiency was determined by SDS-PAGE, autoradiography and detection by X-ray film.

2.3.7 Immunoprecipitation (IP)

Protein G-sepharose beads (50 µl) were transferred to an eppendorf using a cut pipette tip. The beads were washed 3 times in 100 µl of 1 x PBS to remove excess storage buffer. To pre-clear the sample, 10 µl of IVT mix or 40 µl of cell lysate was added to 490 µl of Nek2 extraction buffer (NEB) solution (50 mM Hepes-KOH, pH 7.4, 5 mM $MnCl_2$, 10 mM $MgCl_2$, 5 mM EGTA, 2 mM EDTA, 100 mM NaCl, 5 mM KCl, 0.1% $_{(v/v)}$ Nonidet P-40, 30 µg/ml Rnase A, 30 µg/ml Dnase I, 1 mM phenylmethylsulfonyl fluoride (PMSF), 10 µg/ml leupeptin, 1 µg/ml pepstatin A, 1% aprotinin $_{(v/v)}$, 20 mM β-glycerophosphate, 20 mM sodium fluoride). Pre-washed beads (10 µl) was added to the diluted protein mix and incubated for 30 minutes at 4^0C with rotation. The protein/bead mix was spun for 15 seconds and the supernatant transferred to a new tube on ice. Anti-myc antibody was added to the supernatant and incubated for 1 hour on ice. The remaining beads were blocked with rabbit reticulocyte lysate diluted in NEB buffer by rotating at 4^0C for 30 minutes. This was followed by 3 washes in 100 µl of NEB and resuspended in 50 µl of NEB. Blocked bead slurry (40 µl) was added to the protein-antibody mix and incubated at 4^0C for 60 minutes with rotation. The protein/bead/antibody mixture was spun in a cooled centrifuge at 11,300 g for 15 seconds to collect the antibody bound protein attached to beads. Finally, the beads were either stored at -80^0C or washed 3 times in 100 µl of kinase buffer for a kinase assay.

2.3.8 Kinase Assay

Immune-complex beads were washed 3 times in 100 µl of kinase buffer (50 mM Hepes.KOH, pH 7.4, 5 mM $MnCl_2$, 5 mM β-glycerophosphate, 5 mM sodium fluoride, 1 mM dithiothreitol (DTT)). The supernatant was then completely aspirated, and the beads resuspended in 45 µl of kinase buffer containing additional components: 4 µM ATP, 10 µCi ^{32}P-γ-[ATP], 0.5 mg/ml dephosphorylated β-casein (substrate protein), and incubated at 30^0C for 30 minutes. The kinase reaction was stopped by adding 50 µl of 3x Laemmli protein sample buffer and samples boiled at 95^0C for 3 minutes prior to SDS-PAGE analysis. Finally, the gel was exposed to X-ray film to detect the phosphorylated β-casein.

2.4 Protein expression and purification

2.4.1 Expression of proteins in bacteria

Prokaryotic expression vectors were transformed into *E. coli* (Rosetta DE3, BL21). One colony was selected and added to a starter culture of 5 ml LB containing appropriate antibiotic and grown O/N shaking at 37^{0}C. The starter culture was added to 1 litre of pre-warmed LB and grown at 30^{0}C until the OD_{600} reached 0.2 (approximately 2 hours). β-D-isopropyl-thiogalactopyranoside (IPTG) was then added to a final concentration of 1 mM to induce protein expression. The cultures were grown for 5 hours at 30^{0}C with shaking.

2.4.2 Purification of His- and GST- tagged fusion proteins

Bacterial cultures were spun at 6000 g for 20 minutes and the supernatant removed. The pellet was resuspended in 20 ml lysis buffer (50 mM NaH_2PO_4 pH 8.0, 300 mM NaCl (plus 10 mM imidazole for His-tagged proteins) containing 1 mg/ml of lysozyme on ice. The sample was incubated on ice for 30 minutes before sonication on ice (MSE soniprep 150, 10 mm probe, amplitude 12 μm) with six 10 second bursts at 200-300 W with a 10 second cooling period between bursts. The sample was then centrifuged at 11,000 rpm for 45 minutes at 4^{0}C in a Sorvall SS-34 rotor to remove cell debris. The supernatant was stored at -80^{0}C as soluble protein. This soluble protein (4 ml) was purified by passing through a column containing 1 ml of Ni-NTA (nickel nitrilotriacetic acid) beads (for His-tagged proteins) or glutathione beads (for GST-tagged proteins). The column was washed with 8 ml of wash buffer (8 ml lysis buffer plus 1M NaCl) then four 1 ml volumes of elution buffer (lysis buffer plus 150 mM imidazole) were passed through the column to elute the protein. Samples were taken throughout the procedure for SDS-PAGE analysis to determine the solubility and purity of the eluted protein.

2.5 Cell biology techniques

2.5.1 Maintenance and storage of cells

U2OS cells were grown at 37^{0}C in a 5% CO_2 environment. The cells were grown in Dulbecco’s Modified Eagles Medium (DMEM) supplemented with 10% fetal bovine serum (FBS) and penicillin-streptomycin (100 IU/ml and 100 μg/ml, respectively). Every 3-4 days the cells on each dish were split to prevent overcrowding. The medium was removed and the cells washed in 1x PBS. Each dish was incubated with PBS containing 0.5 mM EDTA for 5 minutes. The cell suspension was pipetted up and down to separate the cells. The cell suspension (75%) was transferred to a waste container. Fresh media was added to the remaining cell suspension. The plate was gently agitated and then placed in the incubator. Cells were stored long-term by freezing in liquid nitrogen. Cells were grown to 80-90% confluent then washed in 1 x PBS. Cells were lifted from the plates by incubating with PBS-

EDTA for 8 minutes and transferred to a centrifuge tube and spun at 454 g for 5 minutes. The supernatant was aspirated and pellet resuspended in 1 ml of 10% DMSO/90% FBS in cryotubes. Cells were gradually frozen from -20 ^{0}C to -80 ^{0}C O/N then stored in liquid nitrogen.

2.5.2 Transfection of cells

Cells were grown on either 10 cm dishes or 6 well plates in order to reach 80% confluency prior to transfection. Plasmid DNA (4 μg (10 cm dish) or 1 μg (per well)) was mixed with 1000 μl or 250 μl of DMEM medium (without FBS or Pen/Strep), respectively. In a separate tube, 16 μl or 4 μl of lipofectamine reagent (Invitrogen) was mixed with 1000 μl or 250 μl of DMEM, respectively. The lipofectamine mixture was then added to the DNA mixture and incubated at room temperature for 20-30 minutes. The medium on the cells was replaced with fresh DMEM (containing 10% FCS and 1% Pen/Strep). The lipofectamine/DNA mixture was added dropwise to each plate, producing a final volume of 10 ml (10 cm dish) or 2.5 ml (per well). After incubation at 37^{0}C for 4-6 hours, the medium was replaced with DMEM (containing 10% FBS and 1% Pen/Strep). At 24 hours post-transfection the cells were either lysed or fixed in methanol.

2.5.3 Cell extractions

Cells were lifted as described previously. Resuspended cells were transferred to a sterile falcon tube and centrifuged at 3225 g for 5 minutes. The supernatant was removed, the pellet resuspended in 200 μl of NEB lysis buffer and transferred to an eppendorf on ice. The lysate was stored on ice for 30 minutes before being passed through a 26 G needle 6 times and centrifuged at 10000 rpm (lab bench microcentrifuge) for 10 minutes at 4^{0}C. The supernatant was transferred to a fresh eppendorf on ice. Supernatant (10 μl) was transferred to a new eppendorf for a BCA assay to calculate the protein concentration. The remainder was stored at -80^{0}C until required.

2.5.4 Cell cycle analysis

Cells (1 x 10^4) were seeded on 6 cm dishes. After 24 hours cells were lifted from the plate and centrifuged for 5 minutes at 806 g. The supernatant was removed and the pellet resuspended in 2 ml PBS. Ice cold ethanol (2 ml) was added dropwise whilst vortexing. The cells were stored at 4^{0}C. After 24 hours the cells were spun down at 244 g for 10 minutes and the pellet resuspended in 800 μl of 1 x PBS to which 100 μl of propidium iodide (50 μg/ml) and 100 μl of RNaseA (1 mg/ml) were added. The cells were incubated at 4^{0}C for 16 hours.

The stained cells were then transferred to FACS tubes and resuspended prior to cell cycle analysis using a Becton Dickinson FACScan II flow cytometer. Cell preparations were examined using Cell Quest software and analysed using a Modfit LT programme.

2.6 Immunofluorescence microscopy

U2OS cells were plated into 6 well dishes containing circular glass acid-etched coverslips and incubated for at least 24 hours. All medium was removed from the wells and the wells washed in 1x PBS. Approximately 2 mls of ice cold (-20^0C) methanol was added to each well to fix the cells and the coverslips stored at –20^0C O/N. The methanol from each dish was then removed and the coverslips washed 3 times in 1 x PBS at 5 minute intervals to rehydrate the cells. 1% BSA in 1 x PBS solution (2 mls) was added to each coverslip for 10 minutes to block non-specific binding sites. The coverslips were then washed in 1 x PBS every 5 minutes for 15 minutes. Next the coverslips were placed cell side down on 200 μl drops of 3% BSA containing primary antibodies on Nesco film in a moist chamber for 1 hour. The coverslips were then washed 3 times in 1 x PBS over 5 minute periods. A secondary antibody solution previously tested for non-specific labelling, was then prepared in 3% BSA-1 x PBS in an eppendorf. The cell side of each coverslip was then placed on 200 μl of secondary antibody solution on fresh Nesco film in a moist chamber for 1 hour. The coverslips were washed in 1 x PBS every 5 minutes for 15 minutes. The coverslips were then dipped in distilled water and placed onto 40 μl drops of mounting fluid (80% glycerol, 3% n-propylgallate) on a glass microscope slide. The edges of each coverslip were sealed with clear nail varnish and left to dry for 10 minutes. The slides were stored at 4^0C and viewed using a 63x or 100x oil objective lens on a Nikon TE300 microscope equipped for fluorescence microscopy. Images were captured using an ORCA ER Hamamatsu cooled CCD camera driven by Openlab software (Improvision). All images were imported into PhotoShop (Adobe), pseudocoloured and printed.

2.7 Antibody generation and purification

2.7.1 Phosphospecific antibody generation

A synthetic phosphorylated peptide TSFAKpTFVGTPC, corresponding to amino acids 170-180 of the activation loop of human Nek2 plus a C-terminal cysteine residue, was synthesised by Severn Biotechnology Ltd. The peptide was then used to immunise two rabbits chosen after examination of the pre-immune sera. The reactivity of the immune sera against endogenous, *in vitro* translated and transfected Nek2 proteins was determined by Western blotting, dot blots and immunofluorescence microscopy.

2.7.2 Preparation of affinity purification columns

Two columns were prepared, one with the phosphorylated-peptide (phospho column) and the other with the non-phosphorylated version of the same peptide (non-phospho-column). The peptides were covalently coupled via the C-terminal cysteine to a sulfolink coupling gel support provided by Pierce Biotechnology according to manufacturer’s instructions. The columns were stored at 4^0C.

2.7.3 Affinity purification of Nek2 phosphospecific antibodies

The peptide coupled columns were equilibrated to room temperature and washed to remove excess storage buffer. Serum (1.5 ml) was applied to each column and the columns incubated for 1 hour according to the manufacturer’s protocol. The flow through from each column was collected and stored at 4^0C. The flow through from the non-phospho-column was labelled as the phosphospecific antibody. The columns were washed in sample buffer and the wash retained. The bound protein was eluted by applying glycine buffer and collected in 1 ml fractions. A BCA assay was performed on all fractions and the most concentrated stored at 4^0C. The affinity of the flow through to detect a phosphorylated peptide was then compared to that of the bound protein.

2.8 Quantification techniques

2.8.1 Quantification of protein concentration

Protein concentration was determined by a Bicinchoninic acid (BCA) assay following manufacturer’s instructions (Pierce). Protein concentrations were estimated by correlating absorbance values to values of protein concentrations from a standard curve of BSA concentrations.

2.8.2 Scintillation counting

Bands on dried Coomassie Blue stained radioactive gels were cut out and placed in scintillation vials. Scintillation fluid (3 mls) was added to each vial. Samples were analysed for 1 minute using a Beckman Coulter$_{TM}$ LS6500 Multi-purpose Scintillation Counter. The counts per minute obtained for each sample indicated the level of radioactivity incorporated into the substrate.

2.8.3 Quantification of kinase activity

The kinase activity of different Nek2 proteins was determined using an *in vitro* kinase assay. Firstly, the amount of radioactivity incorporated into the substrate protein was determined by calculating the mean scintillation counts per minute for each sample minus the background. This was expressed as a percentage of the activity of the Nek2A-WT kinase, which was taken as 100%. Secondly, the amount of Nek2 protein immunoprecipitated for each reaction was quantified using NIH image. The protein bands on a scanned Western blot of the IPs were selected and the mean pixel intensity calculated. The background value was subtracted and the amount of protein present in each IP calculated as a percentage of the amount of Nek2-WT protein, which was taken as 1.0. The activity of each protein previously calculated by scintillation counting was then divided by the amount of protein immunoprecipitated.

2.8.4 Quantification of centrosome splitting

Centrosome splitting was determined by assessing the distance between two centrosomes within each cell by immunofluorescence microscopy following staining, usually with antibodies against γ-tubulin. U2OS cells were chosen for this technique as the centrioles are generally close together therefore any centrosome separation is clearly visible. Centrosomes were classed as split if the centrosomes were greater than 2 μm apart, otherwise they were classed as non-split. Transfected cells were identified by the anti-myc antibody staining (green) at the centrosome. Cells were counted in each field of view moving across the coverslip in a way that ensures the same cells are not counted twice. One hundred transfected cells were counted per coverslip in 3 separate experiments performed on different occasions. The number of cells exhibiting split centrosomes was expressed as a percentage of the total cells counted.

2.8.5 Quantification of protein band intensity

The relative abundance of protein within a band observed on a gel or autorad was measured using NIH image software. Intensity measurements were taken by selecting a region of interest box which remained the same size when calculating each protein band. The box covered the size of the biggest band and the pixel intensity within this box was measured. A background measurement was taken and subtracted from the total intensity for each sample.

The intensities were compared in a histogram to identify changes in abundance of the protein in question.

2.8.5 Statistics

Unless otherwise stated, statistical significance was deteremined using the standard student's *t*-test. A *p*-value of ≤ 0.05 was considered significant.

Chapter Three

Regulation of the Nek2 Protein Kinase by Autophosphorylation

3.1 Introduction

Increasing evidence supports a crucial role for the Nek2 protein kinase both in cell cycle progression and centrosome organisation. Some possible substrates for Nek2 protein have been identified, although it remains unclear which sites are targeted for phosphorylation by Nek2. The activity of almost all kinases is regulated by protein phosphorylation. This frequently occurs within the activation loop (T-loop) of the catalytic domain. The activation loop is a 20-25 amino acid sequence between and including the DFG motif and the APE motif (Johnson et al., 1996). Phosphorylation of this activation loop activates the kinase by stabilising the active conformation or destabilising the inactive conformation and ensuring the correct positioning for substrate binding and phosphate transfer to occur (Johnson et al., 1996). This was first described in protein kinase A (PKA) and many other protein kinases have since been identified which are activated by phosphorylation of their T-loop residues. Examples of these kinases and the position of their phosphorylation sites are Plk1 (T210), Pak1 (T212), Msp1 (T676) and Nek6 (S206) (Banerjee et al., 2002; Belham et al., 2003; Jang et al., 2002; Mattison et al, 2007). Similar to these kinases Nek2 undergoes autophosphorylation, is predominantly phosphorylated on serine and threonine residues and contains a conserved activation loop (residues 159-186) within the catalytic domain (Fry et al, 1995). However, it is not fully understood how Nek2A is regulated by phosphorylation.

Thirteen autophosphorylation sites have been identified within Nek2 by mass spectrometry, which may play a role in the regulation of Nek2 activity (Figure 1.10). It is possible that Nek2A may undergo autophosphorylation at multiple sites in order to achieve full activation. Autophosphorylation within the N-terminal kinase domain is most likely to regulate Nek2 activity. However, autophosphorylation within the C-terminal domain may have various consequences in terms of Nek2 regulation, as this region contains the PP1 binding site that regulates Nek2 kinase activity and sites involved in Nek2 degradation, as well as localisation. In addition, the C-terminus may exert its own regulation of Nek2A activity by acting as an autoinhibitory domain by interacting with the N-terminal domain, thus blocking the active site. Phosphorylation of the C-terminus may therefore prevent autoinhibition.

A previous PhD student in the lab, Dr. Baxter, generated a series of phosphorylation site mutants of the Nek2 kinase based on the residues identified by mass spectrometry (Baxter, 2006). She used a site-directed mutagenesis approach to introduce mutations at the phosphorylation site to create potentially hyperactive or inactive Nek2 proteins (Figure 1.11). Serines (S) or threonines (T) were mutated to the acidic residues, aspartate (D) or glutamate (E) respectively, in an attempt to mimic the shape and charge of a phosphorylated residue. In addition, serines and threonines were mutated to alanine to mimic the unphosphorylated state of Nek2 and prevent phosphorylation.

Preliminary results did not show any significant difference in activity upon mutation of T170 and S171 compared to WT-Nek2A (Figure 1.11). In contrast, mutation of T175 to alanine abolished Nek2A activity *in vitro,* whereas mutation to glutamate resulted in a hyperactive kinase (Figure 1.11). Mutation of T179 and S241 to alanine, or to glutamate or aspartate, respectively, significantly reduced Nek2 kinase activity (Figure 1.11). Dr. Baxter also generated single constructs that contained combined mutations of four autophosphorylation sites, S387, S390, S397 and S403 within the C-terminus. These sites were all mutated to alanine in one construct (Nek2A-SA_4) and to aspartate in another construct (Nek2A-SD_4). Mutation of these sites had little effect upon binding of PP1 to Nek2A despite the proximity to the PP1 binding site (residues 383-386). The Nek2A-SD_4 mutations produced a hyperactive kinase, though mutation of these sites to alanine did not affect Nek2A activity *in vitro* or *in vivo* (Figure 1.11). She concluded that Nek2A is regulated by phosphorylation at T175 and by structural or secondary autophosphorylation events at positions T179 and S241. Phosphorylation of T175 is thought to be essential for stabilising the active conformation of Nek2 for substrate binding and phospho transfer. On the other hand it is possible that phosphorylation of T179 and S241 is inhibitory. However, the role of autophosphorylation in the C-terminal region of Nek2A remains obscure.

Dr. Baxter initiated the characterisation of many constructs outlined in Figure 1.11. However, in several cases the activity was only partially tested or never tested by each of the assays indicated in Figure 1.11. The first aim of the project was therefore to complete the Nek2 autophosphorylation study initiated by Dr. Baxter in order to obtain a better understanding of how the Nek2 kinase is regulated and identify which residues are crucial for controlling Nek2 activity. First those mutants not yet made were generated by incorporating a number of point mutations into a pRcCMV:myc-Nek2A vector using a site-directed mutagensis approach. These Nek2 mutants were then characterised as well as some of those previously generated by Dr. Baxter. The consequence of these mutations on Nek2A activity was then analysed by performing two standard experiments: (i) *in vitro* translation of Nek2A constructs, followed by IP and an *in vitro* kinase assay using β-casein as the substrate (active Nek2A kinases will incorporate ^{32}P into the substrate β-casein); (ii) transfection of myc-tagged Nek2A constructs into U2OS cells and quantification of centrosome splitting as a measure of Nek2 activity *in* *vivo*. The level of activity of these mutants obtained by these *in vivo* and *in vitro* techniques would reveal the importance of these sites.

A recent crystallisation study by Prof. S. Smerdon (NIMR, London) has enabled a crystal structure for the N-terminal catalytic domain of the human Nek2A to be obtained. This structure was derived using a T175A mutant kinase domain bound to a pyrrole-indolinone inhibitor (SU11652), so Nek2 is in an inactive state. Comparing the crystal structures of the N-terminal catalytic domain of Nek2A and Aurora A kinase identified a novel αT-helix in Nek2A. This novel αT-helix consists of 5 amino acids (162-166) at the N-terminal end of the activation loop. The role of this αT-helix is unknown, but it may help regulate the positioning of the activation loop, thus blocking and unblocking the active site (Figure 1.7).

Analogue-sensitive kinases are protein kinases which have been engineered to allow inhibitors which are ATP analogues to bind non-competitively only to the engineered kinase (Blethrow et al., 2004; Gregan et al., 2008). This provides a mechanism for inactivating a kinase of interest *in vivo* and *in vitro*. Analogue-sensitive kinases are generated by mutating a bulky, hydrophobic amino acid in subdomain V of the hydrophobic pocket that binds ATP, for an amino acid with a smaller side chain. This changes the shape of the ATP binding pocket allowing an inhibitor molecule, commonly 1NM-PP1, to bind and inhibit the engineered kinase but not the wild-type kinase. The amino acid which is altered is known as the gatekeeper residue. The gatekeeper residue is a conserved residue that can be identified from a sequence alignment of family members. In Nek2A, the gatekeeper residue was identified as M86 using a protein database which aligned the protein sequences of Nek family members (http://kinase.ucsf.edu/ksd/). An analogue specific Nek2A kinase which can be reversibly blocked could be used *in vitro* to identify novel substrates and *in vivo* to determine physiological function.

3.2 Results

3.2.1 Validating the activity assays with wild-type and kinase-inactive Nek2A

Two assays were performed in order to determine the activity of each construct *in vivo* and *in vitro*. These assays were first performed using wild-type Nek2A and Nek2-KR. The kinase-inactive Nek2A-KR construct has a lysine (K) to arginine (R) mutation at position 37 within the ATP binding site which prevents ATP binding and results in significantly reduced kinase activity (Figure 3.1A). Firstly, myc-Nek2A and myc-Nek2A-KR were translated *in vitro* and immunoprecipitated using an anti-myc antibody. The immune complexes were then incubated with kinase buffer containing ^{32}P-γ-[ATP] and casein as the substrate at 30^{0}C for 30 minutes. The amount of protein precipitated was determined by Western blot, while the kinase activity of each Nek2A construct was calculated by scintillation counting of the β-casein substrate (Figure 3.1B and C). The activity was then normalised to the amount of protein precipitated. Kinase activity for Nek2A-WT was set at 100%. In comparison, the Nek2A-KR mutant possessed only 4% activity.

Secondly, an *in vivo* centrosome splitting assay was performed to determine whether the Nek2A constructs localised to the centrosome and induced centrosome splitting. Transfection of wild-type Nek2A into U2OS cells has been consistently shown to induce splitting of centrosomes by >2 µm in 40-60% of interphase cells, whereas only 10% of interphase cells transfected with inactive Nek2A or untransfected cells show split centrosomes (Fry et al., 1998b; Meraldi and Nigg, 2001). Active Nek2A is thought to phosphorylate proteins such as C-Nap1 and rootletin, which are components of the intercentriolar linkage joining a pair of centrioles resulting in separation of the two centrioles (Bahe et al., 2005; Fry et al., 1998a). Based on this evidence, a centrosome splitting assay has been developed as an indication of Nek2A activity in cells. At 24 hours post transfection, U2OS cells are fixed in methanol and probed with antibodies which detect the myc-tagged Nek2A constructs and γ-tubulin which identifies the centrosome. Myc-Nek2A-WT and myc-Nek2A-KR both localised to the centrosome. As predicted, myc-Nek2A-WT induced centrosome splitting in 52% of cells, whereas myc-Nek2A-KR induced centrosome splitting in only 12% of cells. These results confirm that Nek2A-WT is active and the Nek2-KR protein is inactive in this assay.

3.2.2 Phosphomimetic mutations of T170 and S171 increase Nek2A kinase activity

Mass spectrometry performed at the NIMR had identified T170 or S171 as a possible autophosphorylation site, although in information provided by Invitrogen with their recombinant Nek2 kinase only S171 was identified as an autophosphorylation site. However, it is possible that both sites may be phosphorylated. Both sites are located at the start of the activation loop of Nek2A, near residues T175 and T179, which have been previously studied and found to be essential autophosphorylation sites for Nek2A kinase activity. The T170 and S171 sites had been partially characterised by Dr. Baxter in so much as she had made individual T170A, T170E, S171A and S171D mutations in myc-tagged Nek2A constructs and transfected them into cells. She showed that all four mutant Nek2A constructs localised to the centrosome and that centrosome splitting counts for all mutants were similar to those for Nek2A-WT kinase (Baxter, 2006). However, counts from previous splitting assays for various Nek2A mutants, including the T175E mutant that shows hyperactivity in an *in vitro* kinase assay, never rise above Nek2A-WT levels of splitting. A splitting efficiency of 50-60% is therefore considered to be the maximum observable and it is likely that mechanisms exist in cells that prevent centrosome splitting from occurring at higher frequencies. From her data, Dr. Baxter was therefore able to conclude that the mutations do not inhibit Nek2 activity *in vivo*.

This project was initiated at this point to continue the characterisation of these mutants. To assess the activity of these mutants *in vitro*, the mutant constructs were translated *in vitro*, immunoprecipitated and a sample of each examined by Western blotting in order to quantify the level of immunoprecipitation. Next, *in vitro* kinase assays were performed using β-casein as a substrate. Mutation of T170 to alanine induced marginally higher kinase activity than Nek2A-WT, whereas mutation of S171 to alanine did not alter Nek2A kinase activity (Figure 3.2). In contrast, T170E and S171D mutations both resulted in clearly hyperactive kinases. The activity of the Nek2A-T170E mutant was at least 3 times higher than that obtained with the Nek2A-WT, whilst Nek2A-S171D was at least twice as active as Nek2A-WT kinase (Figure 3.2). Upon statistical analysis the results obtained using T170E were found to be highly significant ($P < 0.005$) although disappointingly the results obtained for S171D were of borderline significance ($P = 0.1$). This suggests that autophosphorylation at residues T170 and S171 leads to increased Nek2A kinase activity, although autophosphorylation at these sites is not essential for Nek2A to be in an active state.

3.2.3 Mutation of S356 and S368 does not alter Nek2A activity or localisation

The S356 and S368 sites lie in the regulatory C-terminal domain. The S356 site lies just downstream of the leucine zipper motif of Nek2. It is therefore possible that phosphorylation of this site may regulate Nek2 homodimerisation via this coiled-coil leucine zipper motif. Both sites also lie within the region shown to determine centrosome localisation, so phosphorylation of these sites may regulate localisation. To test these possibilities, these sites were mutated to both alanine and aspartate to determine the effects upon Nek2 kinase activity and localisation. The proteins were translated *in vitro*, immunoprecipitated and kinase assays performed using casein as the substrate as previously described (Figure 3.3). None of the mutations had a significant effect upon Nek2 kinase activity *in vitro* ($P>0.5$ for all except K37R). Similarly, each mutant was found to localise at the centrosome (Figure 3.4). Finally, the centrosome splitting counts revealed no significant difference between the mutants and the Nek2A-WT kinase ($P>0.5$ for all except K37R). These results suggest that phosphorylation of S356 and S368 is not required for Nek2 activity or localisation.

3.2.4 Mutation of S296 or S428 does not alter Nek2A activity or localisation

The S296 and S428 residues lie within the non-catalytic domain of Nek2A. S296 lies at the start of the non-catalytic domain just upstream of the leucine zipper, while S428 lies towards the extreme C-terminal end of Nek2A. It is possible that the C-terminal domain acts as an autoinhibitory domain. If this is true, then mutation of S428 may relieve this inhibitory mechanism and increase Nek2A kinase activity. Individual S296A, S296D, S428A and S428D mutations were made in myc-tagged Nek2A constructs. These mutant constructs were translated *in vitro*, immunoprecipitated using an anti-myc antibody and the immunoprecipitates subjected to a kinase assay with casein as the substrate (Figure 3.5B). After normalisation for the amount of protein precipitate, it appeared that mutation of S296 or S428 to alanine or aspartate had no effect on Nek2 activity as they exhibited a similar level of activity as WT-Nek2A kinase. $P> 0.05$ for all mutants except K37R suggesting there is no significanrt difference compared to the WT kinase (Figure 3.5C). However, one should remain cautious about the result as the amount of protein precipitated varied between the different constructs and the level of activity for S296D and S428A was statistically different to WT. The S296 and S428 mutants were then transfected into U2OS cells and stained with a myc antibody to detect the mutant construct and γ-tubulin to detect the centrosome (Figure 3.6A). The S296 and S428 mutations all induced levels of centrosome splitting similar to that of wild-type Nek2A in 3 separate experiments (Figure 3.6B). Thus, it may be concluded that phosphorylation at these two sites is not essential for Nek2A activity or localisation.

3.2.5 Individual mutation of S387 does not affect Nek2A kinase activity

S387 lies immediately downstream of the KVHF motif (383-386) which binds PP1, within the non-catalytic domain of Nek2A. It is possible that the phosphorylation of S387 may stimulate the release of PP1, relieving Nek2 of this inhibition. Thus an increase in Nek2 activity may be observed with the phosphomimetic S387D mutant. However, a combined mutant including S387D made by Dr. Baxter had not shown increased activity (Baxter, 2006). Additional work by an undergraduate student in the lab, Miss N. Sahota, had created individual S387F and S387E mutations in myc-tagged Nek2A constructs. For this project, these constructs were translated *in vitro*, immunoprecipitated them using an anti-myc antibody and subjected the immunoprecipitates to *in vitro* kinase assays with casein as the substrate (Figure 3.7B). Both S387 mutants exhibited a similar level of kinase activity to WT-Nek2A with no significant difference detected (P>1) (Figure 3.7C). The S387 mutants were then transfected into U2OS cells and stained with an anti-myc antibody (green) to detect the mutant construct and an anti-γ-tubulin antibody (red) to detect the centrosomes (Figure 3.8A). Again, both S387 mutants induced levels of centrosome splitting similar to that of wild type Nek2A in 3 separate experiments (Figure 3.8B). P>1 suggesting there was no significance difference between the activities of the S387 mutants compared to WT kinase. Thus, it was concluded that autophosphorylation of S387 is not essential for Nek2A activity and nor is it likely to stimulate Nek2A activity.

3.2.6 Deletion of the last 61 residues from the C-terminus creates a hyperactive Nek2A protein

It was hypothesised that Nek2A might be negatively regulated through an auto-inhibitory reaction of the non-catalytic domain and the kinase domain reminiscent of certain other protein kinases. Initial experiments carried out by Dr. Baxter involved the generation of a truncated GFP-Nek2A-ΔC25 mutant construct that lacked the C-terminal 25 amino acids. This mutant construct was transfected into cells and kinase assays performed on immunoprecipitated protein suggested that this mutant kinase was significantly more active compared to WT-Nek2A (Baxter, 2006). Prof. Andrew Fry has previously created three myc-Nek2A constructs named myc-Nek2-ΔC24 and myc-Nek2-ΔC51 truncated at positions 421 and 394, respectively (Figure 3.9A). He also created a myc-Nek2B construct. Nek2B is a splice variant of Nek2A which lacks the last 61 amino acids of the C-terminus present in Nek2A (Figure 3.9A). These constructs were transiently transfected into U2OS cells and stained with an anti-myc antibody to detect the mutant construct and an anti-γ-tubulin

antibody to detect the centrosome. All constructs localised to the centrosome consistent with previous data that the centrosomal targeting region lies within residues 333-370 (Hames et al., 2005) (Figure 3.9B). Next the Nek2 constructs were translated *in vitro* and immunoprecipitated using an anti-myc antibody. A kinase assay was performed with the immunoprecipitate using casein as the substrate (Figure 3.10B). The kinase activity of each mutant was calculated by scintillation counting and quantified against the amount of protein immunoprecipitated compared to WT-Nek2A kinase which was set at 100%. The kinase activity of the myc-Nek2A-ΔC_{24} and myc-Nek2A-ΔC_{51} constructs was similar to that of Nek2A. However, Nek2B exhibited a significantly higher level of kinase activity compared to Nek2A kinase. These results suggest that truncation of the last 61 residues of the C-terminus of Nek2 increases the activity of the kinase.

3.2.7 Mutation of A163 in the αT-helix leads to loss of Nek2A activity

A recently solved crystal structure of the Nek2 kinase domain revealed the presence of a novel αT-helix close to the active site. This helix would appear to block the entrance to the active site thus inactivating the kinase. Mutation of a key residue within the αT-helix may cause the collapse of the αT-helix and induce the activation loop to move away from the active site. This might create a constitutively active kinase. Interestingly, S241 had previously been shown to be an autophosphorylation site and despite the fact that it is far from the active site, mutation to an alanine or aspartate created an inactive kinase thus suggesting that this residue plays an important role in the regulation of Nek2 activity. One possible explanation is that phosphorylation of S241 might cause the αT-helix to melt. It was hypothesised that an A163G point mutation may cause the helix to collapse and compensate for the inhibitory effect induced by S241A or S241D mutations. If this hypothesis was true, then it would be expected that an A163G/S241A or A163G/S241D mutant would exhibit increased kinase activity compared to an S241A or D mutant.

An A163G point mutation was introduced into the S241A and S241D mutant Nek2 constructs previously created in the lab to create double mutants. To determine the effect of an A163G mutation alone a single point mutation was also introduced into the myc-Nek2A construct. These Nek2 constructs were translated *in vitro* and immunoprecipitated using a myc antibody. A kinase assay was then performed on the immunoprecipitate using casein as the substrate (Figure 3.11). The kinase activity of each mutant was calculated by scintillation counting and quantified against the amount of protein immunoprecipitated compared to Nek2A kinase

which was set at 100%. As previously shown, the S241A and S241D mutants were found to be inactive. Unexpectedly, an A163G mutation in the T-helix created an inactive kinase rather than a constitutively active kinase. Not surprisingly the A163G/S241A or D double mutants were also found to be inactive. All the mutant Nek2 kinases exhibited similar levels of inactivity compared to the Nek2A-K37R protein. $P< 0.001$ for all mutant kinases compared to WT kinase suggesting there is a significant decrease in kinase activity (Figure 3.11). Thus, it can be concluded that collapse of the αT-helix inactivates rather than activates Nek2A.

3.2.8 Mutation of other residues within the αT-helix results in loss of Nek2A kinase activity

Following the observation that an A163G point mutation in the αT-helix creates an inactive Nek2A kinase, two additional αT-helix mutants, αT3 and αT4 were generated. The double mutant, αT3, contains an I165G in addition to the A163G mutation. The triple mutant, αT4 contains combined L162K, R164K and L166K mutations. The aim was to determine whether artificially collapsing the helix in different ways also results in a loss of Nek2A kinase. Triple and double point mutations were created in myc-tagged Nek2A constructs. These mutant constructs were translated *in vitro*, immunoprecipitated using an anti-myc antibody and the immunoprecipitates subjected to a kinase assay with casein as the substrate (Figure 3.12B). The kinase activity was calculated by scintillation counting and quantified against the amount of protein immunoprecipitated (Figure 3.12B). Values were compared to WT-Nek2 which was set at 100%. Similar to the A163 mutants, the αT3 and αT4 mutants also exhibited a highly significant loss of kinase activity compared to WT kinase ($P>0.001$) (Figure 3.12A). Thus, any disruption of the αT-helix leads to loss of Nek2 activity.

3.2.9 Mutation of the gatekeeper residue M86 leads to loss of Nek2A kinase activity

The M86 residue lies within the ATP-binding pocket of the catalytic domain of Nek2A. M86 is proposed to act as the gatekeeper residue and limit the size of the nucleotide that can access the active site. Mutation of M86G to glycine or alanine may widen the ATP binding pocket thus allowing not only ATP but also the ATP analogue, 1NM-PP1, to bind. If this was true then mutation of M86 would generate an analogue-sensitive Nek2A kinase which will be active in the absence, but inactive in the presence of the inhibitor, 1NM-PP1. The aim was to generate a Nek2 kinase whose activity can be switched off by the addition of this drug allowing the consequences of inhibiting Nek2A to be investigated. Individual M86G and generate a Nek2 kinase whose activity can be switched off by the addition of this drug allowing the consequences of inhibiting Nek2A to be investigated. Individual M86G and M86A mutations were created in myc-tagged Nek2A constructs. These mutant constructs were translated *in vitro*, immunoprecipitated using an anti-myc antibody and the immunoprecipitate subjected to a kinase assay with casein as the substrate (Figure 3.13B). Unexpectedly, both the M86 mutants exhibited a highly significant loss of kinase activity compared to WT-Nek2A ($P>0.001$), with a similar level of activity to that exhibited by the inactive Nek2-K37R mutant (Figure 3.13C). This means that simple mutation of the M86 gatekeeper residue cannot be used to generate an analogue-sensitive Nek2A kinase.

3.3 Discussion

In this chapter the role of 7 out of a possible 13 autophosphorylation sites within the catalytic and non-catalytic domain of Nek2A as identified by mass spectrometry was investigated. Previous data indicated that T175 is most probably the primary site of autophosphorylation within the activation loop with a second sequential autophosphorylation event occurring at T179. However, additional phosphorylation sites may be required for full activation of the kinase. These results suggest that phosphorylation of residues T170 and S171 within the activation loop are both likely to contribute to Nek2A kinase activity. Phosphomimetic mutations of T170 and S171 produced increased levels of kinase activity and maximal levels of centrosome splitting, although mutation to an unphosphorylated state did not reduce Nek2A kinase activity. Therefore, phosphorylation of these sites is not essential for Nek2 kinase activity, but appears to enhance Nek2A activity and may fine-tune the overall activity of Nek2 *in vivo*. The phosphorylation of T175 and T179 is most likely required for the release of the activation loop from the active site thus allowing entry of substrates. The phosphorylation of T170 and S171 may not be required to release the activation loop, but may stabilise the activation loop in the open conformation, thus facilitating access of substrates to the active site and greatly increasing the rate of phosphorylation (Nolen et al., 2004). In addition, phosphorylation of these activation loop residues may create extra ionic interactions with the αC helix within the N-lobe, thereby promoting tighter closure of the N- and C-lobes, increasing kinase activity (Huse and Kuriyan, 2002).

In addition to these two residues, the roles of S296, S356, S368, S387 and S428 present in the non-catalytic C-terminal domain were investigated. It was proposed that these residues might play a role in regulating Nek2 kinase activity possibly by influencing its dimerisation or interaction with PP1. In particular, S296 and S356 are found close to either end of the leucine zipper motif and so phosphorylation of these sites could alter homodimerisation. In turn, this could further regulate trans-autophosphorylation and phosphorylation of activation loop residues (Kang et al., 2004). S387 is positioned immediately after the PP1 binding site and phosphorylation of this site could prevent PP1 binding thus enhancing Nek2A activity. Finally, S428 is located towards the extreme C-terminus, which may act as an autoinhibitiory domain; therefore, phosphorylation of this residue may influence the autoinhibitory activity of this domain. *In vitro* kinase assays were performed on immunoprecipitated proteins, as well as centrosome splitting assays on transfected cells to determine whether mutation of these sites altered Nek2 kinase activity. However, these results did not show any significant difference in kinase activity upon mutation of these sites to alanine or putative phosphomimetic residues. These results therefore suggest that these C-terminal sites are not important for regulating Nek2A activity or its centrosomal localisation. If these sites are autophosphorylation sites, they may play other roles that are undetectable in these two assays. One possibility is that phosphorylation of C-terminal residues may facilitate the interaction of Nek2A with various substrate proteins. For example, phosphorylation of MCAK is required to facilitate the tight interaction of MCAK with microtubules so that MCAK can carry out its function in promoting microtubule depolymerisation (Ems-McClung et al., 2004).

Autoinhibition provides a second mechanism by which many kinases are regulated in addition to autophosphorylation. A well characterised example is Plk1 for which C-terminal truncation significantly increases kinase activity (Jang et al., 2002; Mundt et al., 1997). Kinase assays were performed with two truncated Nek2A mutants as well as a myc-Nek2B construct to investigate whether the extreme C-terminal region of Nek2A acts as an autoinhibitory domains. If this was true then deletion of these C-terminal residues may confer hyperactivity. This was observed in the case of Nek2B which showed a 20% increase in Nek2 kinase activity compared to WT kinase. However, the kinase activities of myc-Nek2-ΔC_{24} and myc-Nek2-ΔC_{51} truncated at positions 421 and 394, respectively were unchanged compared to wild-type Nek2A in this assay. This latter observation supports the previous result that mutation of the potential phosphorylation site S428 has no effect on the kinase activity of Nek2A. An explanation for these results may be that an autoinhibitory domain does exist in the Nek2 kinase which is missing in Nek2B hence inducing hyperactivity (which is unlikely caused by the lack of the PP1 binding site as phosphatase inhibitors were present in the assay). However, a truncation of 24 or 51 residues is not considerable enough to affect the autoinhibitory domain. These results suggest that the C-terminal amino acids may be important for activation of the kinase and may act as autoinhibitory domain. It is possible that the conditions of this assay may not have been appropriate for autoinhibition to occur and may explain why an increase in activity was only observed for Nek2B. In some proteins which exhibit autoinhibition, the C-terminus is proteolytically cleaved and subsequently forms a complex with the kinase domain of the truncated protein, as seen for example in the calcium ion channel, Ca(V)1.2 (Hulme et al., 2006). If this is true of Nek2A then the wild-type-Nek2A kinase may not be able to undergo autoinhibition as the cleavage enzymes are not present in the kinase buffer. Another possibility is that the Nek2A kinase is not folded into the correct tertiary structure *in vitro* to allow autoinhibition to occur in this assay. This kinase assay did not support previous evidence by Dr. Baxter which showed a Nek2A construct with a 25 amino acid deletion conferred hyperactivity. However, Dr. Baxter’s result was obtained with a GFP-tagged construct immunoprecipitated from transfected cells rather than from protein generated by *in vitro* translation. More investigation is clearly required to reconcile these differences and draw firm conclusions on whether the C-terminal of Nek2A is indeed an autoinhibitory domain.

Next, the role of the novel αT-helix identified in the crystal structure of the catalytic N-terminal domain of Nek2 complexed with a small molecule inhibitor was investigated (Rellos et al., 2007). The αT-helix is present at the N-terminal end of the activation loop. It was hypothesised that an A163G mutation may artificially collapse the αT-helix moving the activation loop away from the active site thus creating a constitutively active kinase. Furthermore, mass spectrometry had identified S241 at the C-terminal end of the catalytic domain as an autophosphorylation site and mutational analysis had revealed that this is a critical site for regulating Nek2A kinase activity despite its distance from the active site. It was hypothesised that the hyperactivity induced by an A163G mutation might counter-balance the inhibitory mutation of S241. To test this hypothesis, kinase assays were performed with A163G, S241A, S241D and the double mutants: S241A/A163G and S241D/A163G. Unexpectedly, all of these Nek2 mutants displayed complete loss of kinase activity. Indeed, an A163G mutation alone created an inactive Nek2A kinase and thus could not rescue the inactivity caused by S241 mutations. Although this result did not support the proposed model, it did show that this residue is clearly important for Nek2A activity. Further attempts to collapse the αT-helix by inserting lysines or glycines at alternating positions of the αT-helix also led to loss of kinase activity. The Nek2A-L162K/R164K/L166K triple mutant was inactive indicating that at least one if not all these residues are also critical for Nek2A activation. Although the Nek2A-A163G/I165G double mutant was also inactive, this could be due to the presence of the A163G mutation which individually exhibits inactivity. Single mutants of these 4 residues would need to be generated and their activities tested to confirm that mutation of any residue of this helix confers inactivity on the kinase. In summary, these results suggest that mutation of αT-helix residues creates inactive Nek2A kinases. An explanation for this result may be that mutation causes the αT-helix to collapse into the active site blocking the entry of substrates rather than promoting its movement away from the active site.

The crystal structures of inactive kinases are known to exhibit plasticity in the kinase domain that allows distinct conformations to be formed in response to interactions with compounds such as small molecule inhibitors (Huse and Kuriyan, 2002). This has since been shown to be the case for Nek2A. Recent evidence suggests that the αT-helix identified in the crystal structure of Nek2A is in fact a structure induced by the binding of the small molecule inhibitor (R. Bayliss (ICR) and A. Fry; unpublished data). Nevertheless these results suggest that this region of the kinase is critically important for Nek2A activation, as mutation of these residues leads to inactivity.

Lastly, the effect of mutating the M86 gatekeeper residue was investigated. This site was mutated to glycine or alanine in an attempt to alter the shape of the ATP-binding pocket to facilitate the binding of the ATP analogue, 1NM-PP1. Mutation of M86 was not expected to alter Nek2A activity using ATP as the substrate. However, IVT-IP kinase assays indicated that mutation of M86 resulted in loss of kinase activity. Since this kinase was inactive, the consequences of inactivating Nek2A with 1NM-PP1 could not be investigated. One explanation is that mutation of M86 causes the shape of the ATP binding pocket to change in such a way that ATP can no longer bind thus creating an inactive kinase. This result is not unique as it has been found with other kinases that compensatory mutations are required together with the gatekeeper mutation in order to create an analogue sensitive kinase.

A summary of the various Nek2A mutants investigated and their activities in each assay performed are shown in Figure 3.14. The Nek2A mutants investigated in this thesis are indicated in blue. One proposal is that Nek2A activity is likely to be regulated by phosphorylation at the primary site, T175, and by secondary phosphorylation events at T170 and S171 in order to achieve full activation. In addition, Nek2A is further regulated by phosphorylation at T179 and S241 which are necessary for Nek2A activation and may play structural roles by forming interactions required to orientate the N- and C-lobes into the correct conformation for the kinase to be active. These results further suggest that Nek2A is not regulated by autoinhibition.

Chapter Four

Generation, Purification and Characterisation of a Phosphospecific Nek2 Antibody

4.1 Introduction

Overexpression of the Nek2 protein and amplification of the Nek2 gene has been found in various types of human tumours, including breast tumours, choloangiocarcinomas, gastric adenocarcinomas, osteosarcomas and lymphoma (Hayward et al., 2004; de Vos et al., 2003; Kokuryo et al., 2007; Loo et al., 2004; Wai et al., 2002; Weiss et al., 2004). Overexpression of Nek2A in cultured cells results in aneuploid cells with supernumerary centrosomes, whereas ablation of Nek2 inhibits cells growth and induces apoptosis (Faragher and Fry, 2003; Fletcher et al., 2004; Hayward et al., 2004; Kokuryo et al., 2007). Together, these data strongly support Nek2 as a novel target for therapeutic intervention in the treatment of cancer.

Nek2 exhibits differential expression between normal and tumour tissue and is susceptible to inhibition by small molecule inhibitors which compete for binding at its ATP binding pocket (Hayward, 2007). Our ultimate goal is to design a specific and potent inhibitor of Nek2 kinase activity which is capable of killing or arresting cancer cells overexpressing Nek2. Recently, more specific cancer therapies which target the defects that drive tumour formation rather than traditional therapies which target all proliferating cells in a non-specific manner have been investigated. One common defect frequently associated with tumour progression is aberrant kinase expression. Therefore a number of small molecule inhibitors have been developed which inhibit kinase activity by competing with ATP for the catalytic binding pocket, thus stabilising the inactive comformation of the kinase. Presently, there are over 25 kinases for which putative inhibitors have been generated, some of which are licensed for clinical use (Dancy and Sausville, 2003). These include the mitotic kinases, Aurora-A and Plk1. Aurora-A and Plk1 are upregulated in multiple human tumours and are closely associated with tumour progression. Inhibitors of these kinases induce mitotic arrest and apoptosis selectively in cancer cells which overexpress these kinases (Taylor and Peters, 2008).

Phosphospecific antibodies are frequently used to assess the therapeutic efficacy for potential small molecule inhibitors. There are over 300 phosphospecific antibodies commercially available against specific phosphoproteins. These include anti-phospho T210 Plk1 antibody and an anti-phospho T288 Aurora-A antibody (Mandell, 2003). The development of a Nek2 phosphospecific antibody would allow the specific detection of Nek2 activated by phosphorylation. At present only antibodies which detect total Nek2 kinase are available. Phosphorylation at specific residues commonly in the activation loop of protein kinases is thought to induce a conformational change which results in kinase activation (Mandell, 2003).

Previous studies by Dr. J. Baxter identified T175 within the activation loop of Nek2 as a critical phosphorylation site. This was shown using a myc-Nek2-T175A mutant that had reduced kinase activity and a significant reduction in efficiency of centrosome splitting, and a myc-Nek2-T175E mutant that was hyperactive (Rellos et al., 2006). In addition, the importance of T175 is supported by its position within the activation loop. Many other kinases such as Plk1 have a threonine residue at an equivalent site to T175 in Nek2 which is critical for activation of the kinase. In Plk1 this residue is threonine 210 (Jang et al., 2002). As a result of these studies, a peptide mimicking a region of the activation loop containing a phosphorylated T175 site was synthesised by Severn Biotechnology Ltd and injected into rabbits. This method of immunisation of animals with a synthetic peptide is commonly used to generate phosphospecific antibodies. The Nek2 phosphospecfic antibody was purified from the antiserum. This was achieved by removing the antibodies that bind to the unphosphorylated peptide by using a non-phospho-peptide affinity column. The reactivity and specificity of this antibody with Nek2 was investigated by various techniques. In parallel, an antibody developed against the same phospho-T175 containing peptide by Millenium Pharmaceuticals (Boston, USA) was also characterised. This pT175 antibody generated promising results as a Nek2 phospho-specific antibody. However, due to the commercial implications of using a phosphospecific antibody generated by a pharmaceutical company in further research and in a drug discovery project, an alternative approach of generating a successful phosphospecific antibody was sought.

AbD Serotec creates custom monoclonal antibodies without the need for animal immunisation using a HuCAL GOLD® antibody library. This library contains more than 15 million human antibody specifications in Fab format prefabricated in *E. coli* or phage libraries. Thirty-four well microtitre plates coated with the phosphorylated peptide were screened against this library by ELISA. Several high affinity binders were then chosen using CysDisplay™ technology. The 6 positive candidates were expressed in bacteria and affinity purified and sent to the lab for characterisation. The most promising antibodies were then provided on a larger scale. The generation of a successful phosphospecific antibody has provided the lab with a very useful tool for directly measuring Nek2A activity. This antibody has enabled the timing of Nek2 activation and the location of active Nek2 during the cell cycle to be determined. In the long term, this antibody will also allow the lab to test the efficiency of potential Nek2A inhibitors in drug discovery projects.

4.2 Results

4.2.1 Pre-screening of rabbit sera

Eight different rabbit sera, numbered 10654-10661, were pre-screened by Western blotting and immunofluorescence microscopy (Figure 4.1). U2OS cells were lysed and extracts separated by SDS-PAGE and blotted onto nitrocellulose membrane. The eight lanes were cut and individually incubated with 8 µl of each rabbit serum (1:250) in 2 mls of 5% milk-PBST for 1 hour. The strips were probed with anti-rabbit AP-conjugated secondary antibody (1:7500) in 5% milk-PBST for 1 hour. After developing for 5 minutes, bands corresponding to proteins of various size were observed for each rabbit sera. Rabbit sera 10654, 10659, 10660 and 10661 did not reveal any strongly staining proteins or any proteins of a similar size to Nek2A (48 kDa). Immunofluorescence microscopy was performed by staining U2OS cells with the different rabbit sera (1:250) and using γ-tubulin antibody (1:500) to detect the centrosome (red) and Hoechst 33258 (1:10,000) to stain the DNA (blue). Rabbit sera 10655, 10656 and 10658 revealed strong centrosomal staining. Centrosomal staining could also be seen with rabbit sera 10657 but to less of an extent. Rabbit sera 10660 and 10661 did not stain the centrosome but areas of the cytoplasm were stained suggesting these sera were detecting cytoplasmic structures. Finally, only faint centrosomal staining was observed with rabbit sera 10654 and 10659 with few brighter spots elsewhere. From these two pre-screening techniques, rabbits 10654 and 10659 were chosen to be injected with our pT175 peptide.

4.2.2 The immune sera stain centrosomes more strongly than the pre-immune sera

Rabbits 10654 and 10659 were immunised with the phosphorylated peptide conjugated to keyhole limpet haemocyanin according to a standard immunisation protocol (Figure 4.2A). The terminal bleeds were collected and the immune sera compared to the pre-immune sera corresponding to that rabbit by immunoflorescence microscopy. U2OS cells were grown on coverslips and fixed with methanol. They were stained with either the pre-immune or immune serum of either rabbit 10654 or 10659. In addition, the cells were stained with γ-tubulin antibody (1:500) to detect the centrosome (red) and Hoechst 33258 (1:10,000) to stain the DNA (blue) (Figure 4.2). Images were captured at the same exposure and gain to allow fair comparison. The immune sera stained centrosomes more strongly than the corresponding pre-immune sera for both rabbits, although it was more obvious for rabbit 10654.

4.2.3 The immune sera for rabbits 10654 and 10659 detect the peptides more strongly than the pre-immune sera

Serial dilutions of the phosphorylated (PP) and non-phosphorylated (NP) peptides were created ranging from 0.002 mM to 1 mM (Figure 4.3). 1 µl drops of each peptide solution were dotted onto a nitrocellulose membrane and blocked in 5% BSA-TBST. The membrane was cut into strips and incubated with either the pre-immune or immune serum of either rabbit 10654 or 10659 before developing with an anti-rabbit secondary antibody. The dot blot indicates that the immune sera for both rabbits detect the peptides more strongly than the pre-immune sera, but that the immune sera detect the phosphorylated and non-phosphorylated peptides with similar efficiency (Figure 4.3). This was not surprising as the sera had yet to be purified.

4.2.4 The purified pT175 antibody detects the phosphorylated peptide more strongly than the non-phosphorylated peptide

A sulfolink coupling gel support was prepared by covalently coupling the non-phosphorylated peptide to the column. Immune serum 10659 was applied to the peptide coupled column according to the manufacturer’s protocol. The flow through from this column was labelled as the phosphospecific antibody (Figure 4.4A). The column was washed in sample buffer and the wash retained. The bound protein was eluted and collected in 1 ml fractions. A BCA assay was performed on all fractions and the most concentrated stored at 4^0C. Drops (1 µl) of the phosphopeptide and non-phosphopeptide were dotted onto nitrocellulose membrane and blocked in 5% BSA-TBST for 30 minutes. The peptides were then probed with either the flow through, wash or elution (1:50) from the column diluted in 5% BSA-TBST (Figure 4.4B). The dot blot suggests non-phospho-specific Nek2 antibodies bound to the NP-coupled column whilst pT175 specific antibodies did not bind and flowed through the column (Figure 4.4B). The dot blot shows that the flow through strongly detects the phosphorylated peptide although it weakly detects the non-phosphorylated peptide (Figure 4.4B). The flow through was applied to the NP coupled column for a second time in an attempt to remove these non-phospho Nek2 antibodies and the flow through collected. This was labelled as pT175 Ab B. The purification process was repeated with rabbit serum 10654, although the flow through contained equal quantities of phospho- and non-phospho-specific antibodies (pT175 Ab A). At this point a third potential phosphospecific antibody was included which was generated from rabbit sera supplied by Millennium Pharmaceuticals (pT175 Ab C). This antibody had been purified but only partially characterised by a previous PhD student (Baxter, 2006). Serial dilutions of the phosphorylated peptide (PP) and non-phosphorylated (NP) peptide

ranging from 0.002 mM to 1 mM and 1 μl of each peptide solution dotted onto nitrocellulose membrane. The membrane was blocked in 5 % BSA-TBST and then probed with one of the three purified Nek2 pT175 antibodies (1:100) diluted in 5 % BSA-TBST. The pT175 antibody A developed from sera 10654 weakly detected phosphorylated and non-phosphorylated peptide equally. However, pT175 antibody B generated from rabbit sera 10659 strongly detected the phosphorylated peptide and only very weakly detected non-phosphorylated peptide which disappeared as the peptide concentration was reduced to 0.2 mM. T175 antibody C from Millennium Pharmaceuticals generated the most promising result as it only detected the phosphorylated but not the non-phosphorylated peptide (Figure 4.4C).

4.2.5 Generation and characterisation of an inactive Nek2 KD-K37R/D141A kinase

The data presented above indicate that the purified antibodies could detect the phosphorylated peptide by dot blot analysis. Next it was determined whether these antibodies could also detect Nek2 protein phosphorylated on T175. We recently published data on the structure and regulation of Nek2 (Rellos *et al*., 2007). As part of this study a bacterial expression vector encoding a His-tagged Nek2 kinase domain (KD) construct with a double mutation of D141A and K37R was generated. This mutant kinase domain proved to be completely inactive and unable to undergo autophosphorylation even when expressed in bacteria. This protein is not expected to be phosphorylated at position T175 unlike the single Nek2-K37R mutant which still exhibits some kinase activity when produced in large amounts. These reagents therefore provide a method for characterising the specificity of phosphospecific antibodies. The two His-tagged Nek2 kinase domain constructs were expressed in Rosetta bacteria. Protein expression was induced by incubating with IPTG (Figure 4.5). The bacterial culture was centrifuged and the pellets were resuspended in lysis buffer containing lysozyme prior to centrifugation. The aliquots of induced and uninduced bacteria, as well as of the pellet and supernatant after extraction, were resuspended in sample buffer. The proteins in these extracts were separated by SDS-PAGE and analysed by Coomassie Blue staining (Figure 4.5A). As these proteins were His-tagged, they were purified by mixing the cleared lysate with Ni-NTA slurry. The bead-lysate mixture was then added to a purification column and subsequently washed. The protein was eluted from the column with imidazole-containing elution buffer and collected in 4 fractions. The flow through, wash and elution fractions collected during the purification process were analysed by SDS-PAGE (Figure 4.5B). A band corresponding to the two purified proteins can be seen in the elution fractions. Elution fraction 2 contained the most concentrated protein and a dilution series was analysed by SDS-PAGE and Coomassie Blue staining (Figure 4.5C).

The activity of these mutant Nek2 kinase domains was characterised by performing an *in vitro* kinase assay. Equal quantities of purified Nek2-KD-K37R and Nek2-KD-K37R/D141A kinases were incubated with kinase buffer containing ^{32}P-γ-[ATP] in the presence and absence of β-casein at 30^0C for 30 minutes. The kinase reactions were stopped by the addition of 3 x sample buffer and boiling for 5 minutes. The proteins within each kinase mixture were separated by SDS-PAGE and analysed by Coomassie Blue staining and autoradiography (Figure 4.6). The Coomassie Blue stained gel indicates equal concentrations of these two proteins. The autoradiograph shows that the Nek2-KD-K37R protein undergoes autophosphorylation and phosphorylates the substrate β-casein. In comparison, the Nek2-KD-K37R/D141A kinase does not phosphorylate β-casein and does not autophosphorylate.

4.2.6 pT175 Ab C detected the Nek2-KD-K37R but not Nek2-KD-K37R/D141A protein

To test whether the purified phosphospecific antibodies were specific for phosphorylated Nek2 protein, the purified Nek2-KD-K37R and Nek2-KD-K37R/D141A proteins were separated by SDS-PAGE and blotted onto nitrocellulose membrane. The membrane was stained with Ponceau which showed that the quantity of Nek2 protein loaded into each lane was equal across every lane. Next, the membrane was blocked in 5% BSA-TBST then probed with the purified pT175 antibodies B and C and the corresponding non-phospho-specific antibodies. Disappointingly, the pT175 antibody B did not show a preference for either purified kinase and detected both kinases to the same extent which was also observed with its corresponding non-phospho-specific Nek2 Ab B (Figure 4.7). The non-phospho-specific Nek2 antibody C detected both purified kinases to an equal extent, whereas the pT175 antibody C detected the Nek2-KD-K37R more strongly than the Nek2-KD-D141A/K37R. Although this result suggests that the pT175 Ab C antibody is more specific for phosphorylated than non-phosphorylated Nek2, it is not clear whether it is specific for phosphorylated Nek2 rather than other phosphorylated kinases.

4.2.7 pT175 Ab C detects endogenous Nek2 in U2OS lysates and stains the centrosome and midbody in U2OS cells

To determine whether the pT175 Ab C detects endogenous Nek2 in cells, Western blotting and immunofluorescence microscopy were performed. Untransfected U2OS lysates were separated by SDS-PAGE and blotted onto nitrocellulose membrane. The membrane was divided and blocked with 5% BSA-TBST. The membrane was probed with the purified non-phospho-specific Ab C and the pT175 Ab C and a commercial monoclonal Nek2 antibody to detect endogenous Nek2. The pT175 antibody detected a band corresponding to the size of Nek2 although not as strongly as the other two antibodies (Figure 4.8A). Immunofluorescence microscopy was performed to determine whether the pT175 antibody C detects endogenous Nek2 at the centrosomes in cells. U2OS cells were fixed with methanol and probed with Hoechst 33258 to stain the DNA, pT175 Ab C and the monoclonal Nek2 antibody (Figure 4.8B). Immunofluorescent images were taken of cells in interphase, metaphase and telophase. The pT175 antibody colocalised with Nek2 at the centrosome in interphase cells but the signal was still present in metaphase cells unlike the Nek2 monoclonal antibody which loses its signal, consistant with the proposal that Nek2A is degraded prior to metaphase (Hames et al., 2001). In addition, the pT175 Ab C antibody detected the midbody at telophase. Hence, it is not clear that this antibody is specifically detecting Nek2 in cells. Furthermore, as it was generated by Millennium Pharmaceuticals, it would be difficult to use this reagent in a drug discovery project that was independent of Millenium Pharmaceuticals.

4.2.8 The Six potential Nek2 pT175 phosphospecific antibodies generated by HuCAL technology

As a result a Nek2 pT175 phospho-specific antibody was generated by using recombinant antibody technology employed by AbD Serotec Technologies. For this purpose, the same phosphorylated peptide (Figure 4.2A) was conjugated to BSA or human transferrin (Trf) and used to screen for positive binders against the HuCAL library. Using an ELISA assay, six high affinity binders were identified as potential phosphospecific antibodies, and named AbD1 to AbD6 (Figure 4.9). These antibodies were sent to the laboratory for further characterisation. First of all, dot blotting was carried out to confirm that these antibodies detect specifically the phosphorylated peptide. The phosphorylated peptide (PP) tagged with either BSA or Trf and non-phosphorylated peptide tagged with BSA at 1mM were dotted onto nitrocellulose membrane. The membrane was blocked in 5% BSA-TBST, cut into strips and incubated with AbD1-6. The membrane strips were then incubated with an anti-human Fab

fragment AP-conjugated secondary antibody and developed by the addition of alkaline phosphatase reagents. The dot blot indicates that all six recombinant antibodies detect the phosphorylated peptide irrespective of the conjugated tag but they do not detect the non-phosphorylated peptide (Figure 4.10A). Next, serial dilutions of the phosphorylated (PP) and non-phosphorylated (NP) peptides ranging from 0.002 mM to 1 mM were dotted onto a nitrocellulose membrane and blocked in 5% BSA-TBST. The membrane was cut into strips and incubated with AbD1-6 before developing with an anti-human Fab fragment AP-conjugated antibody (Figure 4.10B). The dot blot confirms that all six antibodies detect specifically the phosphorylated peptide in a dose-dependent manner. However, of the six AbD1, 2, 3 and 6 gave the strongest reactivity with AbD4 and 5 being considerably weaker.

4.2.9 AbD1 detects centrosomes in prophase U2OS cells

Immunofluorescence microscopy was performed to determine whether AbD1-6 could stain centrosomes in U2OS cells and, more importantly, whether they stained centrosomes specifically in prophase when Nek2 is thought to be active. U2OS cells were fixed with methanol and probed with AbD1-6. These antibodies were then detected by using an anti-myc tag antibody as the recombinant HuCAL antibodies carry an N-terminal Myc-His fusion. In addition, cells were stained with a γ-tubulin antibody to detect the centrosomes. Immunofluorescent images of cells in prophase probed with each recombinant antibody are shown in Figure 4.11A, although the precise timing of prophase differs slightly between the representative cells. AbD1 colocalised with γ-tubulin at the centrosomes in prophase, but possible spindle association was also observed. AbD2-6 did not produce a detectable signal at the centrosomes. Interestingly, AbD5 specifically detected the midbody between dividing cells at telophase (Figure 4.11B). These observations were based on viewing 10 prophase cells stained with each antibody.

4.2.10 AbD1, 2, 3 and 6 detect Nek2-KD-K37R and Nek2-KD-K37R/D141A bacterially expressed proteins

Next it was tested whether AbD1-6 could detect bacterially expressed Nek2 protein in a phosphorylated or unphosphosphorylated state by Western blotting. Purified Nek2-KD-K37R and Nek2-KD-K37R/D141A proteins were incubated in kinase buffer with ATP for 30 minutes at 30^0C to allow autophosphorylation. The proteins were then separated by SDS-PAGE and blotted onto nitrocellulose membrane. The membrane was blocked in 5% BSA-TBST then probed with AbD1-6 or the commercial anti-Nek2 monoclonal antibody and developed by ECL-plus. The intensity of each band was then quantitated using Image J

software and the measurements displayed as a histogram (Figure 4.12B). The Nek2 mAb antibody detected both purified kinases equally, whereas AbD1, 2, 3 detected Nek2-KD K37R kinase significantly more than the unphosphorylated Nek2-KD-D141A/K37R kinase. Although this result suggests these antibodies are phosphospecific, it is not clear whether they are specific for phosphorylated Nek2 rather than other phosphorylated kinases.

4.2.11 Recombinant antibodies AbD1, 2, and 3 detect the full-length recombinant His-Nek2A protein preferentially after ATP incubation

We then investigated whether AbD1-6 could detect purified full-length His-Nek2A kinase pre-incubated with or without ATP. Purified Nek2A kinase was incubated in kinase buffer in the presence or absence of ATP at 30^0C for 30 minutes. Parallel reactions were performed with and without ^{32}P-γ-ATP. The proteins in the radioactive kinase reactions were separated by SDS-PAGE and the gel analysed by Coomassie Blue staining and autoradiography (Figure 4.13A). This indicated that Nek2A kinase pre-incubated with ATP is significantly autophosphorylated in contrast to Nek2A kinase pre-incubated without ATP which is only weakly phosphorylated. The proteins in the non-radioactive kinase reactions were then separated by SDS-PAGE and blotted onto nitrocellulose membrane and probed with AbD1-6 or a total Nek2 monoclonal antibody (Figure 4.13B). Finally, the membrane was developed using ECL plus for varying lengths of time. After a 5 second exposure the total Nek2 mAb detected the Nek2A kinase in the presence or absence of ATP to equal extents although pre-incubation with ATP led to an upshift on the gel that would support the notion of autophosphorylation. In comparison, AbD1, 2, and 3 detected preferentially the phosphorylated Nek2A pretreated with ATP.

4.2.12 AbD1 detects specifically the mitotic kinase Nek2A *in vitro*

Of the three antibodies that specifically detected phosphorylated Nek2, AbD1 gave the strongest and most selective signal. Next, it was determined whether AbD1 might also detect other mitotic kinases. The activation loop sequence of Nek2 surrounding T175 was first aligned with Nek6, Nek7, Aurora-A and Plk1. This showed significant divergence around the phosphorylation site (Figure 4.14A). To then determine experimentally whether AbD1 specifically detects other mitotic kinases, purified Nek2, Nek6, Nek7, Aurora-A and Plk1 kinases were incubated in kinase buffer in the presence or absence of ATP. An aliquot of each kinase reaction was taken to which ^{32}P-γ-ATP was added. All reactions were incubated at 30^0C for 30 minutes before being separated by SDS-PAGE. The gel containing radioactive sample was stained with Coomassie Blue, dried and subjected to autoradiography indicating

that all kinases had been phosphorylated to a higher level by preincubation in the presence of ATP (Figure 4.14B). The gel containing non-radioactive sample was either silver-stained to show equal loading of each kinase or blotted onto nitrocellulose membrane. The membrane was then probed with AbD1 and developed by ECL plus (Figure 4.14B). This result clearly shows that AbD1 specifically detects the Nek2A kinase and not other mitotic kinases.

4.2.13 Recombinant AbD1 detects centrosomes specifically from prophase to metaphase

Having demonstrated the specificity of AbD1 for phosphorylated Nek2, the antibody was used to investigate where and when Nek2 is active during the cell cycle. U2OS cells were fixed with methanol and probed with AbD1 which was detected by using an anti-myc tag antibody. In addition, the cells were stained with an anti-γ-tubulin antibody to detect the centrosomes. Immunofluorescence microscopy images of cells in interphase and different stages of mitosis are shown in Figure 4.15. AbD1 detected Nek2 at the centrosomes specifically from early prophase through to metaphase. However, the signal starts to weaken after prometaphase so that by metaphase a signal can be observed in some cells, but not others. This corresponds precisely with the time at which Nek2A is degraded (Hayes et al., 2006).

4.2.14 Nek2A does not colocalise with kinetochores

To investigate this possibility, immunofluorescence microscopy was performed using AbD1 and an anti-CENP antibody to stain the centromeres. U2OS cells were fixed with methanol and probed with AbD1 to detect active Nek2 in addition to an anti-centromere antibody which detects the centromere (Figure 4.16). AbD6 did not colocalise with CENP at the centromeres arguing against previous suggestions that chromatin and kinetochore proteins, such as HMGA2 and Hec1, are substrates of Nek2 at least during mitosis in cultured U2OS cells.

4.3 Discussion

The aim of this chapter was to develop a phosphospecific antibody against T175 that specifically detects activated Nek2. Not only would this allow the time and location at which Nek2 is activated to be measured directly, but it would also enable the efficacy of small molecule inhibitors of Nek2 to be tested.

In order to generate a phosphospecific antibody, three antisera generated using phosphorylated peptide as immunogens in rabbits were tested. Two of these (phospho-antibody A and B) were generated under contract from Seven Biotechnology Ltd., whilst a third phospho-antibody C was provided through collaboration with Millennium Pharmaceuticals. Following a one step purification, characterisation of these antibodies indicated that phospho-antibody A did not specifically detect the phosphorylated over the non-phosphorylated peptide, whereas phospho-antibody B did detect the phosphorylated peptide more strongly than the non-phosphorylated peptide. Phospho-antibody C exhibited the strongest selectivity for the phosphopeptide over the non-phosphorylated peptide. After further characterisation of phospho-antibodies B and C, it was found that phospho-antibody C detected a bacterially expressed Nek2 kinase domain which was able to autophosphorylate more strongly than one that was unable to undergo autophosphorylation. In comparison, phospho antibody B detected both proteins equally and did not show any preference for the phosphorylated over the non-phosphorylated Nek2 proteins. Further characterisation of phospho-antibody C revealed that the antibody could detect endogenous Nek2 in U2OS lysates, albeit weakly. The antibody also stained the centrosome in mitosis, although it still detected the spindle poles in metaphase and anaphase and the midbody in telophase cells. Whilst Nek2A is degraded in prometaphase, it is possible that the pT175 antibody is detecting active Nek2B which is not degraded in mitosis. However, it is also possible that the antibody may be detecting a protein other than Nek2 in mitotic cells. RNAi depletion of Nek2 proteins would be required to rule out this possibility.

Despite the promising data with phospho-antibody C, it is important to bear in mind that this antibody was made through collaboration with Millennium Pharmaceuticals. This would have implications in terms of commercial rights if used in a separately funded drug discovery project. We therefore attempted to generate a phosphospecific antibody by using recombinant antibody technology developed by AbD Serotec which uses a library of recombinant Fab fragment clones to screen for potential antibodies. Six recombinant antibodies were identified by AbD Serotec based on ELISA assay as detecting the phosphorylated peptide but not the unphosphorylated peptide. All six antibodies also showed strong selectivity for phosphorylated versus non-phosphorylated peptide by dot blot analysis. AbD1, 2 and 3 detected a bacterially expressed fragment of the Nek2 kinase domain that was able to autophosphorylate more strongly than a fragment that was incapable of autophosphorylation. In addition, AbD1, 2 and 3 specifically detected full-length Nek2A protein which had been preincubated with ATP to allow it to autophosphorylate. Immunostaining suggested that AbD1 produced strong centrosomal staining at prophase which was absent in interphase. Slight spindle staining was also evident with AbD1 highlighting the possibility that the AbD1 may also detect a microtubule associated protein or that active Nek2 associates with the microtubules as well as the centrosome. In comparison, AbD2-6 did not detect centrosomes, although AbD3 often stained two dots which were perpendicular to the γ-tubulin containing dots. Interestingly, AbD5 produced strong staining at the midbody between a pair of dividing cells. From these experiments AbD1 looked the most promising as a phosphospecific Nek2 antibody. Indeed, it was confirmed that AbD1 specifically detects the phosphorylated Nek2 kinase in comparison to a number of other phosphorylated mitotic kinases. Following this characterisation, AbD1 was identified as a phosphospecific pT175 Nek2 antibody.

Finally, AbD1 was used to determine when and where Nek2 was activated in cells by immunofluorescence microscopy. AbD1 detected active Nek2 at the centrosomes from early prophase to metaphase. This coincides with the time at which centrosome separation occurs and supports previous evidence that Nek2A is degraded following ubiquitination by the APC/C prior to mitotic exit (Hames et al., 2001; Hayes et al., 2006).   AbD1 was also used to investigate claims that Hec1 and Sgo1 are substrates of Nek2. These proteins localise to kinetochores and contribute to accurate chromosome segregation through regulation of spindle assembly checkpoint signalling and chromosome cohesion, respectively (Chen et al., 2002; Fu et al., 2007). U2OS cells were costained with AbD1 and an anti-centromere antibody. AbD1 clearly did not colocalise with kinetochores suggesting that active Nek2 does not colocalise with Hec1 or Sgo1. Therefore, it seems unlikely that these proteins are phosphorylated by Nek2 at least in U2OS cells, contradicting proposals that these proteins are substrates of Nek2 and that Nek2 functions to control chromosome segregation at kinetochores (Chen et al., 2002; Fu et al., 2007). Moreover, no association of active Nek2 with mitotic chromatin was observed suggesting that Nek2 does not directly regulate mitotic chromatin condensation through interaction and phosphorylation of HMGA2.

In conclusion, a phosphospecific antibody raised against pT175 within the Nek2 activation loop has been successfully generated. Recently, a previous PhD student in the lab, Dr. D. Hayward, developed two assays for measuring Nek2 activity through measuring phenotypes associated with active Nek2, namely displacement of rootletin from centrosomes and premature centrosome separation (Hayward, 2007). The aim was to use these assays to assess the effectiveness of small molecule inhibitors of Nek2 kinase activity (Hayward, 2007). However, the availability of a phosphospecific antibody will provide a more direct measurement of Nek2 activity in cells providing an alternative assay for the Nek2 drug discovery project.

Chapter Five

Investigation into the Consequences of Cdk1 Inhibition on Nek2 Activity and Centrosome Cohesion

5.1 Introduction

The mechanisms which regulate centrosome duplication and cohesion in mammalian cells are still poorly understood. In terms of centrosome duplication, one recently proposed mechanism suggests that centriole disengagement in anaphase licenses centriole reduplication (Tsou and Stearns, 2006; Wong and Stearns, 2003). Timely centriole disengagement and subsequent centriole duplication is regulated by separase activity. Separase is a protease which cleaves cohesin rings, thus stimulating sister chromatid segregation in anaphase (Uhlmann et al., 2000). Separase activity is regulated by at least two mechanisms: binding of securin and phosphorylation dependent binding of cyclin B1 (Gorr et al., 2005; Lindqvist et al., 2007). Securin forms a complex with separase which contributes to its inhibition, while Cdk1 phosphorylates separase at S1126 which allows Cdk1-cyclin B1 to bind and inhibit separase (Holland and Taylor, 2006).

Cdk1 activation is required for mitotic entry, whereas Cdk1 inactivation is required for mitotic exit. Cdk1 is activated by dephosphorylation by the phosphatase, Cdc25, and inactivated by destruction of cyclin B1 triggered by the APC/C (Lindqvist et al., 2007). Once cyclin B1 is destroyed this would relieve its inhibition of separase, whilst APC/C-mediated destruction of securin would relieve the second mechanism of separase inhibition. This coordinated activation of separase is thought to promote centriole disengagement. Furthermore, it has been suggested that centriole disengagement is a prerequisite for the recruitment of intercentrosomal linker proteins necessary for re-establishment of centrosome cohesion in the subsequent interphase (Tsou and Stearns, 2006).

Nek2 plays a major role as a key regulator of centrosome cohesion. Nek2 localises to the centrosome where it triggers the dissociation of intercentriolar linkage proteins allowing centrosome separation at the G_2/M transition. Nek2A activity is negatively regulated by PP1 which in turn is negatively regulated by Cdk1-cyclin B1 phosphorylation. Inhibition of PP1 induces premature centrosome separation similar to Nek2 overexpression (Fry et al., 1998; Helps et al., 2000; Mi et al., 2007). Therefore, activation of Cdk1-cyclin B1 may indirectly lead to Nek2 activation at the G_2/M transition.

The aim of the work described in this chapter was to determine the consequences of Cdk1 inhibition on Nek2 activity and centrosome cohesion. For this purpose, Cdk1 was inhibited using a selective small molecule inhibitor of Cdk1, RO-3306. RO-3306 is an ATP competitive inhibitor which has a 15-fold selectivity for Cdk1 over eight other human kinases, including PKA and ERK (Vassilev et al., 2006). However, this comparison did not assess the effect of RO-3306 on Nek2. Importantly, RO-3306 appears to be an excellent tool for cell synchronisation of proliferating human cell lines, such as HCT116, SW480 and HeLa, in G_2 phase, while Cdk1 inhibition by RO-3306 was fully reversible for up to 20 hours. However, after longer periods of treatment, increasing number of cells underwent apoptosis (Vassilev et al., 2006). The specific objectives of this chapter were to test whether RO-3306 inhibited Nek2 activity directly *in vitro* or *in vivo* and to look at the consequences of RO-3306 treatment on centrosome morphology.

5.2 Results

5.2.1 RO-3306 induces a reversible G_2/M arrest in U2OS cells

In order to determine whether the Cdk1 inhibitor, RO-3306, induced a G_2/M arrest in U2OS cells, cells were grown in 6 cm dishes and treated with 20 µM RO-3306 for 16 hours. The cells were released from drug treatment by washing in fresh medium and then incubated for increasing times alongside untreated asynchronous U2OS cells. Cells were then examined by flow cytometry. The cell cycle profiles for untreated and treated U2OS cells at each time point are shown in Figure 5.1. RO-3306 treatment induced a substantial G_2/M arrest, whilst upon release from drug treatment, cells cycled into mitosis and subsequent G_1, represented by the increasing 2N peak at the expense of the 4N peak. After a 24 hour release, the cell cycle profile began to resemble that of asynchronous cells. Hence, RO-3306 treatment can be used to induce a substantial but reversible G_2/M arrest in U2OS cells.

5.2.2 RO-3306 inhibits Cdk1 but not Nek2A kinase *in vitro*

To confirm that RO-3306 does indeed inhibit Cdk1 activity and determine whether it can also inhibit Nek2A activity directly, *in vitro* kinase assays were performed. Purified recombinant Cdk1/cyclin B and Nek2A kinases were added to a kinase assay containing ^{32}P-γ-[ATP], β-casein and either 0.02, 0.2, 2.0 or 20 µM RO-3306 or DMSO carrier alone (Figure 5.2A). After a 30 minute incubation at 30^0C, the reaction products were analysed by SDS-PAGE, Coomassie Blue staining and autoradiography. The β-casein bands were then excised from the gels and the degree of ^{32}P incorporation calculated by scintillation counting. The kinase activities of Cdk1 and Nek2A in response to RO-3306 treatment were displayed as histograms (Figure 5.2B). As the concentration of RO-3306 increased, the extent to which the substrate β-casein was phosphorylated by Cdk1 was reduced. There was 60% inhibition at 20 µM RO-3306 indicating that Cdk1 activity is inhibited by RO-3306 in vitro. In contrast, β-casein phosphorylation by Nek2A was not considerably reduced in response to increasing RO-3306 concentration, indicating that RO-3306 does not directly inhibit Nek2A at the concentrations used.

5.2.3 RO-3306 does not prevent premature centrosome splitting in response to Nek2A overexpression

Next, it was determined whether RO-3306 could directly inhibit Nek2A activity *in vivo*. This was tested by measuring the ability of overexpressed Nek2A to stimulate premature centrosome splitting in the presence or absence of RO-3306. Moreover, this would test whether Nek2A-induced premature centrosome separation was dependent upon Cdk1 activity.

U2OS cells were transfected with myc-Nek2A-WT and 4 hours later treated with 20 µM RO-3306. At 20 hours post-transfection, U2OS cells were fixed and stained with an anti-myc antibody to detect the myc-tagged Nek2A construct and anti-γ-tubulin antibody to identify the centrosomes. The transfected myc-Nek2A-WT protein localised to the centrosome in the presence or absence of RO-3306 (Figure 5.3A). Although the image representing a RO-3306 treated cell shows some nucleolar staining, this is not typical of RO3306 treated cells but it is a commonly observed phenotype of myc-Nek2 transfected cells. One hundred cells were counted in 3 separate experiments and centrosomes classed as split or non-split. RO-3306 treated cells expressing myc-Nek2A-WT induced centrosome splitting to a similar extent to that observed in cells not treated with RO-3306 (Figure 5.3B). $P>0.6$ suggesting there is no significant difference in the results between the treated and untreated cells. This result indicates that RO-3306 does not alter the activity or localisation of transfected Nek2A in cells.

5.2.4 Cdk1 inhibition induces centrosome defects

To determine the effect of Cdk1 inhibition upon centrosome morphology, U2OS cells were treated with 20 µM RO-3306 for 16 hours and centrosomes analysed by immunofluorescence microscopy using an anti-γ-tubulin antibody. Interestingly, 32% of RO-3306 treated cells displayed four γ-tubulin stained spots compared to untreated cells which almost invariably gave two spots (99%) (Figure 5.4A and B). $P< 0.001$ suggests there is a highly significant increase in the number of γ-tubulin stained spots in treated cells compared to untreated cells. The arrangement of the four γ-tubulin stained spots varied between RO-3306 treated cells, although the predominant arrangement was of two separated pairs (31%) or all four spots close together (38%) (Figure 5.4C). The presence of more than two γ-tubulin spots may indicate overduplication of centrosomes or premature disengagement of centrioles.

5.2.5 Release of Cdk1 inhibition leads to multipolar spindle formation

Cdk1 inhibition by RO-3306 was reported to be readily reversible and that release from a RO-3306 induced arrest leads to synchronised entry into mitosis (Vassilev et al., 2006). To determine the consequences of entering mitosis with overduplicated or prematurely disengaged centrioles or overduplicated centrosomes, U2OS cells were arrested with RO-3306 for 16 hours and then released them for 60 minutes. Immunofluorescence microscopy revealed that a significant percentage of cells had entered mitosis, as predicted, compared to untreated cells. This supports the earlier data that the effect of this drug is reversible in U2OS

cells. However, mitotic cells treated with RO-3306 displayed a significantly higher proportion (7%) of multipolar spindles compared to untreated cells (1%) which was found to be highly significant ($P<0.001$ compared to untreated cells) (Figure 5.5). This suggests that the extra γ-tubulin containing spots induced by the presence of RO-3306 are capable of forming additional spindle poles.

5.3 **Discussion**

Cyclin dependent kinases are serine/threonine kinases that require the binding of cyclin for full activity and are essential regulators of cell cycle progression. Activation of Cdk1 is required for mitotic entry, whereas its inactivation is required for mitotic exit (Lindqvist et al., 2007). There is evidence to suggest that activation of Cdk1 by Cdc25c occurs at the centrosome (Bonnet et al., 2008). There is also evidence to show that Cdk1 inactivation in *Drosophila* wing disc cells induces the formation of anomalous centriole configurations, suggesting that Cdk1 inactivation permits centriole reduplication (Viwans et al., 2003). Moreover, Cdk1 has been previously predicted to function as a negative regulator of PP1 which in turn regulates Nek2 kinase activity (Meraldi and Nigg, 2001). Together, these data suggest that Cdk1 may play a role in centrosome cohesion and separation, as well as in the control of centriole duplication. The work in this chapter has focused on investigating the consequences of inhibiting Cdk1 with a small molecule inhibitor, RO-3306, on centrosome cohesion and Nek2 activity.

Firstly, flow cytometry analysis of RO-3306 treated cells confirmed that RO-3306 induced a substantial G_2/M arrest. Secondly, *in vitro* kinase assays showed that RO-3306 directly inhibits the kinase activity of Cdk1, but does not directly inhibit Nek2A kinase activity. Furthermore, addition of RO-3306 to cells does not affect the ability of overexpressed Nek2A to induce centrosome splitting. This also supports the notion that Cdk1 activity is not required for the premature centrosome splitting induced by Nek2A overexpression. This research suggests that Cdk1 inhibition prevents the disassembly of the intercentriolar linkage which normally occurs in response to phosphorylation of C-Nap1 and rootletin by Nek2. This supports a model previously described in which Cdk1 acts upsteam to inhibit PP1 which in turn inhibits Nek2A (Fry et al., 1998b; Helps et al., 2000; Mi et al., 2007). Therefore it is proposed that Cdk1 functions upstream of Nek2.

Thirdly, the consequence of Cdk1 inhibition on centrosome morphology was investigated. Interestingly, four γ-tubulin containing dots were observed in RO-3306 treated G_2/M arrested cells instead of the normal two seen in untreated asynchronous cells. There are two possible explanations for this phenotype. Firstly, that duplicated centrioles were split prematurely or secondly that centrosomes were overduplicated in response to Cdk1 inhibition. This was investigated by M. Samant (an MSc student in the laboratory) by co-staining drug treated HeLa cells with anti-centrin antibodies to detect centrioles and anti-γ-tubulin antibodies to detect centrosomes. Both antibodies stained four foci that were slightly separated from one another (Figure 5.6A). This strongly suggests that the four foci observed in drug treated cells are the result of premature centriole disengagement and not centrosome duplication. This has led to the proposal that Cdk1 activity is required to prevent premature centriole disengagement in G_2 at least in U2OS and HeLa cells. Centriole disengagement normally occurs in late mitosis coincident with the activation of the protease, separase, which is thought to mediate centriole disengagement (Tsou and Stearns, 2006). Separase can be inhibited by a number of mechanisms including its interaction with cyclin B which is mediated by its phosphorylation by Cdk1 (Holland and Taylor, 2006). Therefore, it was proposed that Cdk1 inhibition prevents the inhibitory phosphorylation of separase. Separase then becomes prematurely active resulting in premature centriole disengagement. However, other mechanisms exist which regulate separase activity, such as binding of securin. Hence, to test this hypothesis, future experiments will need to investigate whether separase is active in cells arrested at G_2/M by RO-3306.

Although drug-treated cells often possessed four distinct centrioles that had undergone disengagement, the majority of these were relatively close together and most were commonly arranged as four centrioles together or as two closely-associated pairs of centrioles. This suggests that the intercentriolar linkage is still present. Furthermore, costaining cells for rootletin and C-Nap1 performed by M. Samant frequently revealed the presence of four foci (Figure 5.6B). This indicates that premature centriole disengagement may lead to the premature recruitment of intercentriolar linker components. It also argues that recruitment of linker proteins occurs as a result of disengagement.

Finally, in cells released from drug-mediated G_2/M arrest, a significant increase in the number of multipolar spindles was observed suggesting that prematurely disengaged centrioles were each able to nucleate and organise microtubules and thereby form spindle poles. It was proposed that the release from drug-induced G_2/M arrest leads to activation of Cdk1 and subsequently Nek2 which triggers the disassembly of both the old and new intercentriolar linkages. In turn this allows the production of multipolar spindles containing a single centriole at each spindle pole. This interpretation was supported by TEM analysis of drug-released cells which revealed the presence of single centrioles at spindle poles, although more images need to be obtained to confirm this hypothesis (Figure 5.6C performed by Dr. S. Prosser). Interestingly, premature centriole disengagement and subsequent multipolar spindle formation has also been observed in CHO cells arrested in G_2 by DNA damage in a pathway that would also be expected to inactivate Cdk1 (Hut et al., 2003).

This study therefore provides important insights into the mechanisms of centriole disengagement, centrosome cohesion and the pathway by which Nek2 activity is regulated (Figure 5.7 and 5.8). In summary, the results indicate that the inhibition of Cdk1 at G_2/M causes premature centriole disengagement possibly due to activation of separase. This hypothesis is supported by an observed increase in the number of cells with more than the normal two γ-tubulin staining dots as a result of Cdk1 inhibition. The majority of these γ-tubulin dots were arranged as two separated pairs or as four dots close together. This indicates that premature centriole disengagement has occurred. The possibility that this phenotype could have occurred through overduplication of centrosomes rather than premature centriole disengagement is unlikely as these four dots also stain for centrin suggesting the centrioles are separated (Figure 5.6). Cdk1 inhibition also leads to premature recruitment of intercentriolar linker proteins. This has been observed by immunofluorescence microscopy in which the prematurely disengaged centrioles costained for γ-tubulin and C-Nap1 or rootletin. Release from the drug induced G_2/M arrest leads to Cdk1 activation which in turn activates Nek2 resulting in the breakdown of intercentriolar linker thus allowing centrosome separation. However, as indicated by immunofluorescence microscopy, due to the premature disengagement of centrioles, entry into mitosis is accompanied by formation of multipolar spindles (Figure 5.7 and 5.8). This is supported by the increased number of multipolar spindles observed in RO3306 treated cells compared to control cells. Together these results suggest Cdk1 is an upstream regulator of Nek2 activity.

Chapter Six

Investigating the roles of Nek2 and C-Nap1 in Centrosome Cohesion

6.1 Introduction

Upon mitotic entry, duplicated centrosomes separate and move to opposite ends of the cell forming the spindle poles. However, during interphase unduplicated or duplicated centrosomes remain relatively close together for most of the time. Electron microscopy of isolated centrosomes has revealed the presence of electron dense material between the mother and daughter centrioles. Together, these observations support the existence of a linkage structure connecting mother and daughter centrioles which mediates centrosome cohesion (Fuller et al., 1995; Paintrand et al., 1992). Nek2A is a well characterised regulator of centrosome separation at the onset of mitosis. Endogenous Nek2 activity peaks at G_2/M which correlates with centrosome separation, while overexpression of Nek2A causes premature centrosome splitting in interphase (Faragher and Fry, 2003; Fry et al., 1998a; Fry et al., 1995).

The C-Nap1 protein was isolated in a yeast two-hybrid screen using Nek2A as bait (Fry et al., 1998b). C-Nap1 is a 281 kDa protein which has two globular head domains at its N- and C-termini separated by two large coiled-coil domains with a central proline-rich hinge region predicted to be of non-helical structure. C-Nap1 is located at the proximal ends of centrioles and is able to interact with the centrosome via its C- and N-terminal domains (Mayor et al., 2002; Mayor et al., 2000).

Microinjection of anti-C-Nap1 antibodies, depletion of C-Nap1 by RNAi or overexpression of truncated mutants all induce premature centrosome splitting in cells, supporting the notion that C-Nap1 forms part of the intercentriolar linker (Mayor et al., 2000; Bahe et al., 2005; unpublished data from our laboratory). However, antibodies raised against specific parts of the C-Nap1 molecule consistently revealed two dots at the proximal ends of centrioles rather than staining the area between the centrioles (Mayor et al., 2000). Therefore, C-Nap1 is thought to facilitate the anchorage of other proteins that constitute the core of the intercentriolar linkage connecting the proximal ends of centrioles. Increasing evidence suggests that rootletin is one of these other major components of the intercentriolar linkage. Microscopic studies reveal the presence of rootletin fibers emanating from the proximal ends of centrioles linking the centriolar structures. As for C-Nap1, depletion of rootletin by RNAi also induces centrosome splitting. Meanwhile, depletion of C-Nap1 leads to the displacement of rootlein, whereas depletion of rootletin has no effect upon C-Nap1 localisation. This suggests that C-Nap1 acts as a docking protein for the attachment of rootletin fibers to the centrosome (Bahe et al., 2005).

C-Nap1 is phosphorylated by Nek2A on its C- and N-terminal domains *in vitro* (Fry et al., 1998; Hames, 2002). Overexpression of C-Nap1 results in the formation of large insoluble protein aggregates throughout the cell, which are reduced in size when co-expressed with Nek2A (Mayor et al., 2002). This suggests that phosphorylation of C-Nap1 by Nek2A may affect the oligomerisation or folding of the C-Nap1 protein. C-Nap1 is displaced from the centrosome in response to phosphorylation by Nek2 and the intercentriolar linkage is destroyed.

Similar to C-Nap1, rootletin is also phosphorylated by Nek2 which results in its displacement from the centrosome (Bahe et al., 2005). A model for centrosome separation has been proposed based on our current understanding of the intercentriolar linkage. This model states that increased expression or activity of Nek2A at the G_2/M transition promotes phosphorylation of the intercentriolar linker components, C-Nap1 and rootletin, causing their dissociation which subsequently results in loss of centriole cohesion (Mayor et al., 1999; Fry et al., 2002; O'Regan et al., 2007). Nek2B is also capable of interacting with C-Nap1 which led to the proposal that C-Nap1 is maintained in a phosphorylated state by Nek2B after Nek2A is degraded in early mitosis to ensure the centrosomes remain separated until G_1 (Hames, 2002). It is likely that C-Nap1 and rootletin are then dephosphorylated by PP1 allowing them to reassociate with the newly disengaged centrioles forming a new intercentriolar linkage (Helps et al., 2000).

In this chapter, the regulation of C-Nap1 by phosphorylation by Nek2A was investigated. In particular, it was addressed how C-Nap1 interacts with Nek2, which sites are phosphorylated within C-Nap1 and what happens to the structural conformation of C-Nap1 as a result of this phosphorylation. Therefore, the aim of work described in this chapter was to investigate how these two proteins cooperate to regulate centrosome cohesion.

6.2 Results

6.2.1 Purification of GST-C-Nap1-CTD and –NTD proteins

In order to test the the interactions between C-Nap1 and Nek2A, the C-Nap1-NTD (amino acids 1-488) and CTD (amino acids 1964-2442) were expressed as GST fusion proteins (Figure 6.1A). Full length C-Nap1 is a large protein (281 kDa) that contains extensive coiled-coil domains and hence it would have proved difficult to express and purify as a full-length protein. A previous PhD student had created GST-tagged constructs by inserting the two C-Nap1 domains into the pGEX vector in frame with an N-terminal GST tag (Hames, 2002). GST-CTD and GST-NTD constructs, as well as a construct expressing GST alone, were transformed into the *E. coli* bacterial strain, BL21. Protein expression was induced with 1 mM IPTG for 4 hours at 30^0C. Following lysis and sonication, the GST proteins were purified from the bacterial supernatant using pre-washed glutathionine-sepharose linked beads blocked with rabbit reticulocyte lysate. An aliquot of purified GST, GST-CTD and GST-NTD protein bound beads was resuspended in sample buffer and analysed by SDS-PAGE and Coomassie Blue staining (Figure 6.1B). The GST-tagged C-Nap1-CTD protein has a predicted molecular weight of 78 kDa. In contrast the GST-tagged C-Nap1-NTD protein has a predicted molecular weight of 84 kDa. Bands of similar size corresponding to each protein were observed on the Coomassie Blue stained gel. The GST-tagged C-Nap1-NTD protein migrates slightly faster than C-Nap1-CTD despite having a larger mass, most likely as it is more negatively charged. A number of degradation products can also be observed for both C-Nap1 proteins although to a greater extent for C-Nap1-CTD. All three proteins were correctly expressed at the expected sizes, although the GST-CTD protein contained a number of smaller proteins. These are most likely to be degradation products as previous experiments in the lab had shown that these proteins were recognised by GST antibodies. A previous attempt to alleviate this problem by the addition of protease inhibitors during the purification procedure was unsuccessful.

6.2.2 Intramolecular interactions of C-Nap1

The interactions between C-Nap1 and Nek2 and between different C-Nap1 domains have been previously analysed in the laboratory using the yeast two-hybrid system (Hames, 2002). Growth selection and β-galactosidase activity indicated that the C-Nap1-CTD was capable of binding the C-Nap1-NTD and that the C-Nap1-NTD could also interact with itself. Interaction of the C-Nap1-CTD with itself could not be tested in yeast as the CTD fragment could not be cloned into the yeast vector expressing the GAL4 activation domain. The study also found that both C-Nap1 domains could interact with Nek2A. To confirm these

interactions biochemically, a GST pull-down technique was used. Purified GST, GST-CTD and GST-NTD were bound to glutathione-sepharose beads and the concentration of the bound protein equalised by analysis on SDS-PAGE (Figure 6.2B). Myc-tagged C-Nap1-CTD, C-Nap1-NTD, Nek2A and untagged Rab4 proteins were then prepared by *in vitro* translation (IVT) from a pRcCMV vector in the presence of [^{35}S]-methionine. An aliquot of each sample was analysed by SDS-PAGE followed by autoradiography (Figure 6.2A). The remaining [^{35}S]-labelled proteins were then incubated with equal amounts of GST-protein bound beads before extensive washing. The proteins bound to beads were then analysed by SDS-PAGE followed by autoradiography (Figure 6.2B). [^{35}S]-labelled proteins did not interact with GST alone suggesting that any interactions were not caused by non-specific binding to GST-fused proteins. Equally, the control [^{35}S]-labelled Rab4 protein did not interact with the C-Nap1 proteins. In contrast, [^{35}S]-Nek2A bound strongly to the GST-NTD and GST-CTD fragments of C-Nap1 with similar affinity but did not bind GST alone. Furthermore, [^{35}S]-NTD and [^{35}S]-CTD both bound to GST-CTD and GST-NTD but not GST alone. The interactions between CTD-CTD and NTD-NTD were relatively strong, but the interaction between CTD-NTD was considerably weaker and was not detected using GST-NTD and *in vitro* translated myc-CTD (Figure 6.2B). This is most likely due to the weaker intensity of the myc-CTD protein. The results of this binding assay support the interactions seen in the yeast two-hybrid study, but also indicate that C-Nap1-CTD can interact with itself. In summary, this binding assay suggests that both terminal domains of C-Nap1 are capable of binding Nek2A and each other, providing evidence that C-Nap1 can form hetero- and homo-dimers.

6.2.3 *In vitro* phosphorylation of C-Nap1 by Nek2 kinase

To confirm that both domains of C-Nap1 could be phosphorylated by Nek2, an *in vitro* kinase assay was performed. The purified GST-fused C-Nap1-CTD and -NTD proteins were bound to glutathione beads and were used directly in an *in vitro* kinase assay with purified commercial Nek2A kinase (Figure 6.3). Dephosphorylated casein was used as a positive control as Nek2A readily phosphorylates β-casein. As expected, β-casein was phosphorylated by Nek2A kinase. In addition both GST-NTD and GST-CTD proteins were phosphorylated by Nek2A kinase although less efficiently than β-casein. It is worth noting that the degradation products for C-Nap1-CTD were not phosphorylated by the Nek2A kinase suggesting that the major sites of phosphorylation may be close to the extreme C-terminus. GST alone was not phosphorylated by Nek2A confirming that it is the C-Nap1 domains that are being phosphorylated and not the GST-tag. Nek2A autophosphorylation was also evident at 46 kDa. Interestingly, Nek2A autophosphorylation was increased in the absence of

other substrates.

Next a time-course assay was performed with purified commercial Nek2A kinase taking aliquots of GST-CTD or GST-NTD bound beads resuspended in kinase buffer at regular intervals up to 4 hours. Sample buffer (3 x) was added to stop the reaction. The samples for each time point were separated by SDS-PAGE and the Coomassie Blue stained gel subjected to autoradiography (Figure 6.3B and C). The extent of phosphorylation was measured by scintillation counting of the C-Nap1 proteins excised from the dried gel and plotting the incorporated radioactivity against time (Figure 6.3D and E). The extent of phosphorylation increased to a maximum at 90 minutes before reaching a plateau for both GST-NTD and GST-CTD proteins. GST-CTD incorporated approximately twice as much radiolabelled phosphate as GST-NTD, suggesting that the C-Nap1-CTD may possess twice as many phosphorylation sites as the C-Nap1-NTD.

6.2.4 The ability of the C-Nap1-CTD and -NTD to form heterodimers is reduced as a consequence of phosphorylation by Nek2A

To investigate the effect of Nek2 phosphorylation upon C-Nap1 interactions, a GST pull-down assay was performed following a non-radioactive kinase assay. Equal amounts of beads bound with GST-CTD, GST-NTD or GST alone were resuspended in kinase buffer containing unlabelled ATP in the presence or absence of Nek2A kinase (Figure 6.4). After a 90 minute incubation the protein-beads were then washed and incubated with [^{35}S]-labelled myc-Nek2A. Samples were subjected to SDS-PAGE prior to Coomassie Blue staining and autoradiography. Nek2A was found to bind specifically to beads fused to GST-CTD and GST-NTD but not to GST alone, irrespective of whether the beads had been pre-incubated with Nek2A kinase or not (data not shown). The procedure outlined above was then repeated using [^{35}S]-labelled C-Nap1-CTD and -NTD proteins. Following incubation of GST-tagged C-Nap1 domains with Nek2A kinase, the interaction between CTD-NTD was significantly reduced ($P< 0.05$, $n=4$), but the CTD-CTD and NTD-NTD interactions were unaffected ($P> 0.7$ suggesting no significance) (Figure 6.4).

6.2.5 Identification of sites in C-Nap1 phosphorylated by Nek2

Phosphorylation of C-Nap1 by Nek2 is thought to be required for its displacement from the centrosome resulting in loss of centrosome cohesion (Fry, 2002; Mayor et al., 1999; O’Regan et al., 2007). In order to test this hypothesis, it is necessary to map the sites phosphorylated

by Nek2 and analyse the consequences of their mutation. For this purpose, Nek2 phosphorylated C-Nap1 fragments were prepared for phosphorylation site mapping by mass spectrometry. GST-C-Nap1-CTD and GST-C-Nap1-NTD purified proteins pre-bound to glutathione-sepharose beads were incubated in kinase buffer containing unlabelled ATP and purified Nek2A kinase. The proteins were incubated at 30^0C for 90 minutes as this led to near maximal phosphorylation of the proteins (Figure 6.4B). A sample of unphosphorylated protein was used as a control. These samples were sent to the University of Dundee mass spectrometry facility, where the proteins were separated by SDS-PAGE and stained with Coomassie Blue. The bands corresponding to C-Nap1-CTD and -NTD were excised from the gel, destained and subjected to trypsin digestion overnight. The fragmented peptides were then analysed by LC-MS parent ion scanning mass spectrometry on an Agilent Q-Trap 4000 Triple Quadrupole Mass Spectrometer. The ion data were analysed with Analyser 1.41 software and searches done with Mascot software. The results of the mass spectrometry analysis revealed 8 phosphorylation sites, one site within the N-terminal domain and 7 sites within the C-terminal domain (Figure 6.5). Sequence analysis of the peptides within which these sites were located revealed five residues at 451, 2064, 2102, 2179 and 2394, which lie in a common motif, L/AxxpS/Tϕ where x represents any amino acid and ϕ represents a hydrophobic residue (Figure 6.6). Interestingly, this predicted consensus sequence is similar to that of the structural homologue of Nek2, NIMA, which is FRxpS/Tx. The phenylalanine at position P-3 is similar in charge and hydrophobicity to leucine or alanine observed at position P-3 in C-Nap1. In addition, a previous mass spectrometry analysis of the C-Nap1-CTD protein following phosphorylation by Nek2 had identified two additional phosphorylation sites in the extreme C-terminus, S2417 and S2421, which also lie in the motif LxxpS (Baxter, 2006). This adds further support to our prediction that this represents a common consensus motif for Nek2.

6.3 Discussion

Throughout interphase, mother and daughter centrioles are thought to be physically linked by a cohesive structure termed the intercentriolar linkage. At the G_2/M transition, the intercentriolar linkage is disassembled, allowing duplicated centrosomes to separate to form the poles of the mitotic spindle. This linker is likely to be composed of at least three proteins: C-Nap1, rootletin and Cep68 (Fry et al., 1998; Graser et al., 2007; Yang et al., 2006). C-Nap1 is composed of an N-terminal globular domain, a long coiled-coil, a central hinge region, another long coiled-coil and a C-terminal globular domain. Overexpression of C-Nap1 in cells induces the formation of aggregates suggesting that C-Nap1 has the ability to oligomerise (Mayor et al., 2000). C-Nap1 also interacts with another large coiled-coil protein, rootletin. Both C-Nap1 and rootletin interact with the Nek2 kinase. The current model for centrosome cohesion therefore proposes that phosphorylation of substrates, including C-Nap1 and rootletin, by Nek2 in late G_2 leads to the breakdown of the intercentriolar linkage holding centrosomes together (Mayor et al., 1999; Bahe et al., 2005). However, a detailed molecular characterisation of the intercentriolar linkage and the mechanisms that regulate its assembly and disassembly are far from understood.

The work in this chapter aimed to increase our understanding of how Nek2 and C-Nap1 interactions contribute to the regulation of centrosome cohesion and separation. Results from GST pull-down experiments indicate that both the C-Nap1-CTD and C-Nap1–NTD globular domains can interact with each other and with themselves. This supports previous results obtained using a yeast two-hybrid assay (Hames, 2002). The CTD-CTD and NTD-NTD interactions appeared to be relatively strong compared to the weaker CTD-NTD interactions. Together, this provides compelling evidence that the C-Nap1-CTD and -NTD domains can form hetero- and homo-dimers. In addition, both domains of C-Nap1 can interact with Nek2A. The *in vitro* kinase assays suggest that both the NTD and CTD are phosphorylated by Nek2A. This phosphorylation by Nek2 is thought to trigger the dissociation of C-Nap1 from the centrosome possibly by inducing a structural change in the C-Nap1 molecule. This is based upon by the observation of large C-Nap1 aggregates in cells expressing kinase-dead Nek2A compared to the smaller C-Nap1 aggregates seen in cells expressing active Nek2 (Mayor et al., 2002). To investigate whether phosphorylation of C-Nap1 by Nek2A might induce a structural change in the protein, C-Nap1 fragments were subjected to *in vitro* kinase assays with Nek2A followed by GST-pull down assays. The interactions between the CTD and NTD with Nek2A were unaffected by prior phosphorylation by Nek2A. Similarly, the ability of the C-Nap1 NTD and CTD to form homodimers was also unaffected. However, importantly, the ability of the NTD and CTD to form heterodimers was significantly reduced as a consequence of phosphorylation by the Nek2A kinase. This was demonstrated using both GST-CTD with *in vitro* translated NTD and GST-NTD with *in vitro* translated CTD.

Based on these results, it is proposed that C-Nap1 exists as a dimer probably with an anti-parallel arrangement of the coiled-coils folded at the flexible hinge. This arrangment is similar to that of the SMC (structural maintenance of chromosomes) proteins which constitute the cohesion and condensin complexes (Melby et al., 1998). It is likely that this flexible hinge region is responsible for positioning the terminal domains in close proximity together so that they may interact. The movement of the hinge region may be stimulated by its interaction with centrosomal components. This is suggested by previous research in which overexpression of the hinge region induced centrosome splitting, possibly by sequestering other components of the intercentriolar linkage such as Cep68 or rootletin (Mayor et al., 2000). One proposal is that the globular CTD and NTD of each C-Nap1 molecule may then interact with the same domain on a partner C-Nap1 molecule forming intermolecular homodimers. However, the NTD of each C-Nap1 molecule may also interact with the CTD of either the same molecule forming an intramolecular heterodimer interaction or a partner molecule forming an intermolecular heterodimer interaction (Figure 6.7).

The CTD and NTD domains of the dimer can both interact with and be phosphorylated by Nek2A. As the interaction between the CTD and NTD domains is reduced after phosphorylation by Nek2A, it is proposed that either the intramolecular interaction is disturbed such that C-Nap1 dimers open and close in a scissor-like fashion in response to phosphorylation by Nek2 and that this is aided by the flexibility of the hinge region; or that the intermolecular interaction is lost leading to loss of attraction of neighbouring molecules. Indeed, Nek2 might sit at the centre of the C-Nap1 domain complex and phosphorylate a number of residues which are positioned within the core of the complex, resulting in the dissociation of the NTD from the CTD and the simultaneous displacement of the C-Nap1 molecule from the centrosome. This model fits with results from a truncation study by Dr. Hames which suggested that the NTD binds the CTD at a different site to Nek2A implying that the NTD can interact simultaneously with the CTD and Nek2A (Hames, 2002). In addition, this model accounts for the observation that recombinant C-Nap1-CTD and –NTD both localise to the centrosome, although the central hinge region does not and that C-Nap1 molecules do not localise to the area between two parental centrioles (Mayor et al., 2000). Further research is clearly required to validate this proposed model and increase our

understanding of the interactions which occur between intercentriolar linkage components to regulate centrosome cohesion. Rotary shadowing electron microscopy of full-length C-Nap1 molecules would be a great help in revealing the structural conformation of C-Nap1 with and without phosphorylation by Nek2. Another experiment which could be performed is a yeast two-hybrid screen using the central region of C-Nap1 as bait. This may lead to the identification of novel proteins involved in C-Nap1 regulation or that form part of the intercentriolar linkage.

Previous work has suggested that there may be up to 13 Nek2 phosphorylation sites within the CTD of C-Nap1 as approximately 13 moles of phosphate were incorporated per mole of the C-Nap1 CTD (Helps et al., 2000). However, using mass spectrometry, only 7 Nek2 phosphorylation sites, were identified in the CTD, together with 1 site in the NTD. Two additional Nek2 phosphorylation sites at the extreme C-terminus of C-Nap1 that were previously identified by mass spectrometry were not identified in this study (Joanne Baxter, 2006). However, it is likely that the mass spectrometry analysis was not exhaustive. To determine whether there are additional Nek2 phosphorylation sites within C-Nap1 which were not identified by mass spectrometry, site-directed mutagenesis should be performed to mutate the 10 phosphorylation sites to non-phosphorylatable residues such as alanine or residues that mimic phosphorylation such as aspartate or glutamate. The mutated C-Nap1 proteins can then be expressed in bacteria and used as substrates in Nek2 kinase assays. If there are additional phosphorylation sites then one would expect the extent of phosphorylation of the mutated protein to be reduced but still detectable compared to the wild-type. Furthermore, the mutated C-Nap1 proteins could also be used in GST-pull down assays to determine whether the mutant construct still interacts with Nek2 or other domains of C-Nap1. Finally, mutation of these sites in full-length C-Nap1 constructs would allow the consequences of inhibiting phosphorylation *in vivo* to be determined, for example in terms of localisation to the centrosome.

Finally, the identification of sites that Nek2 targets is important as it allows the identification of a possible consensus sequence motif for Nek2 phosphorylation. Most protein kinases recognise specific sequences up to four residues on either side of the phosphorylated residue which work together to increase the overall selectivity of a kinase for particular substrates (Ubersax and Ferrell, 2007). Consensus phosphorylation sites have been determined for several protein kinases. For example, the NIMA consensus sequence has been defined as FRxS/T, whereas for Nek6 and Nek7 the target sequence is FP/LxFS/TF/Y (Lu et al., 1994;

Belham et al., 2001; Lizcano et al., 2002. The identification of a consensus sequence would help identify the sites on other substrates phosphorylated by the Nek2 kinase. However, the discovery of a consensus motif within a substrate does not necessarily mean that site is phosphorylated. In addition, there are also sites which are phosphorylated which do not conform to the consensus sequence (Ubersax and Ferrell, 2007). Analysis of the sequences surrounding the phosphorylation sites identified in C-Nap1 revealed the common motif of L/AxxS/Tϕ. Seven of the 10 phosphorylation sites identified share this consensus sequence, 6 of which lie in a common motif, LxxS/TL. This suggests there are hydrophobic pockets in the kinase that favour a hydrophobic residue at position P-3 and P+1. A hydrophobic residue at P+1 is also preferred by other protein kinases such as PKA which targets the consensus sequence RRxS/Tϕ. Interestingly, of the autophosphorylation sites identified in Nek2, T175 and T179 lie within the consensus sequence FxxS/Tϕ. The phenylalanine at position P-3 is similar in charge and hydrophobicity to leucine or alanine observed at position P-3 in the C-Nap1 phosphorylation sites. Of the other autophosphorylation sites, S241, S296, S387 and S397 partially conform to the proposed consensus sequence having a hydrophobic residue at P-3, but lacking the hydrophobic residue at P+1. Further analysis of the C-Nap1-CTD sequence suggests that there are over a dozen more serine or threonine residues which share the L/AxxS/Tϕ consensus motif which could represent additional Nek2 phosphorylation sites. Phosphorylation of synthetic peptides with variations on this motif would help identify the importance of these particular residues.

Chapter Seven

Final Discussion

7.1 Nek2 regulation by autophosphorylation

Upon overexpression, the Nek2A protein kinase induces a characteristic phenotype of premature centrosome splitting in interphase cells (Fry et al., 1998b). This loss of centrosome cohesion is thought to occur through the phosphorylation of intercentriolar linker proteins, such as C-Nap1 and rootletin, by the Nek2A kinase (Fry et al., 1998b; Hames, 2002; Bahe et al., 2005). Overexpression of Nek2A in HBL100 breast epithelial cells results in the accumulation of multinucleated cells with supernumerary centrosomes (Hayward et al., 2004). This is a typical hallmark of cancer. In addition, elevated levels of the Nek2 protein or amplification of the Nek2 gene has been observed in many cancer derived cell lines and primary tumours (Hayward et al., 2004; Hayward and Fry, 2005; Loo et al., 2004; Weiss et al., 2004). Therefore understanding how Nek2 activation is regulated in a precise and timely manner is a major goal of this research.

Previous work on Nek2A has identified a leucine zipper motif in the regulatory C-terminal domain that promotes homodimerisation and subsequent trans-autophosphorylation on serine and threonine residues (Fry et al., 1999). Recently, 13 autophosphorylation sites have been identified within Nek2A by mass spectrometry (Baxter, 2006). Of these sites, T175 is likely to be an important site of autophosphorylation, as a phosphomimetic mutation resulted in increased kinase activity, whereas an alanine substitution led to loss of activity. In addition, phosphorylation of Thr 179 and Ser 241 were likely to be important for Nek2 activity, as mutation of these residues led to loss of activity (Rellos et al., 2007).

The first aim of this thesis was to increase our understanding of how Nek2A is regulated by autophosphorylation by studying the remaining autophosphorylation sites within Nek2A using a site-directed mutagenesis approach.

This study found that mutation of either of the activation loop residues T170 and S171 to a phosphomimetic residue created hyperactive kinases. However, mutation of T170 and S171 to alanine had no effect upon Nek2A activity suggesting that autophosphorylation of these sites is not essential for Nek2A activation, but may enhance Nek2A activity perhaps by moving the activation loop further away from the active site, thus increasing access of substrates to the active site. In comparison, mutation of C-terminal residues S296, S356, S368, S387 and S428 to either aspartate or alanine had no effect upon Nek2A activity.

However, they may play roles in regulating some other aspect of Nek2 function that was not measured in the *in vitro* assays performed.

7.1.1 Is there a common mechanism for activation of Nek kinases?

It is thought that autophosphorylation of Nek2 within the activation loop induces a conformational change that allows Nek2 to become fully active and capable of phosphorylating its substrates, such as C-Nap1 and rootletin, to trigger centrosome separation and other mitotic events.

Interestingly, Nek6 and Nek7 are also activated by autophosphorylation of residues within their activation loops which are equivalent in position to autophosphorylation sites within Nek2. Nek6 is primarily phosphorylated at S206, which is the major event leading to Nek6 activation and equivalent to T175 in Nek2, with secondary phosphorylation events at T202, equivalent to the S171 site in Nek2 (Belham et al., 2003). Similarly, it is likely that in Nek7, phosphorylation of T195 primarily activates Nek7 with a secondary phosphorylation event at T191 enhancing Nek7 kinase activity. Furthermore, T170 in Nek2 is in an equivalent position to a potentially phosphorylatable threonine residue in Nek6 and Nek7. Nek9 is primarily phosphorylated at activation loop residue T210 by *in vitro* autoactivation which is equivalent in position to T175 in Nek2 (Tan and Lee, 2004). Interestingly, all members of the Nek kinase family possess a serine or threonine residue in an equivalent position to T175 in Nek2. Nek8 and Nek9 also have a serine residue at an equivalent position to S171 in Nek2, T202 in Nek6 and T191 in Nek7 which could act as a secondary site of phosphorylation as observed in Nek2, Nek6 and Nek7 (Rellos et al., 2006). This similarity in activation loop sequences in Nek kinases highlights the possibility that these kinases may share a common mechanism of activation with phosphorylation of equivalent residues required to fully activate the kinases.

7.1.2 Does the C-terminal domain of Nek2 act as an autoinhibitory domain?

The C-terminal domain of Nek2A contains many regulatory features including two degradation motifs, a KEN-box and MR-tail (Hames et al., 2001), a centrosomal targeting motif (Hames et al., 2005) and a KVHF motif that encodes a PP1 binding site (Helps et al., 2000). PP1 inhibits Nek2 by dephosphorylation. It has been previously shown using a GFP-tagged construct that removal of the last 25 amino acids results in a hyperactive kinase suggesting that the extreme C-terminus of Nek2A may act as an autoinhibitory domain in a similar manner to certain other domains exhibited by other kinases e.g. Plk1 (Baxter, 2006;

Jang et al., 2002; Mundt et al., 1997). However, using myc-tagged constructs, C-terminal truncation of Nek2 by 24 and 51 residues had no effect upon Nek2A activity. In addition mutation of residues S387 and S428 to aspartate or alanine had no effect upon Nek2A activity. However, the splice variant, Nek2B, that has a shorter C-terminus exhibited a higher level of activity compared to Nek2A *in vitro* supporting previous evidence that C-terminal residues act as an autoinhibitory domain which is missing in Nek2B (Hames and Fry, 2002). These data suggest that the C-terminus may function as an autoinhibitory domain which requires further investigation .

7.1.3 Does mutation of residues comprising the αT-helix result in hyperactivity?

Recently, a crystal structure of the catalytic domain of Nek2 complexed with a small molecule inhibitor has been solved (Rellos et al., 2007). This led to the identification of a novel αT-helix at the N-terminal end of the activation loop that appeared to block the active site. Initially, it was thought that the introduction of an A163G mutation in the centre of the helix would cause the helix to collapse freeing the active site and creating a hyperactive Nek2 kinase. It was proposed that this hyperactivity may counterbalance the inhibitory effect of an S241D/A mutation. However, unexpectedly an A163G mutation resulted in loss of kinase activity and did not rescue the inactivity caused by an S241 mutation. Additional mutations of other residues within the αT-helix also resulted in loss of kinase activity. Although these results do not support the original hypothesis, they do highlight this 5 amino acid region as being critical for Nek2 activation. One possibility is that mutation of these residues causes the αT-helix to collapse inside the active site thus inactivating the kinase. Further investigation is required to test this hypothesis and determine the role of this region. Ideally, the 5 residues of the αT-helix should be mutated individually to determine if all the residues are critical for Nek2 activity to the same extent.

7.1.4 Does mutation of the M86 gatekeeper residue alter Nek2A activity?

The generation of analogue-sensitive kinases provides a neat method for selectively inhibiting a specific protein kinase so that the functional consequences can be investigated (Blethrow et al., 2004; Gregan et al., 2007). M86 has been identified as the gatekeeper residue of Nek2 which sits in the ATP binding pocket. It is predicted that mutation of M86 to glycine or alanine would change the shape of the ATP binding pocket allowing an ATP analogue, 1NM-PP1, to bind in a non-competitive manner. However, such a mutant would only be useful if it retained the ability to use ATP as a substrate. Unfortunately, mutation of M86 led to the loss of Nek2A kinase activity, suggesting that the shape of the ATP binding pocket had been changed in such a way that no longer permitted the utilisation of ATP. This result has been observed with some other kinases and additional compensatory mutations are likely to be necessary to create an analogue-sensitive Nek2 kinase (Blethrow et al., 2004; Oh et al., 2007).

7.2 Generation of Nek2 phosphospecific antibodies

The identification of the putative autophosphorylation site T175 within the activation loop of Nek2 has highlighted a particular residue which would allow active Nek2 protein to be distinguished from inactive Nek2 protein. Using this information, we initiated the production of T175 phosphospecific antibodies using two different methods. Firstly, we purified antibodies from two different rabbits immunised with the pT175 phosphopeptide. Unfortunately, following purification, antibody A was not able to distinguish between the phospho- and non-phosphopeptides on a dot blot. The second antibody B detected the phosphopeptide more strongly than the non-phosphopeptide, although antibody B failed to distinguish between phosphorylated and unphosphorylated, bacterially-expressed and purified Nek2 proteins on a Western blot. It is also possible that antibodies A and B recognise other kinases which share a similar activation loop sequence. A third phosphospecific antibody, C, generated from rabbit serum supplied by Millennium Pharmaceuticals (Boston, USA) generated promising results as the antibody specifically detected the phosphopeptide and not the non-phosphopeptide and could detect phosphorylated, bacterially-expressed and purified Nek2 protein on a Western blot. In addition, antibody C could detect centrosomes in mitotic cells. However, due to the commercial implications of using an antibody generated by a pharmaceutical company in Nek2 drug discovery studies, it was felt necessary to generate a phosphospecific antibody by an alternative method.

Therefore six antibodies (AbD1-6) identified by AbD Serotec were characterised by using their recombinant antibody technology, as capable of selectively recognising phosphorylated peptides by ELISA assay. Using dot blot analysis, it was confirmed that all six antibodies strongly recognized the phosphorylated, but not the unphosphorylated, peptide. AbD1, 2 and 3 were capable of detecting a bacterially expressed Nek2 kinase domain fragment capable of autophosphorylation more strongly than a Nek2 fragment incapable of autophosphorylation. The same antibodies also detected a full-length Nek2A protein which had undergone autophosphorylation by pre-treatment with ATP. However, only AbD1 strongly stained centrosomes at prophase but not interphase. Finally, it was confirmed that AbD1 detected specifically the Nek2A kinase and not a number of other mitotic kinases, including Aurora-A and Plk1.

Having successfully established AbD1 as a phosphospecific Nek2 antibody, it was used as a tool for detecting active Nek2 in cells. By immunofluorescence microscopy, it was observed that Nek2 is specifically active in early mitosis being detected from early prophase until metaphase. Indeed, AbD1 stained spindle poles in some metaphase cells but not others. It is known that Nek2A is degraded at this point by the APC/C following ubiquitylation prior to anaphase onset (Hames et al., 2001; Hayes et al., 2006). Using AbD1, it was discovered that active Nek2 does not colocalise with centromeres where the kinetochore proteins, Hec1 and Sgo1, are localised. This suggests that these proteins are not likely to be substrates of Nek2 and that Nek2 does not contribute to the regulation of chromosome segregation or the spindle assembly checkpoint. In addition, AbD1 does not stain chromatin suggesting that HMGA2 is not a substrate of Nek2 in mitotic cells and that Nek2 does not directly regulate mitotic chromatin condensation.

The availability of a Nek2 phosphospecific antibody now allows the direct measurement of Nek2 activity in cells. Therefore, future experiments will involve the use of the Nek2 phosphospecific antibody in assays to determine the effectiveness of a number of small molecule inhibitors of Nek2 in a drug discovery project.

7.3 Does Nek2 activation occur upstream or downstream of Cdk1?

Cdk1 activation is required for mitotic entry, whereas its inactivation stimulates mitotic exit. Cdk1 is inactivated by APC/C-mediated destruction of cyclin B1 (Lindqvist et al., 2007). The destruction of cyclin B1 and securin relieves the inhibitory constraints imposed upon the cysteine protease, separase (Holland and Taylor, 2006). As a result, separase activation is thought to promote both sister chromatid separation and centriole disengagement (Tsou and Stearns, 2006). Centriole disengagement is thought to be a prerequisite for both centriole duplication and the recruitment of proteins to form the intercentriolar linker. This highlights a possible role for Cdk1 in centrosome cohesion (Tsou and Stearns, 2006). Furthermore, Cdk1 acts as a negative regulator of PP1, which in turn, inhibits Nek2 kinase activity (Meraldi and Nigg, 2001). Therefore, activation of Cdk1-cyclin B1 may indirectly lead to Nek2 activation at the G_2/M transition, which subsequently leads to loss of centrosome cohesion. Current evidence therefore suggests that Cdk1 may play roles in regulating centrosome cohesion and centriole duplication. However, this hypothesis is not supported by early studies in *Aspergillus* which suggest that Cdk1 and NIMA are activated independently, since inactivation of either kinase had no effect upon the activity of the other (Osmani et al., 1991).

In order to determine the consequences of Cdk1 inhibition upon Nek2 kinase activity and centrosome cohesion, a small molecule inhibitor of Cdk1, RO-3306 was used. It was confirmed that RO-3306 induced a substantial G_2/M arrest by flow cytometry analysis. We then showed that RO-3306 could directly inhibit the kinase activity of Cdk1 but not Nek2A *in vitro*. In addition, the ability of overexpressed Nek2A to stimulate centrosome splitting in cells was unaffected by RO-3306. Release of RO-3306 treated cells from drug-mediated G_2/M arrest led to mitotic entry, indicating that release from drug arrest leads to the activation of Cdk1. Moreover, the majority of these cells exhibited bipolar spindles, suggesting that Nek2 had also been activated leading to disassembly of the intercentriolar linkage. Together, these data suggest that Cdk1 functions upstream of Nek2A probably by relieving the inhibitory constraints imposed on Nek2A by PP1 (Fry et al., 1998b; Helps et al., 2000; Mi et al., 2007).

Further investigation revealed the presence of four γ-tubulin containing dots in cells treated with RO-3306 compared to the normal two dots observed in untreated cells. These four dots each also contained one dot of centrin suggesting that these foci arose from premature centriole disengagement rather than centrosome overduplication. A proposal is that Cdk1 activity is necessary to prevent premature centriole disengagement until anaphase onset, possibly by preventing the premature activation of separase. However, further investigation is required to test this hypothesis. Future experiments will need to investigate whether separase is active in cells arrested at G_2/M by RO-3306.

The majority of centrioles in RO-3306 treated cells were in close proximity to each other suggesting that they were still connected by the presence of the intercentriolar linkage. This was further supported by the presence of four C-Nap1 and rootletin dots in RO-3306 treated cells. It is proposed that centriole disengagement is a prerequisite for the recruitment of intercentriolar linker components and that these components can be recruited in a premature fashion if centriole disengagement occurs prematurely.

7.4 Nek2 interactions with C-Nap1

7.4.1 Nek2, C-Nap1 and the intercentriolar linkage

During interphase, the mother and daughter centrioles are physically joined by an intercentriolar linker. This remains present both before and after centriole duplication. The linker is likely to be composed of C-Nap1, rootletin and Cep68 (Fry et al., 1998; Graser et al., 2007; Yang et al., 2006). The current model proposes that these proteins are phosphorylated by Nek2 at the G_2/M transition leading to their displacement and the diassembly of the intercentriolar linkage (Bahe et al., 2005; Mayor et al., 1999). The centriole pairs then separate to form the spindle poles. C-Nap1 consists of N-terminal (NTD) and C-terminal (CTD) globular head domains joined by long coiled-coil domains and a central proline rich region that may act as a flexible hinge. In order to increase our understanding of how Nek2 and C-Nap1 interactions contribute to centrosome cohesion, it has been demonstrated that both the CTD and NTD can interact with each other and with themselves suggesting that the C-Nap1-CTD and -NTD domains can form hetero- and homo-dimers. It has also been shown that both the NTD and CTD are phosphorylated by Nek2A and that as a consequence of phosphorylation the ability of the C-Nap1 to form heterodimers was significantly reduced. However, the ability of these domains to form homodimers was unaffected.

A model has been generated based on these results, which also takes into account previous data on centrosome cohesion. Firstly, it is proposed that C-Nap1 exists as a dimer most likely in an anti-parallel arrangement of the coiled-coils folded at the hinge region. The globular CTD and NTD of each C-Nap1 molecule may interact with the same domain on a partner C-Nap1 molecule forming intermolecular homodimers. The NTD of each molecule may also interact with the CTD on either the same molecule or on a partner molecule forming an intramolecular or intermolecular heterodimer interaction, respectively (Figure 7.1). Previous research showed that overexpression of the hinge region induced centrosome splitting, possibly by sequestering other molecules which form the intercentriolar linkage, such as rootletin and Cep68 (Mayor et al., 2000). Previous research also suggested that rootletin forms oligomeric filaments between the pair of centrioles, unlike C-Nap1 which is only observed at the proximal ends of centrioles (Bahe et al., 2005; Yang et al., 2006). Recently, Cep68 has also been observed between a pair of centrioles decorating rootletin fibers (Graser et al., 2004). It is possible that Cep68 may stabilise rootletin fibers.

It is predicted that in late G_2, Nek2 bound to the NTD and CTD phosphorylates a number of residues positioned within the core of these domains, resulting in the dissociation of the NTD from the CTD. It may simultaneously lead to the displacement of C-Nap1 or loss of interaction between C-Nap1 and rootletin leading to disassembly of the intercentriolar linkage. Nek2 also phosphorylates rootletin which may further promote the dissociation of individual intercentriolar components. It has not yet been shown whether Cep68 is also phosphorylated by Nek2.

Further experiments are clearly required to validate this model. These could include rotary shadowing electron microscopy of full length C-Nap1 molecules to give an insight into the structural conformation of C-Nap1 with and without phosphorylation by Nek2. Another approach could involve a yeast two-hybrid screen using the central hinge region of C-Nap1 as bait which may lead to the identification of novel proteins involved in C-Nap1 regulation which could also constitute components of the intercentriolar linkage.

7.4.2 Does a Nek2 target consensus sequence exist?

Most protein kinases recognise a specific consensus sequence within their substrates as a target for phosphorylation. It is likely that this is also true of the Nek2 kinase. The identification of sites that Nek2 phosphorylates may help with the identification of a Nek2 consensus sequence motif. Seven Nek2 phosphorylation sites have been identified in the CTD and one site in the NTD of C-Nap1. However, it is likely that this mass spectrometry analysis was not exhaustive.

Analysis of the sequences surrounding the phosphorylation sites identified in C-Nap1 reveal a common motif of L/AxxS/Tϕ, with LxxS/TL being the preferred motif. This suggests that two hydrophobic pockets exist at P-3 and P+1 within the Nek2 kinase that prefer to interact with a hydrophobic residue on the substrate, similar to PKA. However, the NTD and CTD contain more than a dozen additional serine or threonine residues that lie within this consensus sequence. These may represent additional phosphorylation sites that have not yet been identified by mass spectrometry, or suggest that there are additional requirements for Nek2 to phosphorylate a particular sequence. Sequence analysis of the autophosphorylation sites identified within Nek2 revealed that T175 and T179 lie within the motif FxxS/Tϕ, where the phenylalanine is similar in hydrophobicity to leucine and alanine. In addition, S241, S296, S387 and S397 partially conform to the proposed consensus sequence, although they lack the hydrophobic residue at P+1. Interestingly, half of the phosphorylation sites identified in the Nek2 substrate, Nlp, lie within the consensus motif L/AxS/Txϕ (Baxter, 2006). However, in this case the leucine is positioned at P-2 rather than at position P-3 as predicted in the proposed consensus sequence and the other hydrophobic residue is located at P+2 rather than P+1 as predicted. So there maybe a general requirement for hydrophobic residues upstream and downstream of the phosphorylated residue, but some flexibility over exactly where these are positioned. A crystal structure of the Nek2 kinase domain with a substrate peptide bound would help to resolve this issue.

7.5 Concluding remarks

The research presented in this thesis has provided further insight into Nek2 regulation by autophosphorylation and the consequences of phosphorylation of the substrate C-Nap1 by Nek2. A number of phosphorylation sites have been identified within C-Nap1. Analysis of the sequences surrounding these phosphorylation sites has highlighted a possible Nek2 consensus sequence which has increased our understanding of how this kinase recognises its targets. It may also lead to the identification of additional substrates of Nek2 that are components of the intercentriolar linkage. This study has also provided evidence that C-Nap1 can homo- and hetero-dimerise and that its ability to heterodimerise is reduced in response to phosphorylation by Nek2. This has provided an insight into how the intercentriolar linkage is disassembled during centrosome separation at the G_2/M transition. Work within this thesis has also provided insights into the mechanisms of centriole disengagement, centrosome cohesion and the pathway by which Nek2 activity is regulated. Evidence has been presented that Nek2 functions downstream of Cdk1 and that centriole disengagement is a prerequisite for the recruitment of intercentriolar linker components.

Finally, the data on Nek2 autophosphorylation was used to generate a Nek2 phosphospecific antibody which was used to determine the timing and localisation of activation of Nek2 during the cell cycle. In the future, the phosphospecific antibody should prove an invaluable tool for detecting elevated levels of Nek2 activity in cancer cells and as a biomarker in the development of Nek2 inhibitors for use as novel anti-cancer treatments.

Chapter Eight

Bibliography

Abal, M., Piel, M., Bouckson-Castaing, V., Mogensen, M., Sibarita, J. B. and Bornens, M. (2002) **Microtubule release from the centrosome in migrating cells**. *J. Cell Biol.*, **159**(5): 731-737.

Adams, M., Smith, U. M., Logan, C. V. and Johnson, C. A. (2008) **Recent advances in the molecular pathology, cell biology and genetics of ciliopathies.** *J. Med. Genet.*, **45**(5): 257-267.

Alberts, B., Bray, D., Lewis, J., Raff, M., Roberts, K. and Watson, J. D. (2008) **Molecular biology of the cell**. 5th Edition. *Garland Science publishing*.

Andersen, J. S., Wilkinson, C. J., Mayor, T., Mortensen, P., Nigg, E. A. and Mann, M. (2003) **Proteomic characterization of the human centrosome by protein correlation profiling**. *Nature*, **426**(6966): 570-574.

Andrews, P. D., Knatko, E., Moore, W. J. and Swedlow, J. R. (2003) **Mitotic mechanics: the auroras come into view**. *Curr. Opin. Cell Biol.,* **15**(6): 672-683.

Arama, E., Yanai, A., Kilfin, G., Bernstein, A. and Motro, B. (1998) **Murine NIMA-related kinases are expressed in patterns suggesting distinct functions in gametogenesis and a role in the nervous system**. *Oncogene,* **16**: 1813-1823.

Avides, M. D. C. and Glover, D. M. (1999) **Abnormal spindle protein, Asp, and the integrity of mitotic centrosomal microtubule organizing centers**. *Science,* **283**: 1733-1735.

Avides, M. D. C., Tavares, A., Glover, D. M. (2001) **Polo kinase and Asp are needed to promote the mitotic organizing activity of centrosomes**. *Nat. Cell Bio.,* **3**: 421-424.

Badano, J. L., Mitsuma, N., Beales, P. L. and Katsanis, N. (2006) **The ciliopathies: an emerging class of human genetic disorders.** *Annu. Rev. Genomics Hum. Genet.*, **7**: 125-148.

Bahe, S., Steihof, Y., Wilkinson, C. J., Leiss, F., Nigg, E. A. (2005) **Rootletin forms centriole-associated filaments and functions in centrosome cohesion**. *J. Cell Biol.,* **171**: 27-33.

Bahmanyar, S., Kaplan, D. D., Deluca, J. G., Giddings, T. H. Jr., O'Toole, E. T., Winey, M., Salmon, E. D., Casey, P. J., Nelson, W. J., Barth, A. I. (2008) **beta-Catenin is a Nek2 substrate involved in centrosome separation**. *Genes Dev.,* **22**(1): 91-105.

Banerjee, M., Worth, D., Prowse, D. M., and Nikolic, M. (2002) **Pak1 phosphorylation on t212 affects microtubules in cells undergoing mitosis.** *Curr. Biol.,* **12**(14): 1233-1239.

Barr, A. R and Gergely, F. (2007) **Aurora-A: the maker and breaker of spindle poles**. *J. Cell Sci.,* **120**(17): 2987-2996.

Barr, F. A., Silljé, H. H. and Nigg, E. A. (2004) **Polo-like kinases and the orchestration of cell division**. *Nat. Rev. Mol. Cell. Biol.,* **5**(6): 429-440.

Barton, A. B., Davies, C. J., Hutchison, C. A. and Kaback, D. B. (1992) **Cloning of chromosome I DNA from Saccharomyces cerevisiae: analysis of the FUN52 gene, whose product has homology to protein kinases**. *Gene,* **117**(1): 137-140.

Basto, R., Lau, J., Vinogradova, T., Gardiol, A., Woods, C. G., Khodjakov, A., and Raff, J. W. (2006) **Flies without centrioles**. *Cell*, **125**(7): 1375-1386.

Baxter, J. E. (2006) **Phosphorylation site analysis of the centrosomal Nek2 kinase and its substrates**. *Ph. D Thesis,* University of Leicester.

Belham, C., Comb, M. J. and Avruch, J. (2001) **Identification of the NIMA family kinases NEK6/7 as regulators of the p70 ribosomal S6 kinase**. *Curr. Biol.,* **11**: 1155-1167.

Belham, C., Roig, J., Caldwell, J. A., Aoyama, Y., Kemp, B. E., Comb, M. and Ayruch, J. (2003) **A mitotic cascade of NIMA family kinases. Nercc1/Nek9 activates the Nek6 and Nek7 kinases**. *J. Biol. Chem.,* **278**(37): 34897-34909.

Berdnik, D. and Knoblich, J. A. (2002) **Drosophila Aurora-A is required for centrosome maturation and actin-dependent asymmetric protein localization during mitosis**. *Curr. Biol*., **12**(8): 640-647.

Bettencourt-Dias, M. and Glover, D. M. (2007) **Centrosome biogenesis and function: centrosomics brings new understanding**. *Nat. Rev. Mol. Cell. Biol.,* **8**(6): 451-463.

Blagden, S. P. and Glover, D. M. (2003) **Polar expeditions--provisioning the centrosome for mitosis**. *Nat. Cell Biol.,* **5**(6): 505-511.

Blangy, A., Lane, H. A., d'Hérin, P., Harper, M., Kress, M. and Nigg, E. A. (1995) **Phosphorylation by p34cdc2 regulates spindle association of human Eg5, a kinesin-related motor essential for bipolar spindle formation in vivo**. *Cell,* **83**(7): 1159-1169.

Blethrow, J., Zhang, C., Shokat, K. M. and Weiss, E. L. (2004) **Design and use of analog-sensitive protein kinases**. *Curr. Protoc. Mol. Biol*., **18**(11) 1-19.

Bonnet, J., Coopman, P. and Morris, M. C. (2008) **Characterization of centrosomal localization and dynamics of Cdc25C phosphatase in mitosis.** *Cell Cycle,* **13**: 1991-1998.

Bornens, M. (2002) **Centrosome composition and microtubule anchoring mechanisms**. *Curr. Opin. Cell Biol.,* **14**: 25-34.

Bouckson-Castaing, V., Moudjou, M., Ferguson, D. J., Mucklow, S., Belkaid, Y., Milon, G. and Crocker, P. J. (1996) **Molecular characterization of ninein, a coiled-coil protein of the centrosome**. *J. Cell Sci.,* **109**: 179-190.

Bowers, A. J. and Boylan, J. F. (2004) **Nek8, a NIMA family kinase member, is overexpressed in primary human breast tumors**. *Gene,* **328**: 135-142.

Brinkley, B. R. (2001) **Managing the centrosome numbers game: from chaos to stability in cancer cell division**. *Trends Cell Biol*., **11**(1): 18-21.

Brinkley, B. R. and Goepfert, T. M. (1998) **Supernumerary centrosomes and cancer: Boveri's hypothesis resurrected**. *Cell Motil. Cytoskeleton,* **41**(4): 281-288.

Brunet, S. and Maro, B. (2005) **Cytoskeleton and cell cycle control during meiotic maturation of the mouse oocyte: integrating time and space**. *Reproduction,* **130**(6): 801-811.

Buolamwini, J. K. (2000) **Cell cycle molecular targets in novel anticancer drug discovery**. *Curr. Pharm. Design,* **6**: 379-392.

Casenghi, M., Barr, F. A., Nigg, E. A. (2005) **Phosphorylation of Nlp by Plk1 negatively regulates its dynein-dynactin-dependent targeting to the centrosome**. *J. Cell Sci.,* **118**(21): 5101-5108.

Casenghi, M., Meraldi, P., Weinhart, U., Duncan, P. I., Korner, R. and Nigg, E. A. (2003) **Polo-like kinase 1 regulates Nlp, a centrosome protein involved in microtubule nucleation**. *Dev. Cell,* **5**: 113-125.

Chan, E. H., Santamaria, A., Silljé, H. H. and Nigg, E. A. (2008) **Plk1 regulates mitotic Aurora A function through betaTrCP-dependent degradation of hBora**. *Chromosoma,* **117**(5): 457-469.

Chen, A., Yanai, A., Arama, E., Kilfin, G. and Motro, B. (1999) **NIMA-related kinases: isolation and characterization of murine Nek3 and Nek4 cDNAs, and chromosomal localization of Nek1, Nek2 and Nek3**. *Gene,* **234**(1): 127-137.

Chen, Y., Riley, D. J., Zheng, L., Chen, P. L. and Lee, W. H. (2002) **Phosphorylation of the mitotic regulator protein Hec1 by Nek2 kinase is essential for faithful chromosome segregation**. *J. Biol. Chem.,* **277**(51): 49408-49416.

Cheng, K. Y., Lowe, E. D., Sinclair, J., Nigg, E. A., Johnson, L. N. (2003) **The crystal structure of the human polo-like kinase-1 polo box domain and its phospho-peptide complex**. *EMBO J.,* **22**: 5757-5768.

Cloutier, M., Vigneault, F., Lachance, D. and Seguin, A. (2005) **Characterization of a popular NIMA-related kinase PNek1 and its potential role in meristematic activity**. *FEBS Lett.,* **579**: 4659-4665.

Cohen, P. T. (2002) **Protein phosphatase 1--targeted in many directions**. *J. Cell Sci.,* **115**: 241-256.

Compton, D. A. (2000) **Spindle assembly in animal cells**. *Annu. Rev. Biochem.,* **69**: 95-114.

Cowan, C. R. and Hyman, A. A. (2004) **Asymmetric cell division in C. elegans: cortical polarity and spindle positioning**. *Annu. Rev. Cell Dev. Biol.,* **20**: 427-453.

Dammermann, A. and Merdes, A. (2002) **Assembly of centrosomal proteins and microtubule organization depends on PCM-1.** *J. Cell Biol.,* **159**(2): 255-266.

Dammermann, A., Müller-Reichert, T., Pelletier, L., Habermann, B., Desai, A. and Oegema, K. (2004) **Centriole assembly requires both centriolar and pericentriolar material proteins**. *Dev. Cell,* **7**(6): 815-829.

Dancey, J. and Sausville, E. A. (2003) **Issues and progress with protein kinase inhibitors for cancer treatment**. *Nat. Rev. Drug Discov.,* **2**(4): 296-313.

D'Assoro, A. B., Lingle, W. L. and Salisbury, J. L. (2002) **Centrosome amplification and the development of cancer**. *Oncogene,* **21**: 6146-6153.

de Cárcer, G., Pérez de Castro, I., Malumbres, M. (2007) **Targeting cell cycle kinases for cancer therapy**. *Curr. Med. Chem.*, **14**(9): 969-985.

Deng, C. X. (2002) **Roles of BRCA1 in centrosome duplication**. *Oncogene*, **21**(40): 6222-6227.

de Vos, S., Hofmann, W. K., Thomas, M. G., Krug, U., Schrage, M., Milerr, T. P., Braun, J. G., Wachsman, W., Koeffler, H. P. and Said, J. W. (2003) **Gene expression profile of serial samples of transformed B-Cell lymphomas**. *Lab. Invest.*, **83**(2): 271-285.

Delgehyr, N., Sillibourne, J. and Bornens, M. (2005) **Microtubule nucleation and anchoring at the centrosome are independent processes linked by ninein function**. *J. Cell. Sci.*, **118**: 1565-1567.

Di Agostino, S., Rossi, P., Geremia, R. and Sette, C. (2002) **The MAPK pathway triggers activation of Nek2 during chromosome condensation in mouse spermatocytes**. *Development*, **129**(7): 1715-1727.

Di Agostino, S., Fedele, M., Chieffi, P., Fusco, A., Rossi, P., Geremia, R., Sette, C. (2004) **Phosphorylation of high-mobility group protein A2 by Nek2 kinase during the first meiotic division in mouse spermatocytes**. *Mol. Biol. Cell*, **15**(3): 1224-1232.

Dictenberg, J. B., Zimmerman, W., Sparks, C. A., Young, A., Vidair, C., Zheng, Y., Carrington, W., Fay, F. S. and Doxsey, S. J. (1998) **Pericentrin and gamma-tubulin form a protein complex and are organized into a novel lattice at the centrosome**. *J. Cell Biol.*, **141**: 163-174.

Ditchfield, C., Keen, N. and Taylor, S. S. (2005) **The Ipl1/Aurora kinase family: methods of inhibition and functional analysis in mammalian cells**. *Methods Mol. Biol.*, **296**: 371-381.

Diwan, J. (2006) **Molecular Biochemistry: Microtubule Motors**
http://www.rpi.edu/dept/bcbp/molbiochem/MBWeb/mb2/part1/kinesin.htm

Donaldson, M. M., Tavares, A. A., Ohkura, H., Deak, P. and Glover, D. M. (2001) **Metaphase arrest with centromere separation in polo mutants of Drosophila.** *J. Cell Biol.*, **153**(4): 663-676.

Doxsey, S. (1998) **The centrosome--a tiny organelle with big potential**. *Nat. Genet.*, **20**(2): 104-106.

Doxsey, S. (2001) **Re-evaluating centrosome function**. *Nat. Rev. Mol. Cell Biol.*, **2**: 688-698.

Doxsey, S. (2002) **Duplicating dangerously: Linking centrosome duplication and aneuploidy**. *Mol. Cell*, 439-440.

Doxsey, S., Zimmerman, W. and Mikule, K. (2005) **Centrosome control of the cell cycle**. *Trends Cell Biol.*, **15**: 303-311.

Doxsey, S. J., Stein, P., Evans, L., Calarco, P. D. and Kirschner, M. (1994) **Pericentrin, a**

highly conserved centrosome protein involved in microtubule organization. *Cell,* **76**: 639-650.

Dutertre, S., Descamps, S. and Prigent, C. (2002) **On the role of aurora-A in centrosome function**. *Oncogene,* **21**(40): 6175-6183.

Eckerdt, F., Yuan, J., Saxena, K., Martin, B., Kappel, S., Lindenau, C., Kramer, A., Naumann, S., Daum, S., Fischer, G., Dikic, I., Kaufmann, M. and Strebhardt, K. (2005) **Polo-like kinase 1 (Plk1) mediated phosphorylation of Pin1 stabilizes Pin1 by inhibiting its ubiquitination in human cells**. *J. Biol. Chem.,* **280**(44): 36575-36583.

Egloff, M. P., Johnson, D. F., Moorhead, G., Cohen, P. T., Cohen, P. and Barford, D. (1997) **Structural basis for the recognition of regulatory subunits by the catalytic subunit of protein phosphatase 1**. *EMBO J.,* **16**: 1876-1887.

Elia, A. E., Rellos, P., Haire, L. F., Chao, J. W., Ivins, F. J., Hoepker, K., Mohammad, D., Cantley, L. C., Smerdon, S. J. and Yaffe, M. B. (2003) **The molecular basis for phosphodependent substrate targeting and regulation of Plks by the Polo-box domain**. *Cell,* **115**: 83-95.

Ems-McClung, S. C., Hertzer, K. M., Zhang, X., Miller, M. W. and Walczak, C. E. (2007) **The interplay of the N- and C-terminal domains of MCAK control microtubule depolymerization activity and spindle assembly**. *Mol. Biol. Cell.,* **18**(1): 282-294.

Eley, L., Yates, L. M. and Goodship, J. A. (2005) **Cilia and disease**. *Curr. Opin. Genet. Dev.,* **15**(3): 308-314.

Eto, M., Elliot, E., Prickett, T. D. and Brautigan, D. L. (2002) **Inhibitor-2 regulates protein phosphatase-1 complexed with NIMA-related kinase to induce centrosome separation.** *J. Biol. Chem.,* **277**: 44013-44020.

Fang, G., Yu, H. and Kirschner, M. W. (1998) **Direct binding of CDC20 protein family members activates the anaphase-promoting complex in mitosis and G1.** *Mol. Cell,* **2**(2): 163-171.

Faragher, A. J. and Fry, A. M. (2003) **Nek2A kinase stimulates centrosome disjunction and is required for formation of bipolar mitotic spindles**. *Mol. Biol. Cell,* **14**: 1-14.

Feige, E. and Motro, B. (2002) **The related murine kinases, Nek6 and Nek7, display distinct patterns of expression**. *Mech. Dev.,* **110**(1-2): 219-223.

Fiegauf, M., Benzing, T. and Omran, H. (2008) **When cilia go bad: cilia defects and ciliopathies**. *Nat. Rev. Mol. Cell Biol.,* **8**(11): 880-893.

Fletcher, L., Cernigilia, G. J., Nigg, E. A., Yen, T. J. and Muschel, R. J. (2004) **Inhibition of centrosome separation after DNA damage: a role for Nek2**. *Radiat. Res.,* **162**(2): 128-135.

Fletcher, L., Cerniglia, G. J., Yen, T. J. and Muschel, R. J. (2005) **Live cell imaging reveals distinct roles in cell cycle regulation for Nek2A and Nek2B**. *Biochim. Biophys. Acta,* 1744: 89-92.

Fourest-Lieuvin, A., Peris, L., Gache, V., Garcia-Saez, I., Juillan-Binard, C., Lantez, V. and

Job, D. (2006) **Microtubule regulation in mitosis: tubulin phosphorylation by the cyclin-dependent kinase Cdk1**. *Mol. Biol. Cell,* **17**(3): 1041-1050.

Fry, A. M. (2002) **The Nek2 protein kinase: a novel regulator of centrosome structure.** *Oncogene,* **21**: 6184-6194.

Fry, A. M., Arnaud, L. and Nigg. E. A. (1999) **Activity of the human centrosomal kinase, Nek2 depends on an unusual leucine zipper dimerization motif**. *J. Biol. Chem.,* **274**(23): 16304-16310.

Fry, A. M. and Baxter, J. E. (2006) **Sealed with a Kiz: How Plk1 ensures spindle pole Integrity**. *Dev. Cell.,* **11**(4): 431-432.

Fry, A. M., Descombes, P., Twomey, C., Bacchieri, R. and Nigg, E. A. (2000a) **The NIMA-related kinase X-Nek2B is required for efficient assembly of the zygotic centrosome in Xenopus laevis**. *J. Cell Sci.,* **113** (11): 1973-1984.

Fry, A. M. and Faragher, A. J. (2001) **Identification of centrosome kinases**. *Methods Cell Biol.,* **67**: 305-323.

Fry, A. M., Mayor. T., Meraldi, P., Stierhof, Y., Tanaka, K. and Nigg, E. A. (1998b) **C-Nap1, a Novel centrosomal coiled-coil protein and candidate substrate of the cell cycle – regulated protein kinase Nek2**. *J. Cell Biol.,* **141**(7): 1563-1574.

Fry, A. M., Mayor, T. and Nigg, E. A. (2000b) **Regulating centrosomes by protein phosphorylation**. *Curr. Top. Dev. Biol.,* **49**: 291-312.

Fry, A. M., Meraldi, P. and Nigg, E. A. (1998a) **A centrosomal function for the human Nek2 protein kinase, a member of the NIMA family of cell cycle regulators**. *EMBO J.,* **17**(2): 470-481.

Fry, A. M. and Nigg, E. A. (1997) **Characterization of mammalian NIMA-related kinases**. *Methods Enzymol.,* **283**: 270-282.

Fry, A. M., Schultz, S. J., Bartek, J. and Nigg, E. A. (1995) **Substrate specificity and cell cycle regulation of the Nek2 protein kinase, a potential human homolog of the mitotic regulator NIMA of Aspergillus nidulans**. *J. Biol. Chem.,* **270**: 12899-12905.

Fry, A. M. and Yamano, H. (2006) **APC/C-mediated degradation in early mitosis: how to avoid spindle assembly checkpoint inhibition**. *Cell Cycle*. **5**(14): 1487-1491.

Fu, G., Ding, X., Yuan, K., Aikhionbare, F., Yao, J., Cai, X., Jiang, K. and Yao, X. (2007) **Phosphorylation of human Sgo1 by NEK2A is essential for chromosome congression in mitosis**. *Cell Res.,* **17**(8): 664-665.

Fujioka, T., Takebayashi, Y., Ito, M. and Uchida, T. (2000) **Nek2 expression and localization in porcine oocyte during maturation**. *Biochem. Biophys. Res. Commun.,* **279**(3): 799-802.

Fukasawa, K. (2007) **Oncogenes and tumour suppressors take on centrosomes**. *Nat. Rev. Cancer,* **7**(12): 911-924.

Fukasawa, K. (2008) **p53, cyclin-dependent kinase and abnormal amplification of centrosomes**. *Biochim. Biophys. Acta*. **1786**(1): 15-23.

Fuller, S. D., Gowen, B. E., Reinsch, S., Sawyer, A., Buendia, B., Wepf, R. and Karsenti, E. (1995) **The core of the mammalian centriole contains gamma-tubulin**. *Curr. Biol.,* **5**(12): 1384-1393.

Gaetz, J. and Kapoor, T. M. (2004) **Dynein/dynactin regulate metaphase spindle length by targeting depolymerizing activities to spindle poles**. *J. Cell Biol.,* **166**: 465-471.

Glover, D. M. (2005) **Polo kinase and progression through M phase in Drosophila: a perspective from the spindle poles**. *Oncogene*, **24**(2): 230-237.

Glover, D. M., Leibowitz, M. H., McLean, D. A. and Parry, H. (1995) **Mutations in aurora prevent centrosome separation leading to the formation of monopolar spindles**. *Cell*, **81**(1): 95-105.

Giet, R., Uzbekov, R., Kireev, I. and Prigent, C. (1999) **The Xenopus laevis centrosome aurora/Ipl1-related kinase.** *Biol. Cell*., **91**(6): 461-470.

Golsteyn, R. M., Mundt, K. E., Fry, A. M. and Nigg, E. A. (1995) **Cell cycle regulation of the activity and subcellular localization of PLK1, a human protein kinase implicated in mitotic spindle function**. *J. Cell Biol.,* **129**: 1617-1628.

Gönczy, P., Echeverri, C., Oegema, K., Coulson, A., Jones, S. J., Copley, R. R., Duperon, J., Oegema, J., Brehm, M., Cassin, E., Hannak, E., Kirkham, M., Pichler, S., Flohrs, K., Goessen, A., Leidel, S., Alleaume, A. M., Martin, C., Ozlü, N., Bork, P. and Hyman, A. A. (2000) **Functional genomic analysis of cell division in C. elegans using RNAi of genes on chromosome III**. *Nature*, **408**(6810): 331-336.

Gorr, I. H., Boos, D. and Stemmann, O. (2005) **Mutual inhibition of separase and Cdk1 by two-step complex formation**. *Mol. Cell*, **19**(1): 135-141.

Graf, R. (2002) **DdNek2, the first non-vertebrate homologue of human Nek2, is involved in the formation of microtubule-organizing centers**. *J. Cell Sci.,* **115**(9): 1919-1929.

Grallert, A. and Hagan, I. M. (2002) **Schizosaccharomyces pombe NIMA-related kinase, Fin1, regulates spindle formation and an affinity of Polo for the SPB**. *EMBO J.,* **21**: 3096-3107.

Grallert, A., Krapp, A., Bagley, S., Simanis, V. and Hagan, I. M. (2004) **Recruitment of NIMA kinase shows that maturation of the S. pombe spindle-pole body occurs over consecutive cell cycles and reveals a role for NIMA in modulating SIN activity**. *Genes Dev.,* **18**(9): 1007-1021.

Graser, S., Stierhof, Y. D. and Nigg, E. A. (2007) **Cep68 and Cep215 (Cdk5rap2) are required for centrosome cohesion**. *J. Cell Sci.,* **120**(24): 4321-4331.

Gregan, J., Zhang, C., Rumpf, C., Cipak, L., Li, Z., Uluocak, P., Nasmyth, K. and Shokat, K. M. (2007) **Construction of conditional analog-sensitive kinase alleles in the fission yeast Schizosaccharomyces pombe.** *Nat. Protoc*., **2**(11): 2996-3000.

Gromley, A., Jurczyk, A., Sillibourne, J., Halilovic, E., Mogensen, M., Groisman, I., Blomberg, M. and Doxsey, S. (2003) **A novel human protein of the maternal centriole is required for the final stages of cytokinesis and entry into S phase.** *J. Cell Biol.,* **161**(3): 535-545.

Gumireddy, K., Reddy, M. V., Cosenza, S. C., Boominathan, R., Baker, S. J., Papathi, N., Jiang, J., Holland, J. and Reddy, E. P. (2005) **ON01910, a non-ATP-competitive small molecule inhibitor of Plk1, is a potent anticancer agent**. *Cancer Cell*, **7**(3): 275-286.

Habedanck, R., Stierhof, Y. D., Wilkinson, C. J. and Nigg, E. A. (2005) **The Polo kinase Plk4 functions in centriole duplication.** *Nat. Cell Biol.,* **7**(11): 1140-1146.

Ha Kim, Y., Yeol Choi, J., Jeong, Y., Wolgemuth, D. J. and Rhee, K. (2002) **Nek2 localizes to multiple sites in mitotic cells, suggesting its involvement in multiple cellular functions during the cell cycle**. *Biochem. Biophys. Res. Commun.,* **290**(2): 730-736.

Hames, R. S. (2002) **Cell cycle regulation of the centrosomal kinase Nek2 and its substrate C-Nap1**. *Ph. D Thesis,* University of Leicester.

Hames, R. S., Crookes, R. E., Straatman, K. R., Merdes, A., Hayes, M. J., Faragher, A. J. and Fry, A. M. (2005) **Dynamic recruitment of Nek2 kinase to the centrosome involves microtubules, PCM-1, and localized proteasomal degradation**. *Mol. Biol. Cell,* **16**(4): 1711-1724.

Hames, R. S. and Fry, A. M. (2002) **Alternative splice variants of the human centrosome kinase Nek2 exhibit distinct patterns of expression in mitosis**. *Biochem. J.,* **361**: 77-85.

Hames, R. S., Wattam, S. L., Yamano, H., Bacchieri, R. and Fry, A. M. (2001) **APC/C-mediated destruction of the centrosomal kinase Nek2A occurs in early mitosis and depends upon a cyclin A-type D-box.** *EMBO J.,* **20**(24): 7117-7127.

Hanks, S. K. and Hunter, T. (1995) **Protein kinases 6. The eukaryotic protein kinase superfamily: kinase (catalytic) domain structure and classification.** *FASEB J.,* **9**(8): 576-596.

Hannak, E., Kirkham, M. and Hyman, A. A., Oegema, K. (2001) **Aurora-A kinase is required for centrosome maturation in Caenorhabditis elegans**. *J. Cell Biol.,* **155**(7): 1109-1116.

Hansen, D. V., Hsu, J. Y., Brett, K. K., Jackson. P. K. and Eldridge, A. G. (2002) **Control of the centriole and centrosome cycles by ubiquitination enzymes**. *Oncogene,* **21**: 6209-6221.

Hashimoto, Y., Akita, H., Hibino, M., Kohri, K. and Nakanishi, M. (2002) **Identification and characterization of Nek6 protein kinase, a potential human homolog of NIMA histone H3 kinase**. *Biochem. Biophys. Res. Commun.,* **293**(2): 753-758.

Hayashi, K., Igarashi, H., Ogawa, M. and Sakaguchi, N. (1999) **Activity and substrate specificity of the murine STK2 Serine/Threonine kinase that is structurally related to the mitotic regulator protein NIMA of Aspergillus nidulans**. *Biochem. Biophys. Res. Commun.,* **264**(2): 449-456.

Hayes, M. J., Kimata, Y., Wattam, S. L., Lindon, C., Mao, G., Yamano, H. and Fry, A. M.

(2006) **Early mitotic degradation of Nek2A depends on Cdc20-independent interaction with the APC/C**. *Nat. Cell Biol.,* **8**(6): 607-614.

Hayward, D. (2007) **Validating the NIMA-related kinase Nek2 as a novel chemotherapeutic target**. *Ph. D Thesis,* University of Leicester.

Hayward, D. G., Clarke, R. B., Faragher, A. J., Pillai, M. R., Hagan, I. M. and Fry, A. M. (2004) **The centrosomal kinase Nek2 displays elevated levels of protein expression in human breast cancer**. *Cancer Res.,* **64**(20): 7370-7376.

Hayward, D. G. and Fry, A. M. (2006) **Nek2 kinase in chromosome instability and cancer**. *Cancer Lett.,* **237**: 155–166.

Heald, R., Tournebize, R., Blank, T., Sandaltzopoulos, R., Becker, P., Hyman, A. and Karsenti, E. (1996) **Self-organization of microtubules into bipolar spindles around artificial chromosomes in Xenopus egg extracts**. *Nature*. **382**(6590): 420-425.

Heald, R., Tournebize, R., Habermann, A., Karsenti, E. and Hyman, A. (1997) **Spindle assembly in Xenopus egg extracts; respective roles of centrosomes and microtubule self-organization**. *J. Cell Biol.,* **138**: 615-628.

Helps, N. R., Luo, X., Barker, H. M. and Cohen, P. T. W. (2000) **NIMA-related kinase 2 (Nek2), a cell-cycle-regulated protein kinase localized to centrosomes, is complexed to protein phosphatase 1**. *Biochem. J.,* **349**: 509-518.

Higginbotham, H. R. and Gleeson, J. G. (2007) **The centrosome in neuronal development**. *Trends Neurosci*., **30**(6): 276-283.

Hinchcliffe, E. H., Li, C., Thompson, E. A., Maller, J. L. and Sluder, G. (1999) **Requirement of Cdk2-cyclin E activity for repeated centrosome reproduction in Xenopus egg extracts**. *Science*. **283**(5403): 851-854.

Hinchcliffe, E. H., Miller, F. J, Cham, M., Khodjakov, A. and Sluder ,G. (2001) **Requirement of a centrosomal activity for cell cycle progression through G1 into S phase**. *Science,* **291**(5508): 1547-1550.

Holland, P. M. and Cooper, J. A. (1999) **Protein modification: Docking sites for kinases**. *Curr. Biol.,* **9**: R329-R331.

Holland, A. J. and Taylor, S. S. (2006) **Cyclin-B1-mediated inhibition of excess separase is required for timely chromosome disjunction**. *J. Cell Sci.,* **119**(16): 3325-3336.

Hong, Y. R., Chen, C.H., Chang, J. H., Wang, S., Sy, W. D., Chou, C. K. and Howng, S. L. (2000) **Cloning and characterization of a novel human ninein protein that interacts with the glycogen synthase kinase 3beta**. *Biochim. Biophys. Acta,* **1492**(2-3): 513-516.

Houtgraaf, J. H., Versmissen, J. and van der Giessen, W. J. (2006) **A concise review of DNA damage checkpoints and repair in mammalian cells**. *Cardiovasc. Revasc. Med.,* **7**(3): 165-172.

Hulme, J. T., Yarov-Yarovoy, V., Lin, T. W., Scheuer, T. and Catterall, W. A. (2006) **Autoinhibitory control of the CaV1.2 channel by its proteolytically processed distal C-**

terminal domain. *J. Physiol.*, **576**(1): 87-102.

Huse, M. and Kuriyan, J. (2002) **The conformational plasticity of protein kinases**. *Cell*, **109**(3): 275-282.

Hut, H. M., Lemstra, W., Blaauw, E. H., Van Cappellen, G. W., Kampinga, H. H. and Sibon, O. C. (2003) **Centrosomes split in the presence of impaired DNA integrity during mitosis**. *Mol. Biol. Cell*, **14**(5): 1993-2004.

Ishikawa, H., Kubo, A., Tsukita, S. and Tsukita, S. (2005) **Odf2-deficient mother centrioles lack distal/subdistal appendages and the ability to generate primary cilia.** *Nat. Cell. Biol.*, **7**(5): 517-524.

Jackman, M., Lindon, C., Nigg, E. A. and Pines, J. (2003) **Active cyclin B1-Cdk1 first appears on centrosomes in prophase**. *Nat. Cell Biol.*, **5**(2): 143-148.

Jackson, J. R., Patrick, D. R., Dar, M. M. and Huang, P. S. (2007) **Targeted anti-mitotic therapies: can we improve on tubulin agents?** *Nat. Rev. Cancer*, **7**(2): 107-17.

Jang, Y. J., Ma, S., Terada, Y. and Erikson, R. L. (2002) **Phosphorylation of threonine 210 and the role of serine 137 in the regulation of mammalian polo-like kinase**. *J. Biol. Chem.*, **277**(46): 44115-44120.

Jang, Y. J., Lin, C. Y. and Erikson, R. L. (2002) **Functional studies of the role of the C-terminal domain of mammalian polo-like kinase**. *PNAS*, **99**(4): 1984-1989.

Jeong, Y., Lee, J., Kim, K., Yoo, J. C. and Rhee, K. (2007) **Characterization of NIP2/centrobin, a novel substrate of Nek2, and its potential role in microtubule stabilization**. *J. Cell Sci.*, **120**(12): 2106-2116.

Job, D., Valiron, O. and Oakley, B. (2003) **Microtubule nucleation**. *Curr. Opin. Cell Biol.*, **15**: 111-117.

Johnson, L. N., Noble, M. E. M. and Owen, D. J. (1996) **Active and inactive protein kinases: structural basis for regulation**. *Cell*, **85**: 149-158.

Jones, D. G. and Rosamond, J. (1990) **Isolation of a novel protein kinase-encoding gene from yeast by oligodeoxyribonucleotide probing** *Gene*, **90**, 87-92.

Kandli, M., Feige, E., Chen, A., Kilfin, G. and Motro, B. (2000) **Isolation and characterization of two evolutionarily conserved murine kinases (Nek6 and Nek7) related to the fungal mitotic regulator, NIMA**. *Genomics*, **68**(2): 187-196.

Kang, J., Chen, Y., Zhao, Y. and Yu, H. (2007) **Autophosphorylation-dependent activation of human Mps1 is required for the spindle checkpoint**. *Proc. Natl. Acad. Sci. USA.*, **104**(51): 20232-20237.

Keating, T. J. and Borisy, G. G. (2000) **Immunostructural evidence for the template mechanism of microtubule nucleation**. *Nat. Cell Biol.*, **2**: 352-357.

Kelm, O., Wind, M., Lehmann, W. D. and Nigg, E. A. (2002) **Cell cycle-regulated phosphorylation of the Xenopus polo-like kinase Plx1**. *J. Biol. Chem.*, **277**: 25247-25256.

Khodjakov, A. and Rieder, C. L. (1999) **The sudden recruitment of gamma-tubulin to the centrosome at the onset of mitosis and its dynamic exchange throughout the cell cycle, do not require microtubules**. *J. Cell Biol.,* **146**(3): 585-596.

Khodjakov, A. and Rieder, C. L. (2001) **Centrosomes enhance the fidelity of cytokinesis in vertebrates and are required for cell cycle progression**. *J. Cell Biol.,* **153**: 237-242.

Kim, S., Lee, K. and Rhee, K. (2007) **NEK7 is a centrosomal kinase critical for microtubule nucleation**. *Biochem. Biophys. Res. Commun.*, **360**(1): 56-62.

Kimura, M. and Okano, Y. (2001) **Molecular cloning and characterization of the human NIMA-related protein kinase 3 gene (NEK3)**. *Cytogenet. Cell Genet.*, **95**(3-4): 177-182.

Kinoshita, K., Noetzel, T. L., Pelletier, L., Mechtler, K., Drechsel, D. N., Schwager, A., Lee, M., Raff, J. W. and Hyman, A. A. (2005) **Aurora A phosphorylation of TACC3/maskin is required for centrosome-dependent microtubule assembly in mitosis.** *J. Cell Biol.,* 170(7): 1047–1055.

Kirkham. M., Müller-Reichert, T., Oegema, K., Grill, S. and Hyman, A. A. (2003) **SAS-4 is a C. elegans centriolar protein that controls centrosome size**. *Cell,* **112**(4): 575-587.

Kleylein-Sohn, J., Westendorf, J., Le Clech, M., Habedanck, R., Stierhof, Y. D. and Nigg, E. A. (2007) **Plk4-induced centriole biogenesis in human cells**. *Dev. Cell,* **13**(2): 190-202.

Kochanski, R. S. and Borisy, G. G. (1990) **Mode of centriole duplication and distribution**. *J. Cell Biol.,* **110**(5): 1599-1605.

Kokuryo, T., Senga, T., Yokoyama, Y., Nagino, M., Nimura, Y. and Hamaguchi, M. (2007) **Nek2 as an effective target for inhibition of tumorigenic growth and peritoneal dissemination of cholangiocarcinoma.** *Cancer Res.*, **67**(20): 9637-9642.

Krien, M. J. E., Bugg, S. J., Palatsides, M., Asouline, G., Morimyo, M. and O’Connell, M. J. (1998) **A NIMA homologue promotes chromatin condensation in fission yeast**. *J. Cell Sci.,* **111**: 967-976.

Krien, M. J., West, R. R., John, U. P., Koniaras, K., McIntosh, J. R. and O'Connell, M. J. (2002) **The fission yeast NIMA kinase Fin1p is required for spindle function and nuclear envelope integrity**. *EMBO J.*, **21**(7): 1713-1722.

Lacey, K. R., Jackson, P. K. and Stearns, T. (1999) **Cyclin-dependent kinase control of centrosome duplication.** *PNAS.*, **96**(6): 2817-2822.

Lane, H. A. and Nigg, E. A. (1996) **Antibody microinjection reveals an essential role for human polo-like kinase 1 (plk1) in the functional maturation of mitotic centrosomes**. *J. Cell Biol.*, **135**(6): 1701-1713.

Laoukili, J., Kooistra, M. R., Bras, A., Kauw, J., Kerkhoven, R. M., Morrison, A., Clevers, H. and Medema, R. H. (2005) **FoxM1 is required for execution of the mitotic programme and chromosome stability**. *Nat. Cell Biol.,* **7**: 126-136.

La Terra, S., English, C. N., Hergert, P., McEwen, B. F., Sluder, G. and Khodjakov, A.

(2005) **The de novo centriole assembly pathway in HeLa cells: cell cycle progression and centriole assembly/maturation**. *J. Cell Biol.*, **168**(5): 713-722.

Leach, C., Shenolikar, S., and Brautigan, D. L. (2003) **Phosphorylation of phosphatase inhibitor-2 at centrosomes during mitosis**. *J. Biol. Chem.,* **278**: 26015-26020.

Leidel, S., Delattre, M., Cerutti, L., Baumer, K. and Gönczy, P. (2005) **SAS-6 defines a protein family required for centrosome duplication in C. elegans and in human cells**. *Nat. Cell Biol.*, **7**(2): 115-125.

Leidel, S. and Gönczy, P. (2003) **SAS-4 is essential for centrosome duplication in C elegans and is recruited to daughter centrioles once per cell cycle**. *Dev. Cell,* **4**(3): 431-439.

Leidel, S. and Gönczy, P. (2005) **Centrosome duplication and nematodes: recent insights from an old relationship**. *Dev. Cell,* **9**(3): 317-325.

Letwin, K., Mizzen, L., Motro, B., Ben-David, Y., Bernstein, A. and Pawson, T. (1992) **A mammalian dual specificity protein kinase, Nek1, is related to the NIMA cell cycle regulator and highly expressed in meiotic germ cells**. *EMBO J.*, **11**(10): 3521-3531.

Lindqvist, A., van Zon, W., Karlsson Rosenthal, C. and Wolthuis, R. M. (2007) **Cyclin B1-Cdk1 activation continues after centrosome separation to control mitotic progression**. *PLoS Biol.*, **5**(5): e123.

Liu, Q., Tan, G., Levenkova, N., Li, T., Pugh, E. N. Jr., Rux, J. J., Speicher, D. W. and Pierce, E. A. (2007) **The proteome of the mouse photoreceptor sensory cilium complex.** *Mol. Cell. Proteomics,* **6**(8): 1299-1317.

Liu, S., Lu, W., Obara, T., Kuida, S., Lehoczky, J., Dewar, K., Drummond, I. A. and Beier, D. R. (2002) **A defect in a novel Nek-family kinase causes cystic kidney disease in the mouse and in zebrafish.** *Development,* **129**(24): 5839-5846.

Lizcano, J. M., Deak, M., Morrice, N., Kieloch, A., Hastie, C. J., Dong, L., Schutkowski, M., Reimer, U. and Alessi, D. R. (2002) **Molecular basis for the substrate specificity of NIMA-related kinase-6 (NEK6)**. *J. Biol. Chem.*, **277**(31): 27839-27849.

Lou, Y., Yao, J., Zereshki, A., Dou, Z., Ahmed, K., Wang, H., Hu, J., Wang, Y. and Yao, X. (2004) **NEK2A interacts with MAD1 and possibly functions as a novel integrator of the spindle checkpoint signaling**. *J. Biol. Chem.*, **279**: 20049-20057.

Lu, K. P. and Hunter, T. (1995) **The NIMA kinase: a mitotic regulator in Aspergillus nidulans and vertebrate cells**. *Prog. Cell Cycle Res.*, **1**: 187-205.

Lu, K. P., Kemp, B. E. and Means, A. R. (1994) **Identification of substrate specificity determinants for the cell cycle-regulated NIMA protein kinase.** *J. Biol. Chem.*, **269**(9): 6603-6607.

Lu, K. P., Osmani, S. A. and Means, A. R. (1993) **Properties and regulation of the cell cycle-specific NIMA protein kinase of Aspergillus nidulans**. *J. Biol. Chem.*, **268**(12): 8769-8776.

Lupas, A. (1996) **Coiled coils: new structures and new functions**. *Trends Biochem. Sci.*, **21**: 375-382.

Mandell, J. W. (2003) **Phosphorylation state-specific antibodies: applications in investigative and diagnostic pathology**. *Am. J. Pathol.*, **163**(5): 1687-1698.

Mantel, C., Braun, S. E., Reid, S., Henegariu, O., Liu, L., Hangoc, G. and Broxmeyer, H. E. (1999) **p21(cip-1/waf-1) deficiency causes deformed nuclear architecture, centriole overduplication, polyploidy, and relaxed microtubule damage checkpoints in human hematopoietic cells.** *Blood,* **93**(4): 1390-1398.

Marshall, W. F. (2001) **Centrioles take center stage**. *Curr. Biol.*, **11**(12): R487-96.

Marumoto, T., Honda, S., Hara, T., Nitta, M., Hirota, T., Kohmura, E. and Saya, H. (2003) **Aurora-A kinase maintains the fidelity of early and late mitotic events in HeLa cells.** *J. Biol. Chem.*, **278**(51): 51786-51795.

Matsumoto, Y., Hayashi, K. and Nishida, E. (1999) **Cyclin-dependent kinase 2 (Cdk2) is required for centrosome duplication in mammalian cells.** *Curr. Biol.*, **9**(8): 429-432.

Matthews, N., Visintin, C., Hartzoulakis, B., Jarvis, A. and Selwood, D. L. (2006) **Aurora A and B kinases as targets for cancer: will they be selective for tumors?** *Expert Rev. Anticancer Ther.*, **6**(1): 109-120.

Mattison, C. P., Old, W. M., Steiner, E., Huneycutt, B. J., Resing, K. A., Ahn, N. G. and Winey, M. (2007) **Mps1 activation loop autophosphorylation enhances kinase activity**. *J. Biol. Chem.*, **282**(42): 30553-30561.

Mayor, T., Hacker, U., Stierhof, Y. and Nigg, E. A. (2002) **The mechanism regulating the dissociation of the centrosomal protein C-Nap1 from mitotic spindle poles**. *J. Cell Sci.,* **115**: 3275-3284.

Mayor, T., Meraldi. P., Stierhof, Y., Nigg, E. A. and Fry, A. M. (1999) **Protein kinases in control of the centrosome cycle.** *FEBS* Lett, **452**: 93-95.

Mayor. T., Stierhof, Y., Tanaka, K., Fry, A. M. and Nigg, E. A. (2000) **The centrosomal protein C-Nap1 is required for cell cycle-regulated centrosome cohesion**. *J. Cell Biol.,* **151**(4): 837-846.

McIntosh, J. R., Grishchuk, E. L. and West, R. R. (2002) **Chromosome-microtubule interactions during mitosis**. *Annu. Rev. Cell Dev. Biol.,* **18**: 193-219.

Melby, T. E., Ciampaglio, C. N., Briscoe, G. and Erickson, H. P. (1998) **The symmetrical structure of structural maintenance of chromosomes (SMC) and MukB proteins: long, antiparallel coiled coils, folded at a flexible hinge**. *J. Cell Biol.*, **142**(6): 1595-1604.

Meraldi, P., Honda, R. and Nigg, E. A. (2002) **Aurora-A overexpression reveals tetraploidization as a major route to centrosome amplification in p53-/- cells**. *EMBO J.,* **21**(4): 483-492.

Meraldi, P., Lukas, J., Fry, A. M., Bartek, J. and Nigg, E. A. (1999) **Centrosome duplication in mammalian somatic cells requires E2F and Cdk2-cyclin A.** *Nat. Cell Biol.*, **1**(2): 88-93.

Meraldi, P. and Nigg, E.A. (2001) **Centrosomal cohesion is regulated by a balance of kinases and phosphatase activities**. *J. Cell Sci.,* **114**: 3749-3757.

Meraldi, P., Honda, R. and Nigg, E. A. (2002) **Aurora-A overexpression reveals tetraploidization as a major route to centrosome amplification in P53$^{-/-}$ cells**. *EMBO J.,* **21**: 483-492.

Merdes, A., Heald, R., Samejima, K., Earnshaw, W. C. and Cleveland, D. W. (2000) **Formation of spindle poles by dynein/dynactin-dependent transport of NuMA**. *J. Cell Biol.,* **149**(4): 851-862.

Mi, J., Guo, C., Brautigan, D. L. and Larner, J. M. (2007) **Protein phosphatase-1alpha regulates centrosome splitting through Nek2.** *Cancer Res.,* **67**(3): 1082-1089.

Mikule, K., Delaval, B., Kaldis, P., Jurcyzk, A., Hergert, P. and Doxsey, S. (2007) **Loss of centrosome integrity induces p38-p53-p21-dependent G1-S arrest**. *Nat. Cell Biol.,* **9**(2): 160-170.

Miller, S. L., Antico, G., Raghunath, P. N., Tomaszewski, J. E. and Clevenger, C. V. (2007) **Nek3 kinase regulates prolactin-mediated cytoskeletal reorganization and motility of breast cancer cells.** *Oncogene*. **26**(32): 4668-4678.

Minoguchi, S., Minoguchi, M. and Yoshimura, A. (2003) **Differential control of the NIMA-related kinases, Nek6 and Nek7, by serum stimulation**. *Biochem. Biophys. Res. Commun,* **301**(4): 899-906.

Mitchison, T. J. and Salmon, E. D. (1992) **Poleward kinetochore fiber movement occurs during both metaphase and anaphase-A in newt lung cell mitosis.** *J. Cell Biol.,* **119**(3): 569-582.

Mitchison, T. J. and Salmon, E. D. (2001) **Mitosis: a history of division**. *Nat. Cell Biol.,* **3**: E17-E21.

Mogensen, M. M. (1999) **Microtubule release and capture in epithelial cells**. *Biol. Cell.,* **91**(4-5): 331-341.

Mogensen, M. M., Mackie, J. B., Doxsey, S. J., Stearns, T. and Tucker, J. B. (1997) **Centrosomal deployment of gamma-tubulin and pericentrin: evidence for a microtubule-nucleating domain and a minus-end docking domain in certain mouse epithelial cells.** *Cell Motil. Cytoskeleton*. **36**(3): 276-290.

Mogensen, M. M., Malik, A., Piel, M., Bouckson-Castaing, V. and Bornens, M. (2000) **Microtubule minus-end anchorage at centrosomal and non-centrosomal sites: the role of ninein**. *J. Cell Sci,* **113** (17): 3013-3023.

Mori, D., Yano, Y., Toyo-oka, K., Yoshida, N., Yamada, M., Muramatsu, M., Zhang, D., Saya, H., Toyoshima, Y. Y., Kinoshita, K., Wynshaw-Boris, A. and Hirotsune, S. (2007) **NDEL1 phosphorylation by Aurora-A kinase is essential for centrosomal maturation, separation, and TACC3 recruitment**. *Mol. Cell Biol.,* **27**(1): 352-367.

Moritz, M., and Agard, D. A. (2001) **Gamma-tubulin complexes and microtubule**

nucleation. *Curr. Opin. Struct. Biol.,* **11**: 174-181.

Moritz, M., Braunfeld, M. B., Guenebaut, V., Heuser, J. and Agard, D. A. (2000) **Structure of the gamma-tubulin ring complex: a template for microtubule nucleation**. *Nat.Cell Biol.* **2**: 365-370.

Moss, D. K., Bellett, G., Carter, J. M., Liovic, M., Keynton, J., Prescott, A. R., Lane, E. B. and Mogensen, M. M. (2007) **Ninein is released from the centrosome and moves bi-directionally along microtubules**. *J. Cell Sci.*, **120**(17): 3064-3074.

Mundt, K. E., Golsteyn, R. M., Lane, H. A. and Nigg, E. A. (1997) **On the regulation and function of human polo-like kinase 1 (PLK1): effects of overexpression on cell cycle progression.** *Biochem. Biophys. Res. Commun*., **239**(2): 377-385.

Musacchio, A. and Hardwick, K. G. (2002) **The spindle checkpoint: structural insights into dynamic signalling**. *Mol. Cell Biol.,* **3**: 731-741.

Nakajima, H., Toyoshima-Morimoto, F., Taniguchi, E. and Nishida, E. (2003) **Identification of a consensus motif for Plk (Polo-like kinase) phosphorylation reveals Myt1 as a Plk1 substrate**. *J. Biol. Chem.,* **278**(28): 25277-25280.

Neef, R., Preisinger, C., Sutcliffe, J., Kopajtich, R., Nigg, E. A., Mayer, T. U. and Barr, F. A. (2003) **Phosphorylation of mitotic kinesin-like protein 2 by polo-like kinase 1 is required for cytokinesis**. *J. Cell Biol.,* **162**: 863-875.

Nigg, E. A. (1998) **Polo-like kinases: positive regulators of cell division from start to finish**. *Curr. Opin. Cell Biol.,* **10**: 776-783.

Nigg, E. A. (2001) **Mitotic kinases as regulators of cell division and its checkpoints**. *Nat. Rev. Mol. Cell Biol.,* **2**: 21-32.

Nigg, E. A. (2002) **Centrosomal aberrations: cause or consequence of cancer progression?** *Nat. Rev. Cancer,* **2**: 815-825.

Nigg, E. A. (2004) **Centrosomes in development and disease**. *Wiley-VCH.*

Nigg, E. A., Blangy, A. and Lane, H. A. (1996) **Dynamic changes in nuclear architecture during mitosis: on the role of protein phosphorylation in spindle assembly and chromosome segregation**. *Exp. Cell Res.,* **229**: 174-180.

Noguchi, K., Fukazawa, H., Murakami, Y. and Uehara, Y. (2004) **Nucleolar Nek11 is a novel target of Nek2A in G1/S-arrested cells**. *J. Biol. Chem.,* **279**(31): 32716-32727.

Noguchi, K., Fukazawa, H., Murakami, Y. and Uehara, Y., 2002. **Nek11, a new member of the NIMA family of kinases, involved in DNA replication and genotoxic stress responses**. *J. Biol. Chem.,* **277**(42): 39655-39665.

Nolen, B., Taylor, S. and Ghosh, G. (2004) **Regulation of protein kinases: controlling activity through activation segment conformation**. *Mol. Cell,* **15**: 661-675.

O'Connell, M. J., Krien. M. J. E. and Hunter, T. (2003) **Never say never. The NIMA-related protein kinases in mitotic control**. *Trends Cell Biol.*, **13**(5): 211-228.

O'Connell, M. J., Norbury, C. and Nurse, P. (1994) **Premature chromatin condensation upon accumulation of NIMA**. *EMBO J.*, **13**(20): 4926-4937.

O'Connell, M. J., Meluh, P. B., Rose, M. D. and Morris, N. R. (1993) **Suppression of the bimC4 mitotic spindle defect by deletion of klpA, a gene encoding a KAR3-related kinesin-like protein in Aspergillus nidulans**. *J. Cell Biol.*, **120**(1): 153-162.

Oh, H., Ozkirimli, E., Shah, S., Harrison, M. L. and Geahlen, R. L. (2007) **Generation of an analog-sensitive Syk tyrosine kinase for the study of signaling dynamics from the B cell antigen receptor.** *J. Biol. Chem.,* **282**(46): 33760-33768.

Ohta, K., Shiina, N., Okumura, E., Hisanaga, S., Kishimoto, T., Endo, S., Gotoh, Y., Nishida, E. and Sakai, H. (1993) **Microtubule nucleating activity of centrosomes in cell-free extracts from Xenopus eggs: involvement of phosphorylation and accumulation of pericentriolar material**. *J. Cell Sci.*, **104** (1): 125-137.

Okuda, M., Horn, H. F., Tarapore, P., Tokuyama,Y., Smulian, A. G., Chan, P. K., Knudsen, E. S., Hofmann, I. A., Snyder, J. D., Bove, K. E. and Fukasawa, K. (2000) **Nucleophosmin/B23 is a target of CDK2/cyclin E in centrosome duplication**. *Cell,* **103**(1): 127-140.

Oshimori, N., Ohsugi, M. and Yamamoto, T. (2006) **The Plk1 target Kizuna stabilizes mitotic centrosomes to ensure spindle bipolarity**. *Nat. Cell Biol.*, **8**(10): 1095-1101.

Osmani, S. A., Engle, D. B., Doonan, J. H. and Morris, N. R. (1988) **Spindle formation and chromatin condensation in cells blocked at interphase by mutation of a negative cell cycle control gene**. *Cell,* **52**(2): 241-251.

Osmani, A. H., McGuire, S. L,, O'Donnell, K. L., Pu, R. T. and Osmani, S. A. (1991) **Role of the cell-cycle-regulated NIMA protein kinase during G2 and mitosis: evidence for two pathways of mitotic regulation**. *Cold Spring Harb. Symp. Quant. Biol.*, **56**: 549-555.

Osmani, S. A., May, G. S. and Morris, N. R. (1987) **Regulation of the mRNA levels of nimA, a gene required for the G2-M transition in Aspergillus nidulans**. *J. Cell Biol.,* **104**(6): 1495-1504.

O'Regan, L., Blot, J. and Fry, A. M. (2007) **Mitotic regulation by NIMA-related kinases.** *Cell Div.*, **2**: 25.

Paintrand, M., Moudjou, M., Delacroix, H. and Bornens, M. (1992) **Centrosome organisation and centriole architecture: their sensitivity to divalent cations.** *J. Struct. Biol.*, **108**: 107-128.

Pelletier, L., O'Toole, E., Schwager, A., Hyman, A. A. and Müller-Reichert, T. (2006) **Centriole assembly in Caenorhabditis elegans**. *Nature*, **444**(7119): 619-623.

Peters, U., Cherian, J., Kim, J. H., Kwok, B. H. and Kapoor, T. M. (2006) **Probing cell-division phenotype space and Polo-like kinase function using small molecules**. *Nat. Chem. Biol.*, **2**(11): 618-626.

Pfleger, C. M. and Kirschner, M. W. (2000) **The KEN box: an APC recognition signal**

distinct from the D box targeted by Cdh1. *Genes Dev.*, **14**(6): 655-665.

Pfleger, C. M., Lee, E. and Kirschner, M. W. (2001) **Substrate recognition by the Cdc20 and Cdh1 components of the anaphase-promoting complex**. *Genes Dev.*, **15**(18): 2396-2407.

Piel, M., Meyer, P., Khodjakov, A., Reider, C. L. and Bornens, M. (2000) **The respective contributions of the mother and daughter centrioles to centrosome activity and behaviour in vertebrate cells**. *J. Cell Biol.,* **149**: 317-330.

Pihan, G. A. and Doxsey, S. J. (1999) **The mitotic machinery as a source of genetic instability in cancer**. *Semin. Cancer Biol.,* **9**: 289-302.

Pines, J. and Rieder, C. L. (2001) **Re-staging mitosis: a contemporary view of mitotic progression**. *Nat. Cell Biol.,* **3**: E3-E6.

Pines, J. (1999) **Four-dimensional control of the cell cycle**. *Nat. Cell Biol.,* **1**: E73-E78.

Ping Lu, K., Osmani, S. A., and Means, A. R. (1993) **Properties and regulation of the cell cycle-specific NIMA protein kinase of *Aspergillus Nidulans***. *J. Biol. Chem.,* **268**(12): 8769-8776.

Polci, R., Peng, A., Chen, P. L., Riley, D. J. and Chen, Y. (2004) **NIMA-related protein kinase 1 is involved early in the ionizing radiation-induced DNA damage response**. *Cancer Res.,* **64**(24): 8800-8803.

Prigent, C., Glover, D.M. and Giet, R. (2005) **Drosophila Nek2 protein kinase knockdown leads to centrosome maturation defects while overexpression causes centrosome fragmentation and cytokinesis failure**. *Exp. Cell Res.,* **303**(1): 1-13.

Prime, G. and Markie, D. (2005) **The telomere repeat binding protein Trf1 interacts with the spindle checkpoint protein Mad1 and Nek2 mitotic kinase**. *Cell Cycle,* **4**(1): 121-124.

Pu, R. T., Xu, G., Wu, L., Vierula, J., O'Donnell, K., Ye, X. S. and Osmani, S. A. (1995) **Isolation of a functional homolog of the cell cycle-specific NIMA protein kinase of Aspergillus nidulans and functional analysis of conserved residues**. *J. Biol. Chem.,* **270**(30): 18110-18116.

Pugacheva, E. N. and Golemis, E. A. (2005) **The focal adhesion scaffolding protein HEF1 regulates activation of the Aurora-A and Nek2 kinases at the centrosome**. *Nat. Cell Biol.,* **7**(10): 937-946.

Quarmby, L. M. and Mahjoub, M. R. (2005) **Caught Nek-ing: cilia and centrioles**. *J. Cell Sci.,* **118**(22): 5161-5169.

Quintyne, N. J., Gill, S. R., Eckley, D. M., Crego, C. L., Compton, D. A. and Schroer, T. A. (1999) **Dynactin is required for microtubule anchoring at centrosomes.** *J. Cell Biol.,* **147**(2): 321-334.

Quintyne, N. J. and Schroer, T. A. (2002) **Distinct cell cycle-dependent roles for dynactin and dynein at centrosomes**. *J. Cell Biol.,* **159**(2): 245-254.

Rapley, J., Baxter, J. E., Blot, J., Wattam, S. L., Casenghi, M., Meraldi, P., Nigg, E. A. and Fry, A. M. (2005). **Coordinate regulation of the mother centriole component Nlp by Nek2 and Plk1 protein kinases**. *Mol. Cell. Biol.,* **25**(4): 1309-1324.

Rellos, P., Ivins, F. J., Baxter, J. E., Pike, A., Nott, T., Parkinson, D-M., Das, S., Howell, S., Fedorov, O., Shen, Q. Y., Fry, A. M., Knapp, S. and Smerdon, S. J. (2007) **Structure and regulation of the human Nek2 centrosomal kinase.** *J. Biol. Chem.*, **282**(9): 6833-6842.

Ren, B., Cam, H., Takahashi, Y., Volkert, T., Jolyon, T., Terragni, J., Young, R. A. and Dynlacht. B. D. (2002) **E2F integrates cell cycle progression with DNA repair, replication, and G_2/M checkpoints**. *Genes Dev.*, **16**: 245-256.

Rhee, K. and Wolgemuth, D. J. (1997) **The NIMA-related kinase 2, Nek2, is expressed in specific stages of the meiotic cell cycle and associates with meiotic chromosomes**. *Development,* **124**(11): 2167-2177.

Roig, J., Mikhailov, A., Belham, C. and Avruch, J. (2002) **Nercc1, a mammalian NIMA-family kinase, binds the Ran GTPase and regulates mitotic progression**. *Genes Dev.* **16**: 1640-1658.

Roig, J., Groen, A., Caldwell, J. and Avruch, J. (2005) **Active Nercc1 protein kinase concentrates at centrosomes early in mitosis and is necessary for proper spindle assembly**. *Mol. Biol. Cell.*, **16**(10): 4827-4840.

Roghi, C., Giet, R., Uzbekov, R., Morin, N., Chartrain, I., Le Guellec, R., Couturier, A., Dorée, M., Philippe, M. and Prigent, C. (1998) **The Xenopus protein kinase pEg2 associates with the centrosome in a cell cycle-dependent manner, binds to the spindle microtubules and is involved in bipolar mitotic spindle assembly**. *J. Cell Sci.*, **111**(5): 557-572.

Saavedra, H. I, Maiti, B., Timmers, C., Altura, R., Tokuyama, Y., Fukasawa, K. and Leone, G. (2003) **Inactivation of E2F3 results in centrosome amplification.** *Cancer Cell*, **3**: 333-346.

Salisbury, J. L., Suino, K. M., Busby, R. and Springett, M. (2002) **Centrin-2 is required for centriole duplication in mammalian cells**. *Curr. Biol.*, **12**(15): 1287-1292.

Saunders, W. (2005) **Centrosomal amplification and spindle multipolarity in cancer cells**. *Semin. Cancer. Biol*., **15**(1): 25-32.

Sawin, K. E. and Mitchison, T. J. (1995) **Mutations in the kinesin-like protein Eg5 disrupting localization to the mitotic spindle.** *Proc. Natl. Acad. Sci. USA.***,** **92**(10): 4289-4293.

Schneeweiss, A., Sinn, H. P., Ehemann, V., Khbeis, T., Neben, K., Krause, U., Ho, A. D., Bastert, G. and Krämer, A. (2003) **Centrosomal aberrations in primary invasive breast cancer are associated with nodal status and hormone receptor expression**. *Int. J. Cancer,* **107**(3): 346-352.

Schultz, S. J., Fry, A. M., Sutterlin, C., Ried, T. and Nigg, E. A. (1994) **Cell cycle-dependent expression of Nek2, a novel human protein kinase related to the NIMA mitotic regulator of Aspergillus nidulans**. *Cell Growth Differ.* **5**: 625-635.

Seki, A., Coppinger, J. A., Jang, C. Y., Yates, J. R. and Fang, G. (2008) **Bora and the kinase Aurora A cooperatively activate the kinase Plk1 and control mitotic entry**. *Science*, **320**(5883): 1655-1658.

Seong, Y. S., Kamijo, K., Lee, J. S., Fernandez, E., Kuriyama, R., Miki, T. and Lee, K. S. (2002) **A spindle checkpoint arrest and a cytokinesis failure by the dominant-negative polo-box domain of Plk1 in U2OS cells**. *J. Biol. Chem.*, 277(35): 32282-32293.

Shalom, O., Shalva, N., Altschuler, Y. and Motro, B. (2008) **The mammalian Nek1 kinase is involved in primary cilium formation.** *FEBS Lett.,* **582**(10): 1465-1470.

Sonn, S., Khang, I., Kim, K. and Rhee, K. (2004) **Suppression of Nek2A in mouse early embryos confirms its requirement for chromosome segregation**. *J. Cell Science,* **117**: 5557-5566.

Stearns, T. and Winey, M. (1997) **The cell center at 100.** *Cell*, **91**(3): 303-309.

Sumara, I., Gimenez-Abian, J. F., Gerlich, D., Hirota, T., Kraft, C., De La Torre, C., Ellenberg, J. and Peters, J. M. (2004) **Roles of polo-like kinase 1 in the assembly of functional mitotic spindles**. *Curr. Biol.*, **14**(19): 1712-1722.

Surpili, M. J., Delben, T. M. and Kobarg, J. (2003) **Identification of proteins that interact with the central coiled-coil region of the human protein kinase NEK1**. *Biochemistry,* **42**: 15369-15376.

Swenson, K. I., Winkler, K. E. and Means, A. R. (2003) **A new identity for MLK3 as an NIMA-related, cell cycle-regulated kinase that is localized near centrosomes and influences microtubule organization**. *Mol. Biol. Cell,* **14**: 156-172.

Takahashi, M., Yamagiwa, A., Nishimura, T., Mukai, H. and Ono, Y. (2002) **Centrosomal proteins CG-NAP and kendrin provide microtubule nucleation sites by anchoring gamma-tubulin ring complex**. *Mol. Biol. Cell,* **13**: 3235-3245.

Takai, N., Hamanaka, R., Yoshimatsu, J. and Miyakawa, I. (2005) **Polo-like kinases (Plks) and cancer**. *Oncogene,* **24**: 287-291.

Tan, B. C-M. and Lee, S-C. (2004) **Nek9, a novel FACT-associated protein, modulates interphase progression**. *J. Biol. Chem.*, **279**(10): 9321-9330.

Tanaka, K. and Nigg, E. A. (1999) **Cloning and characterization of the murine Nek3 protein kinase, a novel member of the NIMA family of putative cell cycle regulators.** *J. Biol. Chem.*, **274**(19): 13491-13497.

Tanaka, K., Parvinen, M. and Nigg, E.A. (1997) **The in vivo expression pattern of mouse Nek2, a NIMA-related kinase, indicates a role in both mitosis and meiosis**. *Exp. Cell Res.,* **237**(2): 264-274.

Tavares, A. A, Glover, D. M. and Sunkel, C. E. (1996) **The conserved mitotic kinase polo is regulated by phosphorylation and has preferred microtubule-associated substrates in Drosophila embryo extracts**. *EMBO J.*, **15**(18): 4873-4883.

Taylor, S. S., Knighton, D. R., Zheng, J., Ten Eyck, L. F. and Sowadski, J. M. (1992) **Structural framework for the protein kinase family**. *Annu. Rev. Cell Biol.*, **8**: 429-462.

Taylor, S. and Peters, J. M. (2008) **Polo and Aurora kinases: lessons derived from chemical biology**. *Curr. Opin. Cell Biol.*, **20**(1): 77-84.

Thompson, H. M., Cao, H., Chen, J., Euteneuer, U. and McNiven, M. A. (2004) **Dynamin 2 binds gamma-tubulin and participates in centrosome cohesion.** *Nat. Cell Biol.*, **6**(4): 335-342.

Toji, S., Yabuta, N., Hosomi, T., Nishihara, S., Kobayashi, T., Suzuki, S., Tamai, K. and Nojima, H. (2004) **The centrosomal protein Lats2 is a phosphorylation target of Aurora-A kinase**. *Genes Cells*, **9**(5): 383-397.

Tsou, M. F. and Stearns, T. (2006) **Controlling centrosome number: licenses and blocks**. *Curr. Opin. Cell Biol.*, **18**(1): 74-78.

Twomey, C., Wattam, S. L., Pillai, M. R., Rapley, J., Baxter, J. E. and Fry, A. M. (2004) **Nek2B stimulates zygotic centrosome assembly in Xenopus laevis in a kinase-independent manner**. *Dev. Biol.*, **265**: 384-398.

Ubersax, J. A. and Ferrell, J. E. Jr. (2007) **Mechanisms of specificity in protein phosphorylation**. *Nat. Rev. Mol. Cell Biol.*, **8**(7): 530-541.

Uhlmann, F., Wernic, D., Poupart, M. A., Koonin, E. V. and Nasmyth, K. (2000) **Cleavage of cohesin by the CD clan protease separin triggers anaphase in yeast.** *Cell*, **103**(3): 375-386.

Urbani, L. and Stearns, T. (1999) **The centrosome**. *Curr. Biol.*, **9**(9): R315-7.

Uto, K., Nakajo, N. and Sagata, N. (1999) **Two structural variants of Nek2 kinase, termed Nek2A and Nek2B, are differentially expressed in Xenopus tissues and development**. *Dev. Biol.*, **208**(2): 456-464.

Uto, K. and Sagata, N. (2000) **Nek2B, a novel maternal form of Nek2 kinase, is essential for the assembly or maintenance of centrosomes in early Xenopus embryos**. *EMBO J.*, **19**(8): 1816-1826.

Vaisberg, E. A., Koonce, M. P. and McIntosh, J. R. (1993) **Cytoplasmic dynein plays a role in mammalian mitotic spindle formation.** *J. Cell Biol.*, **123**(4): 849-858.

van de Weerdt, B. C., Littler, D. R., Klompmaker, R., Huseinovic, A., Fish, A., Perrakis, A., Medema, R. H. (2008) **Polo-box domains confer target specificity to the Polo-like kinase family**. *Biochim. Biophys. Acta*, **1783**(6): 1015-1022.

van Vugt, M. A. and Medema, R. H. (2005) **Getting in and out of mitosis with Polo-like kinase-1**. *Oncogene*, **24**: 2844-2859.

Vasquez, R. J., Gard, D. L. and Cassimeris, L. (1999) **Phosphorylation by CDK1 regulates XMAP215 function in vitro**. *Cell Motil. Cytoskeleton*, **43**(4): 310-321.

Vassilev, L. T., Tovar, C., Chen, S., Knezevic, D., Zhao, X., Sun, H., Heimbrook, D. C. and

Chen, L. **Selective small-molecule inhibitor reveals critical mitotic functions of human CDK1**. *Proc. Natl. Acad. Sci. USA,* **103**(28): 10660-10665.

Vidwans, S. J**.,** Wong, M. L. and O'Farrell, P. H. (2003) **Anomalous centriole configurations are detected in Drosophila wing disc cells upon Cdk1 inactivation.** *J. Cell Sci.,* **116**(1): 137-143.

Vodermaier, H. C. and Peters, J. (2002) **Conspiracy to disarm APC in interphase**. *Nat. Cell Biol.,* **4**: E119-E120.

Wai, D. H., Schaefer, K. L., Schramm, A., Korsching, E., Van Valen, F., Ozaki, T., Boecker, W., Schweigerer, L., Dockhorn-Dworniczak, B. and Poremba, C. (2002) **Expression analysis of pediatric solid tumor cell lines using oligonucleotide microarrays**. *Int. J. Oncol.,* **20**(3): 441-451.

Waizenegger, I. C., Hauf, S., Meinke, A. and Peters, J. M. (2000) **Two distinct pathways remove mammalian cohesin from chromosome arms in prophase and from centromeres in anaphase**. *Cell,* **103**(3): 399-410.

Wang, S., Nakashima, S., Sakai, H., Numata, O., Fujiu, K. and Nozawa, Y. (1998) **Molecular cloning and cell-cycle-dependent expression of a novel NIMA (never-in-mitosis in Aspergillus nidulans)-related protein kinase (TpNrk) in Tetrahymena cells**. *J. Biochem.,* **334** (1): 197-203.

Wang, X., Yang, Y. and Dai, W. (2006) **Differential subcellular localizations of two human Sgo1 isoforms: implications in regulation of sister chromatid cohesion and microtubule dynamics**. *Cell Cycle,* **5**(6): 635-640.

Wang, X., Yang, Y., Duan, Q., Jiang, N., Huang, Y., Darzynkiewicz, Z. and Dai, W. (2008) **sSgo1, a major splice variant of Sgo1, functions in centriole cohesion where it is regulated by Plk1**. *Dev. Cell,* **14**(3): 331-341.

Warnke, S., Kemmler, S., Hames, R. S., Tsai, H. L., Hoffmann-Rohrer, U., Fry, A. M., and Hoffmann, I. (2004) **Polo-like kinase-2 is required for centriole duplication in mammalian cells**. *Curr. Biol.,* **14**: 1200-1207.

Wei, W., Ayad, N. G., Wan, Y., Zhang, G., Kirschner, M. W. and Kaelin, W. G. J. (2004) **Degradation of the SCF component Skp2 in cell-cycle phase G1 by the anaphase-promoting complex**. *Nature,* **428**(6979): 194-198.

Weiss, M. M., Kuipers, E. J., Postma, C., Snijders, A. M., Pinkel, D., Meuwissen, S. G., Albertson, D. and Meijer, G. A. (2004) **Genomic alterations in primary gastric adenocarcinomas correlate with clinicopathological characteristics and survival.** *Cell Oncol.*, **26**(5-6): 307-317.

Wiese, C. and Zheng, Y. (2006) **Microtubule nucleation: gamma-tubulin and beyond.** *J. Cell Sci.,* **119**(20): 4143-4153.

Wittmann, T., Hyman, A. and Desais, A. (2001) **The spindle: a dynamic assembly of microtubules and motors**. *Nat. Cell Biol.,* **3**: E28-E34.

White, M. C. and Quarmby, L. M. (2008) **The NIMA-family kinase, Nek1 affects the**

stability of centrosomes and ciliogenesis. *BMC Cell Biol.*, **9**: 29.

Wong, C. and Stearns, T. (2003) **Centrosome number is controlled by a centrosome-intrinsic block to reduplication**. *Nat. Cell Biol.*, **5**(6): 539-544.

Wonsey, D. R. and Follettie, M. T. (2005) **Loss of the forkhead transcription factor FoxM1 causes centrosome amplification and mitotic catastrophe**. *Cancer Res.*, **65**(12): 5181-5189.

Woods, C. G., Bond, J. and Enard, W. (2005) **Autosomal recessive primary microcephaly (MCPH): a review of clinical, molecular, and evolutionary findings**. *Am. J. Hum. Genet.*, 76(5): 717-728.

Wu, W., Baxter, J. E, Wattam, S. L., Hayward, D. G., Fardilha, M., Knebel, A., Ford, E. M., da Cruz e Silva, E. F. and Fry, A. M. (2007) **Alternative splicing controls nuclear translocation of the cell cycle-regulated Nek2 kinase.** *J. Biol. Chem.*, **282**(36): 26431-26440.

Wu, Z. Q., Yang, X., Weber, G. and Liu, X. (2008) **Plk1 Phosphorylation of TRF1 is essential for its binding to telomeres**. *J. Biol. Chem.*, **283**(37): 25503-25513.

Yamamoto, Y., Matsuyama, H., Furuya, T., Oga, A., Yoshihiro, S., Okuda, M., Kawauchi, S., Sasaki, K. and Naito, K. (2004) **Centrosome hyperamplification predicts progression and tumor recurrence in bladder cancer**. *Clin Cancer Res.*, **10**(19): 6449-6455.

Yang, J., Adamian, M. and Li, T. (2006) **Rootletin interacts with C-Nap1 and may function as a physical linker between the pair of centrioles/basal bodies in cells.** *Mol. Biol. Cell*, **17**(2): 1033-1040.

Yang, J., Liu, X., Yue, G., Adamian, M., Bulgakov, O. and Li, T. (2002) **Rootletin, a novel coiled-coil protein, is a structural component of the ciliary rootlet.** *J. Cell Biol.*, **159**(3): 431-440.

Yao, J., Fu, C., Ding, X., Guo, Z., Zenreski, A., Chen, Y., Ahmed, K., Liao, J., Dou, Z. and Yao, X. (2004) **Nek2A kinase regulates the localization of numatrin to centrosome in mitosis**. *FEBS Lett.* **575**: 112-118.

Yin, M. J., Shao, L., Voehringer, D., Smeal, T. and Jallal, B. (2003) **The serine/threonine kinase Nek6 is required for cell cycle progression through mitosis**. *J. Biol. Chem.*, **278**(52): 52454-52460.

Yissachar, N., Salem, H., Tennenbaum, T. and Motro, B. (2006) **Nek7 kinase is enriched at the centrosome, and is required for proper spindle assembly and mitotic progression**. *FEBS Lett.*, **580**(27): 6489-6495.

Young, A., Dictenberg, J. B., Purohit, A., Tuft, R. and Doxsey, S. J. (2000) **Cytoplasmic dynein-mediated assembly of pericentrin and gamma tubulin onto centrosomes**. *Mol. Biol. Cell*, **11**(6): 2047-2056.

Zhang, W., Fletcher, L. and Muschel, R. J. (2005) **The role of polo-like kinase 1 in the inhibition of centrosome separation after ionizing radiation**. *J. Biol. Chem.*, **280**(52): 42994-42999.

Zheng, Y., Wong, M. L., Alberts, B. and Mitchison, T. (1995) **Nucleation of microtubule assembly by a gamma-tubulin-containing ring complex.** *Nature*, **378**(6557): 578-583.

Zhu, F., Lawo, S., Bird, A., Pinchev, D., Ralph, A., Richter, C., Müller-Reichert, T., Kittler, R., Hyman, A. A. and Pelletier, L. (2008) **The mammalian SPD-2 ortholog Cep192 regulates centrosome biogenesis.** *Curr. Biol.*, **18**(2):136-141.

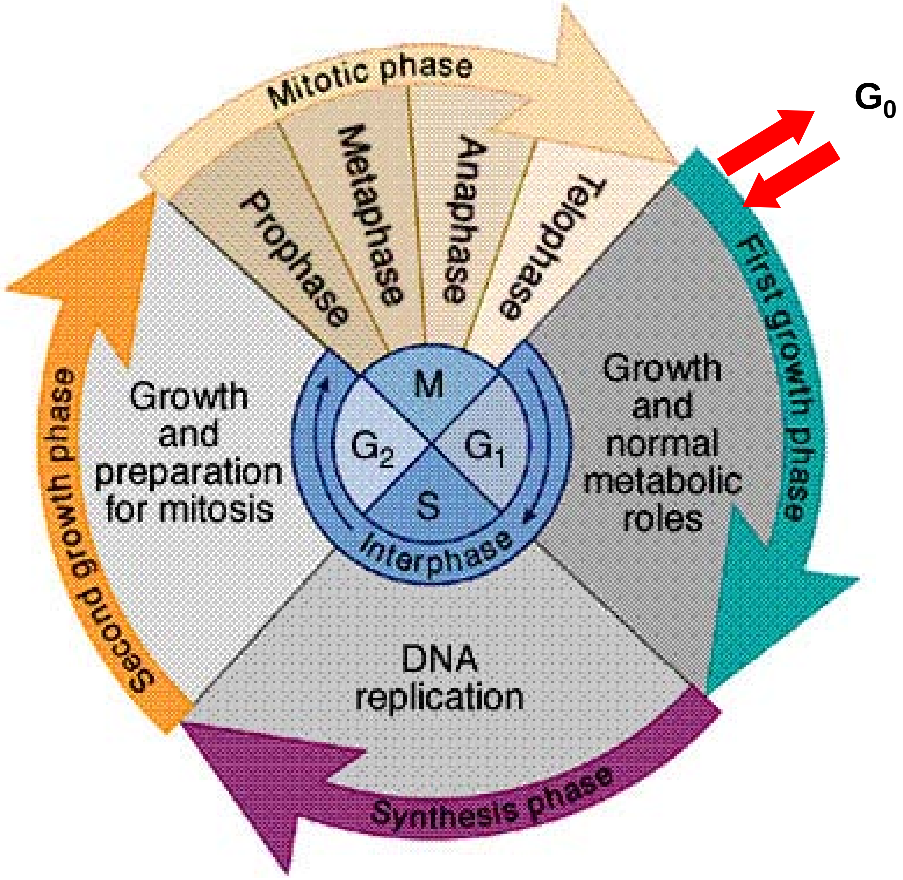
G_0
Mitotic phase
Prophase
Metaphase
Anaphase
Telophase
First growth phase
Growth and normal metabolic roles
M
G_1
G_2
S
Interphase
Growth and preparation for mitosis
Second growth phase
DNA replication
Synthesis phase

Figure 1.1 The eukaryotic cell cycle

The cell cycle consists of interphase (G_1, S and G_2) and mitosis, which can be subdivided as indicated above. Cells with no growth signals can enter a state of quiescence (G_0). Diagram reproduced from http://bhs.smuhsd.org/bhsnew/academicprog/science/vaughn/Student%20Projects/Paul%20&%20Marcus/Cell_Replication.html by Ethan Kensler, 2002.

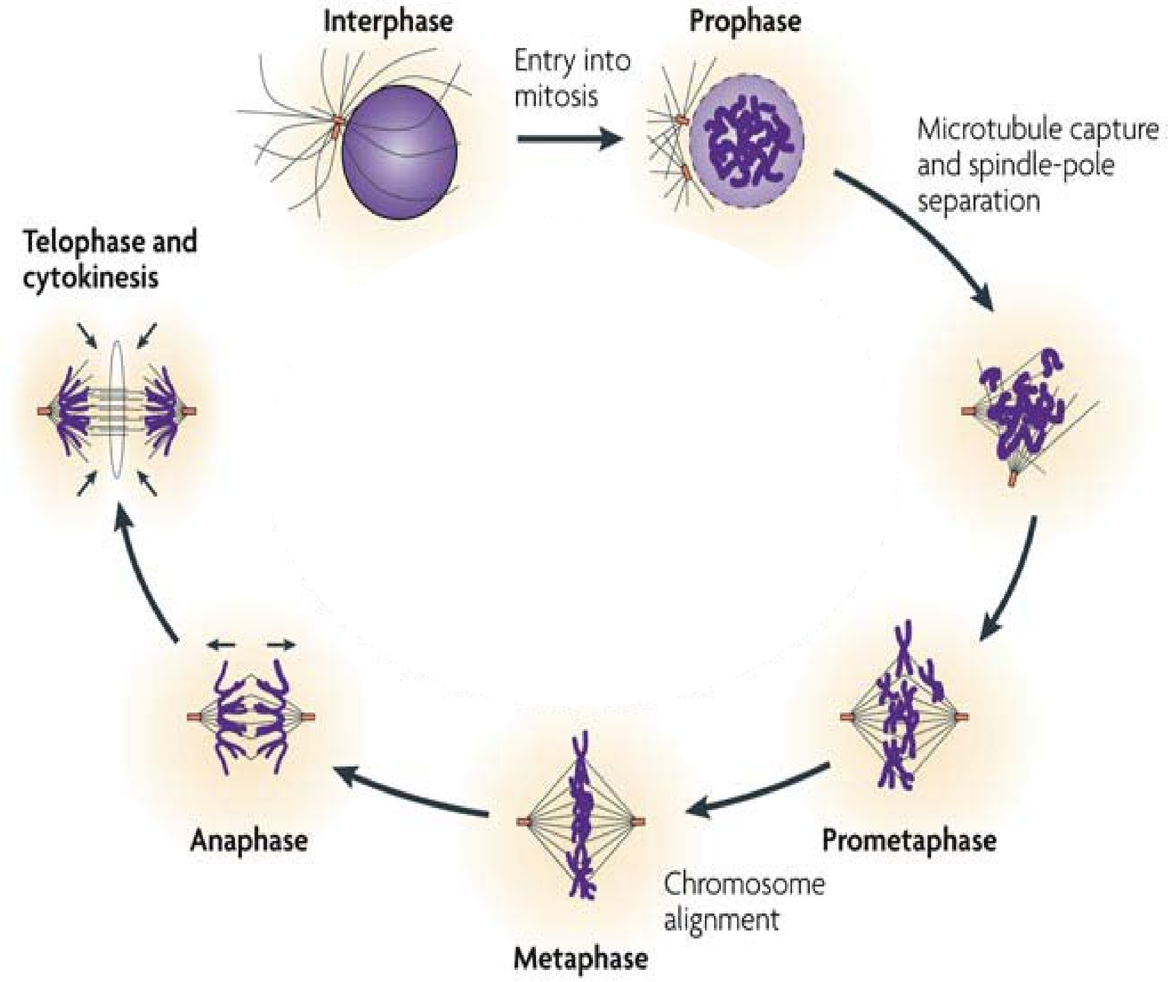
Interphase
Entry into mitosis
Prophase
Microtubule capture and spindle-pole separation
Prometaphase
Chromosome alignment
Metaphase
Anaphase
Telophase and cytokinesis

Figure 1.2 Mitosis

The schematic diagram highlights the different stages of mitosis. During prophase the chromosomes condense and the centrosomes start to separate. After the nuclear envelope breaks down the mitotic spindle starts to assemble as the chromosomes become attached to the microtubules (prometaphase). Once the chromosomes are aligned across the equator of the spindle (metaphase) the sister chromatids are pulled to opposite spindle poles (anaphase). The chromosomes then decondense, a cleavage furrow forms and the cell separates into two daughter cells (telophase and cytokinesis). Diagram adapted from Jackson *et al.*, Nature Reviews Cancer, 2007.

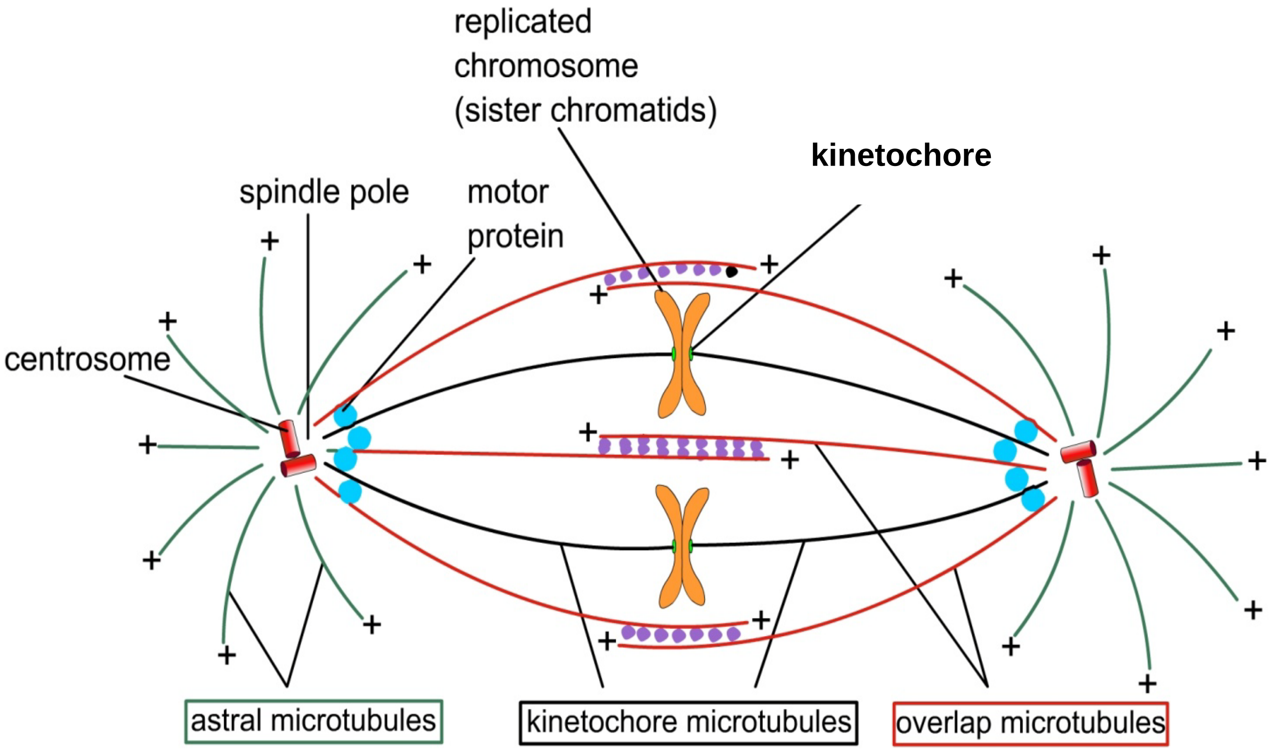
replicated chromosome (sister chromatids)
kinetochore
spindle pole
motor protein
centrosome
+
astral microtubules
kinetochore microtubules
overlap microtubules

Figure 1.3 The mitotic spindle

A schematic diagram of the mitotic spindle in metaphase showing the arrangement of three 3 types of microtubules, chromosomes and spindle poles. Microtubules are polar. Their minus ends are anchored to the centrosome whilst their fast growing plus ends grow outwards away from the centrosome (indicated by +). The continuous growth and shrinkage of microtubules is regulated by motor proteins which bind to the sides (purple spots) or the ends (blue spots) of microtubules. The motor proteins travel along microtubules and promote the assembly and stability of the microtubule array. Diagram taken from website, http://219.221.200.61/ywwy/zbsw(E)/edetail11.htm.

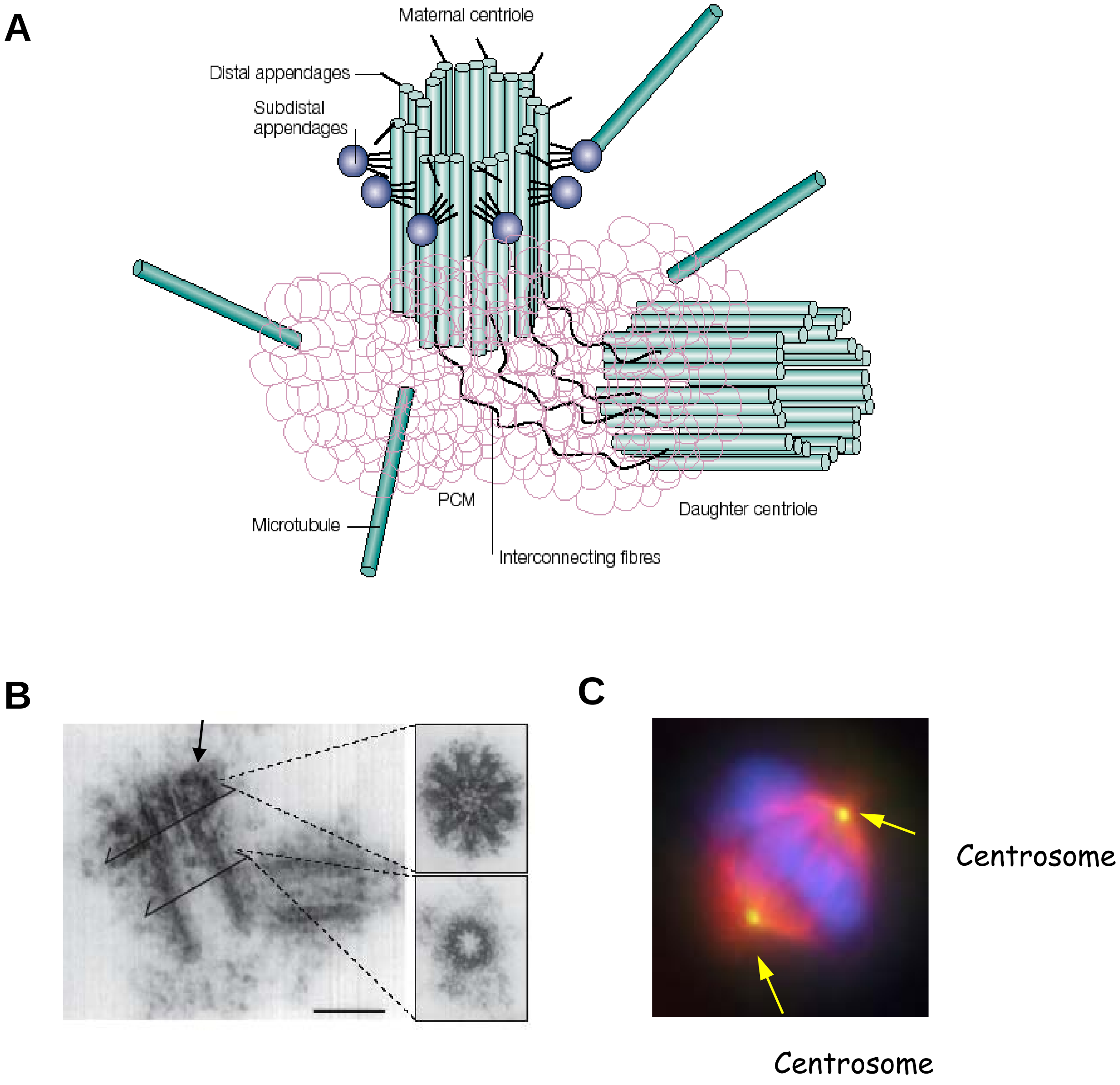
A
Maternal centriole
Distal appendages
Subdistal appendages
PCM
Daughter centriole
Microtubule
Interconnecting fibres
B
C
Centrosome
Centrosome

Figure 1.4 Centrosome structure

A. Schematic representation of the mammalian centrosome (taken from Doxsey, 2001). **B.** Electron microscopy image showing the structure of the centrioles. The distal appendages at the distal end of the mother centriole are indicated by the arrow. Taken from Bettencourt-Dias and Glover, 2007. **C.** Immunofluorescence microscopy image of a mitotic cell indicating the centrosomes (yellow) which form the spindle poles during mitosis to mediate accurate chromosome segregation. The microtubule network is shown in red and the DNA in blue. Image courtesy of Prof. Andrew Fry.

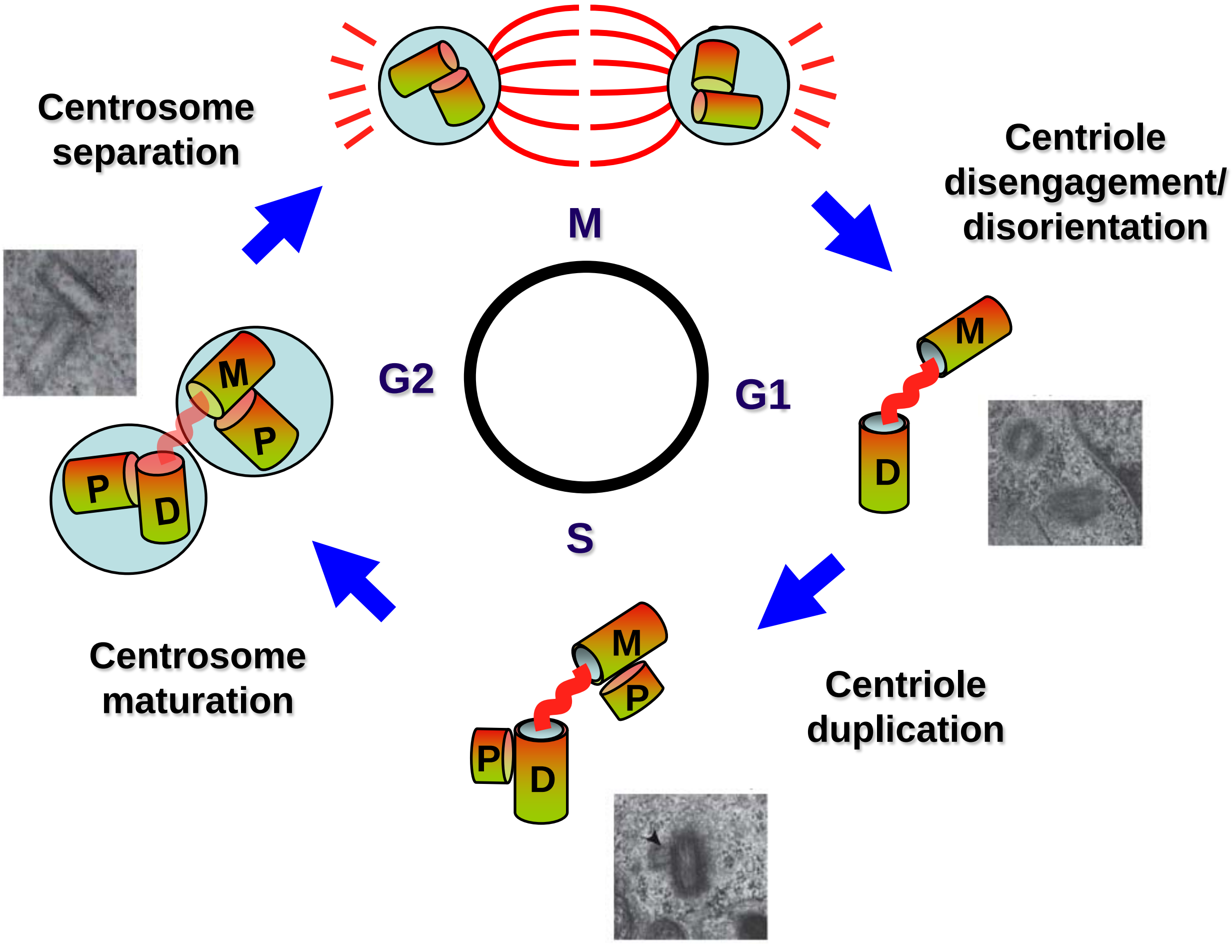
Centrosome separation
M
Centriole disengagement/ disorientation
G2
G1
S
M
P
D
Centrosome maturation
Centriole duplication

Figure 1.5 The centrosome duplication cycle

Diagramatic representation of the centrosome duplication cycle accompanied by electron microscope images of each stage (taken from Bettencourt-Dias and Glover, 2007). In late mitosis/ early G1 the centrioles disengage or disorientate allowing a new procentriole (P) to develop from the side of the older centriole during S phase as indicated by the arrowhead in the electron microscope image. In G2/M the procentrioles mature before the intercentriolar linkage between the two older centrioles (red strand) breaks down and the two centrosomes separate to form the spindle poles. After mitosis is complete each daughter cell receives one centrosome.

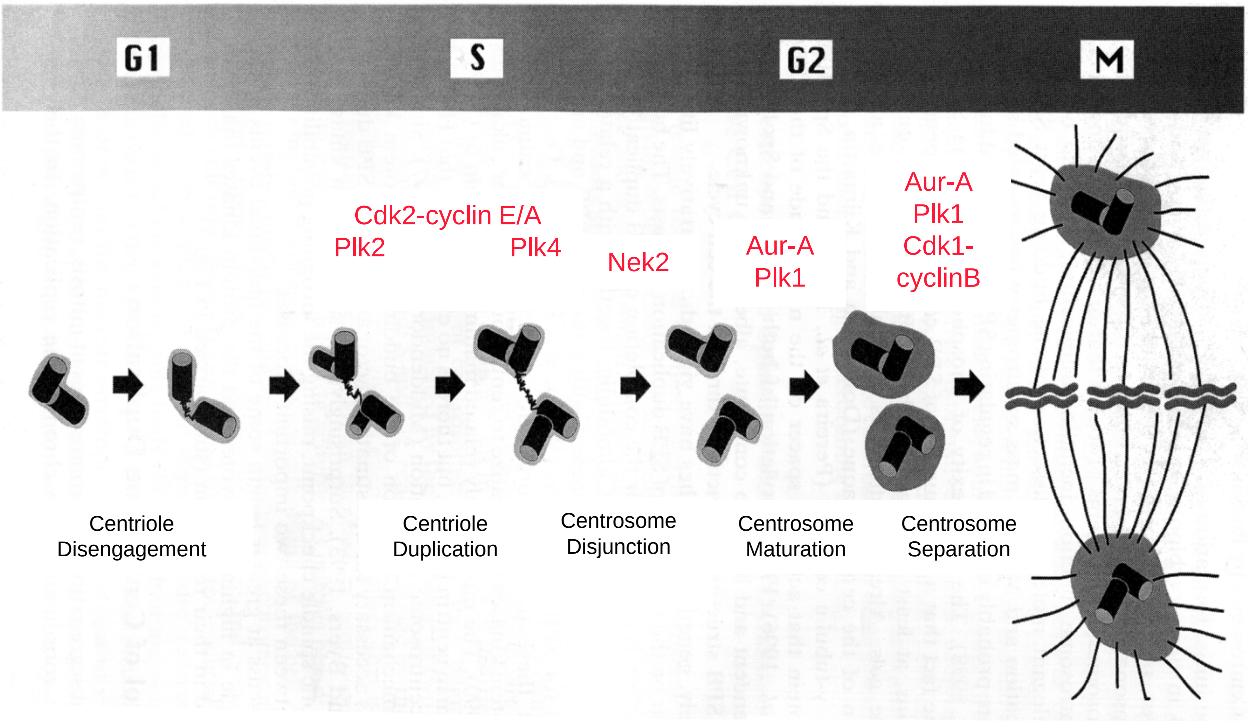
G1
S
G2
M
Cdk2-cyclin E/A
Plk2
Plk4
Nek2
Aur-A
Plk1
Aur-A
Plk1
Cdk1-
cyclinB
Centriole Disengagement
Centriole Duplication
Centrosome Disjunction
Centrosome Maturation
Centrosome Separation

Figure 1.6 **Protein kinase regulation of the centrosome duplication cycle**

The cartoon shows the events of the centrosome duplication cycle in relation to the cell cycle in a mammalian cell. Protein kinases that regulate specific steps in the centrosome cycle are indicated in red. Figure adapted from Fry et al., 2000b.

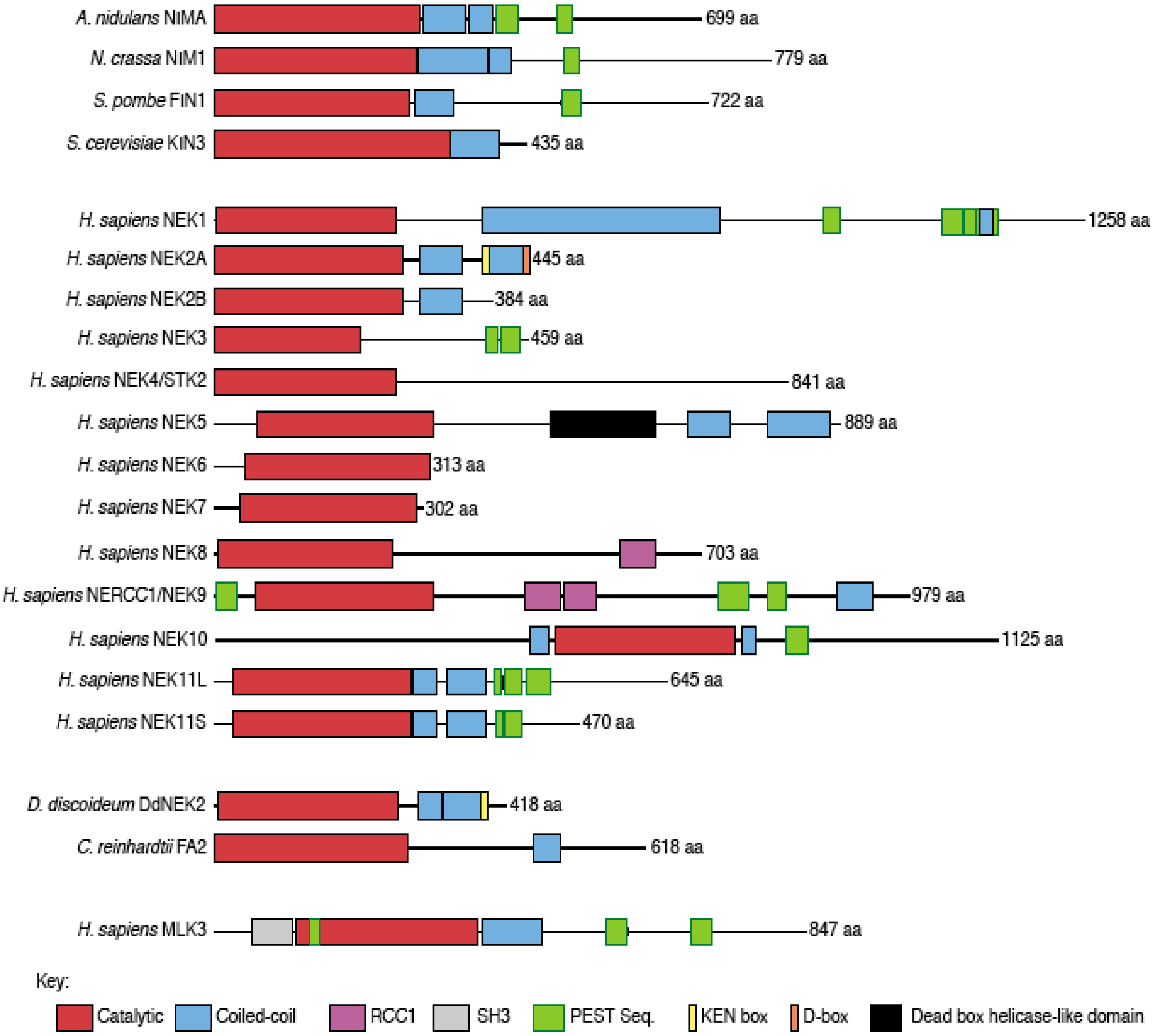
A. nidulans NIMA
699 aa
N. crassa NIM1
779 aa
S. pombe FIN1
722 aa
S. cerevisiae KIN3
435 aa
H. sapiens NEK1
1258 aa
H. sapiens NEK2A
445 aa
H. sapiens NEK2B
384 aa
H. sapiens NEK3
459 aa
H. sapiens NEK4/STK2
841 aa
H. sapiens NEK5
889 aa
H. sapiens NEK6
313 aa
H. sapiens NEK7
302 aa
H. sapiens NEK8
703 aa
H. sapiens NERCC1/NEK9
979 aa
H. sapiens NEK10
1125 aa
H. sapiens NEK11L
645 aa
H. sapiens NEK11S
470 aa
D. discoideum DdNEK2
418 aa
C. reinhardtii FA2
618 aa
H. sapiens MLK3
847 aa
Key:
Catalytic
Coiled-coil
RCC1
SH3
PEST Seq.
KEN box
D-box
Dead box helicase-like domain

Figure 1.7 NIMA-related kinases

Structures of the NIMA-related kinase family. Fungi encode a single NIMA-related kinase, whereas there are 11 members of this family in *H. sapiens*. Homologues have also been identified in the green algae *Chlamydomonas reinhardtii* and the amoeba, *Dictostylium discoideum*. NIMA kinases consist of an N-terminal catalytic domain and a C-terminal domain containing various motifs such as coiled-coils or RCC1-like motifs that most likely facilitate protein-protein interactions, as well as motifs including PEST, KEN and D-boxes which regulate proteolytic degradation. Similarities in sequence and organisation of the C-terminal region of NIMA-related kinases have been reported with the MLK3 kinase. Taken from O'Connell et al., 2003.

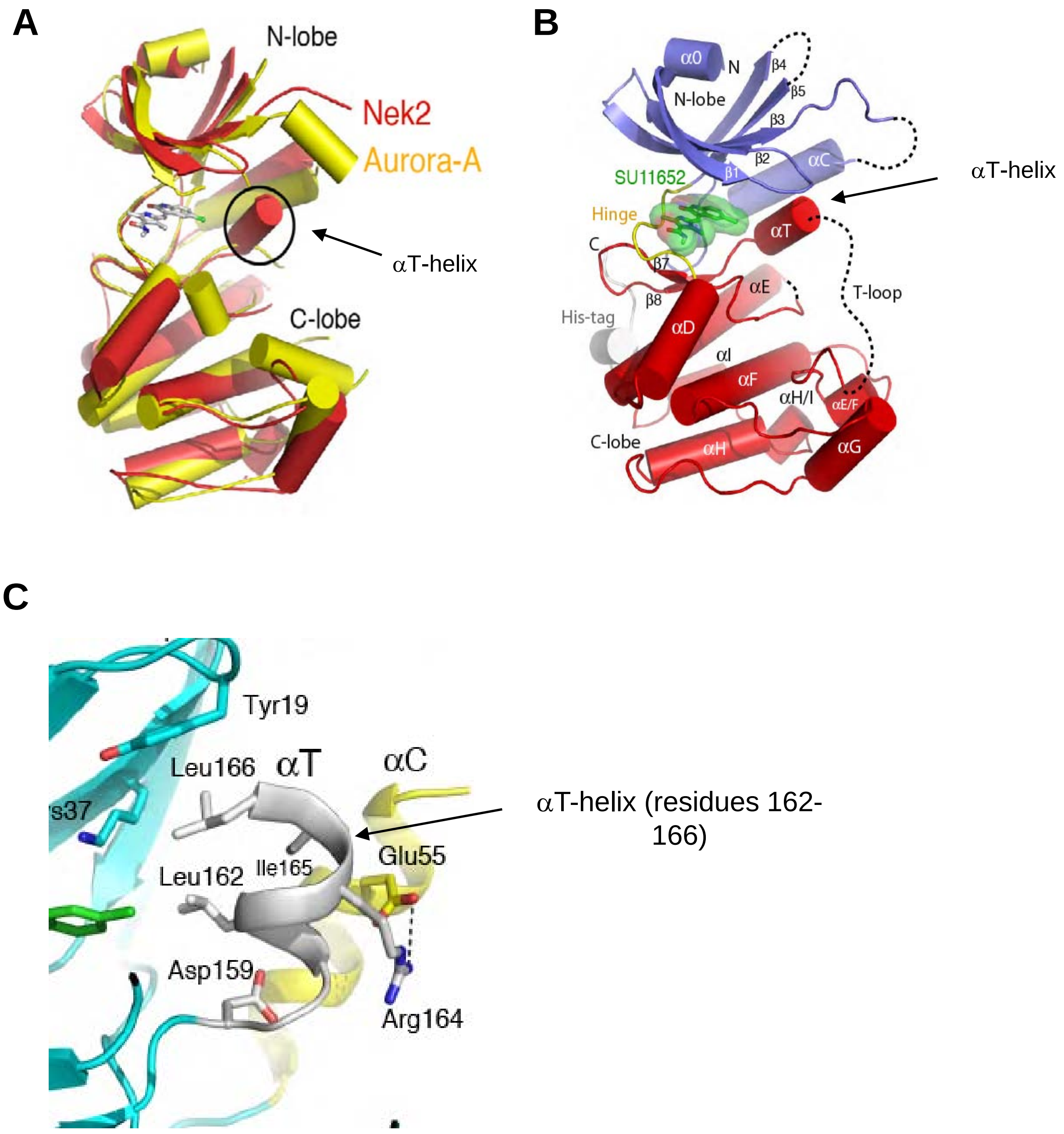
A
N-lobe
Nek2
Aurora-A
αT-helix
C-lobe
B
α0
N
β4
β5
N-lobe
β3
β2
αC
β1
SU11652
αT-helix
Hinge
αT
C
β7
αE
T-loop
β8
His-tag
αD
αI
αF
αH/I
αE/F
C-lobe
αH
αG
C
Tyr19
Leu166
αT
αC
s37
αT-helix (residues 162-166)
Leu162
Ile165
Glu55
Asp159
Arg164

Figure 1.8 Crystal structure of the N-terminal catalytic domain of Nek2

(**A**) Comparison of the crystal structures of the N-terminal catalytic domains of Nek2 (red) and Aurora-A (yellow). Nek2 has a novel αT-helix not present in Aurora-A. (**B**) Crystal structure of the catalytic domain of Nek2 with an inhibitor (SU11652) drug bound. (**C**) The αT-helix consists of 5 amino acids (162-166) which form a helical structure at the N-terminal end of the activation loop. Figure taken from Rellos et al. (2007).

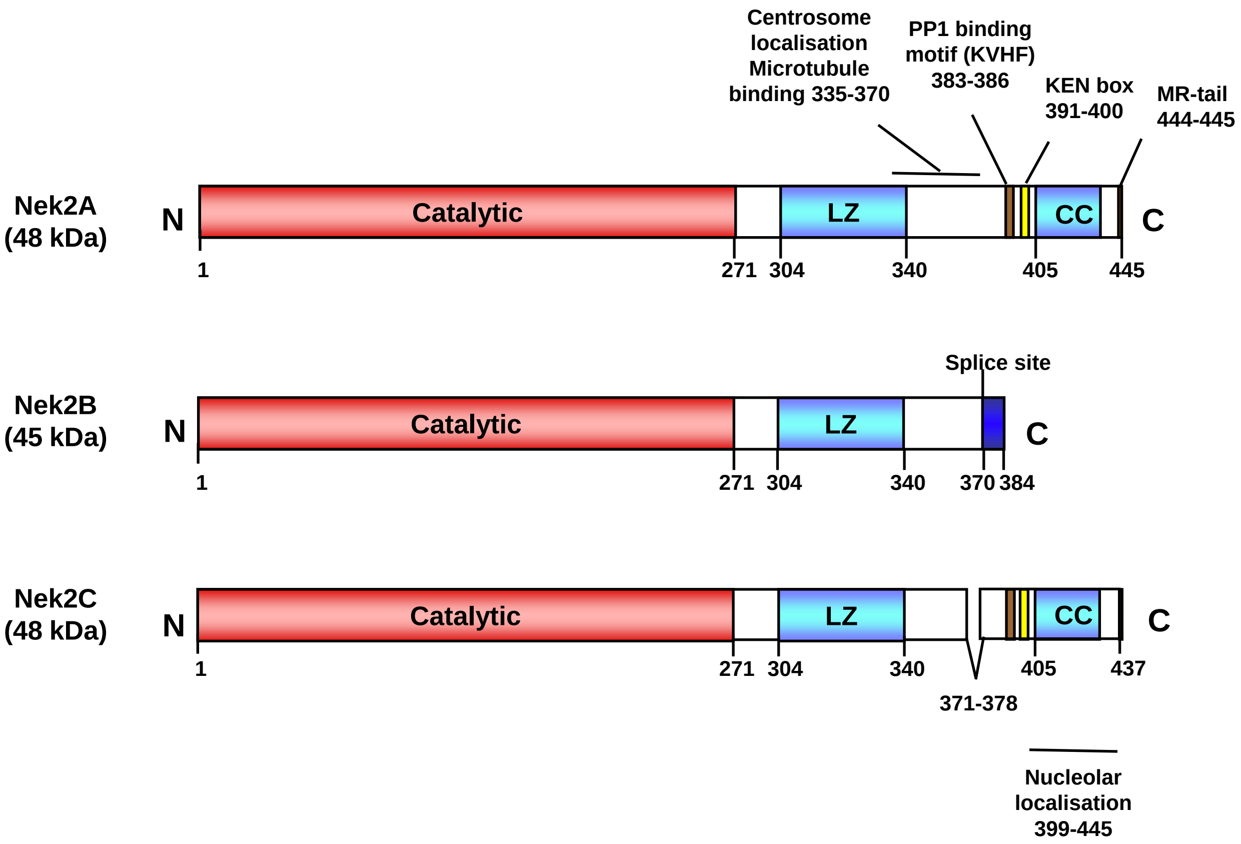
Centrosome localisation Microtubule binding 335-370
PP1 binding motif (KVHF) 383-386
KEN box 391-400
MR-tail 444-445
Nek2A (48 kDa)
N
Catalytic
LZ
CC
C
1
271
304
340
405
445
Splice site
Nek2B (45 kDa)
N
Catalytic
LZ
C
1
271
304
340
370
384
Nek2C (48 kDa)
N
Catalytic
LZ
CC
C
1
271
304
340
405
437
371-378
Nucleolar localisation 399-445

Figure 1.9 The structure of Nek2A, Nek2B and Nek2C

Schematic diagram of the human Nek2 isoforms are shown. These proteins all contain an N-terminal catalytic kinase domain and a coiled-coil region known as a leucine zipper (LZ) which allows the protein to dimerise and auto-phosphorylate. In addition to these regions, Nek2A and Nek2C contain a second coiled-coil region (CC), a PP1 binding site and motifs (KEN box and MR-tail) that allow their degradation at the onset of mitosis (Fry, 2002). Nek2C has an 8 amino acid excision at the Nek2A/B splice site. Motifs that promote centrosome localisation, microtubule binding and nucleolar localisation are also indicated. Reproduced from Hayward and Fry, 2005.

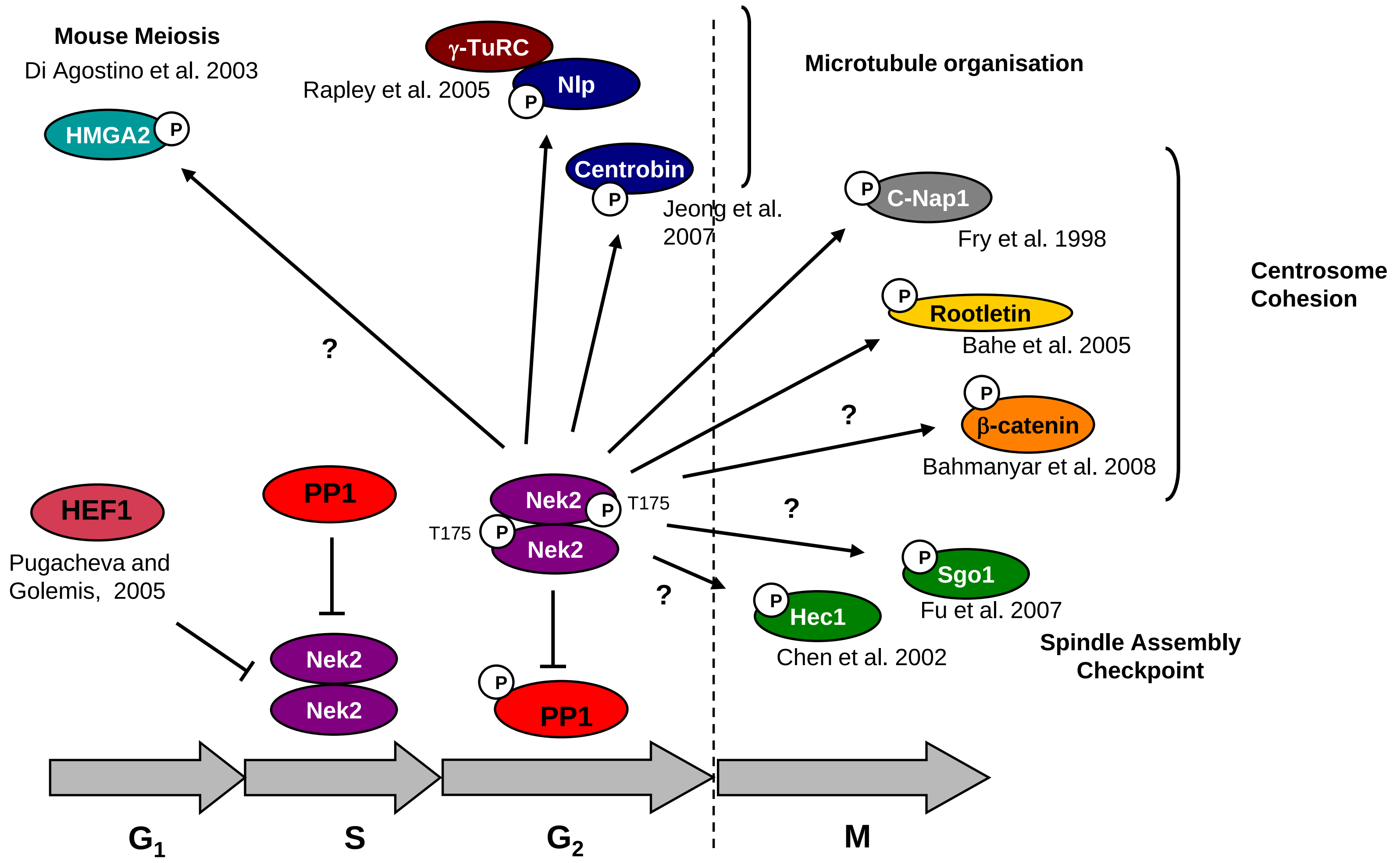

Mouse Meiosis
Di Agostino et al. 2003
HMGA2
P
γ-TuRC
Nlp
P
Rapley et al. 2005
Centrobin
P
Jeong et al. 2007
Microtubule organisation
C-Nap1
P
Fry et al. 1998
Rootletin
P
Bahe et al. 2005
β-catenin
P
Bahmanyar et al. 2008
Centrosome Cohesion
?
?
?
?
HEF1
Pugacheva and Golemis, 2005
PP1
Nek2
Nek2
Nek2
Nek2
P
P
T175
T175
P
PP1
Sgo1
P
Fu et al. 2007
Hec1
P
Chen et al. 2002
Spindle Assembly Checkpoint
G1
S
G2
M

Figure 1.10 Nek2 substrates

Nek2 exists in cells as a dimer. Nek2 activity in interphase is inhibited by HEF1 and protein phosphatase 1 (PP1). PP1 is inactivated at the G2/M transition by Inh2 allowing Nek2 to become active. Once the activity of Nek2 overcomes that of PP1, Nek2 can dephosphorylate and inhibit PP1, further enhancing Nek2 activity by a positive feedback mechanism. Once active, Nek2 can phosphorylate numerous substrates at the G2/M transition in order to mediate several mitotic events. Relevant references are shown next to each proposed substrate of Nek2.

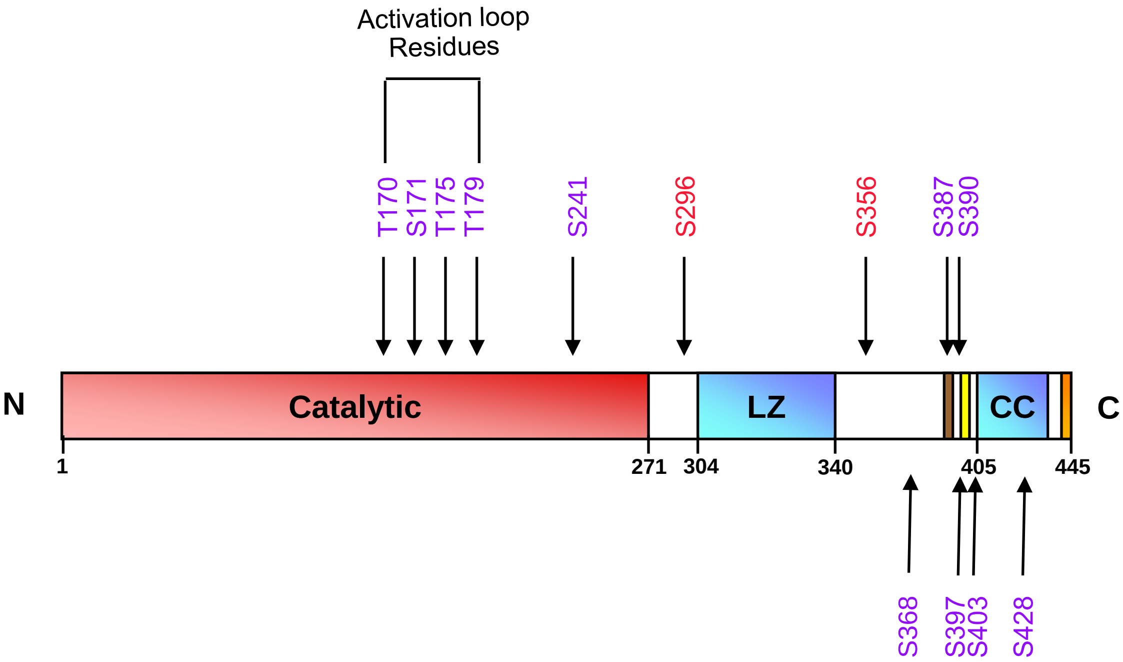
Activation loop
Residues
T170
S171
T175
T179
S241
S296
S356
S387
S390
N
Catalytic
LZ
CC
C
1
271
304
340
405
445
S368
S397
S403
S428

Figure 1.11 Mass spectrometry reveals thirteen autophosphorylation sites within Nek2A

Schematic diagram of the human Nek2A protein sequence indicating the positions of 13 autophosphorylation sites relative to the known functional domains of Nek2. The brown bar indicates the PP1 binding site and the yellow bar indicates the KEN-box. The orange bar indicates the MR-tail. Eleven of these autophosphorylation sites, indicated in blue, were identified through collaboration with Prof. S. Smerdon (NIMR, London), while 2 additional sites indicated in red, were identified by Invitrogen during their analysis of a Nek2 protein that they had expressed in insect cells.

Phosphorylation Site	Mutant Constructs	Combined Mutations	Localised at Centrosome?	Centrosome Splitting Assay (%)	IVT-IP Kinase Assay (%)	Activity of Mutant
WT	WT		YES	58.2	100	NA
K37	K37R		YES	12	3.5	Inactive
T170	T170A T170E		YES YES	53 55.5	- -	Active Active
S171	S171A S171D		YES YES	56 69	- -	Active Hyperactive?
T175	T175A T175E		YES YES	21.25 67.25	32.8 165	Inactive Hyperactive
T179	T179A T179E		YES YES	34 31	36.8 26.6	Inactive Inactive
S241	S241A S241D		YES YES	11.6 18.6	15 16.3	Inactive Inactive
S296	- -		- -	- -	- -	- -
S356	- -		- -	- -	- -	- -
S368	- -		- -	- -	- -	- -
S387						
S390		SA$_4$	YES	63.9	161.7	Hyperactive
S397		SD$_4$	YES	61.3	108.9	Active
S403						
S428	- -		- -	- -	- -	- -

Figure 1.12 A summary of data available before starting this project on Nek2A autophosphorylation sites

The table shows a summary of the Nek2A autophosphorylation sites and mutants created and studied by a previous PhD student, Dr. Baxter. These are compared to the wild-type Nek2A kinase (WT) and a construct carrying a mutation in an essential residue in the ATP-binding site (K37R). Dr. Baxter initiated the characterisation of these constructs but in some cases the activity was only partially tested or never tested (-). The relative activities of these mutants compared to wild-type kinase using one *in vivo* and one *in vitro* assay are outlined in the table.

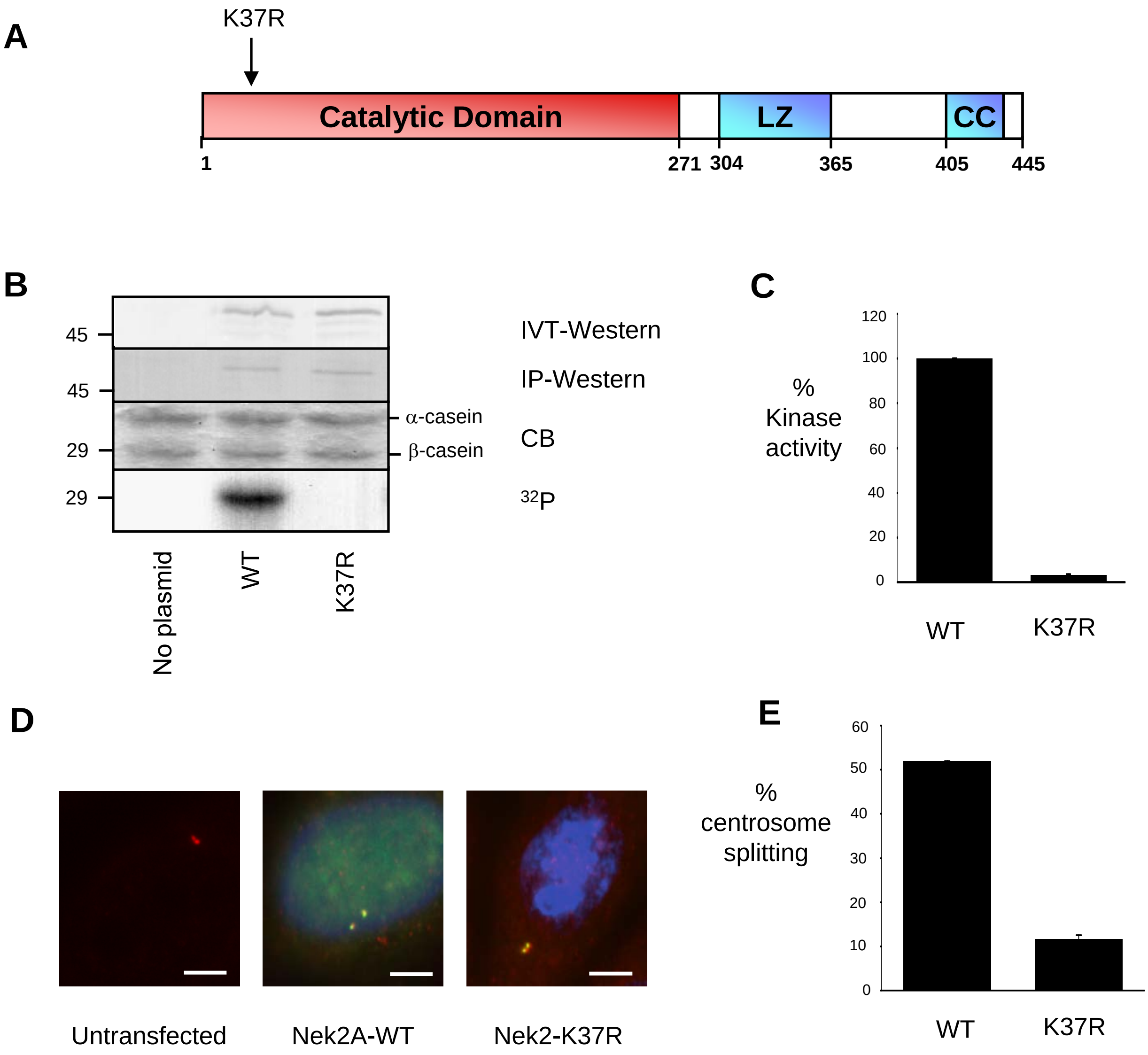

Figure 3.1 Assays to determine Nek2A kinase activity *in vitro* and *in vivo*

A. Schematic diagram of Nek2A indicating the position of the K37R mutation within the catalytic domain. **B.** The pRcCMV:myc-Nek2A-WT and Nek2A-K37R constructs were translated *in vitro* (IVT-Western) then immunoprecipitated using anti-myc antibody and either Western blotted with anti-Nek2 antibody followed by an AP-conjugated anti-rabbit secondary antibody (IP-Western), or incubated with kinase buffer containing ^{32}P-γ-[ATP] and the substrate casein. Proteins were separated by SDS-PAGE and stained with Coomassie Blue (CB). Autoradiography (^{32}P) revealed that Nek2A-WT, but not Nek2A-K37R, incorporates radioactivity into the substrate β-casein. Molecular weights (kDa) are indicated on the left. **C.** Histogram represents the kinase activity of Nek2A-WT and Nek2A-K37R based on 3 separate experiments. Kinase activity was calculated by scintillation counting and normalised for the amount of protein precipitated. **D.** U2OS cells were transfected with either myc-Nek2A-WT or myc-Nek2A-K37R for 24 hours. U2OS cells were fixed with methanol and stained with anti-myc antibody to detect the Nek2A construct (green), anti-γ-tubulin antibody to detect the centrosome (red) and Hoechst 33258 to detect the DNA (blue). Merged images are shown. A non-transfected control cell stained for γ-tuhulin is also shown. Scale bars, 10 µm. **E.** Approximately 100 transfected cells were counted in each of 3 experiments as possessing either split (>2 µm apart) or non-split centrosomes.

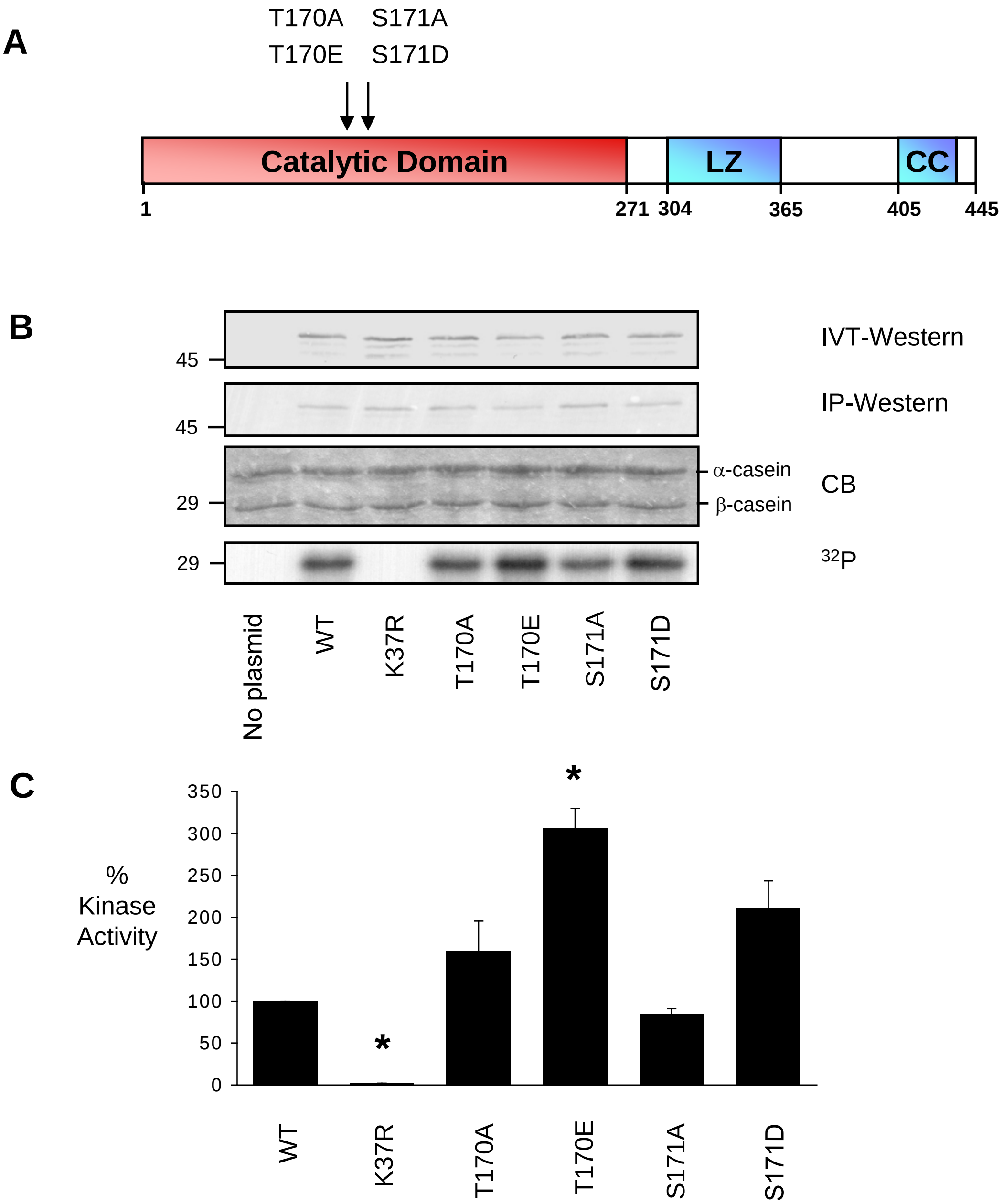

Figure 3.2 Mutation of T170 or S171 to glutamate or aspartate, respectively, results in hyperactive Nek2A proteins

A. Schematic diagram of Nek2A indicating the positions of the T170 and S171 mutations in the catalytic domain. **B.** The pRcCMV:myc-Nek2A-WT, Nek2A-KR, Nek2A-T170A, Nek2A-T170E, Nek2A-S171A and Nek2A-S171D constructs were translated *in vitro* (IVT-Western) then immunoprecipitated with an anti-myc antibody and either Western blotted with anti-Nek2 antibodies followed by an AP-conjugated anti-rabbit secondary antibody (IP-Western), or incubated with ^{32}P-γ-[ATP] and the substrate casein at 30^{0}C for 30 mins. Proteins were separated by SDS-PAGE, stained with Coomassie Blue (CB) and exposed to autoradiography (^{32}P). Molecular weights (kDa) are indicated on the left. **C.** The histogram displays the kinase activity of each mutant based on 3 separate experiments. Kinase activity was calculated by scintillation counting and then normalised to the amount of protein immunoprecipitated. * $P< 0.005$ for T170E and K37R compared to WT kinase.

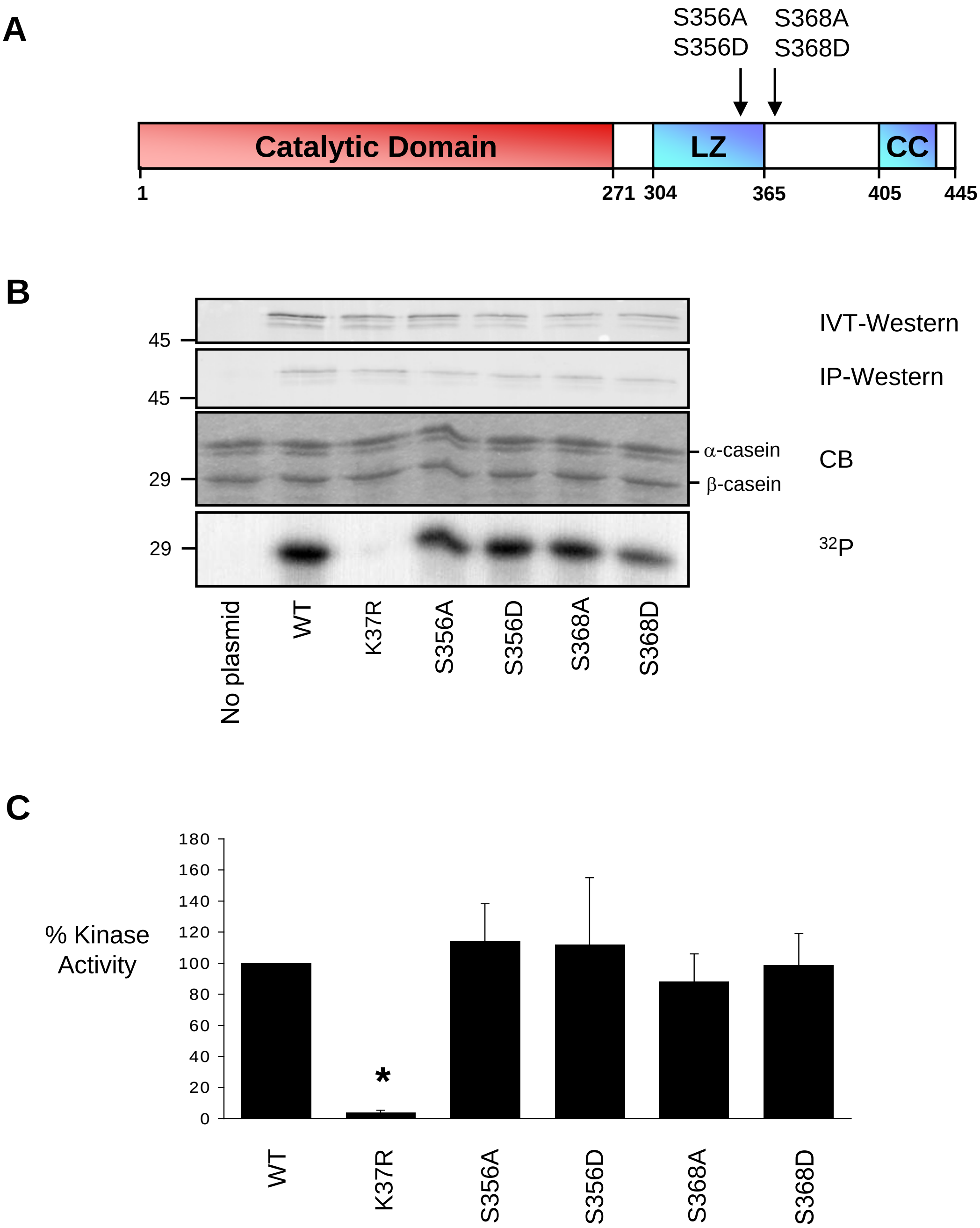

Figure 3.3 Mutation of S356 or S368 does not alter Nek2A kinase activity

A. Schematic diagram of Nek2A indicating the positions of the S356 and S368 mutants in the non-catalytic domain. **B.** The myc-Nek2A-WT, Nek2A-KR, Nek2A-S356A, Nek2A-S356D, Nek2A-S368A and Nek2-S368D proteins were translated *in vitro* (IVT-Western), immunoprecipitated using an anti-myc antibody and either Western blotted with anti-Nek2 antibody followed by an AP-conjugated anti-rabbit secondary antibody (IP-Western) or incubated with kinase buffer containing ^{32}P-γ-[ATP] and the substrate casein. Proteins were separated by SDS-PAGE, stained with Coomassie Blue (CB) and exposed to autoradiography (^{32}P). Molecular weights (kDa) are indicated on the left. **C.** The histogram represents the kinase activity of each mutant based on 3 separate experiments. Kinase activity was calculated by scintillation counting and normalising for the amount of protein precipitated. * $P<0.05$ compared to WT kinase.

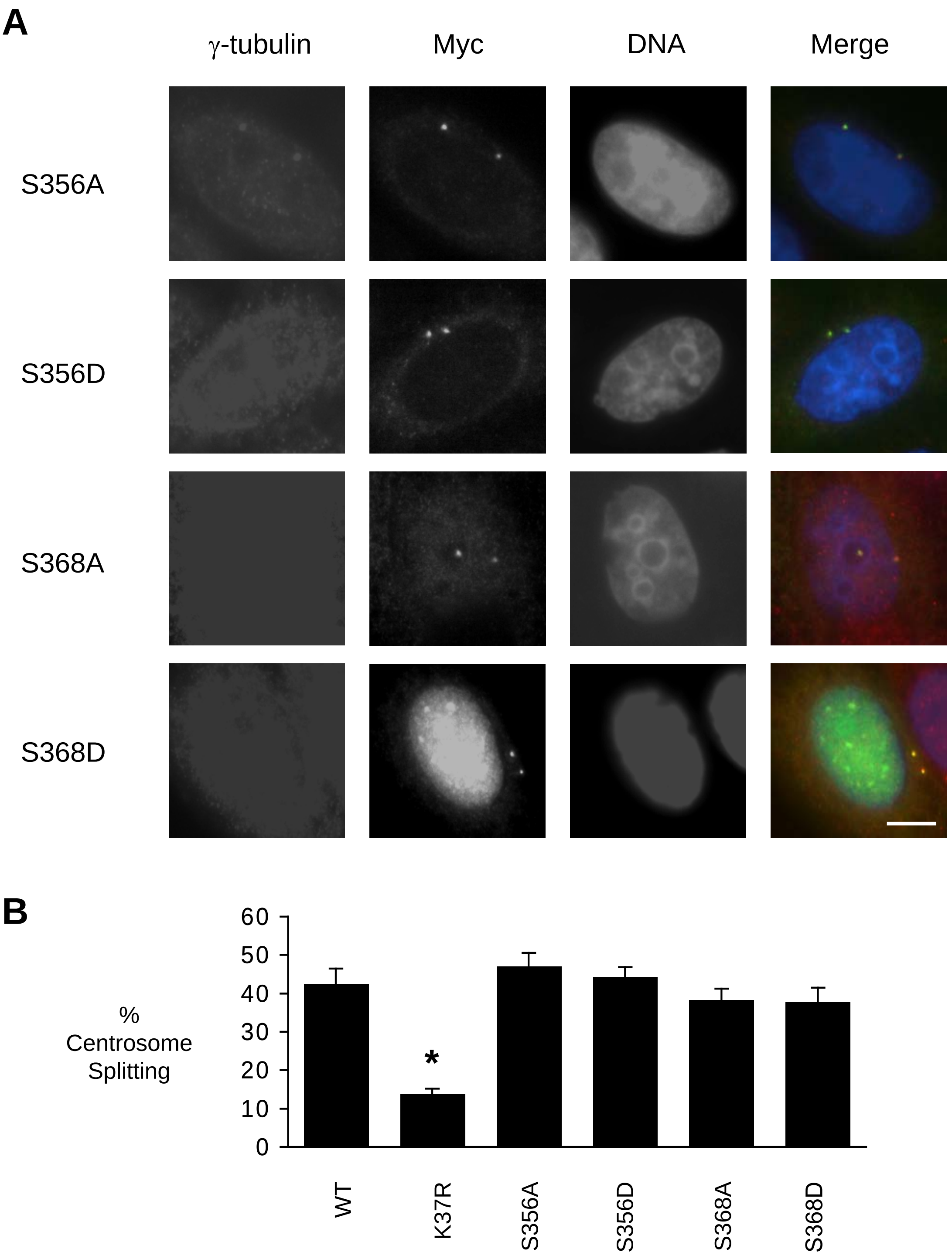
A
γ-tubulin
Myc
DNA
Merge
S356A
S356D
S368A
S368D
B
% Centrosome Splitting
60
50
40
30
20
10
0
*
WT
K37R
S356A
S356D
S368A
S368D

Figure 3.4 Mutation of S356 or S368 does not alter Nek2A activity or localisation in cells

A. U2OS cells were transfected with myc-Nek2A-S356A, myc-Nek2A-S356D, myc-Nek2A-S368A or myc-Nek2A-S368D for 24 hours. Cells were fixed with methanol and stained with anti-myc-antibody to detect the Nek2A construct (green), anti-γ-tubulin antibody to detect the centrosome (red) and Hoechst 33258 to detect the DNA (blue). All mutant Nek2A proteins localise to the centrosome. Merged images are shown. Scale bar, 10 μm. **B.** Approximately 100 cells were counted in 3 separate experiments and the centrosomes scored as split (>2 μm) or non-split. The histogram illustrates the number of split centrosomes observed for each protein based on 3 experiments. * $P<0.05$ compared to WT kinase.

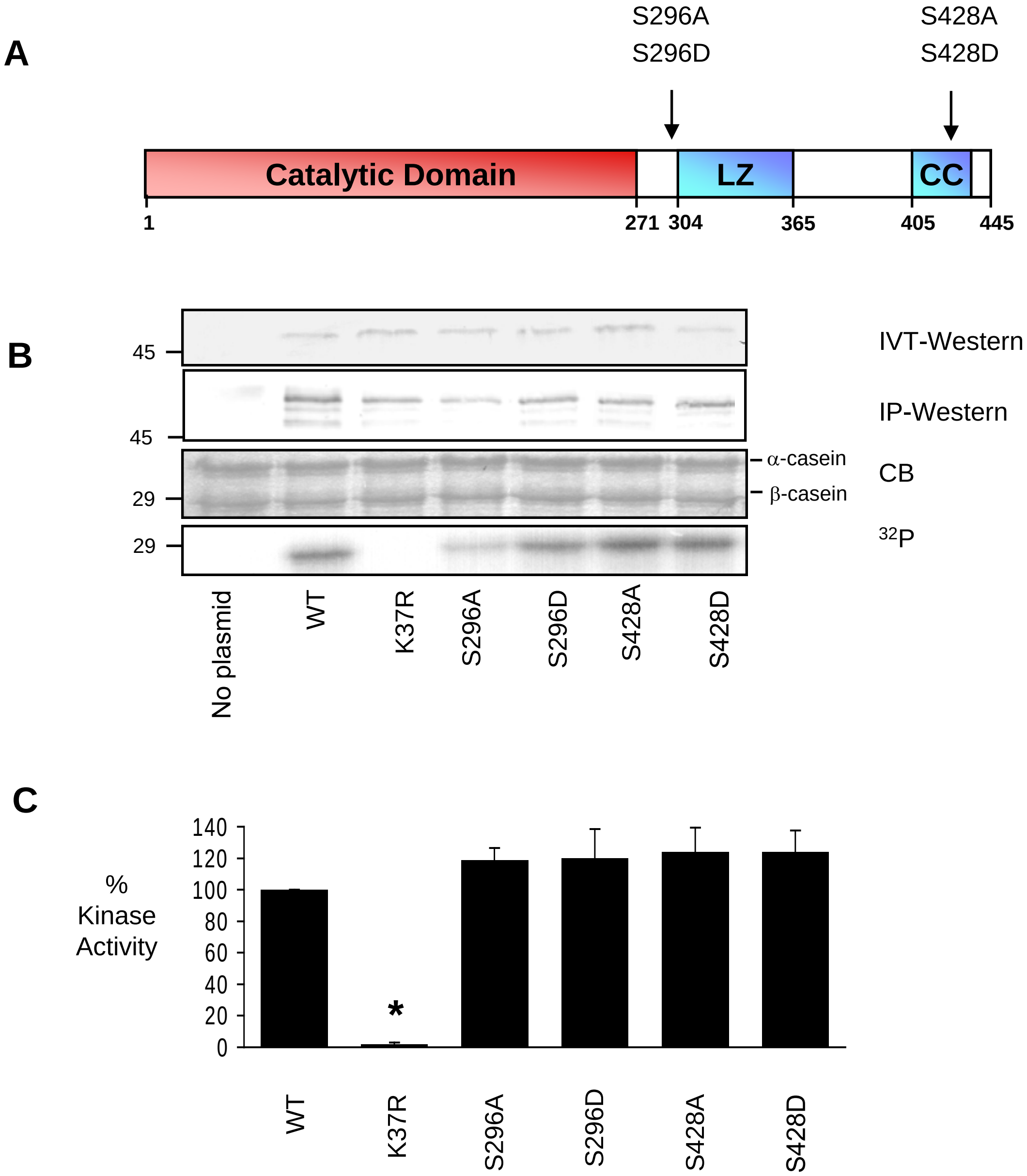

Figure 3.5 Mutation of S296 or S428 has no effect upon Nek2A kinase activity

A. Schematic diagram of Nek2A indicating the positions of the S296 and S428 in the non-catalytic domain. **B.** The myc-Nek2A-WT, Nek2A-KR, Nek2A-S296A, Nek2A-S296D, Nek2A-S428A and Nek2-S428D proteins were translated *in vitro* (IVT-Western), immunoprecipitated using anti-myc antibody and either Western blotted with an anti-Nek2 antibody followed by an AP-conjugated anti-rabbit secondary antibody (IP-Western) or incubated with kinase buffer containing ^{32}P-γ-[ATP] and the substrate casein. Proteins were separated by SDS-PAGE, stained with Coomassie Blue (CB) and exposed to autoradiography (^{32}P). Molecular weights (kDa) are indicated on the left. **C.** The histogram represents the kinase activity of each mutant based on at least 3 separate experiments. Kinase activity was calculated by scintillation counting and normalised for the amount of protein precipitated.* $P<0.05$ for K37R compared to WT.

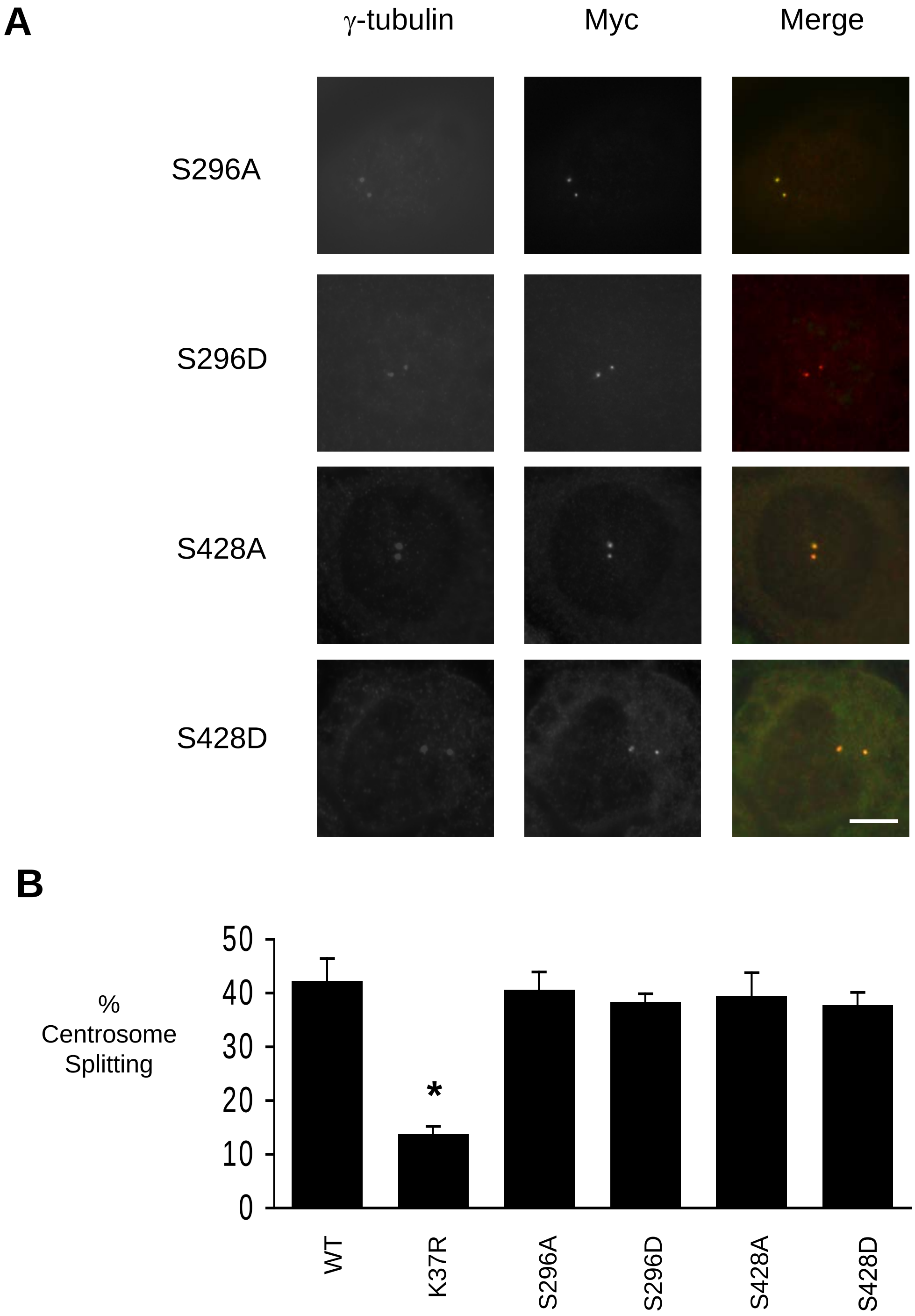

Figure 3.6 Mutation of S296 or S428 does not alter Nek2A activity in cells

A. U2OS cells were transfected with myc-Nek2A-S296A, myc-Nek2A-S296D, myc-Nek2A-S428A or myc-Nek2A-S428D constructs for 24 hours. Cells were fixed with methanol and stained with anti-myc-antibody to detect the Nek2A construct (green), anti-γ-tubulin antibody to detect the centrosome (red). Merged images are shown. All mutant Nek2A proteins localise to the centrosome. Scale bar, 10 μm. **B.** Approximately 100 cells were counted in each experiment and the centrosomes scored as split (>2 μm apart) or non-split. The histogram illustrates the number of split centrosomes observed for each Nek2A mutant based on 3 separate experiments. * $P<0.05$ compared to WT kinase.

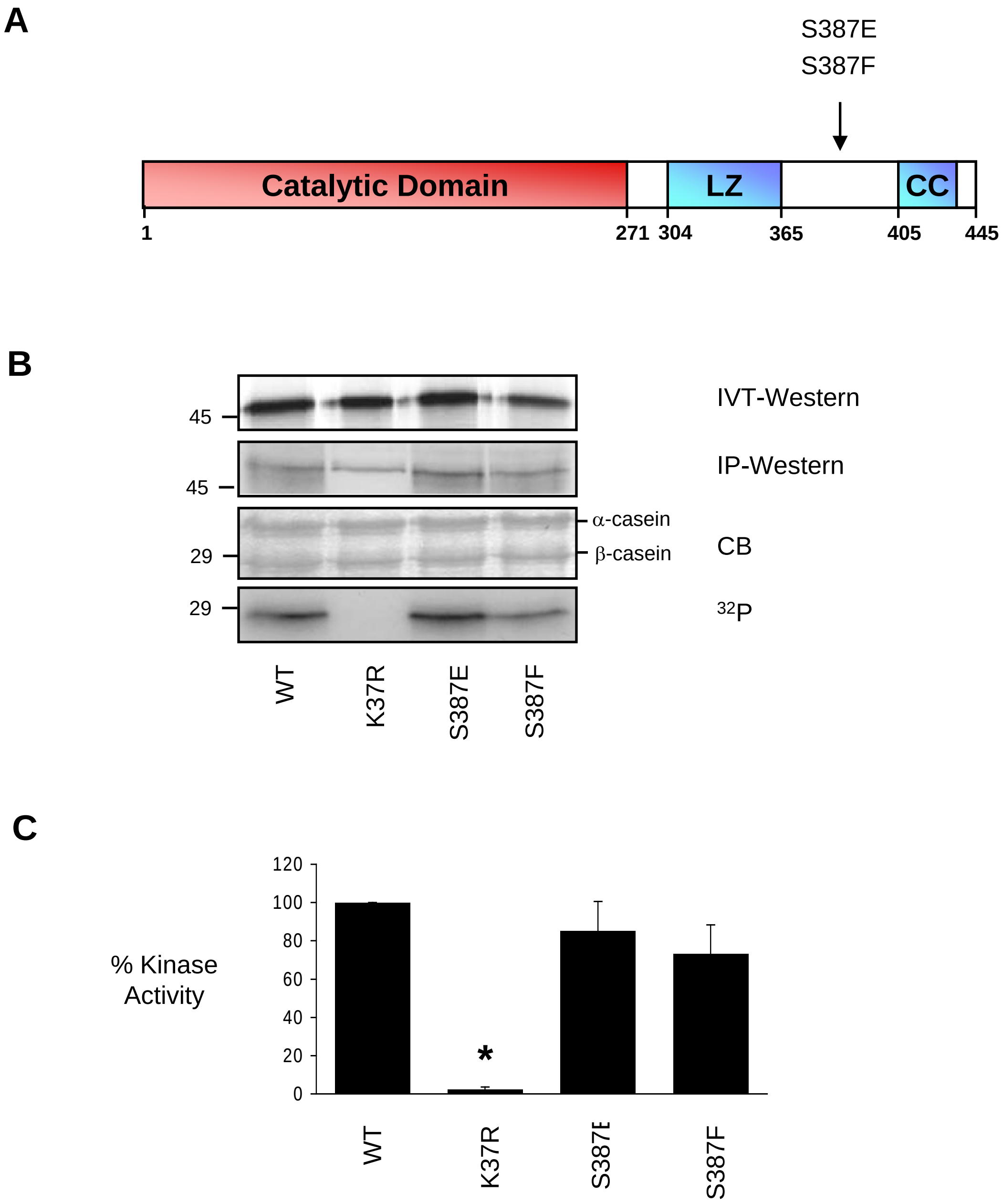

Figure 3.7 Mutation of S387 does not affect Nek2A activity

A. Schematic diagram of Nek2A indicating the position of the S387 mutants in the non-catalytic domain. **B.** The myc-Nek2A-WT, Nek2A-KR, Nek2A-S387E and Nek2A-S387F proteins were translated *in vitro* (IVT), then immunoprecipitated using anti-myc antibody and either Western blotted with an anti-Nek2 antibody followed by an AP-conjugated anti-rabbit secondary antibody (IP-Western), or incubated with kinase buffer containing ^{32}P-γ-[ATP] and the substrate casein. Proteins were separated by SDS-PAGE, stained with Coomassie Blue (CB) and exposed to autoradiography (^{32}P). Molecular weights (kDa) are indicated on the left. **C.** The histogram represents the kinase activity of each mutant based on at least 3 separate experiments. Kinase activity was calculated by scintillation counting and normalised for the amount of protein precipitated. * P> 0.1 for all mutants except K37R compared to WT kinase.

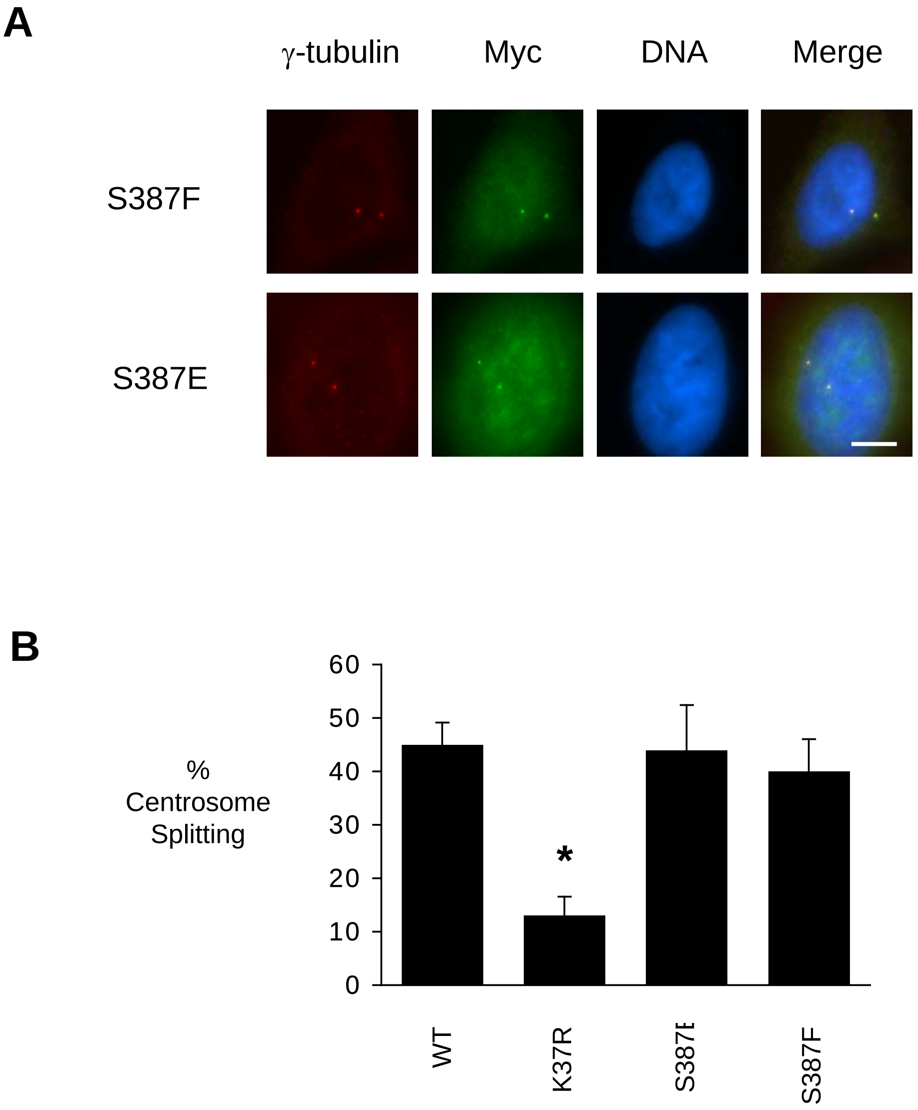

Figure 3.8 Mutation of S387 has no effect on Nek2A activity in cells

A. U2OS cells were transfected with myc-Nek2A-S387E or myc-Nek2A-S387F constructs for 24 hours. Cells were fixed with methanol and stained with anti-myc antibody to detect the Nek2A construct (green), anti-γ-tubulin antibody to detect the centrosome (red) and Hoechst 33258 to detect the DNA (blue). Merge images are shown. All mutant Nek2A proteins localise to the centrosome. Scale bar, 10 μm. **B.** Approximately 100 cells were counted in each experiment and the centrosomes scored as split (>2 μm apart) or non-split. The histogram illustrates the number of split centrosomes observed for each Nek2A mutant based on 3 separate experiments. * P> 0.1 for all mutants except K37R compared to that of WT.

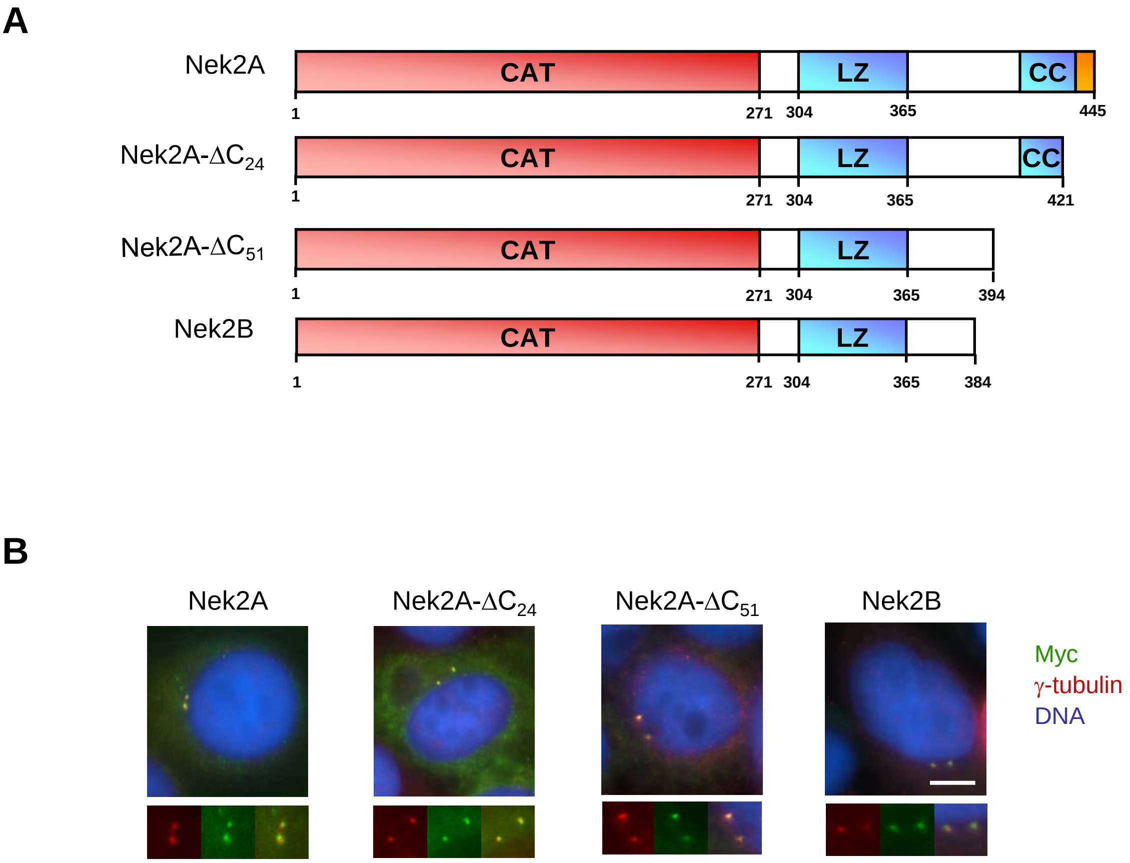
A
Nek2A
CAT
LZ
CC
1
271
304
365
445
Nek2A-ΔC24
CAT
LZ
CC
1
271
304
365
421
Nek2A-ΔC51
CAT
LZ
1
271
304
365
394
Nek2B
CAT
LZ
1
271
304
365
384
B
Nek2A
Nek2A-ΔC24
Nek2A-ΔC51
Nek2B
Myc
γ-tubulin
DNA

Figure 3.9 Deletion of C-terminal residues does not alter Nek2 localisation to the centrosome

A. Schematic diagrams of full length WT-Nek2A, Nek2B and two truncated Nek2A constructs indicating the position of each C-terminal deletion. **B.** U2OS cells were transfected with myc-Nek2A-WT, Nek2A-ΔC_{24}, Nek2A-ΔC_{51}, and Nek2B constructs for 24 hours. Cells were fixed with methanol and stained with anti-myc-antibody to detect the Nek2A construct (green), anti-γ-tubulin antibody to detect the centrosome (red) and Hoechst 33258 to detect the DNA (blue). Merged images as well as a magnified image of the stained centrosomes are shown. Scale bar, 10 µm. All mutant Nek2A proteins localise to the centrosome.

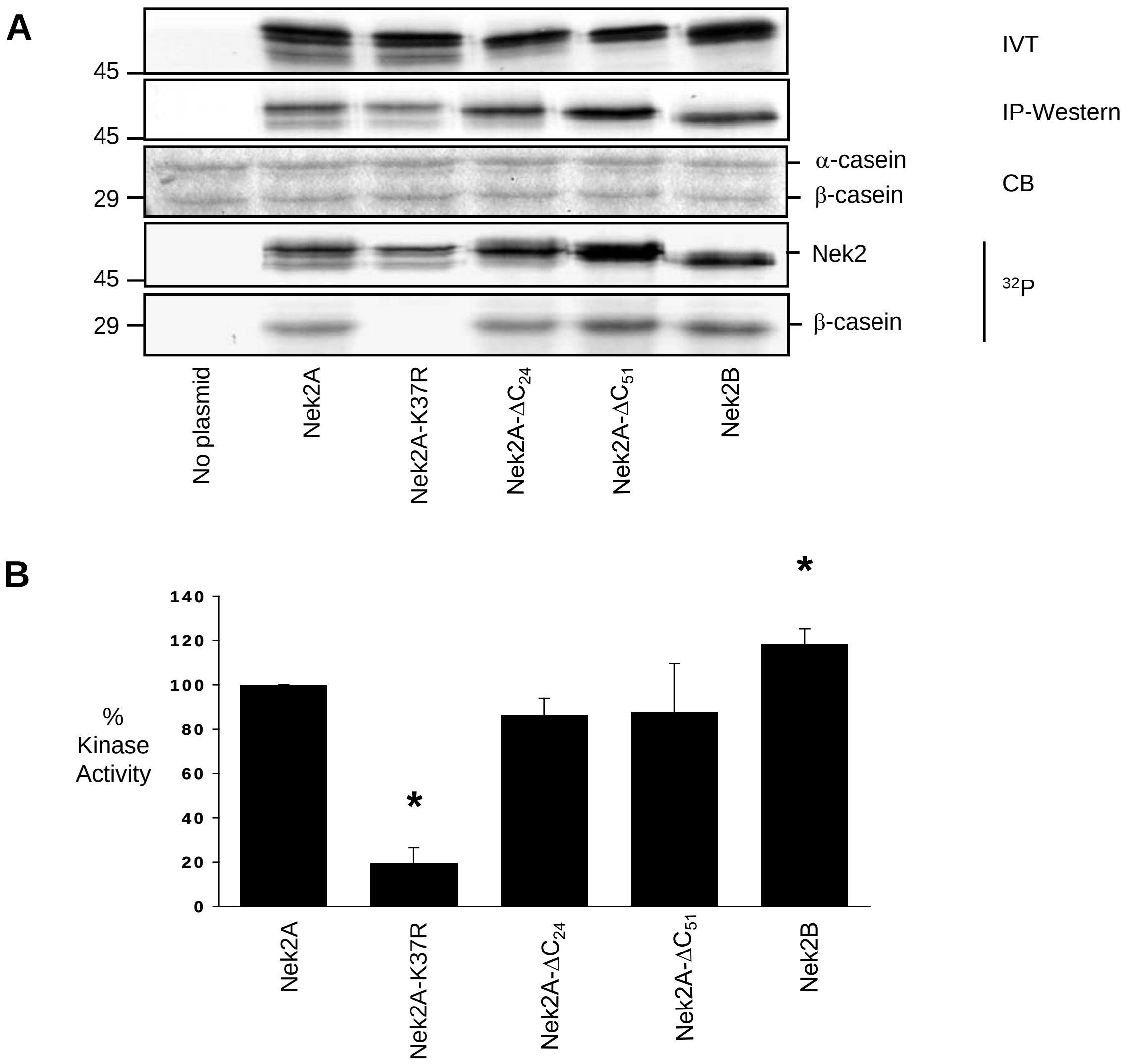

Figure 3.10 Deletion of the last 61 residues from the C-terminus creates a hyperactive Nek2A protein

A. The myc-Nek2A-WT, Nek2A-KR, Nek2A-ΔC_{24}, Nek2A-ΔC_{51} and Nek2B proteins were translated *in vitro* (IVT), immunoprecipitated using anti-myc antibody (IP), and either Western blotted with anti-Nek2 antibodies (IP-Western) or incubated with ^{32}P-γ-[ATP] and the substrate casein at 30^{0}C for 30 mins. Proteins were separated by SDS-PAGE, stained with Coomassie Blue (CB) and exposed to autoradiography (^{32}P). Molecular weights (kDa) are indicated on the left. **B.** The histogram displays the kinase activity of each mutant based on 3 separate experiments. Kinase activity was calculated by scintillation counting and then equalised to the amount of protein immunoprecipitated. * $P< 0.01$ compared to WT kinase.

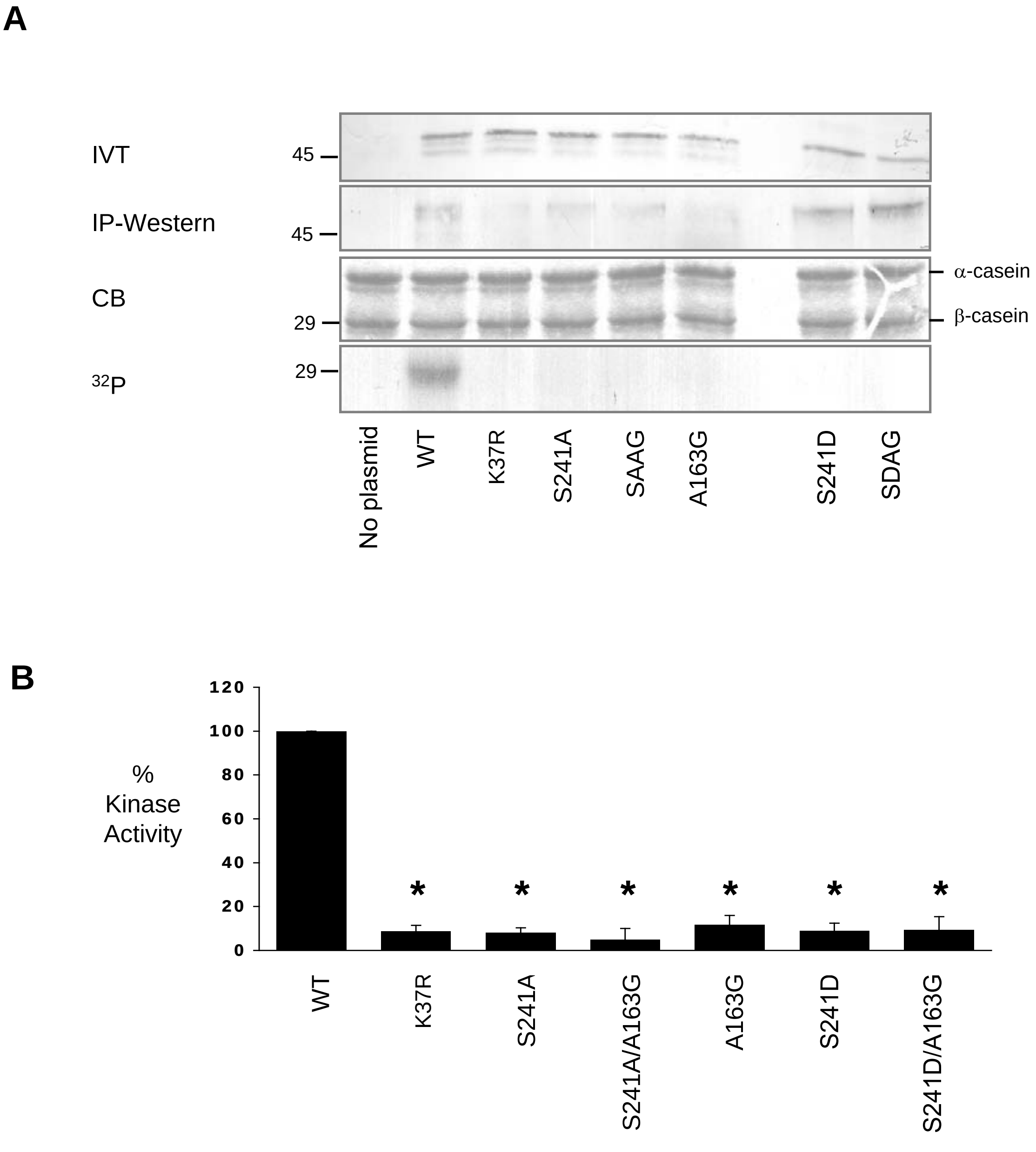

Figure 3.11 Mutation of A163 in the αT-helix inactivates Nek2

A. The Nek2A-WT, KR, S241A, S241A/A163G, A163G, S241D and S241D/A163G proteins were translated *in vitro* (IVT), immunoprecipitated using an anti-myc antibody (IP), and either Western blotted with anti-Nek2 antibodies (IP-Western) or incubated with ^{32}P-γ-[ATP] and the substrate casein at 30^{0}C for 30 mins. Proteins were separated by SDS-PAGE, stained with Coomassie Blue (CB) and exposed to autoradiography (^{32}P). Molecular weights (kDa) are indicated on the left. **B.** Histogram displaying the kinase activity of each mutant based on 3 separate experiments. Kinase activity was calculated by scintillation counting and then equalised to the amount of protein immunoprecipitated. * $P< 0.001$ compared to WT kinase.

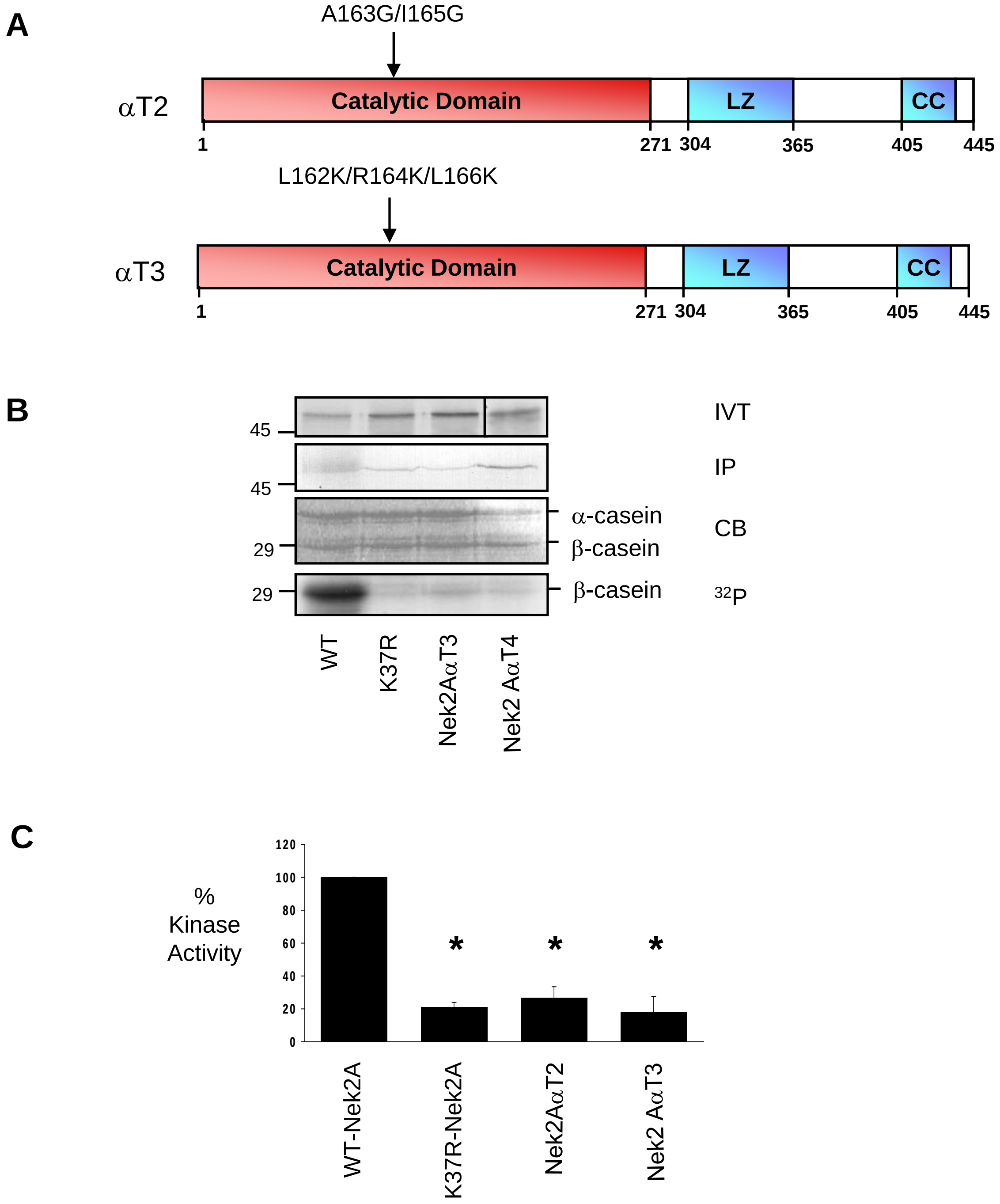

Figure 3.12 Additional mutations in the αT-helix cause loss of Nek2A activity

A. Schematic diagram of Nek2A indicating the positions of the mutations in the αT2 and αT3 construct. **B.** The myc-Nek2A-WT, Nek2A-KR, Nek2A-αT2 and Nek2A-αT3 proteins were translated *in vitro* (IVT), then immunoprecipitated using an anti-myc antibody and either Western blotted with an anti-Nek2 antibody (IP-Western) or incubated with kinase buffer containing ^{32}P-γ-[ATP] and the substrate casein. Proteins were separated by SDS-PAGE, stained with Coomassie Blue (CB) and exposed to autoradiography (^{32}P). Molecular weights (kDa) are indicated on the left. **C.** The histogram represents the kinase activity of each mutant based on at least 3 separate experiments. Kinase activity was calculated by scintillation counting and normalised for the amount of protein precipitated. * $P < 0.001$ compared to WT.

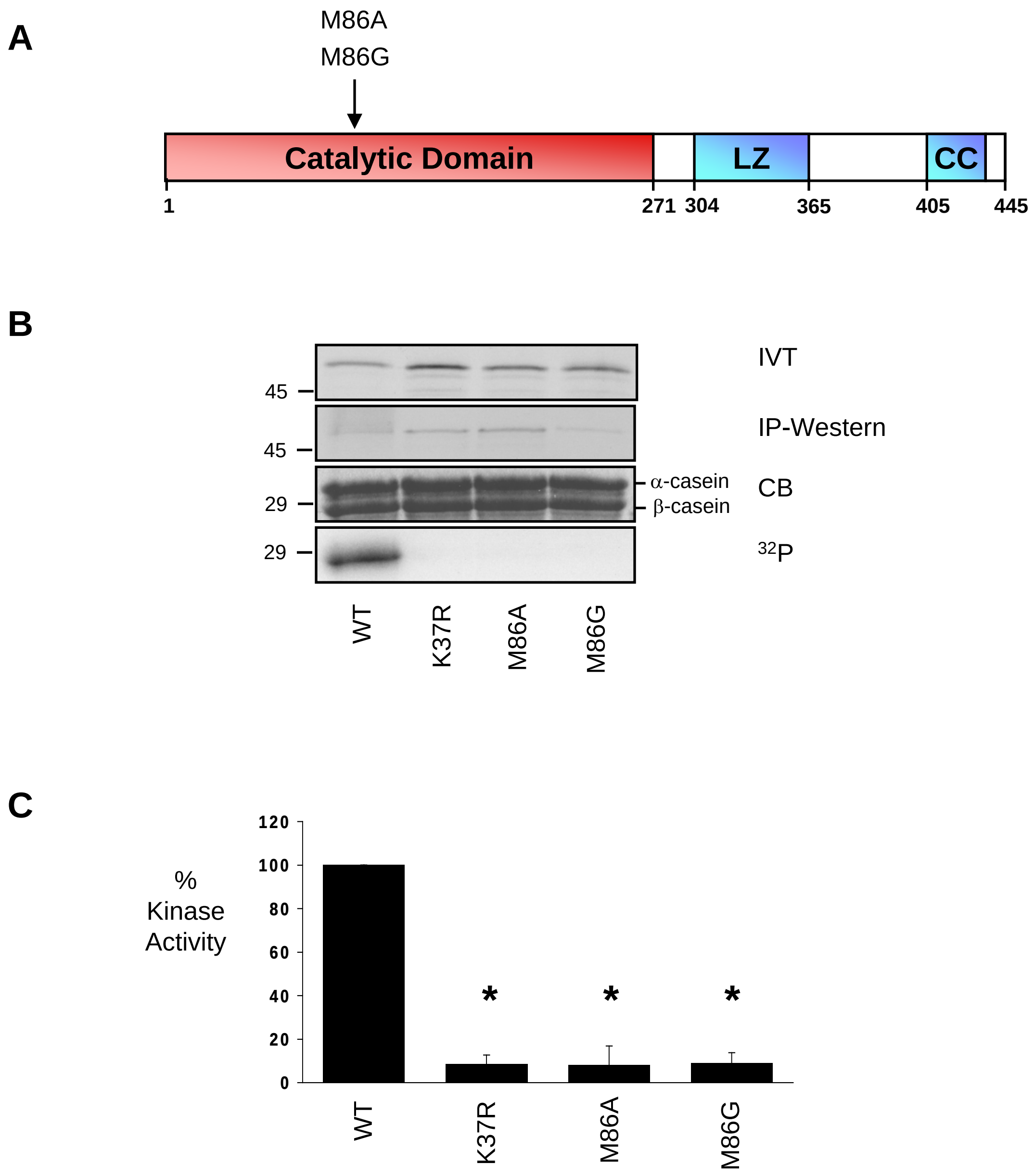

Figure 3.13 Mutation of the gatekeeper residue M86 leads to loss of Nek2A activity

A. Schematic diagram of Nek2A indicating the position of the M86 mutation in the catalytic domain. **B.** The myc-Nek2A-WT, Nek2A-KR, Nek2A-M86A and Nek2A-M86G proteins were translated *in vitro* (IVT), then immunoprecipitated using an anti-myc antibody and either Western blotted with an anti-Nek2 antibody (IP-Western) or incubated with kinase buffer containing ^{32}P-γ-[ATP] and the substrate casein. Proteins were separated by SDS-PAGE, stained with Coomassie Blue (CB) and exposed to autoradiography (^{32}P). Molecular weights (kDa) are indicated on the left. **C.** The histogram represents the kinase activity of each mutant based on at least 3 separate experiments. Kinase activity was calculated by scintillation counting and normalised for the amount of protein precipitated. * $P< 0.001$ compared to WT.

Phosphorylation Site	Mutant Constructs	Combined Mutations	Localised at Centrosome?	Centrosome Splitting Assay (%)	IVT-IP Kinase Assay (%)	Activity of Mutant
WT	WT		YES	58.2	100	NA
K37	K37R		YES	12	3.5	Inactive
T170	T170A T170E		YES YES	53 55.5	160 237	Hyperactive Hyperactive
S171	S171A S171D		YES YES	56 69	85 167	Active Hyperactive
T175	T175A T175E		YES YES	21.25 67.25	32.8 165	Inactive Hyperactive
T179	T179A T179E		YES YES	34 31	36.8 26.6	Inactive Inactive
S241	S241A S241D		YES YES	11.6 18.6	15 16.3	Inactive Inactive
S296	S296A S296D		YES YES	41 38	118.6 119.9	Active Active
S356	S356A S356D		YES YES	47 44	114 112	Active Active
S368	S368A S368D		YES YES	38 38	88 99	Active Active
S387	S387F S387E		YES YES	40 44	73.2 85.2	Active Active
S387/S390/S397/ S403		SA_4 SD_4	YES YES	63.9 61.3	161.7 108.9	Hyperactive Active
S428	S428A S428D		YES YES	39 38	140 124.1	Active Active

Figure 3.14 A summary of the consequences of mutations in Nek2A autophosphorylation sites

The table shows a summary of the Nek2A autophosphorylation sites and mutants analysed. Those studied by previous students, Dr. Baxter and Miss N. Sahota are indicated in black. Those sites which have been characterised in this chapter are highlighted in blue. These are compared to the wild-type Nek2A kinase (WT) and a construct carrying a mutation in the essential ATP-binding site (K37R). The relative activities of these mutants compared to wild-type kinase using one *in vivo* and one *in vitro* assay are outlined in the table.

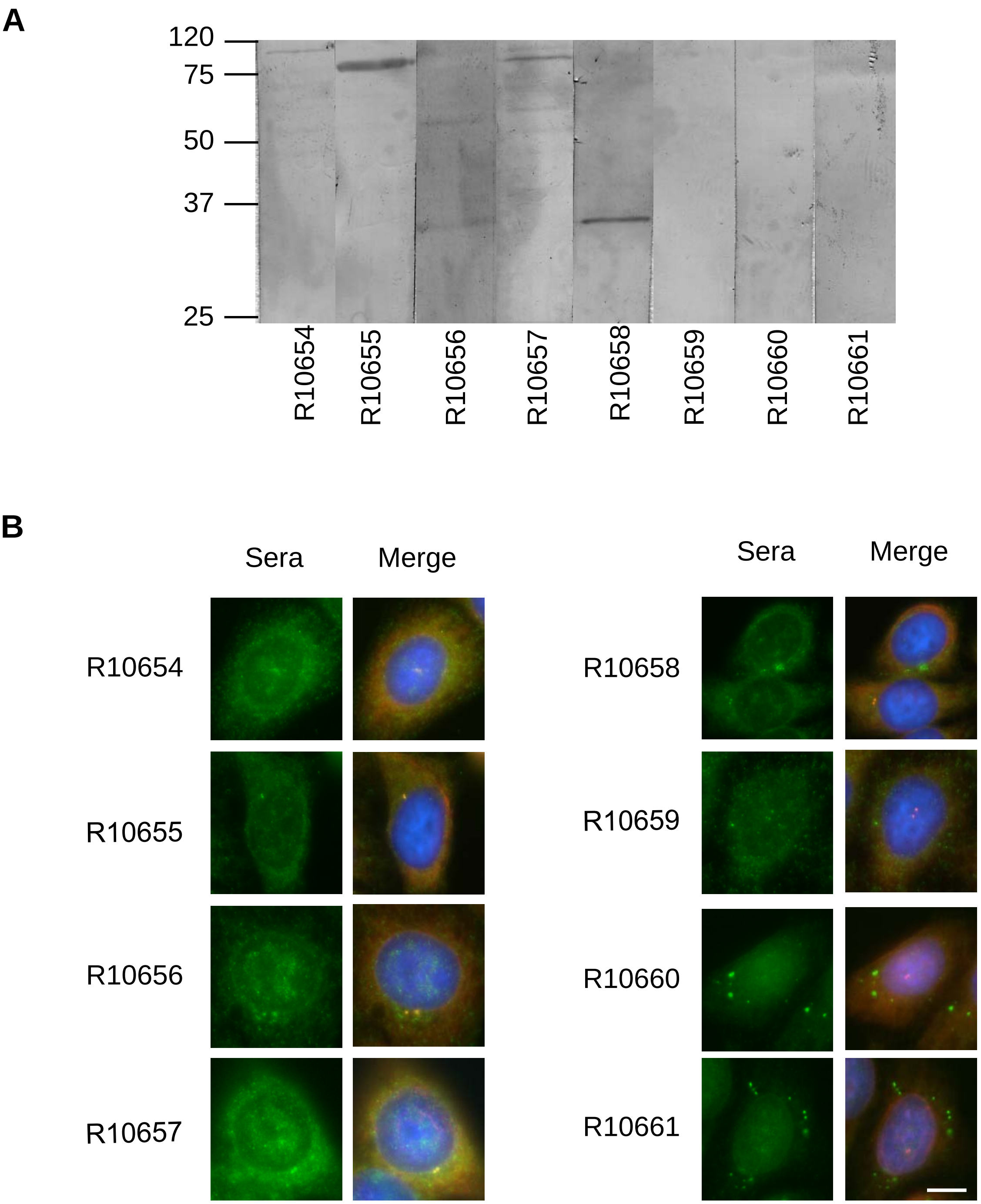
A
120
75
50
37
25
R10654
R10655
R10656
R10657
R10658
R10659
R10660
R10661
B
Sera
Merge
Sera
Merge
R10654
R10655
R10656
R10657
R10658
R10659
R10660
R10661

Figure 4.1 Prescreening of rabbit sera

A. U2OS cells were lysed and extracts separated by SDS-PAGE and blotted onto nitrocellulose membrane. The membrane was divided and probed with a corresponding rabbit serum. Molecular weights (kDa) are indicated on the left. **B.** U2OS cells were grown on coverslips and fixed with methanol. Cells were stained with corresponding rabbit serum (green), anti-γ-tubulin antibody to detect the centrosome (red) and Hoechst 33258 to detect the DNA (blue). Cells were also stained with the secondary anti-rabbit 488 antibody alone to ensure there was no non-specific labelling. Merged images taken using the same exposure and gain for all samples are shown. Scale bar, 10 μm.

A

PP — TSFAKpTFVGTPC —

NP — TSFAKTFVGTPC —

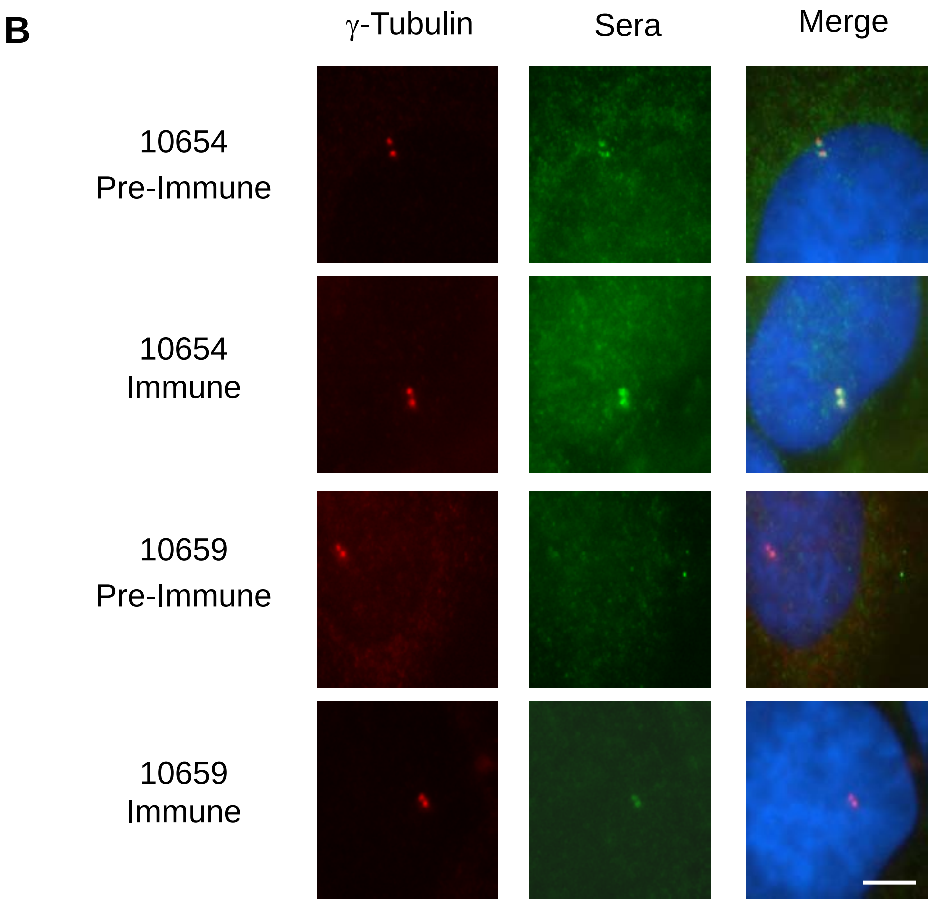

Figure 4.2 Immune sera 10654 and 10659 stain the centrosomes more strongly than the pre-immune sera

A. The sequence of a short peptide designed to correspond to part of the Nek2 protein surrounding the T175 residue. The upper peptide sequence contains a phosphorylated T175 residue (PP). This peptide was injected into rabbits 10654 and 10659. The sequence of the non-phosphorylated peptide (NP) is also shown. **B.** U2OS cells were grown on coverslips and fixed with methanol. Cells were stained with either the preimmune or terminal bleed from each rabbit (green), anti-γ-tubulin antibody to detect the centrosome (red) and Hoechst 33258 to detect the DNA (blue). Merged immunofluorescent images taken using the same exposure and gain between slides are shown. Scale bar, 10 μm. The intensity of centrosomal staining was stronger in the immune than the pre-immune sera for both rabbits.

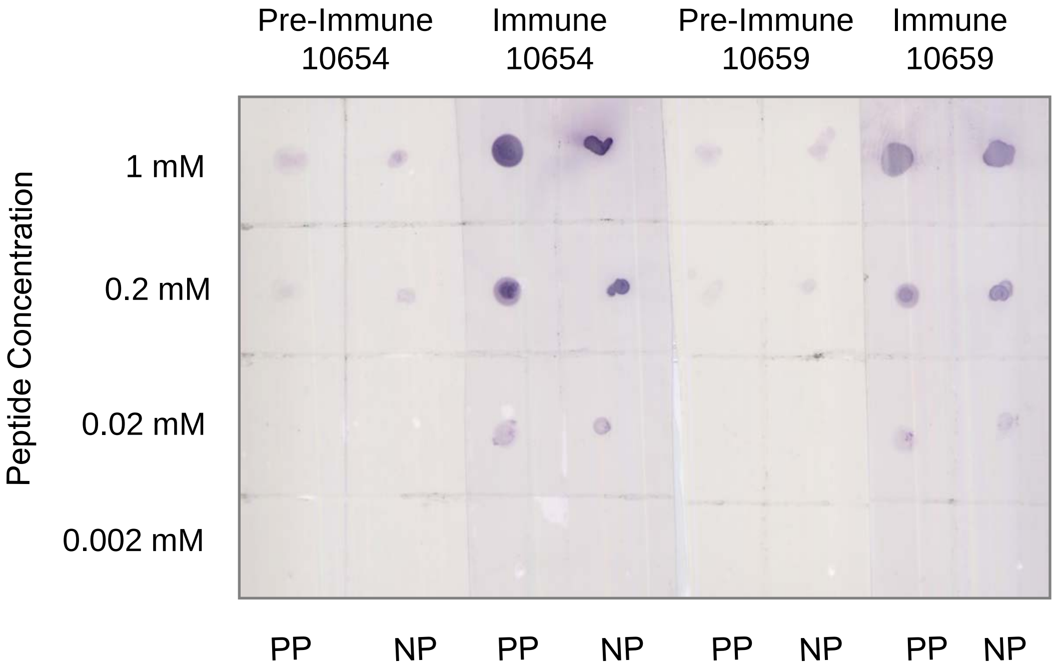
Pre-Immune 10654
Immune 10654
Pre-Immune 10659
Immune 10659
Peptide Concentration
1 mM
0.2 mM
0.02 mM
0.002 mM
PP
NP
PP
NP
PP
NP
PP
NP

Figure 4.3 The immune sera for rabbits 10654 and 10659 detect phosphorylated peptide more strongly than the pre-immune sera

Serial dilutions of phosphorylated (PP) and non-phosphorylated (NP) peptide were dotted onto nitrocellulose membrane and probed with either pre-immune or immune sera from either rabbit 10654 or 10659.

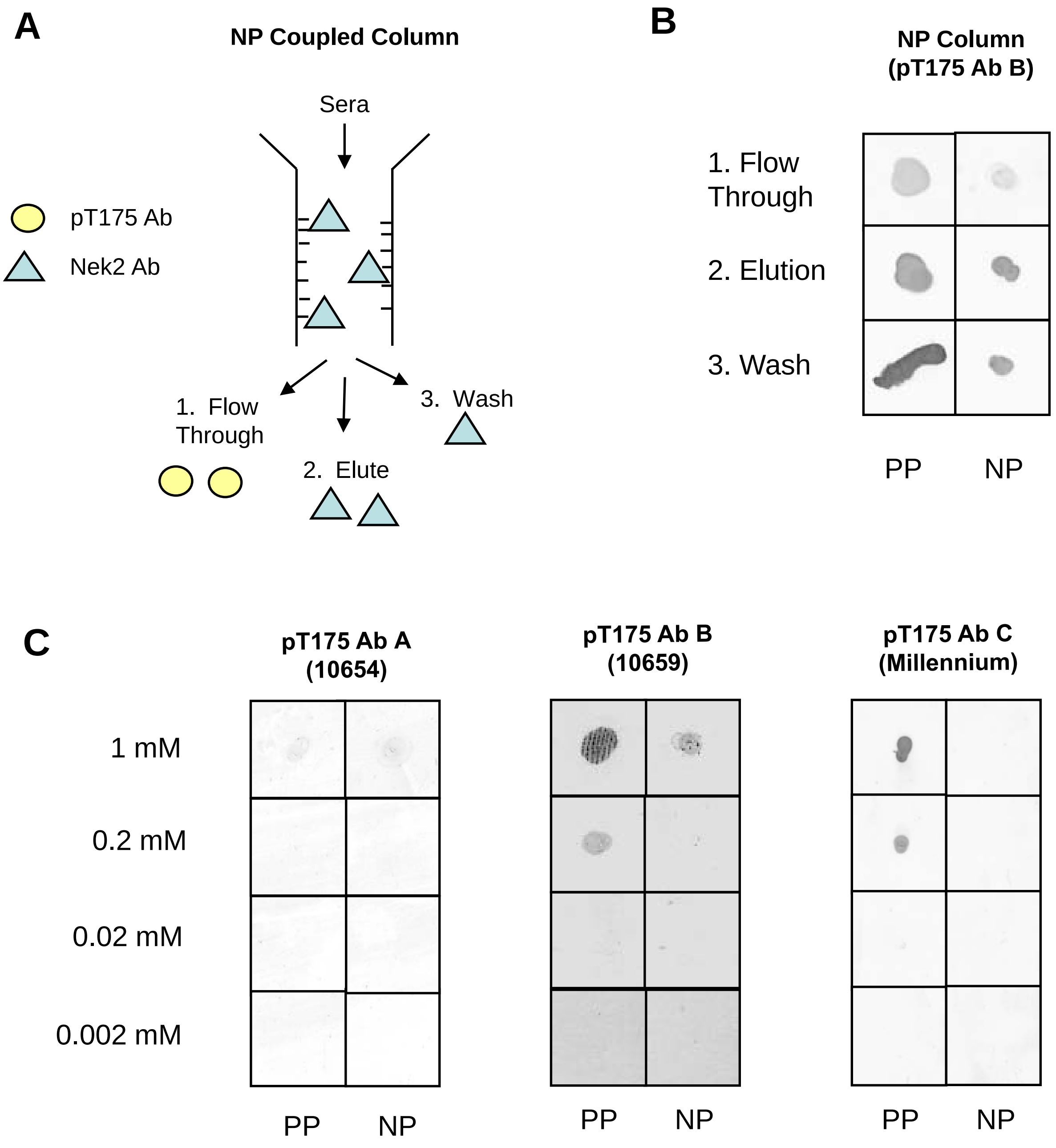
A
NP Coupled Column
Sera
pT175 Ab
Nek2 Ab
1. Flow Through
2. Elute
3. Wash
B
NP Column (pT175 Ab B)
1. Flow Through
2. Elution
3. Wash
PP
NP
C
pT175 Ab A (10654)
pT175 Ab B (10659)
pT175 Ab C (Millennium)
1 mM
0.2 mM
0.02 mM
0.002 mM
PP
NP
PP
NP
PP
NP

Figure 4.4 Two of the purified pT175 antibodies detect the phosphorylated peptide more strongly than the non-phosphorylated peptide

A. Schematic diagram of the purification of phosphospecific pT175 antibodies. Non-phosphorylated (NP) peptide was coupled to an agarose gel support. Serum was then applied to the column and the flow through collected. The column was then washed and the bound protein eluted. The flow through would be expected to contain the pT175 antibody. **B.** An equal volume of the phosphorylated (PP) and non-phosphorylated (NP) peptide was dotted onto nitrocellulose membrane and incubated with either the flow through, wash or elution following purification of pT175 Ab B. The flow through detected the phosphopeptide more strongly than the non-phosphorylated peptide. **C.** A serial dilution of each peptide was dotted onto nitrocellulose membrane and incubated with 3 potential purified pT175 antibodies (1:50). The pT175 antibody B and C detected phosphopeptide more strongly than non-phosphopeptide.

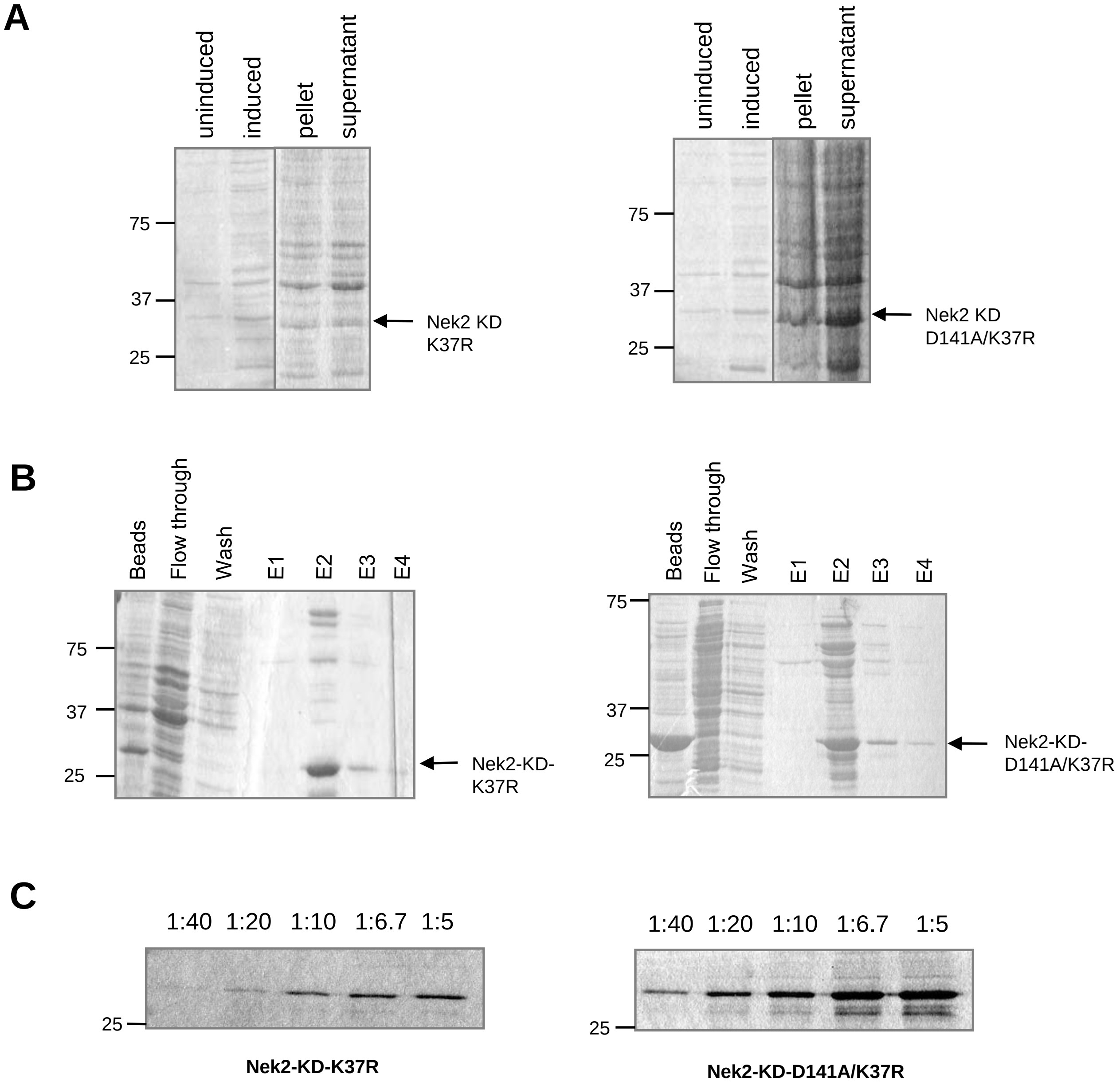
A
uninduced
induced
pellet
supernatant
75
37
25
Nek2 KD
K37R
uninduced
induced
pellet
supernatant
75
37
25
Nek2 KD
D141A/K37R
B
Beads
Flow through
Wash
E1
E2
E3
E4
75
37
25
Nek2-KD-
K37R
Beads
Flow through
Wash
E1
E2
E3
E4
75
37
25
Nek2-KD-
D141A/K37R
C
1:40
1:20
1:10
1:6.7
1:5
25
Nek2-KD-K37R
1:40
1:20
1:10
1:6.7
1:5
25
Nek2-KD-D141A/K37R

Figure 4.5 Expression and purification of Nek2-KD-K37R and Nek2-KD-K37R/D141A proteins

A. Bacterial expression of Nek2-KD-K37R and Nek2-KD-K37R/D141A proteins was induced by adding 1 mM IPTG for 4 hours at 18^0C. The bacterial cultures were centrifuged and the pellets lysed prior to centrifugation. Aliquots of bacteria before and after induction, as well as of the pellets and supernatants after lysis were analysed by SDS-PAGE and Coomassie Blue staining. **B.** The Nek2 proteins were purified by passing the lysates over Ni-NTA beads. The proteins were eluted from the column and collected in 4 fractions. The uninduced, pellet, supernatant, flow-through, wash and elution fractions were analysed by SDS-PAGE and Coomassie Blue staining. Bands corresponding to the Nek2-KD-K37R and Nek2-KD-D141A/K37R proteins can be seen in the elution fractions. **C**. A serial dilution for Elution 2 for each protein was analysed by SDS-PAGE and Coomassie Blue staining. Molecular weights (kDa) are indicated on the left.

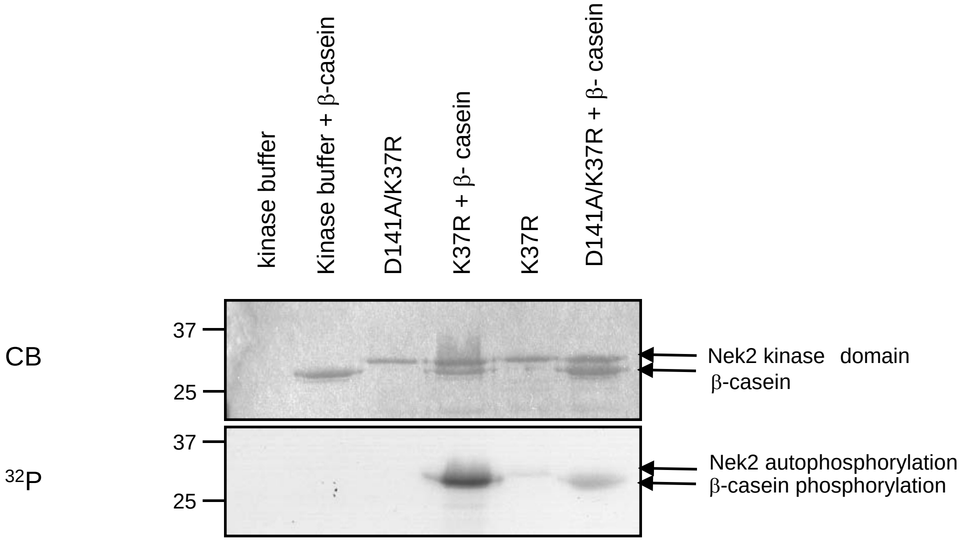
kinase buffer
Kinase buffer + β-casein
D141A/K37R
K37R + β- casein
K37R
D141A/K37R + β- casein
CB
37
25
Nek2 kinase domain
β-casein
32P
37
25
Nek2 autophosphorylation
β-casein phosphorylation

Figure 4.6 Nek2-KD-K37R/D141A kinase is an inactive kinase incapable of autophosphorylation

Purified Nek2-KD-K37R/D141A and Nek2-KD-K37R kinases were incubated in kinase buffer containing ^{32}P-γ-ATP in the presence or absence of β-casein for 30 minutes at 30^{0}C. Samples without Nek2 protein in the presence or absence of β-casein were used as negative controls. The proteins in each reaction were separated by SDS-PAGE and analysed by Coomassie Blue staining (CB) and autoradiography (^{32}P). Molecular weights (kDa) are indicated on the left. A faint band corresponding to autophosphorylation can be observed for the Nek2-KD-K37R kinase which is not present in Nek2-KD-K37R-D141A kinase.

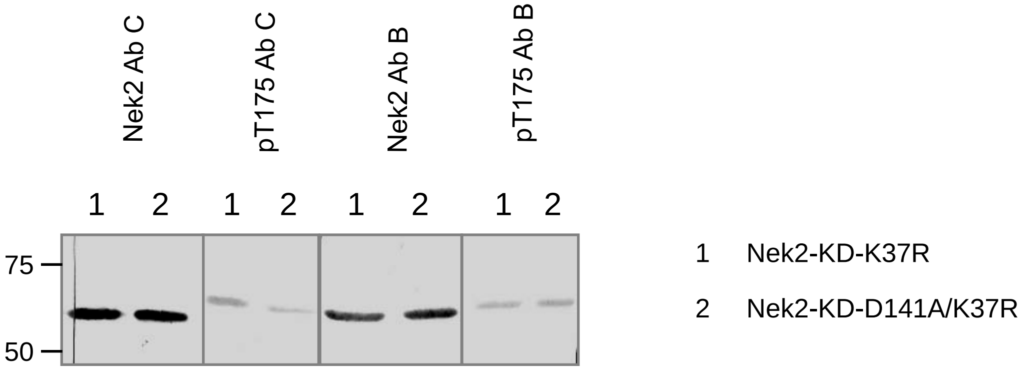
Nek2 Ab C
pT175 Ab C
Nek2 Ab B
pT175 Ab B
1 2 1 2 1 2 1 2
75
50
1 Nek2-KD-K37R
2 Nek2-KD-D141A/K37R

Figure 4.7 pT175 Ab C detected Nek2-KD-K37R kinase but not unphosphorylated Nek2-KD-K37R/D141A kinase.

Purified Nek2-KD-K37R/D141A and Nek2-KD-K37R proteins were incubated in kinase buffer containing ATP for 30 minutes at 30^0C. The kinases were then separated by SDS-PAGE and blotted onto nitrocellulose membrane. The nitrocellulose membrane was stained with Ponceau and equal loading was observed across the 8 lanes. The membrane was divided and blocked in 5% BSA-TBST. The nitrocellulose membrane was probed with purified pT175 antibodies and their corresponding non-phosphospecific Nek2 antibodies (eluted from purification column) diluted 1:250 in 1x TBST. Molecular weights (kDa) are indicated on the left.

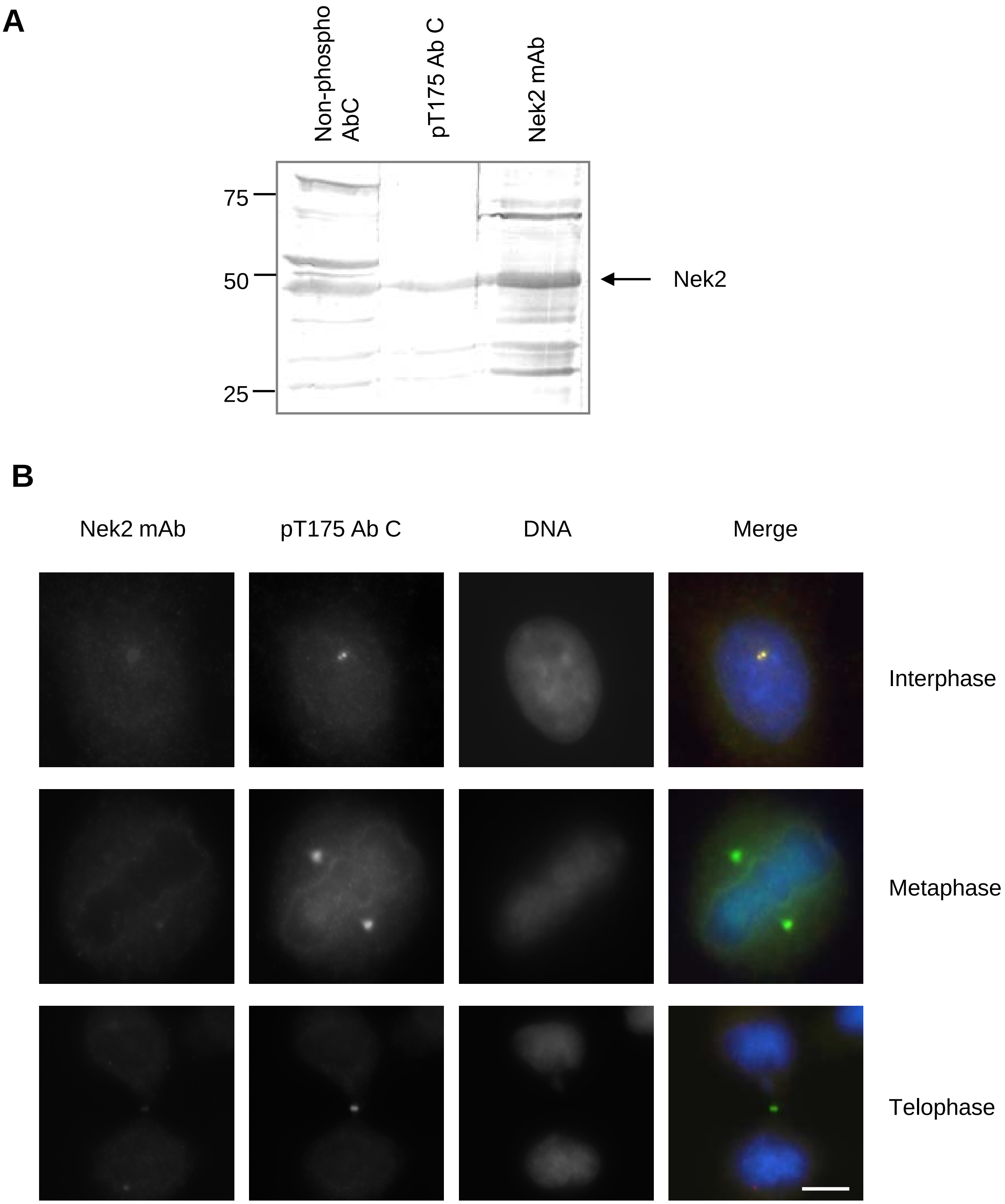
A
Non-phospho AbC
pT175 Ab C
Nek2 mAb
75
50
25
Nek2
B
Nek2 mAb
pT175 Ab C
DNA
Merge
Interphase
Metaphase
Telophase

Figure 4.8 pT175 Ab C detects Nek2 in U2OS lysates

A. U2OS lysates were separated by SDS-PAGE and blotted onto nitrocellulose membrane. The membrane was blocked in 5% BSA-TBST then probed with the non-phospho-specific Ab C, the pT175 Ab C, and a commercial monoclonal Nek2 mAb. All three antibodies detect a band at the predicted size of endogenous Nek2 protein at 48 kDa (arrow). Molecular weights (kDa) are indicated on the left. **B**. U2OS cells were fixed with methanol and probed with pT175 Ab C (green), Nek mAb (red) and Hoechst (blue) to stain the DNA. Images of a cell in interphase, metaphase and telophase are shown. Scale bar, 10 μm. pT175 Ab C stains the centrosome in interphase but also detects the spindle poles in mitosis, unlike the Nek2 mAb. The pT175 Ab C also produces a signal at the midbody in telophase.

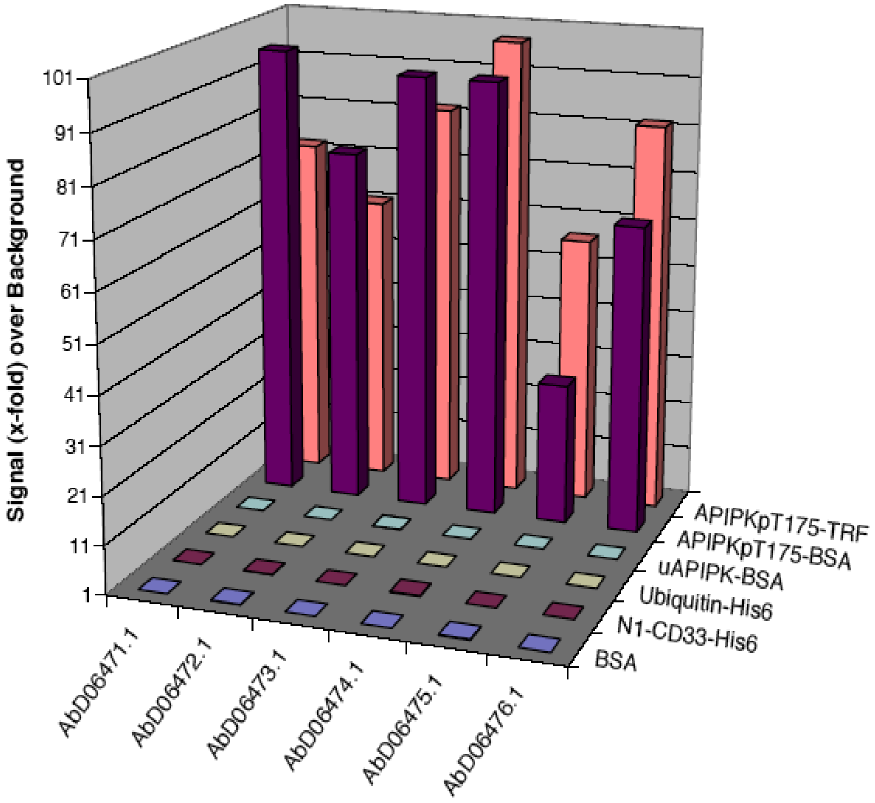

Figure 4.9 ELISA data of the six recombinant pT175 Nek2 antibodies identified by AbD Serotec

AbD06471.1-AbD06476.1 were identified as positive binders of the phosphorylated Nek2 T175 peptide (APIPKpT175) tagged with either Trf or BSA. These antibodies did not bind the non-phosphorylated peptide (uAPIPK) tagged with BSA, BSA alone or proteins Ubiquitin-His6 or N1-CD33-His6. Data kindly provided by AbD Serotec.

A

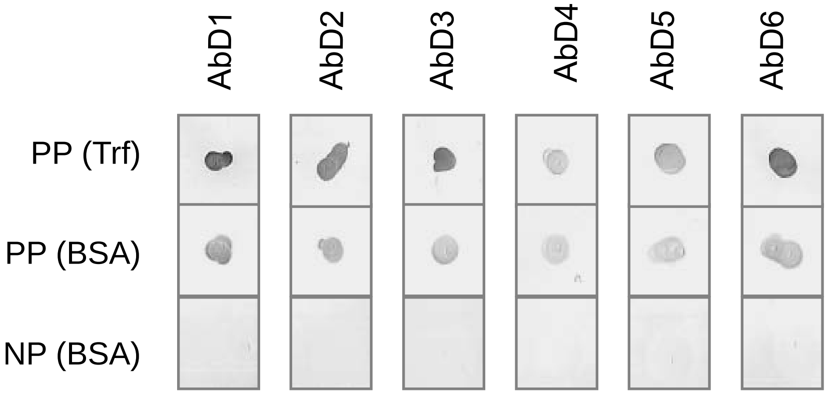
AbD1
AbD2
AbD3
AbD4
AbD5
AbD6
PP (Trf)
PP (BSA)
NP (BSA)

B

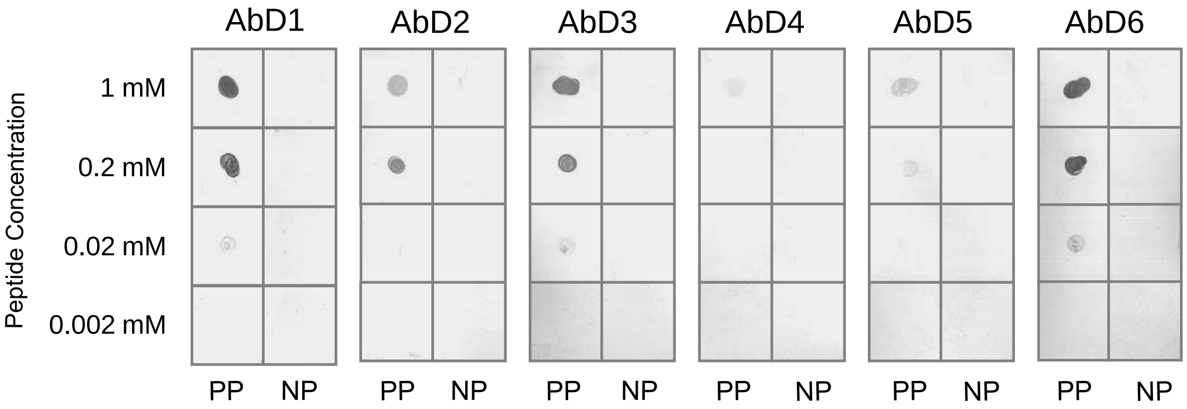
AbD1
AbD2
AbD3
AbD4
AbD5
AbD6
Peptide Concentration
1 mM
0.2 mM
0.02 mM
0.002 mM
PP
NP

Figure 4.10 The six HuCAL pT175 phosphospecific antibodies detect the phosphorylated but not the unphosphorylated peptide

A. Phosphorylated peptide tagged with either Trf or BSA and non-phosphorylated peptide tagged with BSA were dotted onto nitrocellulose membrane and probed with the 6 potential recombinant antibodies named AbD1-AbD6. **B**. A serial dilution of phosphorylated (PP) and non-phosphorylated (NP) peptide was dotted onto nitrocellulose membrane and probed with recombinant antibodies AbD1-6. Dot blots were developed using an anti-human Fab fragment AP-conjugated secondary antibody.

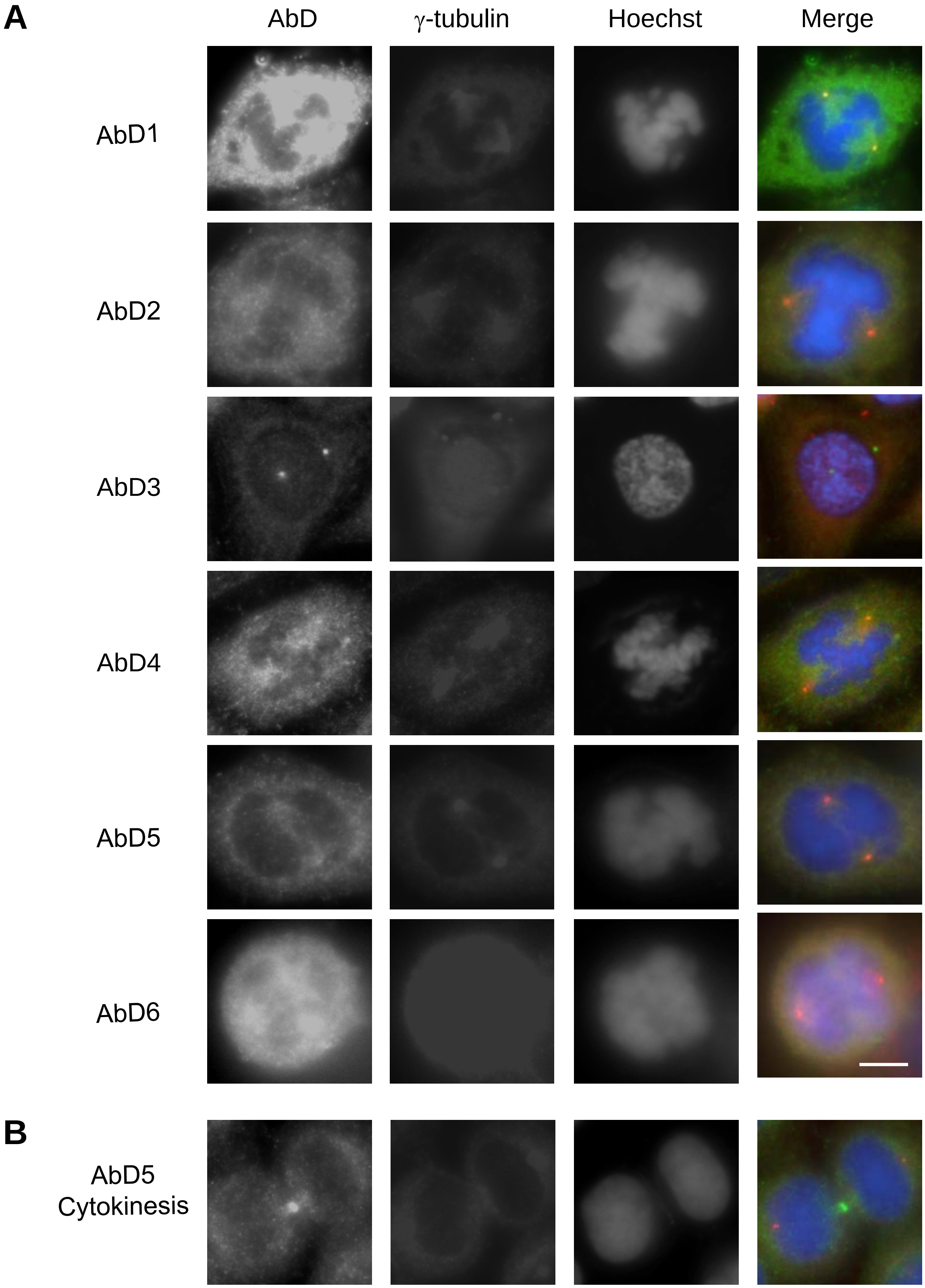

Figure 4.11 AbD1 detects centrosomes in U2OS cells

A. U2OS cells were fixed with methanol and stained with one of recombinant antibodies, AbD1-6 (green). In addition cells were also stained with anti-γ-tubulin antibody to detect the centrosomes (red) and Hoechst 33258 to detect the DNA (blue). Images were taken of mitotic cells in prophase, stained with each antibody, although there are slight differences in the precise stages of prophase exhibited by the representative cells. These observations are based on viewing 10 cells stained with each antibody. Scale bar, 10 μm. AbD1 strongly detects centrosomes in prophase although possible spindle association is also highlighted. **B**. Interestingly AbD5 produced a strong signal at the midbody in cells undergoing cytokinesis.

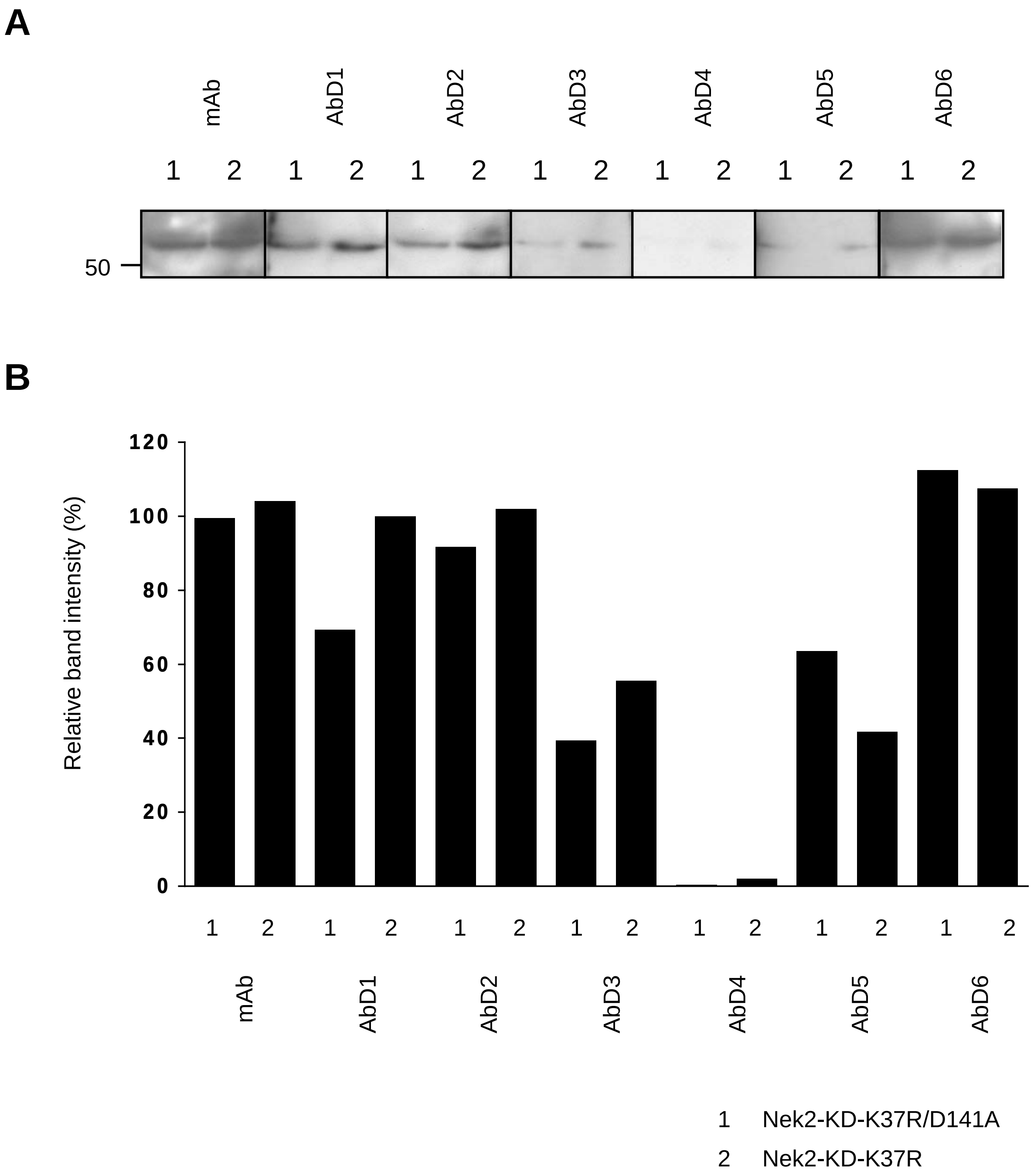

Figure 4.12 AbD1, 2 and 3 preferentially detect Nek2-KD-K37R rather than Nek2-KD-K37R/D141A bacterially expressed protein

A. Nek2-KD-K37R (lane 2) and Nek2-KD-K37R/D141A (lane 1) purified proteins were incubated in kinase buffer containing ATP for 30 minutes at 30^0C. Sample buffer was added to stop the reaction. The proteins were then separated by SDS-PAGE and blotted onto nitrocellulose membrane. The membrane was cut into strips and probed with either total Nek2 mAb or one of AbD1-6. The membrane was developed by ECL. **B.** The intensity of each band was measured using Image J software and the measurements displayed as a histogram with the intensity of the mAb staining of the Nek2-KD-K37R/D141A protein set as 100%.

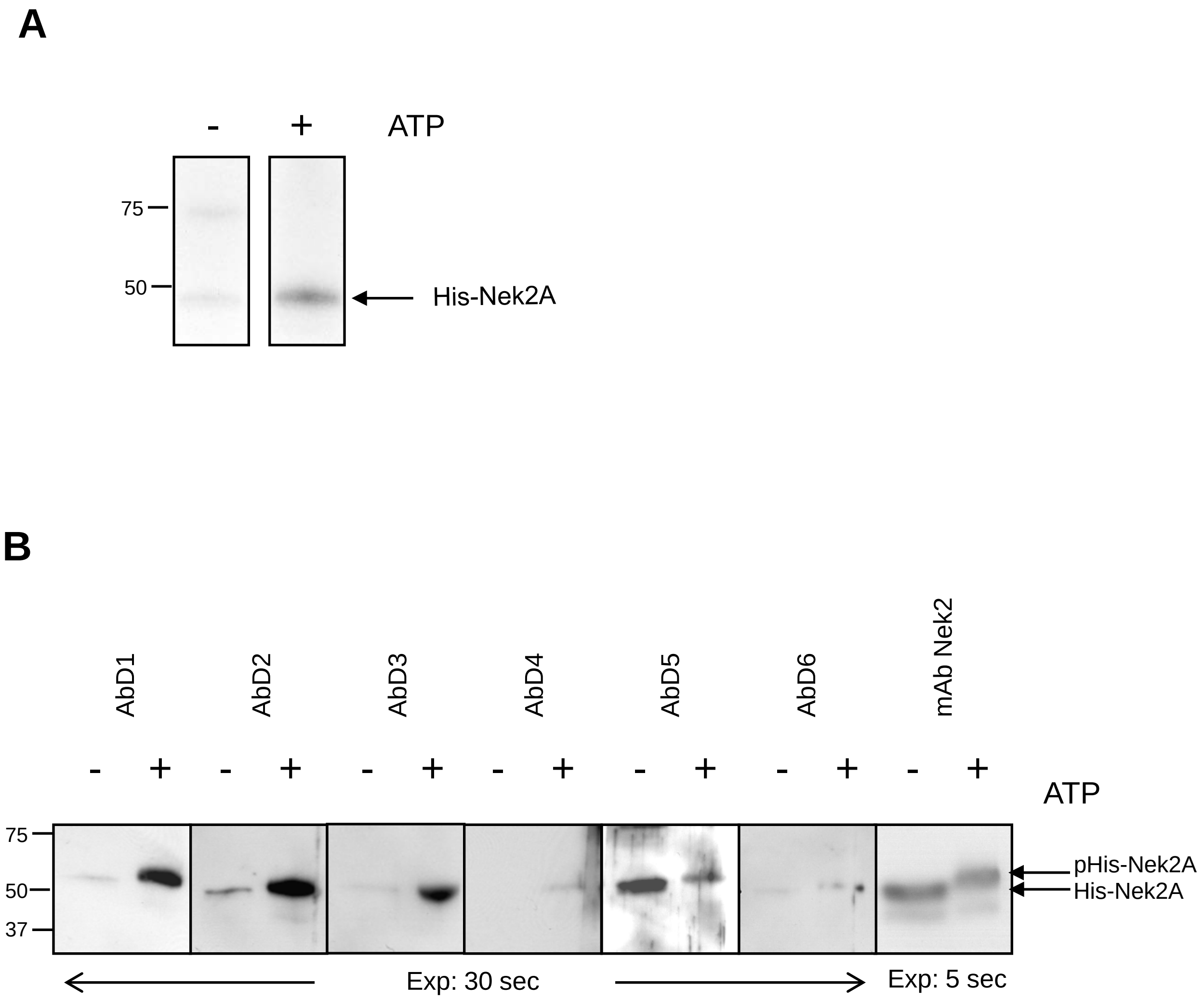
A
- + ATP
75
50
His-Nek2A
B
AbD1
AbD2
AbD3
AbD4
AbD5
AbD6
mAb Nek2
- + - + - + - + - + - + - +
ATP
75
50
37
pHis-Nek2A
His-Nek2A
Exp: 30 sec
Exp: 5 sec

Figure 4.13 Recombinant antibodies AbD1, 2 and 3 detect phosphorylated His-Nek2A after ATP incubation but not untreated His-Nek2

A. Purified His-Nek2A kinase was incubated in kinase buffer in the presence (+) or absence (-) of ATP. An aliquot of each Nek2A mixture was taken and γ-P^{32}-ATP was added and kinase reactions incubated at 30^0C for 30 minutes. The proteins were analysed by SDS-PAGE and autoradiography. **B**. The proteins in the non-radioactive samples were separated by SDS-PAGE, blotted onto nitrocellulose membrane and cut into strips. Each strip was probed with either one of AbD1-6 or the monoclonal Nek2 antibody (mAb) followed by an incubation with anti-human-HRP conjugated antibody. Finally, the membrane strips were developed by ECL Plus. A band corresponding to phosphorylated His-Nek2A is indicated. Molecular weights (kDa) are indicated on the left.

A

- TSFAKTFVGTP -	Nek2
- TTAAHSLVGTP -	Nek6
- TTAAHSLVGTP -	Nek7
- SSRRTTLCGTL -	Aurora A
- GERKKTLCGTP -	Plk1

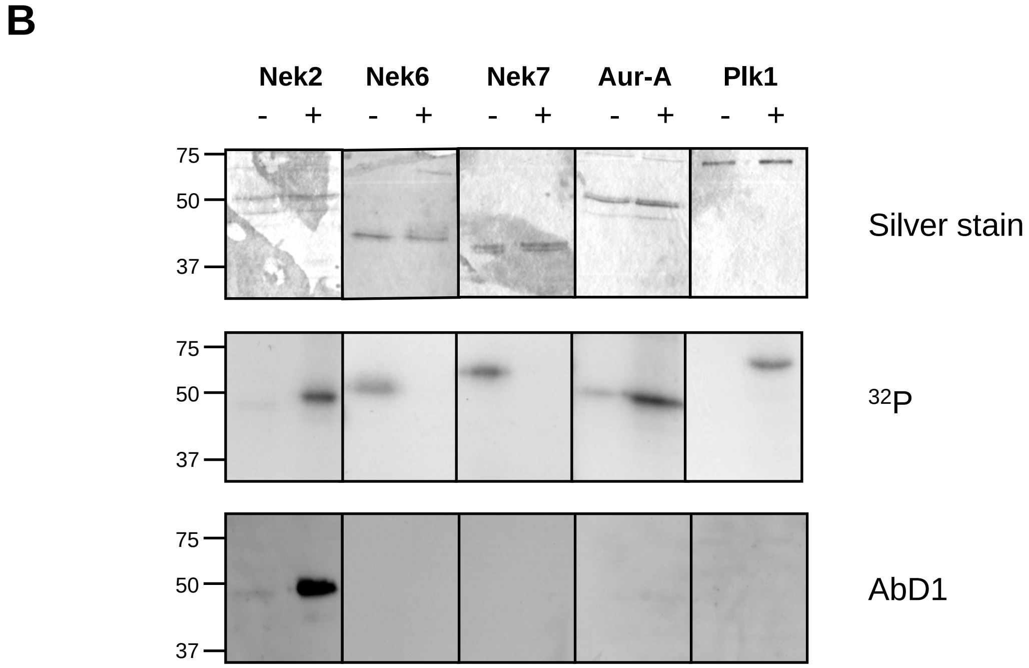

Figure 4.14 AbD1 detects specifically the mitotic kinase, Nek2 *in vitro*

A. Comparison of the activation loop sequences of Nek2 and other mitotic kinases. The primary autophosphorylation site required for kinase activation is highlighted in red. In Nek2 this is Thr175 to which the phosphospecific antibody was raised. **B**. Purified mitotic kinases as indicated were diluted in kinase buffer in the presence (+) or absence (-) of ATP. An aliquot of each kinase reaction was taken and γ-^{32}P-ATP added. All reactions were then incubated at 30^{0}C for 30 minutes and proteins separated by SDS-PAGE. One gel was silver stained to show equal loading. The gel containing radioactive sample was stained with Coomassie Blue and exposed to autoradiography. The third gel was blotted onto nitrocellulose membrane and probed with AbD1. The membrane was developed by ECL plus. Molecular weights (kDa) are indicated on the left.

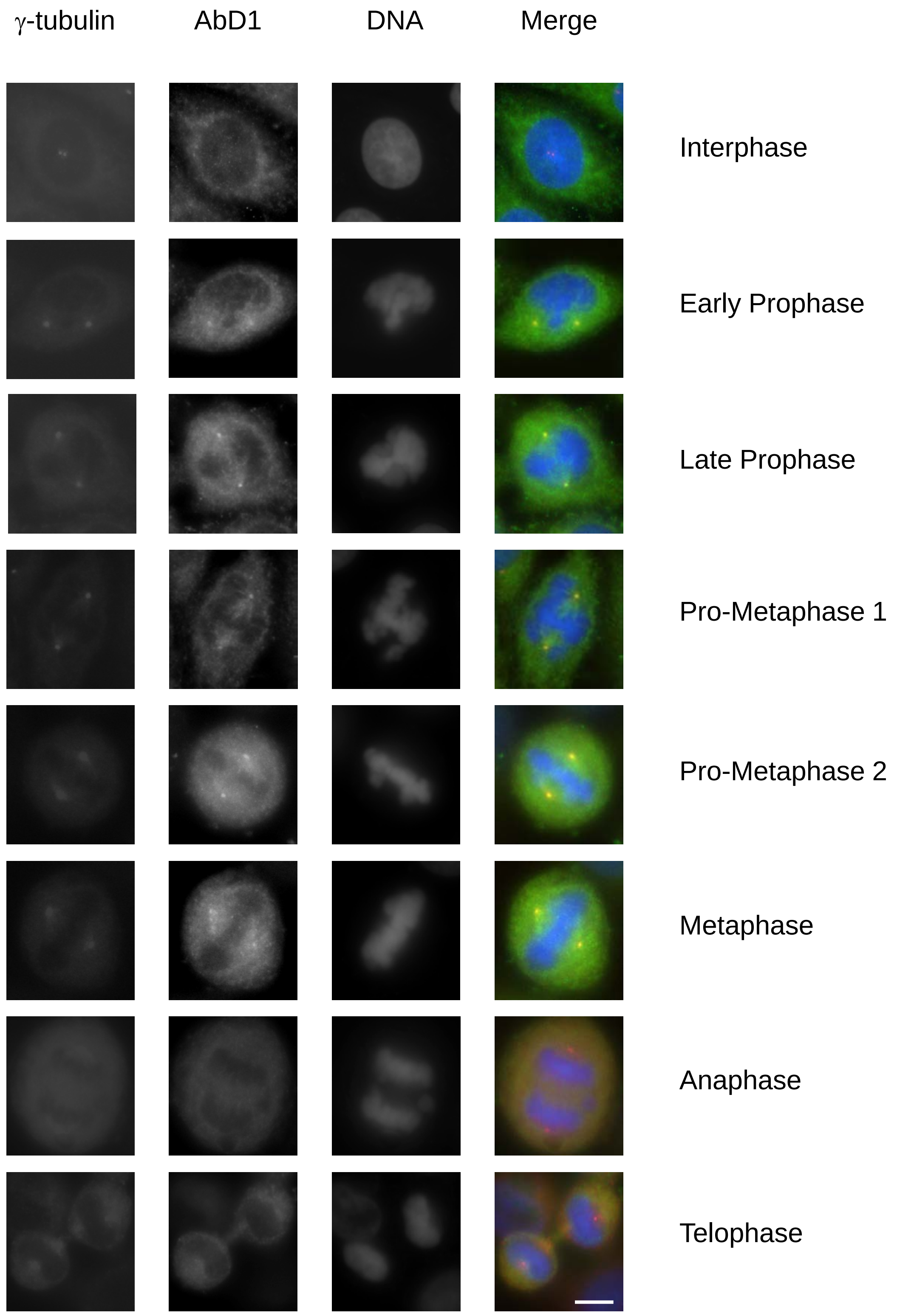
γ-tubulin
AbD1
DNA
Merge
Interphase
Early Prophase
Late Prophase
Pro-Metaphase 1
Pro-Metaphase 2
Metaphase
Anaphase
Telophase

Figure 4.15 AbD1 detects centrosomes specifically in prophase cells

U2OS cells were fixed with methanol and stained with a γ-tubulin antibody to detect the centrosomes (red), AbD1 to detect active Nek2 (green) and Hoechst 33258 to detect the DNA (blue). Images were taken of cells either in interphase or in the different stages of the mitosis as indicated. Scale bar, 10 µm.

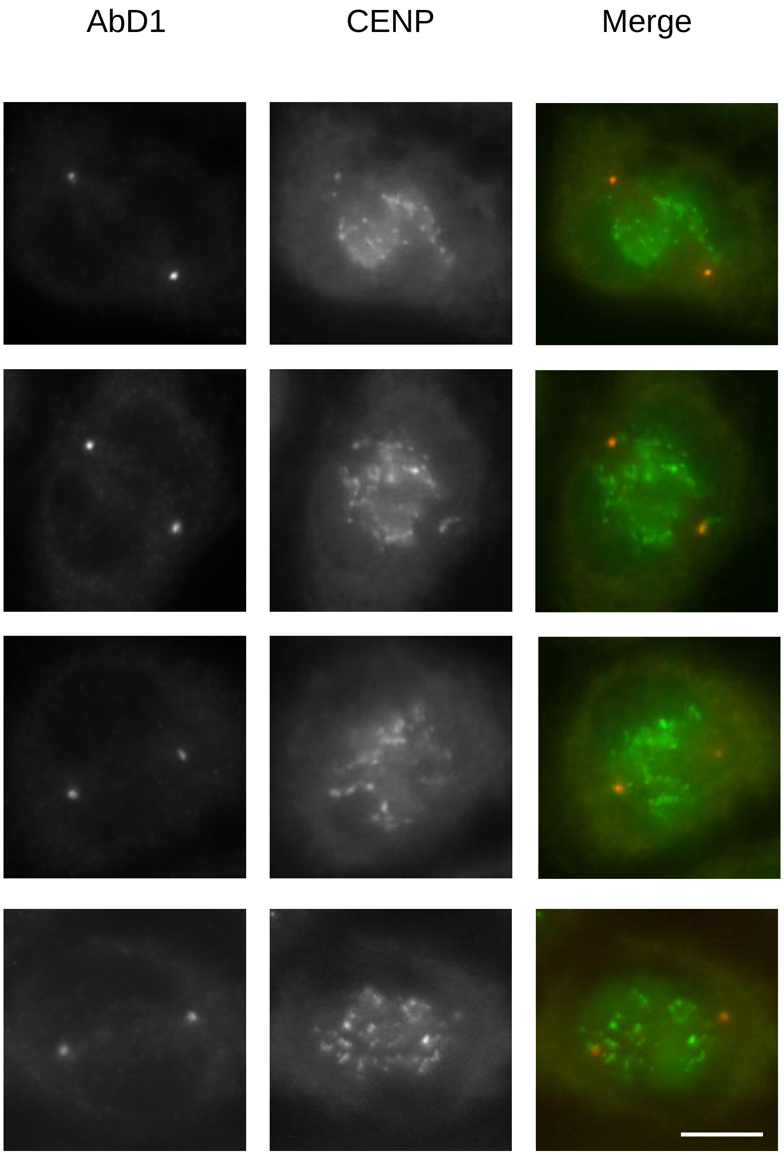

Figure 4.16 Nek2 does not colocalise with kinetochores

U2OS cells were fixed with methanol and stained with AbD1 to detect active Nek2 (red in merge), an anti-CENP antibody to detect centromeres (green in merge). Immunofluorescence microscopy images were taken of mitotic cells in prophase when Nek2A is activated. Merged images of CENP and γ-tubulin are shown. Scale bar, 10 μm. Clearly, the AbD1 signal did not colocalise with kinetochores.

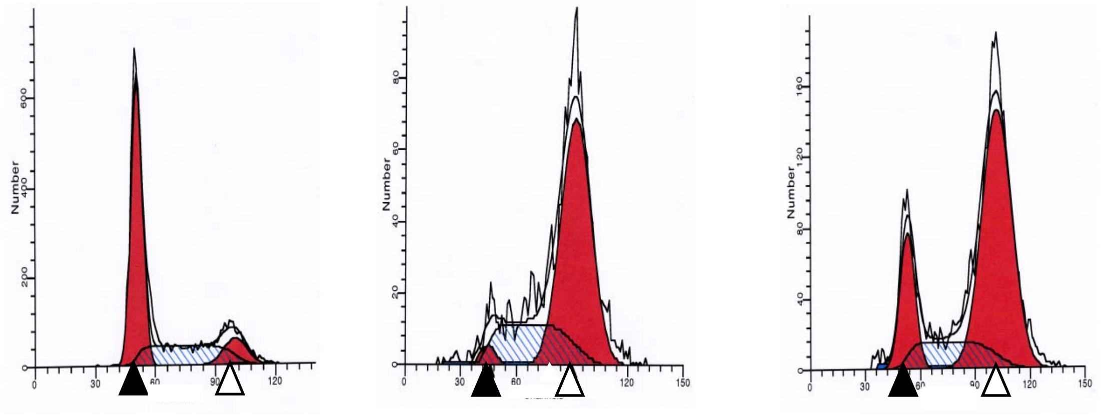

Asynchronous RO-3306 arrested 2 hr release

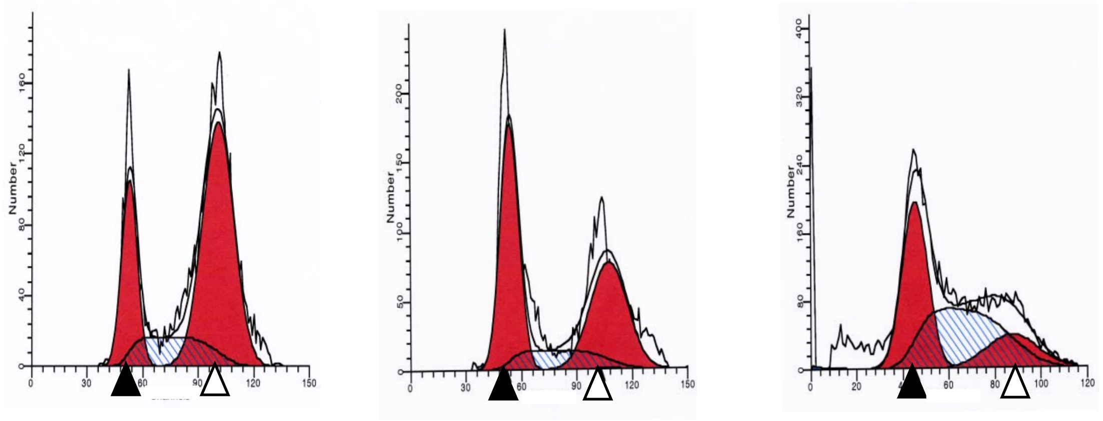

4 hr release 8 hr release 24 hr release

Figure 5.1 RO-3306 induces a G2/M arrest in U2OS cells

U2OS cells were either untreated (asynchronous) or treated with 20 µM RO-3306 for 16 hours (RO-3306 arrested). The cells were then released by washing out the drug and replacing with fresh medium. The cells were harvested after 2, 4, 8 and 24 hours as indicated. The cells were stained with PI and analysed by flow cytometry. Stained cells were examined using Cell Quest software and analysed using a ModFit program. Cells containing 2N DNA are represented by the first peak (▲) and 4N DNA represented by the second peak (△).

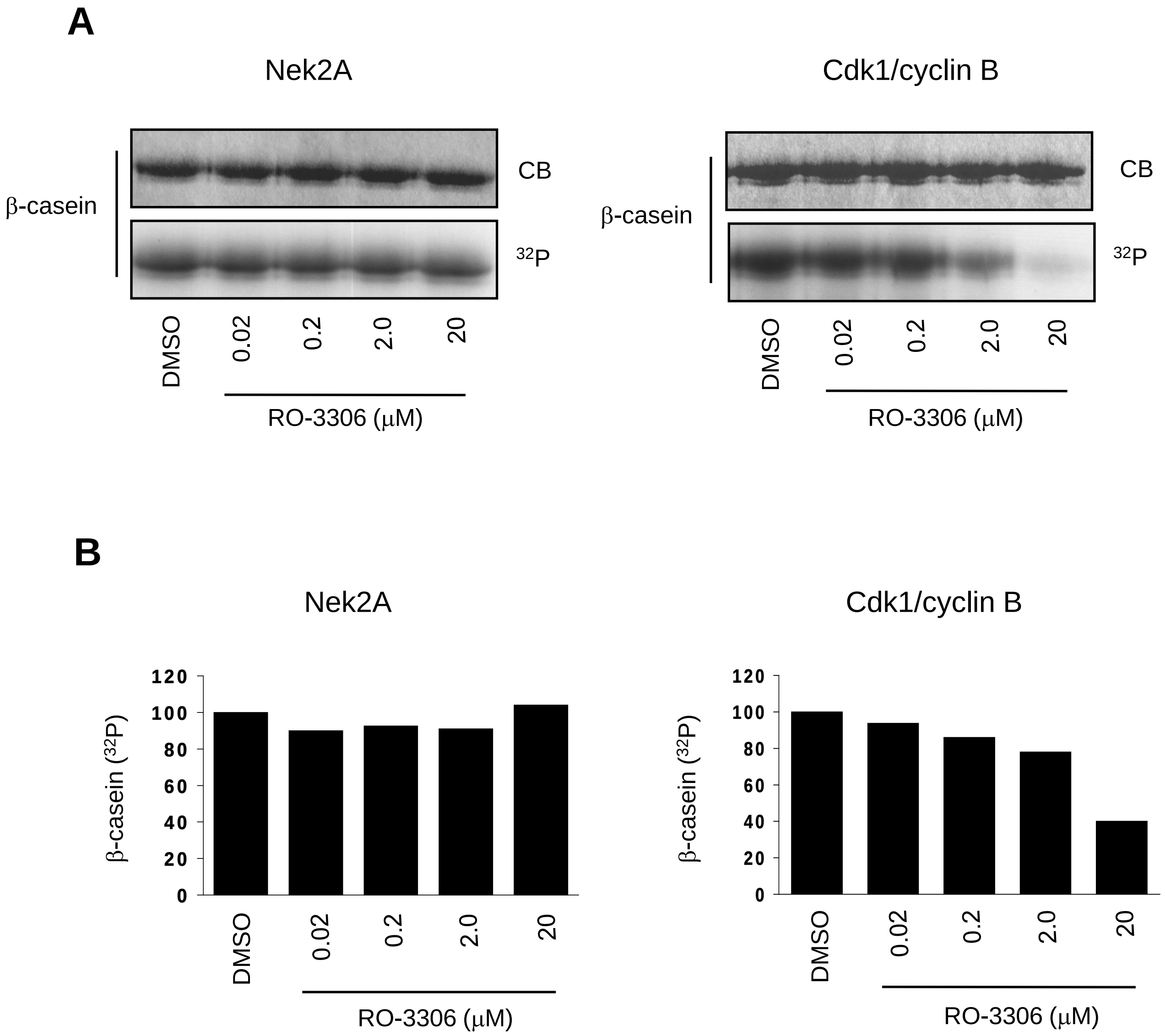

Figure 5.2 RO-3306 inhibits Cdk1 but not Nek2A kinase activity *in vitro*

A. Purified recombinant Nek2A and Cdk1/cyclin B kinases were incubated in kinase buffer containing ^{32}P-γ-[ATP], the substrate β-casein and DMSO or RO-3306 at a range of concentrations (0.02-20 μM). The addition of DMSO acted as a negative control. Following an incubation of 30 minutes at 30^{0}C, the proteins were separated by SDS-PAGE and stained with Coomassie Blue (CB). The dried gel was subjected to autoradiography (^{32}P). The β-casein band is shown. **B**. The kinase activity of Nek2A and Cdk1/cyclin B was calculated by scintillation counting of the β-casein excised from the dried gels and shown in the histogram relative to the activity in the presence of DMSO alone. This experiment was performed once.

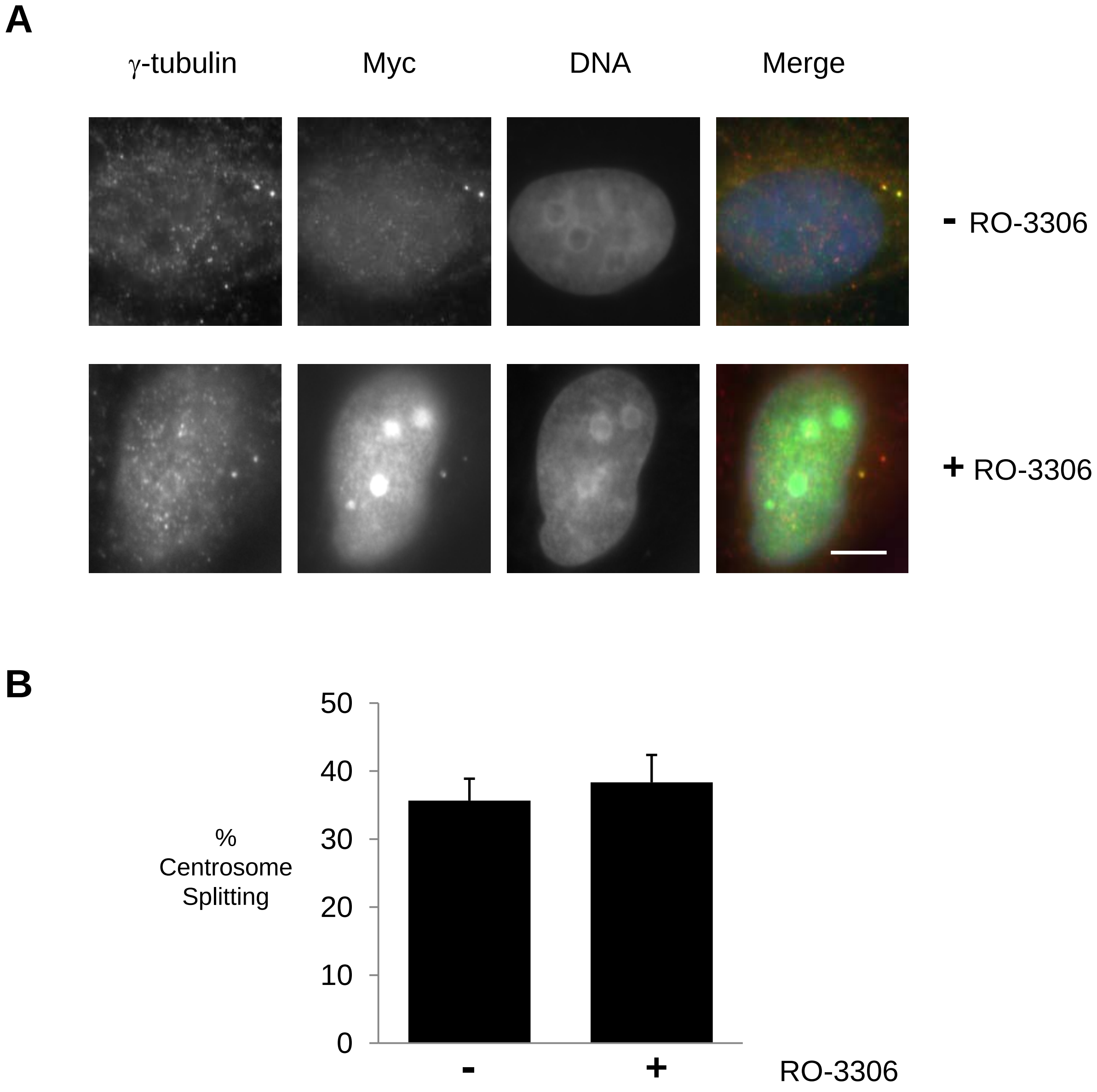
A
γ-tubulin
Myc
DNA
Merge
- RO-3306
+ RO-3306
B
50
40
30
20
10
0
% Centrosome Splitting
-
+
RO-3306

Figure 5.3 RO-3306 does not prevent centrosome splitting in U2OS cells transfected with myc-Nek2A-WT

A. U2OS cells were transfected with a myc-Nek2A-WT construct and treated with or without 20 µM RO-3306. After 16 hours, cells were fixed with methanol and stained with an anti-Myc antibody to detect the Nek2A construct (Myc, green), an anti-γ-tubulin antibody to detect the centrosome (red) and Hoechst 33258 to detect the DNA (blue). Merge images are shown. Scale bar, 10 µm. **B.** Approximately 100 cells were counted in three separate experiments and the centrosomes scored as split (> 2 µm) or non-split. The percentage of cells with split centrosomes in the presence or absence of RO-3306 is illustrated by the histogram.

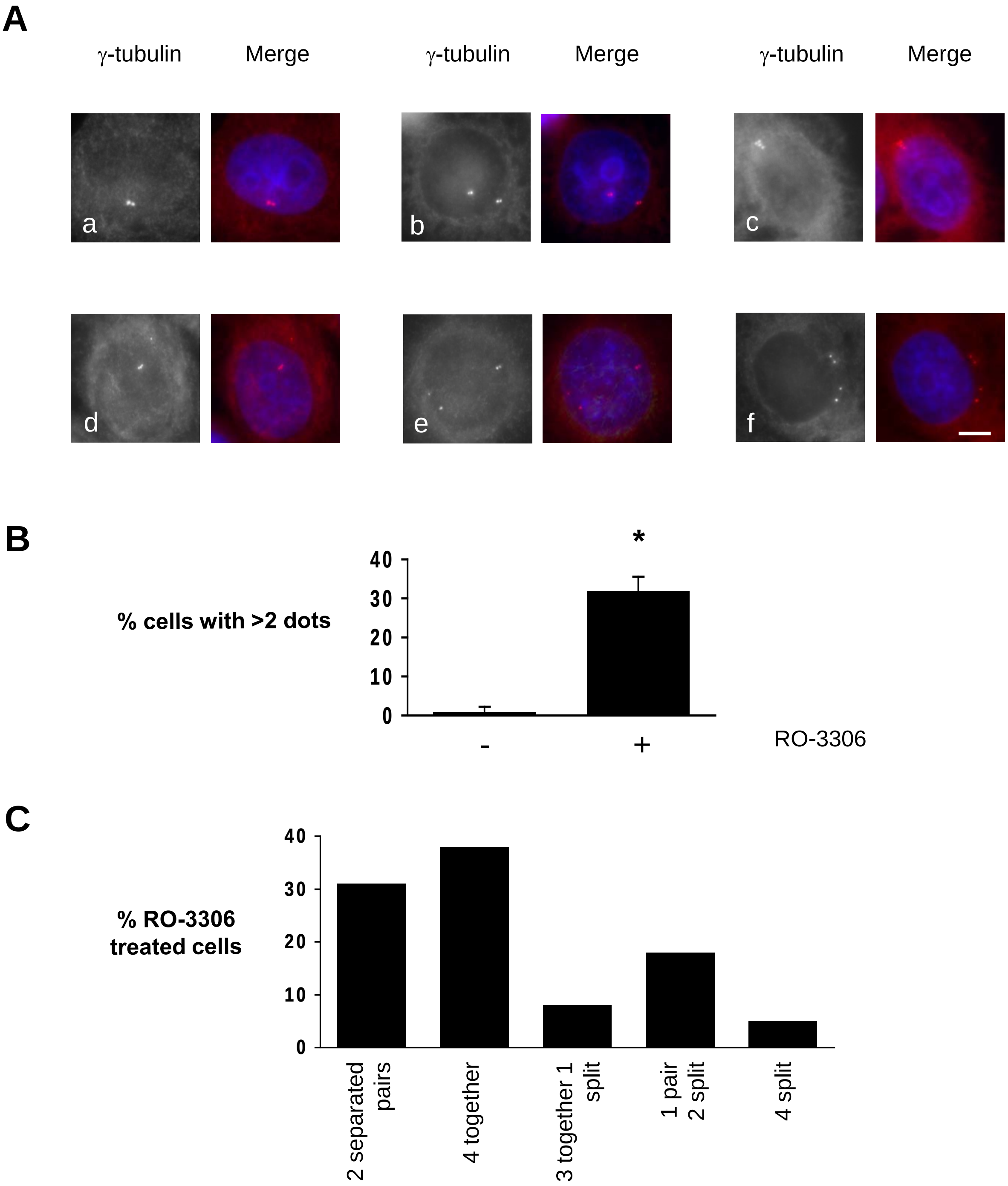

Figure 5.4 RO-3306 induces centrosome defects in U2OS cells

A. U2OS cells were treated with or without RO-3306 (20 μM) for 16 hours before being fixed in cold methanol and staining with an anti-γ-tubulin antibody to detect the centrosomes (red) and Hoechst 33258 to detect the DNA (blue). Images of γ-tubulin staining and a merge image are shown for six representative cells, all treated with RO-3306 (a-f). Scale bar, 10 µm. **B.** Approximately 100 cells were counted in three separate experiments and scored for 2 dots (e.g. image a in panel A) or >2 dots (e.g. images b-f in panel A). * $P< 0.001$ compared to untreated cells. **C.** In cells treated with RO-3306, 100 cells were counted for their distribution of centrosomes stained with anti-γ-tubulin antibodies. The histogram illustrates the number of cells with either 2 separated pairs (b), 4 together (c), 3 together/1 split (d), 1 pair/2 split (e) or all 4 split (f). This experiment was performed once.

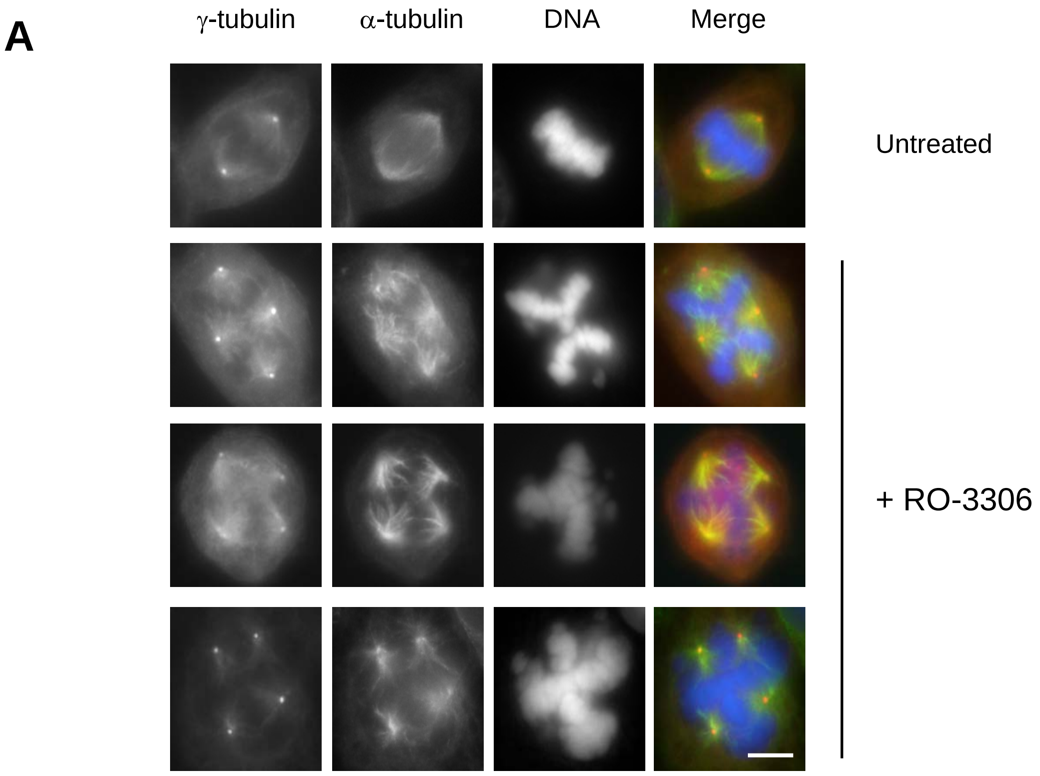

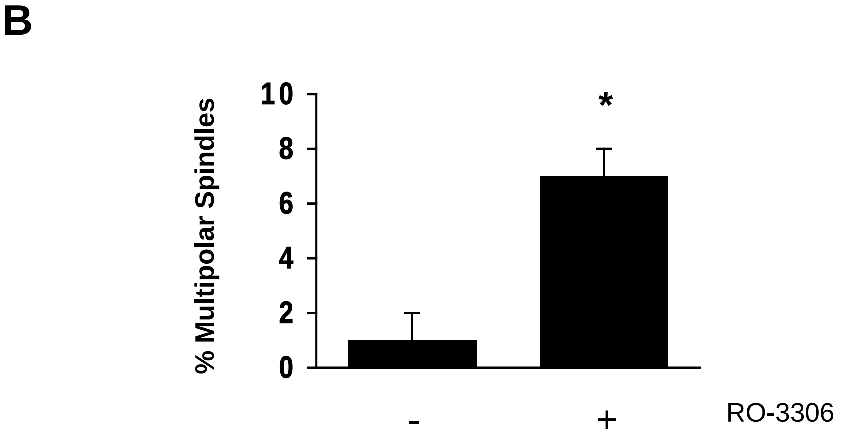

Figure 5.5 RO-3306 induces spindle defects in U2OS cells

A. U2OS cells were treated with or without RO-3306 (20 μM) for 16 hours. Following a 1 hour release from drug treatment, the cells were fixed in cold methanol and stained with an anti-γ-tubulin antibody to detect the centrosomes (red), an anti-α-tubulin antibody to detect microtubules (green) and Hoechst 33258 to detect the DNA (blue). Merge images are shown. Scale bar, 10 μm. **B.** Approximately 50 mitotic cells were counted in three separate experiments and the spindles scored as bipolar or multipolar. The histogram shows the number of cells with multipolar spindles observed in RO-3306-treated and untreated cells. * $P < 0.001$ compared to untreated cells.

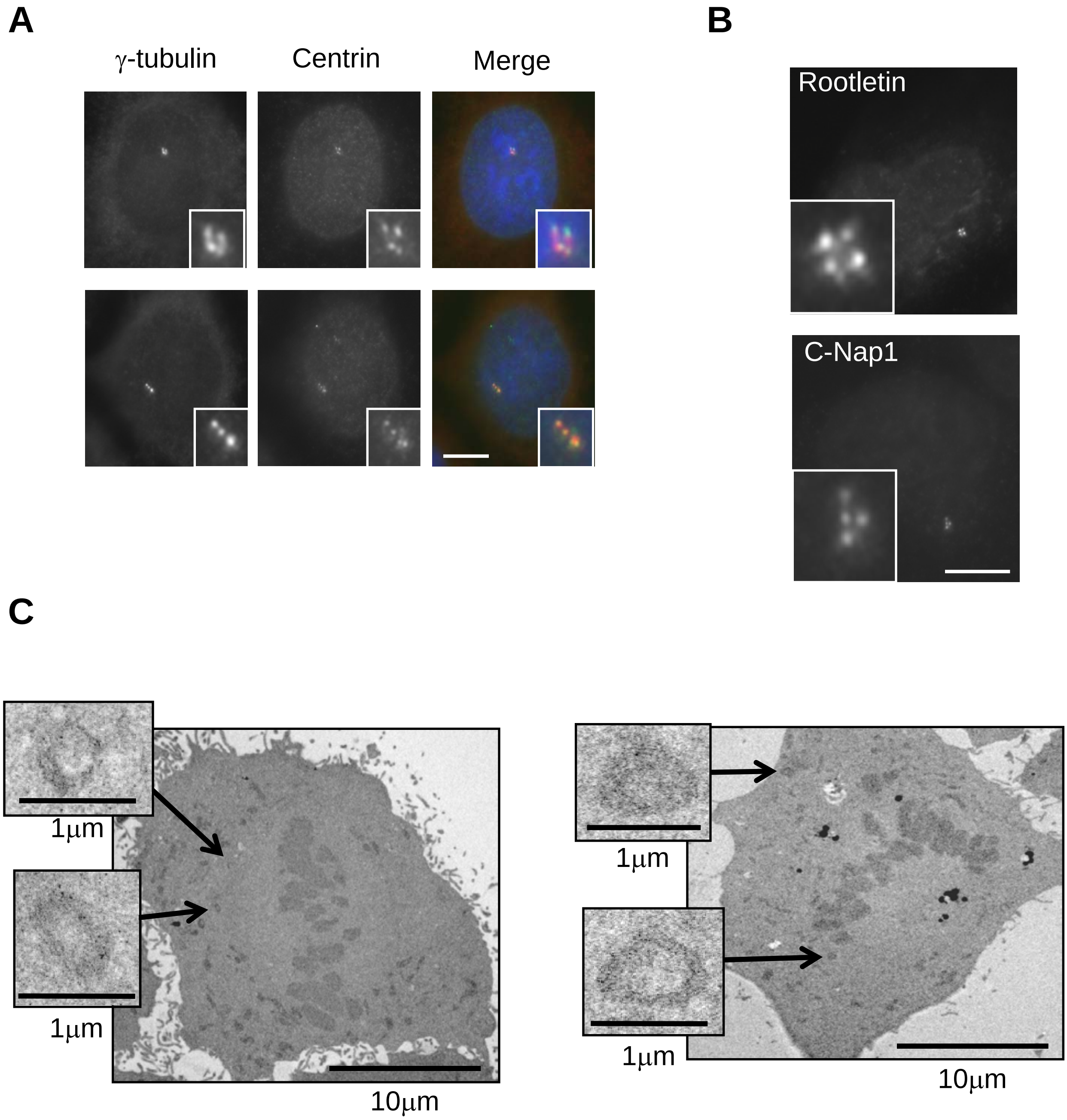

Figure 5.6 Cdk1 inhibition results in premature centriole disengagement and premature recruitment of intercentriolar proteins

A. HeLa cells treated with 20 μM RO-3306 for 20 hours were co-stained with anti-centrin and anti-γ-tubulin antibodies. Using immunofluorescence microscopy, each γ-tubulin focus was found to associate with one centrin focus. The presence of four slightly separated centrin foci suggests that premature centriole disengagement has occurred. **B**. RO-3306 treated HeLa cells were stained with Anti-C-Nap1 and rootletin antibodies. Four foci of C-Nap1 and rootletin were observed in these cells. This suggests that C-Nap1 and rootletin are recruited to the prematurely disengaged centrioles in G2/M arrested cells. **C**. TEM analysis of HeLa cells that had been treated for 1 hour with RO-330 and then released for 1 hour confirmed the presence of a single centriole at each spindle pole. Figures kindly provided by M. Samant and S. Prosser.

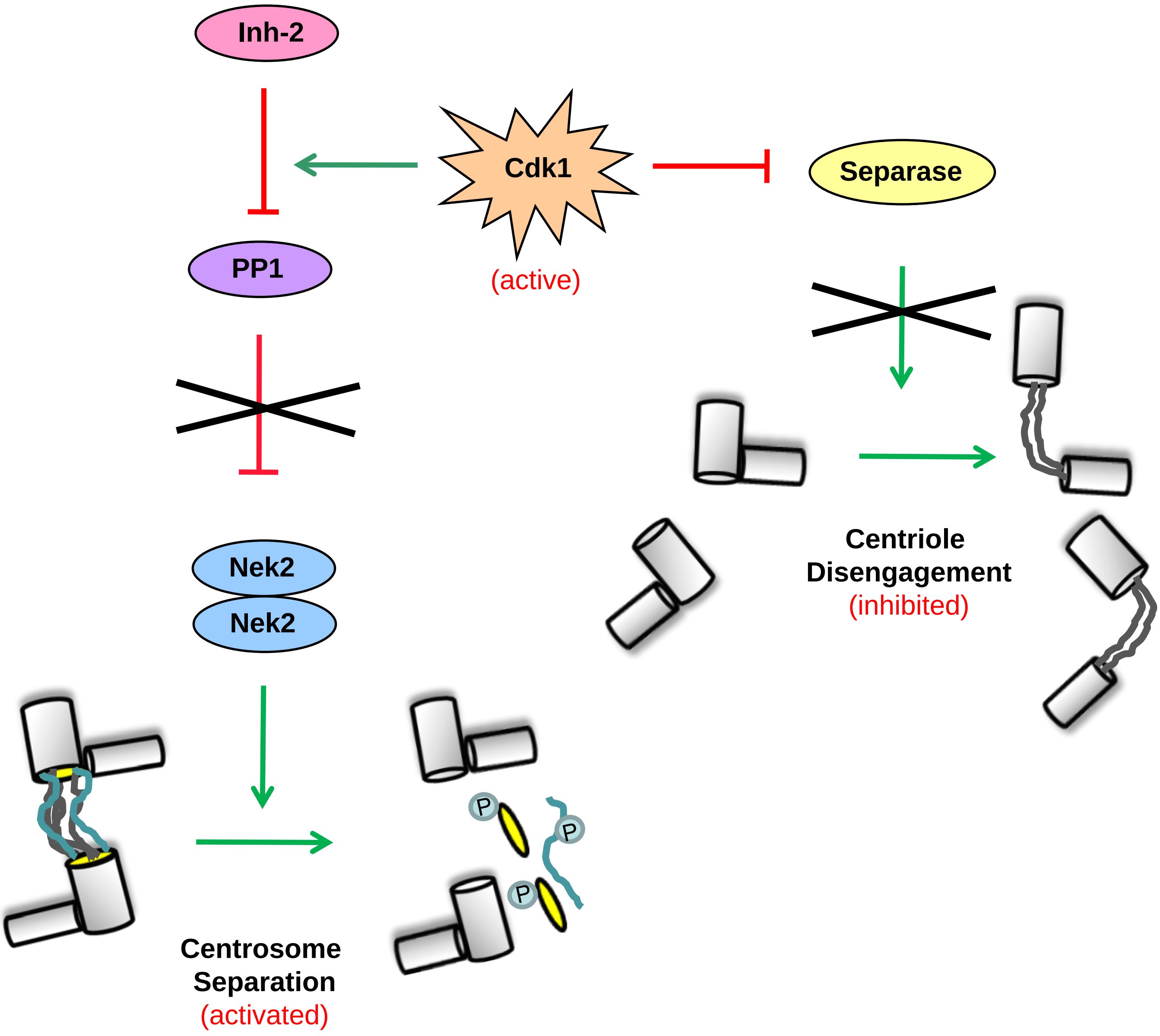
Inh-2
Cdk1
(active)
Separase
PP1
Centriole
Disengagement
(inhibited)
Nek2
Nek2
P
P
P
Centrosome
Separation
(activated)

Figure 5.7 A model for the role of Cdk1 in the activation of Nek2 and prevention of premature centriole disengagement

Nek2, which exists in cells predominantly as a dimer, triggers centrosome separation through phosphorylation of intercentriolar proteins, at the G_2/M transition (see Chapter 6). During interphase, Nek2 activity is restrained by PP1. However, at G_2/M, activation of Cdk1 leads to PP1 inhibition through recruitment of inhibitor-2 (Inh-2). Nek2 is therefore active and able to promote centrosome separation at G2/M. Secondly, Cdk1 can inhibit separase, which prevents the premature disengagement of centrioles.

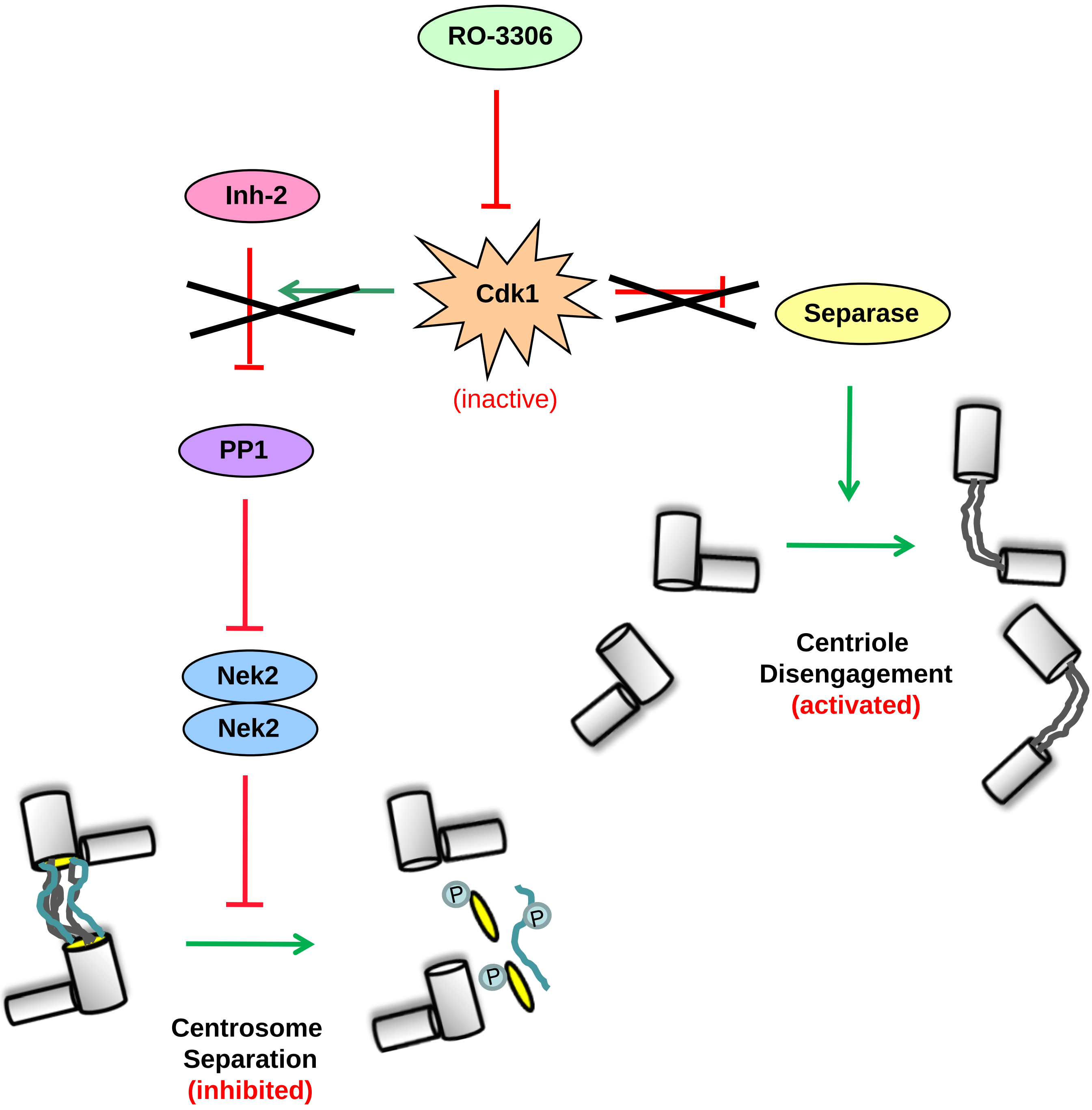
RO-3306
Inh-2
Cdk1
(inactive)
Separase
PP1
Nek2
Nek2
Centriole
Disengagement
(activated)
P
P
P
Centrosome
Separation
(inhibited)

Figure 5.8 A model for the consequences of Cdk1 inhibition by RO-3306 upon Nek2 activation and centriole disengagement

Nek2, which exists in cells predominantly as a dimer, triggers centrosome separation through phosphorylation of intercentriolar proteins, at the G_2/M transition (see Chapter 6). During interphase, Nek2 activity is restrained by PP1. However, at G_2/M, activation of Cdk1 leads to PP1 inhibition through recruitment of inhibitor-2 (Inh-2). However, when Cdk1 is inactivated by RO-3306, Cdk1 can no longer trigger the inhibition of PP1 through Inh-2. Therefore, PP1 remains active and inhibits Nek2 which in turn inhibits centrosome separation from occurring at G2/M. Secondly, inhibition of Cdk1 prevents Cdk1 from inhibiting separase. As a result, separase is prematurely activated which causes the premature disengagement of centrioles. This may also lead to the premature recruitment of intercentriolar linker proteins in the absence of Nek2 activity.

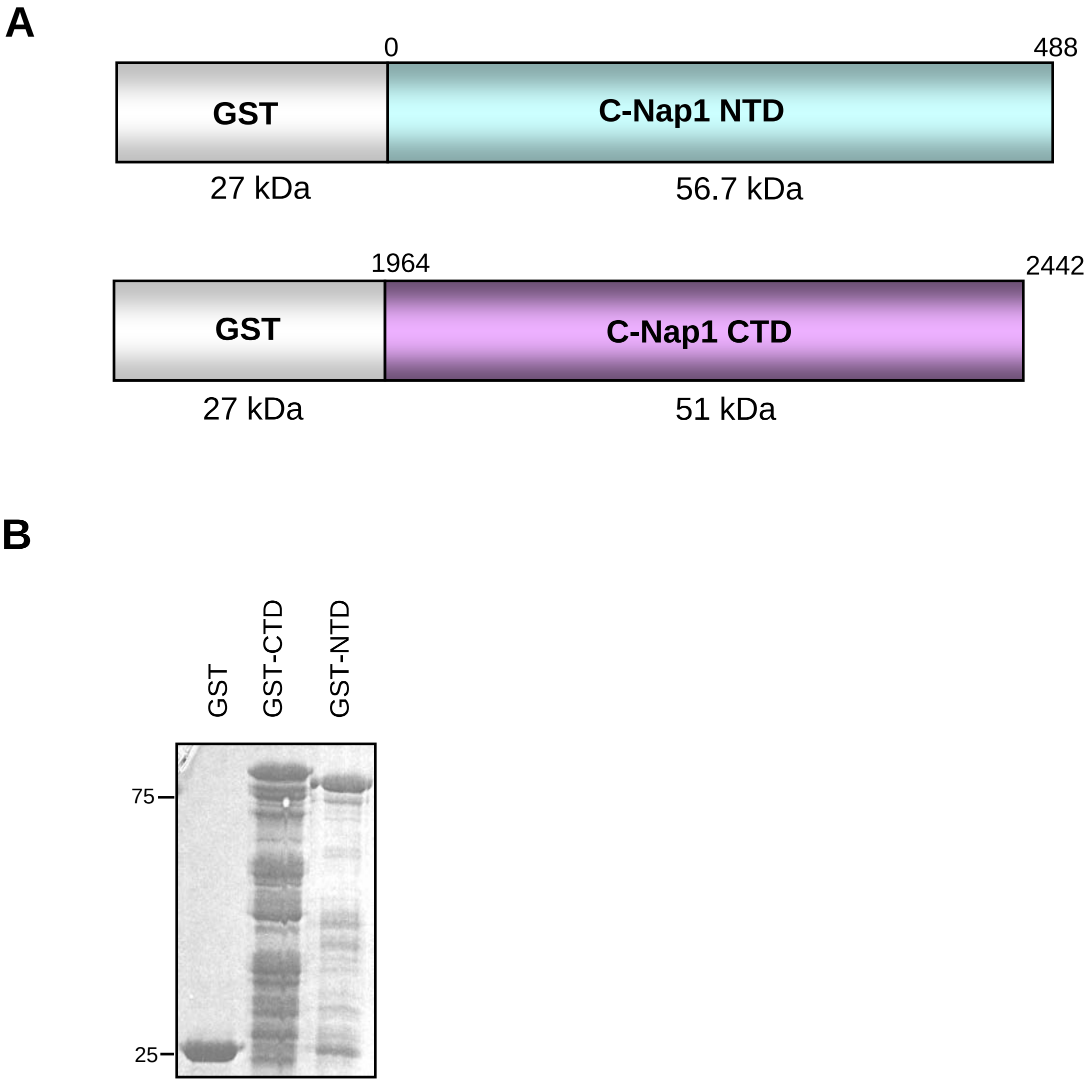
A
0
488
GST
C-Nap1 NTD
27 kDa
56.7 kDa
1964
2442
GST
C-Nap1 CTD
27 kDa
51 kDa
B
GST
GST-CTD
GST-NTD
75
25

Figure 6.1 Purification of GST-C-Nap1-CTD and GST-C-Nap1-NTD

A. A schematic diagram of GST fused C-Nap1-CTD and -NTD proteins and their predicted molecular weights (kDa). The amino acid residue number with respect to full-length C-Nap1 is also indicated. **B**. GST alone, GST-CTD and GST-NTD fusion proteins coupled to glutathione sepharose beads were analysed by SDS-PAGE and Coomassie Blue staining. Molecular weights (kDa) are indicated on the left.

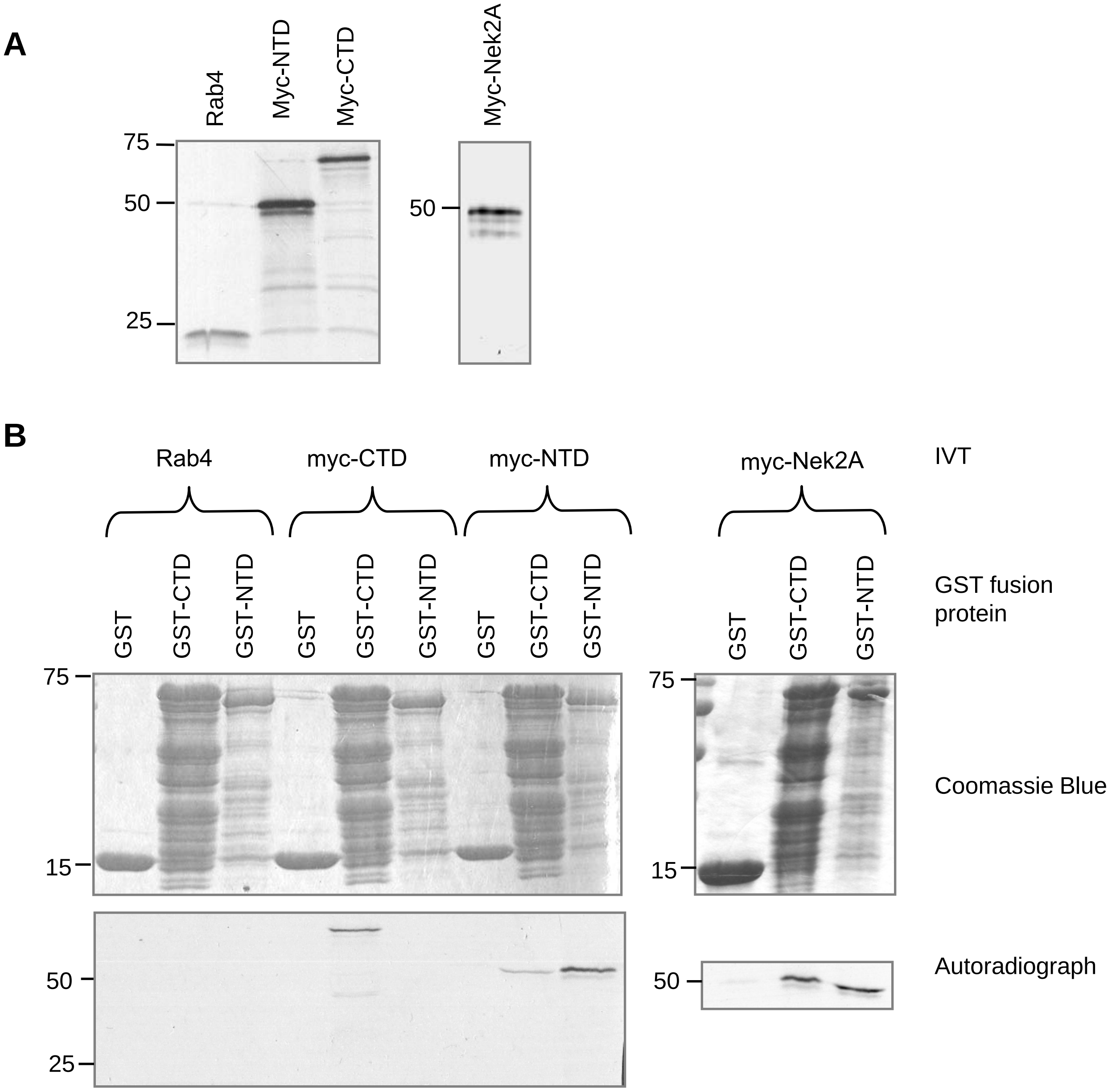
A
Rab4
Myc-NTD
Myc-CTD
Myc-Nek2A
75
50
25
50
B
Rab4
myc-CTD
myc-NTD
myc-Nek2A
IVT
GST
GST-CTD
GST-NTD
GST
GST-CTD
GST-NTD
GST
GST-CTD
GST-NTD
GST
GST-CTD
GST-NTD
GST fusion protein
75
15
75
15
Coomassie Blue
50
25
50
Autoradiograph

Figure 6.2 ***In vitro*** **GST pull down assays with C-Nap1 and Nek2 proteins**

A. Rab4, C-Nap1-CTD, C-Nap1-NTD and Nek2A proteins were generated by *in vitro* translation (IVT) prepared in the presence of [^{35}S] methionine. An aliquot was analysed by SDS-PAGE followed by autoradiography. **B**. GST fusion proteins as indicated were coupled to sepharose beads and incubated with the [^{35}S]-labelled proteins indicated above for 2 hours at 4^{0}C. The beads were then washed and analysed by SDS-PAGE, Coomassie Blue staining and autoradiography. Molecular weights for each protein are indicated on the left (kDa).

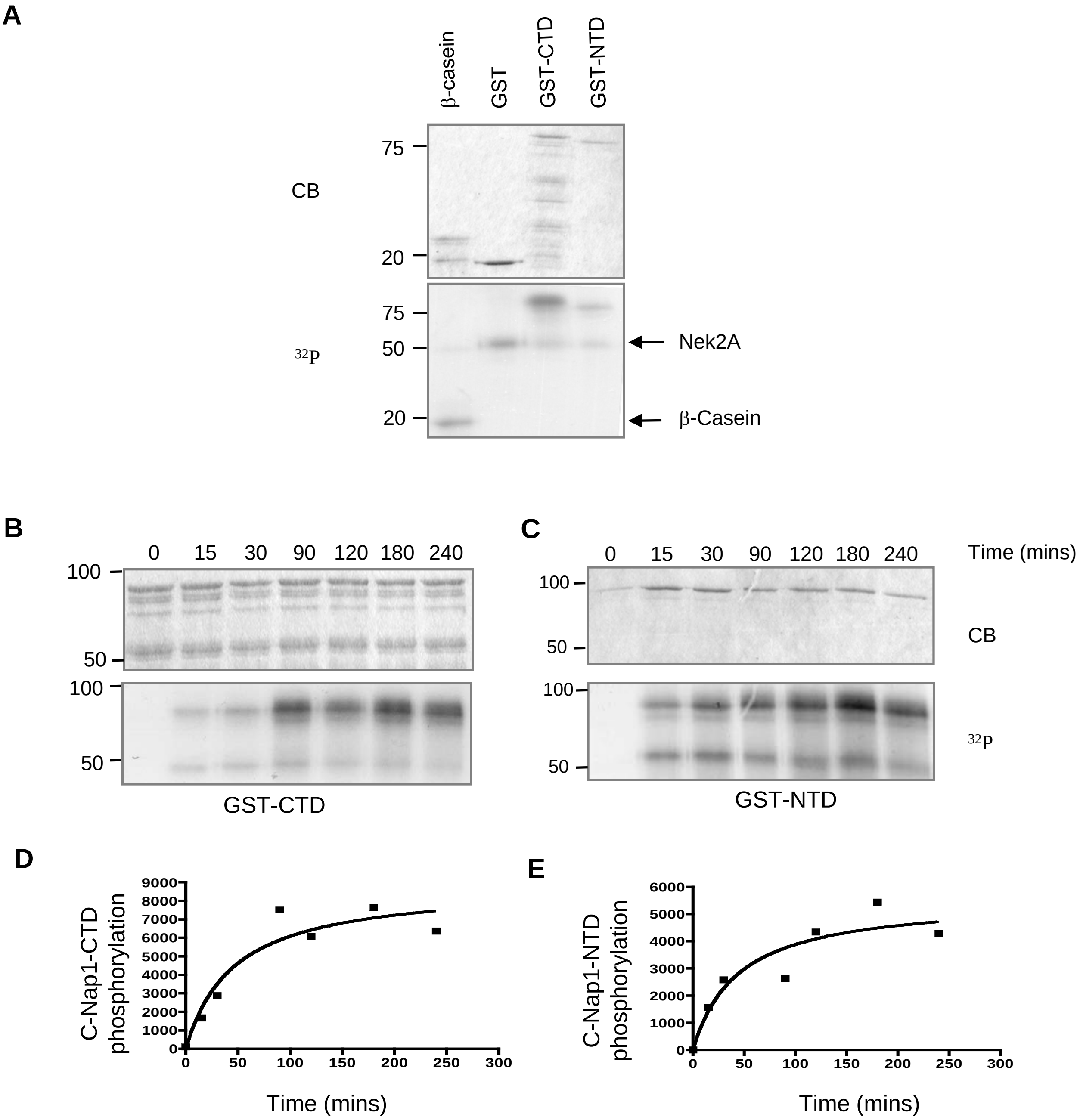

Figure 6.3 C-Nap1-CTD and -NTD can be phosphorylated by Nek2 kinase

A. GST, GST-CTD and GST-NTD coupled to beads or β-casein alone were incubated with kinase buffer containing purified Nek2A kinase and ^{32}P-γ-ATP. Samples were analysed by SDS-PAGE followed by Coomassie Blue staining (CB) and autoradiography (^{32}P). Casein phosphorylation and Nek2A autophosphorylation are indicated on the right (arrows). Molecular weights are indicated on the left (kDa). A kinase assay was performed as described above for GST-CTD **(B)** and GST-NTD **(C)** bound beads. Extracts of beads were taken at regular intervals from 0 to 4 hours. The samples were separated by SDS-PAGE and the Coomassie Blue stained gel (CB) was exposed to autoradiography (^{32}P). **D** & **E.** The amount of radioactivity incorporated by the CTD and NTD proteins was calculated by scintillation counting and plotted against time. This experiment was performed once.

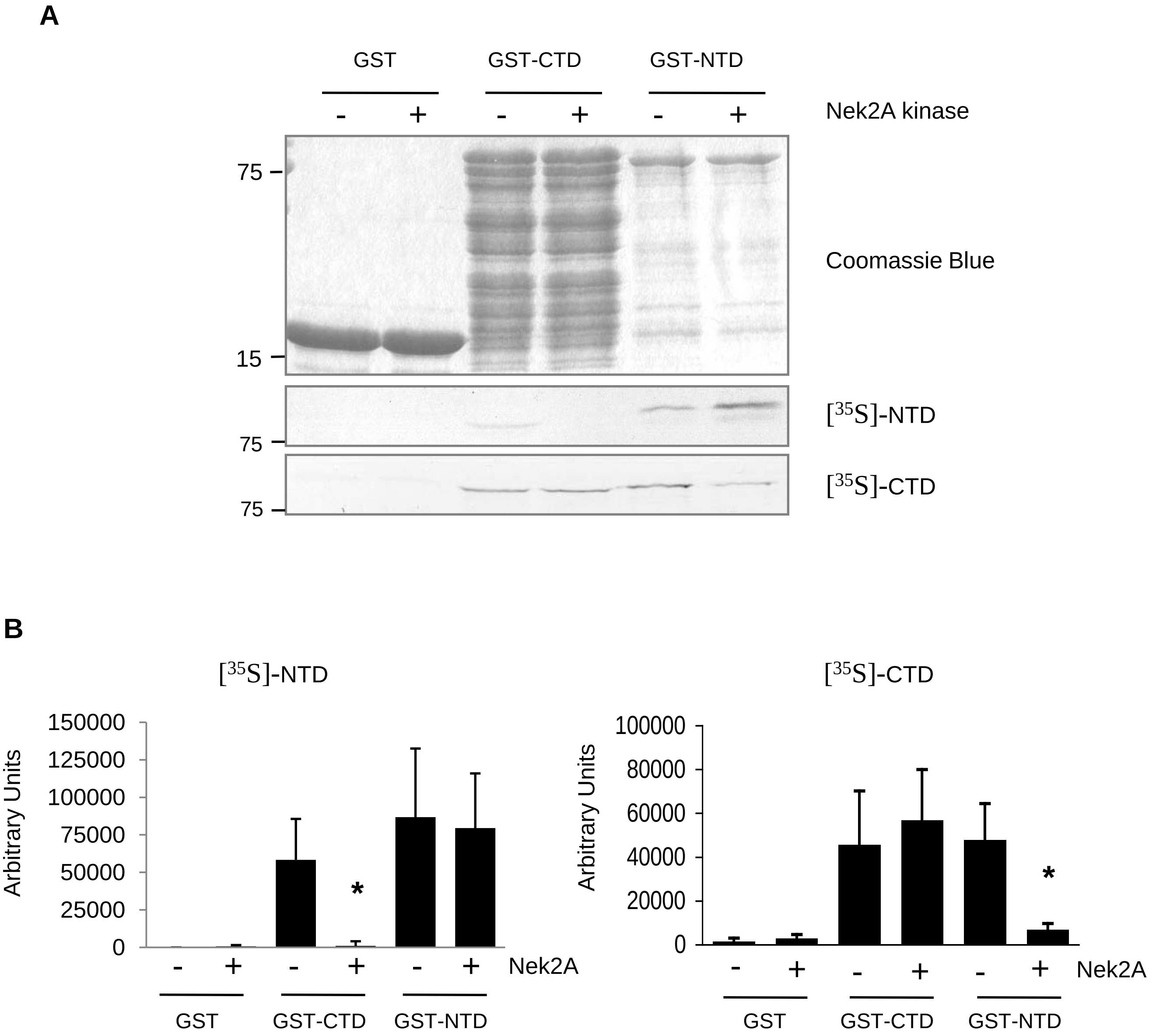

Figure 6.4 The ability of C-Nap1-CTD and -NTD to form heterodimers is significantly reduced as a consequence of phosphorylation by Nek2

A. GST, GST-CTD and GST-NTD proteins were coupled to glutathione-sepharose linked beads and resuspended in kinase assay buffer containing ATP in the presence and absence of purified Nek2A kinase for 30 minutes at 30^{0}C. After washing, the protein bound beads were then incubated with [^{35}S]-labelled C-Nap1-CTD and -NTD proteins. Samples were separated by SDS-PAGE and Coomassie Blue stained. Dried gels were exposed to autoradiography. Molecular weights are indicated on the left of each panel (kDa). **B**. The histograms show that the interaction between C-Nap1-CTD and -NTD is reduced as a consequence of phosphorylation by Nek2A kinase. Autoradiographs were quantified using NIH image software to measure the intensity of each band. Standard error bars are shown, based on four separate experiments. * $P<0.05$ suggesting there is a significant loss of interaction between GST-CTD and GST-NTD following phosphorylation by Nek2.

A

1 metrspglnn mkpqslqlvl eeqvlalqqq maenqaaswr klknsqeaqq
51 rqatlvrklq akvlqyrswc qelekrleat ggpipqrwen veepnldell
101 vrleeeqqrc eslaevntql rlhmekadvv nkalredvek ltvdwsrard
151 elmrkesqwq meqeffkgyl kgehgrllsl wrevvtfrrh flemksatdr
201 dlmelkaehv rlsgslltcc lrltvgaqsr epngsgrmdg repaqlllll
251 aktqelekea hersqeliql ksqgdlekae lqdrvtelsa lltqsqkqne
301 dyekmikalr etveiletnh telmeheasl srnaqeekls lqqvikditq
351 vmveegdnia qgsghensle ldssifsqfd yqdadkaltl vrsvltrrrq
401 avqdlrqqla gcqeavnllq qqhdqweeeg kalrqrlqkl tgerdtlagq
451 **t**vdlqgevds lskerellqk areelrqqle vleqeawr

B

1964 ealqealgka haalqgkeqh lleqaelsrs leastatlqa sldacqahsr
2014 qleealriqe geiqdqdlry qedvqqlqqa laqrdeelrh qqereqllek
2064 **s**laqrvqenm iqekqnlgqe reeeeirglh qsvrelql**t**l aqkeqeilel
2114 retqqrnnle alphshktsp meeqslklds leprlqrele rlqaalrqte
2164 areiewreka qdlal**s**laqt kasvsslqev amflqasvle rdseqqrlqd
2214 eleltrrale kerlh**s**pgat **s**taelgsrge qgvqlgevsg veaepspdgm
2264 ekqswrqrle hlqqavarle idrsrlqrhn vqlr**s**tleqv ererrklkre
2314 amraaqagsl eiskatassp tqqdgrgqkn sdakcvaelq kevvllqaql
2364 tlerkqkqdy itrsaqtsre laglhhslsh **s**llavaqape atvleaetrr

2414 lde**s**ltq**s**lt spgpvllhps psttqaasr

Figure 6.5 Identification of sites within the N- and C-terminal domains of C-Nap1 phosphorylated by Nek2

GST-C-Nap1-NTD and GST-C-Nap1-CTD proteins were incubated with Nek2A and ATP in kinase buffer for 30 minutes at 30^0C. The proteins were then separated by SDS-PAGE and stained with Coomassie Blue, subjected to trypsin digestion and analysed by mass spectrometry by Douglas Lamont and Axel Knebel at the Mass Spectrometry Facility at the University of Dundee. The complete protein sequences of the C-Nap1-NTD (amino acids 1-488) and C-Nap1-CTD (amino acids 1964-2442) protein fragment are shown in **A** and **B,** respectively. The phosphorylation sites identified are indicated in red. One phosphorylation site was found in the NTD, whereas 7 sites were found in the CTD. In addition, two Nek2 phosphorylation sites identified in a previous study by Baxter (2006) are indicated in blue.

A

xxFRxS/Txx

B

pThr451	tlagqtvdlqg
pSer2064	qllekslaqrv
pThr2102	relqltlaqke
pSer2179	qdlalslaqtk
pSer2229	kerlhspgats
pSer2234	spgatstaelg
pSer2298	nvqlrstleqv
pSer2394	hslshsllava
pSer2417	rrldesltqsl
pSer2421	esltqsltspg

C

xxL/AxxS/Tϕ

Figure 6.6 Comparison of the phosphorylation consensus sequence for NIMA and those sites phosphorylated by Nek2 in C-Nap1

A. The consensus site for phosphorylation by the *Aspergillus* NIMA kinase. The phenylalanine within this sequence is thought to be very important. **B**. The sites within C-Nap1 phosphorylated by Nek2A and identified by mass spectrometry are indicated in red. **C**. Based on the sites shown in B, a consensus sequence for phosphorylation of substrates by Nek2A is proposed.

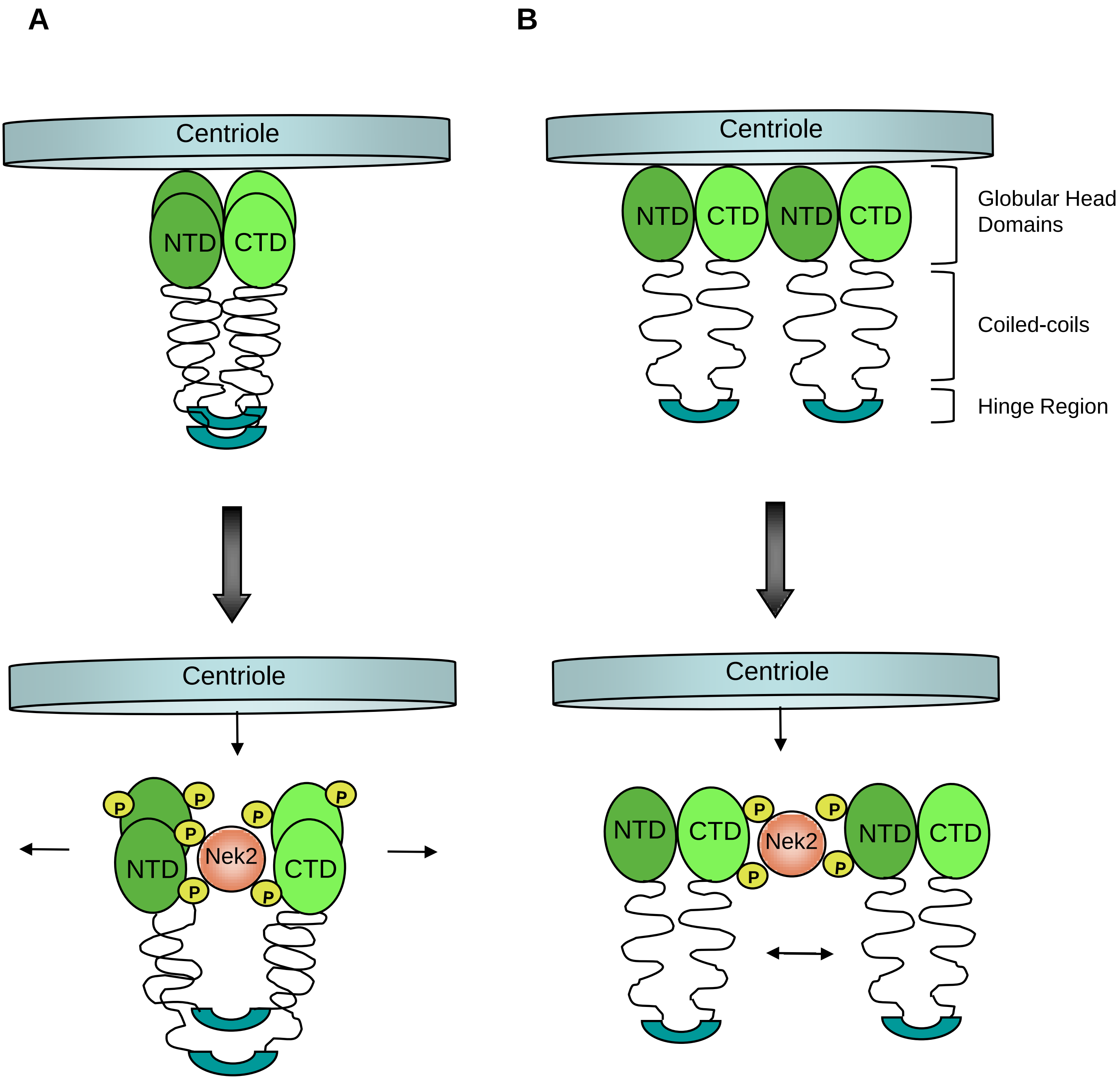

Figure 6.7 Proposed model of how C-Nap1 interactions may be regulated in response to phosphorylation by Nek2

Schematic models showing how C-Nap1 might exist as a dimer and how its phosphorylation by Nek2 could stimulate a change in its conformation and its displacement from the centrosome. The CTD-CTD and NTD-NTD interact strongly, but the CTD-NTD interactions are considerably weaker. Nek2 interacts with the CTD and NTD domains of the dimer and this experimental evidence suggests that these CTD-NTD interactions are lost upon phosphorylation by Nek2. Therefore, it is proposed that either (A) intramolecular interactions may be disturbed by Nek2 phosphorylation and that C-Nap1 dimers may open and close in a scissor-like action in response to Nek2 phosphorylation, or (B) that intermolecular interactions are lost upon phosphorylation by Nek2. Of course it is also possible that Nek2 regulates both intra- and inter-molecular interactions simultaneously.

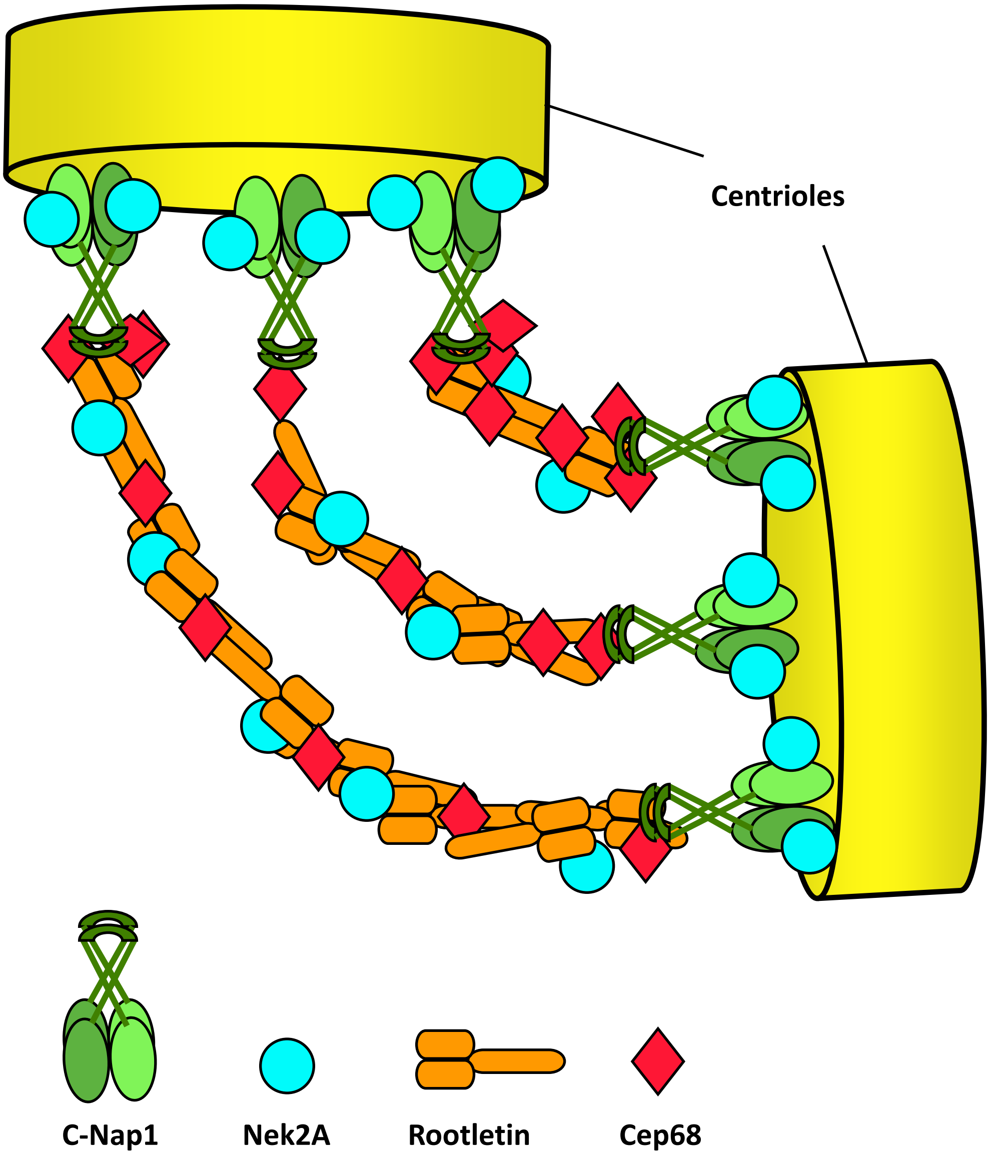

Figure 7.1 A model of the intercentriolar linkage connecting paired centrioles
Schematic diagram representing a model of centrosome cohesion. In this model, rootletin fibers form the linkage between the proximal ends of centrioles. Cep68 decorates the rootletin fibers and may stabilise the rootletin homopolymers. Cep68 may also interact with C-Nap1 possibly via its flexible hinge region. Nek2A interacts with the N- and C-terminal globular domains of C-Nap1, as well as with rootletin. The proposal is that phosphorylation of C-Nap, rootletin, and possibly Cep68, by Nek2A at the G2/M transition leads to conformational changes in these proteins that cause loss of interactions and displacement from the centrosome. Ultimately, this triggers collapse of the intercentriolar linkage promoting centrosome separation at the onset of mitosis.